

# **PERFORMANCE EVALUATION OF THE CRUMB RUBBER MODIFIED BITUMEN CONTAINING WARM-MIX ADDITIVES**

M.Sc. Thesis  
Jirawat Buchagul  
2019, Delft, The Netherlands



# **PERFORMANCE EVALUATION OF THE CRUMB RUBBER MODIFIED BITUMEN CONTAINING WARM-MIX ADDITIVES**

THESIS

for the degree Master of Science (M.Sc.) in Structural Engineering,  
Faculty of Civil Engineering,  
Delft University of Technology,  
to be defended publicly on the 24<sup>th</sup> of April, 2019

by  
Jirawat Buchagul  
born in Bangkok, Thailand

Graduation Committee:

Dr. Xueyan Liu	TU Delft, Chair
Prof. dr. ir. S.M.J.G Erkens	TU Delft
Prof. dr. ir. Erik Schlangen	TU Delft
Ir. Martin van de Ven	TU Delft
Haopeng Wang	TU Delft
Wim Migchels	Kargro Recycling

An electronic version of this thesis is available at <http://repository.tudelft.nl/>.

## **Acknowledgements**

This master thesis is submitted as a partial fulfilment of the requirements for the acquisition of the Master of Science degree in Civil Engineering, with specialization in Road & Railway Engineering. This work would not have been done without the advice and support of many people. Therefore, I would like to express my sincere gratitude to people who have helped me to make this master thesis possible.

First, and foremost, I would like to thank my advisor Dr. Xueyan Liu for providing me the opportunity and inviting me to join this project.

My great thanks go to my wonderful supervisor, Haopeng Wang, who have always supported and guided me. Throughout my thesis working period, he provided good working ideas, assistance for laboratory and experimental works, encouragement, valuable advice, and good company. This work would not be possible without his support, and I truly appreciated.

In addition, I would like to express my sincere gratitude to the committee members for providing valuable comments on this work at both the kick-off and green-light meetings.

I would also like to thank Ing. Michele van Aggelen and Ing. Marco Poot for providing all the lab and technical assistance in the Pavement Engineering laboratory of TU Delft.

Finally, I would like to thank my family, friends, and all special people in my life for their love, support and encouragement throughout my study.

## Abstract

The crumb rubber modified bitumen (CRMB) has been utilized in pavement industries to mainly reduce the environmental impacts of the wasted tires by turning unwanted scrap tires into new bituminous materials. However, the relatively high viscosity compared to the conventional asphalt is the major drawback of the CRMB. The higher mixing and working temperatures are thus required in order to achieve the desired workability of the CRMB. This results in more asphalt fume emission, higher energy consumption, and more harmful working environments for workers.

Warm mix asphalt (WMA) technologies have been intentionally developed to lower the manufacturing and working temperatures of the asphalt by reducing the viscosity of the asphalt binder. Many studies suggested that coupling CRMB with WMA additives can promote better working conditions and minimize environmental issues of the CRMB.

In this study, experimental works were carried out to evaluate rheological and performance-based properties of the CRMB containing WMA additives in order to investigate the effect of the crumb rubber modifier (CRM) content and WMA additives (wax-based and chemical-base WMA additives) by using only one dynamic shear rheometer (DSR). The performance of the studied binder at high, intermediate, and low road service temperatures were investigated by performing Multiple Stress Creep and Recovery test, Linear Amplitude Sweep test, and 4-mm Dynamic shear rheometer test, respectively. Moreover, the Fourier Transform-Infrared Spectroscopy and the storage stability test were also performed to investigate the effects of the CRM dosage and the WMA additives on the aging susceptibility and the high-temperature storage stability of the binders.

The results show that the incorporation of crumb rubber modifier can clearly improve the overall performance (rutting, fatigue damage, low-temperature thermal cracking resistances), and aging resistance of the asphalt binder in a bitumen-level. The high-temperature storage stability of the CRMB became more stable at the higher dosage of the CRM. Moreover, it was found that the wax-based WMA additive can only enhance the high-temperature rutting resistance but negatively impacted the fatigue and low-temperature damage resistances of both neat and CRM binders. The effect of the chemical-based additive on the neat and CRM binders are different as it improved the performance over the whole service temperature of the neat but lowered the damage resistances of CRMBs. Additionally, the addition of both WMA additives decreased the high-temperature storage stability of the CRMB.

# Contents

## Chapter1 Introduction

1.1 Introduction and Background.....	16
1.2 Study goals.....	19
1.3 Organization of the thesis .....	19

## Chapter 2 Literature review

2.1 Introduction.....	22
2.2 Bitumen .....	22
2.3 Warm mix asphalt (WMA) technologies .....	25
2.3.1 Foaming processes .....	25
2.3.2 Addition of organic or wax-based additives .....	26
2.3.3 Addition of chemical-based additives.....	26
2.4 Crumb rubber modified binder (CRMB) .....	27
2.4.1 History of crumb rubber modified asphalt binder (wet process) .....	27
2.4.2 Crumb rubber modifier production .....	27
2.4.3 Interaction mechanism of crumb rubber particle and bituminous binder .....	28
2.4.4 Storage stability of crumb rubber modified binders .....	29
2.4.5 Warm-mix rubberized asphalt binder .....	30
2.5 Performance-based asphalt binder characterization.....	31
2.5.1 Permanent deformation resistance of asphalt binders.....	34
2.5.2 Fatigue cracking resistance of asphalt binders.....	35
2.5.3 Thermal cracking resistance of asphalt binders .....	36

## Chapter 3 Materials and Sample Preparation

3.1 Introduction.....	39
3.2 Materials .....	39
3.2.1 Base bitumen.....	39
3.2.2 Crumb rubber modifier (CRM).....	40
3.2.3 Warm-mix additives.....	42
3.2.3.1 Wax-based warm-mix additive.....	43
3.2.3.2 Chemical-based warm-mix additive .....	45
3.3 Binder modification method .....	45
3.4 Laboratory aging methods .....	48

3.4.1 Short-term aging .....	48
3.4.2 Long-term aging.....	52
<b>Chapter 4 Rheological Characterization</b>	
4.1 Introduction.....	54
4.2 Oscillatory rheological testing .....	54
4.2.1 Background .....	54
4.2.2 Rheological data representation.....	57
4.2.2.1 Isochronal plots .....	57
4.2.2.2 Isothermal plots .....	58
4.2.2.3 Potential issue of the parallel plates’ gap-height for modified asphalt binders containing particulate matter.....	59
4.2.4 Experimental program.....	62
4.3 Fourier transform infrared spectroscopy (FTIR).....	62
4.3.1 FTIR experimental program .....	65
4.4 Results and Analysis .....	67
4.4.1 Effect of CRM content on the rheological properties .....	67
4.4.2 Effect of WMA additives on the rheological properties .....	69
4.4.3 Aging effect on the rheological properties.....	73
4.5 Summary .....	78
<b>Chapter 5 High-Temperature Performance Characterization</b>	
5.1 Introduction.....	80
5.2 Multiple Stress Creep and Recovery Test.....	80
5.2.1 Background .....	80
5.2.2 Sample preparation and experimental program .....	82
5.3 Results and analysis .....	83
5.3.1 Effect of CRM content on the high-temperature performance .....	83
5.3.2 Effect of WMA additives on the high-temperature performance .....	85
5.3.3 Effect of aging on the high-temperature performance .....	88
5.3.4 Comparison of rutting parameters .....	91
5.4 Summary .....	92
5.4.1 Effect of CRM content on high-temperature performance.....	93
5.4.2 Effect of the WMA additives on high-temperature performance.....	93

5.4.3 Effect of aging on high-temperature performance .....	93
<b>Chapter 6 Intermediate-Temperature Performance Characterization</b>	
6.1 Introduction.....	95
6.2 Linear amplitude sweep test.....	96
6.2.1 Background .....	96
6.2.2 Sample preparation and experimental program .....	98
6.3 Results and analysis .....	98
6.3.1 Effect of CRM content on the intermediate-temperature performance .....	100
6.3.2 Effect of WMA additives on the intermediate-temperature performance .....	101
6.3.3 Effect of aging on the intermediate-temperature performance .....	105
6.3.4 Comparison of asphalt binder fatigue parameters .....	108
6.4 Conclusions.....	109
6.4.1 Effect of CRM content on intermediate-temperature performance .....	109
6.4.2 Effect of WMA additives on intermediate-temperature performance .....	109
6.4.3 Effect of aging on intermediate-temperature performance.....	109
<b>Chapter 7 Low-Temperature Performance Characterization</b>	
7.1 Introduction.....	111
7.2 Dynamic shear rheometer test with application of 4-mm plates.....	111
7.2.1 Background .....	111
7.2.2 Experimental program .....	115
7.3 Results and analysis .....	117
7.3.1 Effect of CRM content on the low-temperature performance .....	117
7.3.2 Effect of WMA additives on the low-temperature performance .....	118
7.4 Summary .....	119
7.4.1 Effect of CRM content on low-temperature performance of the binders.....	120
7.4.2 Effect of WMA additives on low-temperature performance of the binders.....	120
<b>Chapter 8 High-Temperature Storage Stability</b>	
8.1 Introduction.....	122
8.2 Experimental program .....	123
8.3 Results and analysis .....	124
8.4 Summary .....	128
8.4.1 Effect of CRM content on storage stability of CRMB .....	128



8.4.2 Effect of WMA additives on storage stability of CRMB .....	128
<b>Chapter 9 Conclusions and Recommendations</b>	
9.1 Conclusions .....	130
9.2 Recommendations .....	132
References .....	133
Appendix A Effect of aging on rheological properties .....	141
Appendix B Effect of aging on fatigue damage resistance of the binder at the intermediate-temperature .....	146

## List of figures

Figure 1.1: Description of swelling of rubber particles and asphalt binder (Heitzman 1992).....	17
Figure 1.2: Scope and Organization of the study.....	20
Figure 2.1: Asphaltene chemical structure (Read&Whiteoak 2003).....	23
Figure 2.2: Schematic representation of SOL and GEL types of bitumen (Read&Whiteoak 2003). .....	23
Figure 2.3: Aromatic chemical structures (Read&Whiteoak 2003). ....	24
Figure 2.4: Saturates chemical structures (Read&Whiteoak 2003).....	24
Figure 2.5: Scanning Electron Microscope (SEM) images at 200 microns and 400x magnification of rubber particles processed by ambient grinding (left) and cryogenic fracturing (right) (Memon 2011). ....	28
Figure 2.6: Progression of bitumen–rubber interaction at elevated temperature: (a) change in binder viscosity over time, (b) change in particle size over time, and (c) change in binder matrix over time (Abdelrahman 2006).....	29
Figure 2.7: Rut depth vs $G^*/\sin(\delta)$ (A), and rut depth vs $J_{nr}$ (B) (Radhakrishnan et al. 2018)....	35
Figure 3.1: Scanning Electron Microscope (SEM) images at 20 microns and 1000x magnification of base bitumen used in this study. ....	39
Figure 3.2: Crumb rubber modifier with particle sizes ranging from 0 - 0.5 mm. ....	40
Figure 3.3: Scanning Electron Microscope (SEM) images at 200 microns and 100x magnification of crumb rubber particles used in this study. ....	41
Figure 3.4: Gradation curve of crumb rubber modifier used in this study. ....	42
Figure 3.5: The wax-based warm mix additive used in this study.....	43
Figure 3.6: The chemical-based warm mix additive used in this study.....	45
Figure 3.7: Mixing procedures of base bitumen containing warm mix additive. ....	46
Figure 3.8: Laboratory equipment used to prepare crumb rubber modified bitumen.....	47
Figure 3.9: Mixing procedures of CRMB and CRMB containing WMA additive. ....	47
Figure 3.10: Rolling thin film oven test (RTFOT) equipment (left) and the bottles for holding the specimens (right).....	49
Figure 3.11: The modified static oven aging simulation .....	50
Figure 3.12: Rheological characteristics master curve of 70/100 samples conditioned at different short-term aging simulations (reference temperature = 30°C).....	51
Figure 3.13: Carbonyl index (left) and sulfoxide index (right) of the short-term aging simulations. .....	51
Figure 3.14: The ATS Pressure Ageing Vessel. ....	52
Figure 4.1: Configuration of DSR parallel plates. ....	55

Figure 4.2: Stress-strain response of a viscoelastic material. ....	55
Figure 4.3: Representation of complex shear modulus.....	56
Figure 4.4: Example of isochronal plot at different frequencies. ....	58
Figure 4.5: Example of isothermal plot at different temperature.....	58
Figure 4.6: The frequency sweep test results of the CRMB-15.....	59
Figure 4.7: Construction of master curve. ....	61
Figure 4.8: An example of the master curve of the unaged neat bitumen constructed by using the modified CAM model. ....	61
Figure 4.9: FTIR spectrometer working principle (Source: <a href="https://tools.thermofisher.com/content">https://tools.thermofisher.com/content</a> ) .....	63
Figure 4.10: Infrared spectrum of an asphalt binder (the colored areas are used for the calculation of specific ageing indices following (Lamontagne et al. 2001)). ....	64
Figure 4.11: Example of a peak area calculation of the band area $A_{1700}$ . ....	64
Figure 4.12: FTIR spectrometer of Perkin-Elmer. ....	66
Figure 4.13: Sample of FTIR-obtained spectrum of a bituminous binder. ....	66
Figure 4.14: Master curves of complex modulus for the unaged binders at a reference temperature of 30°C showing the effect of CRM concentration. ....	68
Figure 4.15: Master curves of phase angle for the unaged binders at a reference temperature of 30°C showing the effect of CRM concentration. ....	68
Figure 4.16: Complex modulus versus temperature at 10 rad/s showing the CRM concentration effect.....	69
Figure 4.17: Master curves of complex modulus for the unaged binders at a reference temperature of 30°C showing the effect of WMA additives on the base bitumen. ....	70
Figure 4.18: Master curves of phase angle for the unaged binders at a reference temperature of 30°C showing the effect of WMA additives on the base bitumen. ....	70
Figure 4.19: Master curves of complex modulus for the unaged binders at a reference temperature of 30°C showing the effect of WMA additives on the CRMB. ....	71
Figure 4.20: Master curves of phase angle for the unaged binders at a reference temperature of 30°C showing the effect of WMA additives on the CRMB. ....	71
Figure 4.21: Complex modulus versus temperature at 10 rad/s showing the WMA additives effect on the base binder. ....	72
Figure 4.22: Complex modulus versus temperature at 10 rad/s showing the WMA additives effect on the CRM binder.....	72
Figure 4.23: Master curves of complex modulus and phase angle for the 70/100 base binder at a reference temperature of 30°C showing the aging effect.....	73
Figure 4.24: Stiffness index of the asphalt binders at 10 rad/s and at temperature of 30°C.....	74
Figure 4.25: FITR-obtained spectrum of the 70/100 base binder at different aging conditions...	75
Figure 4.26: Carbonyl index (left) and sulfoxide index (right) showing the effect of CRM content. .....	75
Figure 4.27: Carbonyl index showing the effect of the WMA additives.....	76

Figure 4.28: Sulfoxide index showing the effect of the WMA additives. ....	76
Figure 4.29: Effect of CRM content on oxidation product. ....	77
Figure 4.30: Effect of the WMA additives on oxidation product. ....	77
Figure 5.1: A creep and recovery curve for a single cycle (Anderson 2014). ....	81
Figure 5.2: schematic representation of the MSCR test loading sequence showing only two stress levels for illustration (D’Angelo 2009). ....	81
Figure 5.3: Sample preparation and the setup for the MSCR test (25mm plates and 1mm gap). ....	83
Figure 5.4: Effect of CRM content on the creep compliance. ....	84
Figure 5.5: Effect of CRM content on the percent recovery. ....	84
Figure 5.6: Effect of CRM content on the stress sensitivity. ....	85
Figure 5.7: Effect of the WMA additives on the creep compliance of the base binder. ....	86
Figure 5.8: Effect of the WMA additives on the percent recovery of the base binder. ....	86
Figure 5.9: Effect of the WMA additives on the creep compliance of the CRMB. ....	87
Figure 5.10: Effect of the WMA additives on the percent recovery of the CRMB. ....	87
Figure 5.11: Effect of the WMA additives on the stress sensitivity. ....	88
Figure 5.12: Effect of CRM content and the WMA additive on the Jnr index. ....	91
Figure 6.1: Loading Scheme for Amplitude Sweep Test. ....	96
Figure 6.2: The LAS test setup (8mm plate with 2mm gap) ....	98
Figure 6.3: Shear stress and strain diagram from amplitude sweep test showing the effect of CRM content. ....	99
Figure 6.4: Shear stress and strain diagram from amplitude sweep test showing the effect of the WMA additives on the base bitumen. ....	99
Figure 6.5: Shear stress and strain diagram from amplitude sweep test showing the effect of the WMA additives on the CRMB. ....	99
Figure 6.6: Damage characteristic curve showing effect of CRM content. ....	100
Figure 6.7: Fatigue life prediction in function of strain level showing effect of CRM content. ....	101
Figure 6.8: Damage characteristic curve showing effect of WMA additives on the base binder. ....	102
Figure 6.9: Damage characteristic curve showing effect of WMA additives on the CRMB. ....	102
Figure 6.10: Fatigue life prediction in function of strain level showing effect of WMA additives on the base binder. ....	103
Figure 6.11: Fatigue life prediction in function of strain level showing effect of WMA additives on the CRMB. ....	104
Figure 6.12: Predicted fatigue lives at 2.5% strain showing effect of the WMA additives. ....	105
Figure 6.13: Damage characteristic curves showing effect of artificial long-term ageing on the base binder. ....	107
Figure 6.14: Fatigue life predictions in function of strain level showing effect of artificial long-term ageing on the base binder. ....	107

Figure 7.1: Correlation between BBR S(60s) and 4-mm DSR G(7200 s) (Sui. et al 2011). ....	112
Figure 7.2: Correlation between BBR mc(60s) and 4-mm DSR mr(7200 s) (Sui. et al 2011)...	112
Figure 7.3: Storage modulus master curve at a reference temperature.....	113
Figure 7.4: Relaxation modulus master curve at a reference temperature.....	113
Figure 7.5: Correlation between BBR S(60s) and 4-mm DSR G(60 s) Farrar et al. (2015).....	114
Figure 7.6: Correlation between BBR mc(60s) and 4-mm DSR mr(60 s) Farrar et al. (2015). .	115
Figure 7.7: Anton Paar spatula for sample trimming.....	115
Figure 7.8: Setup for the 4-mm DSR test (4-mm plates and 1.75-mm gap).....	116
Figure 7.9: Comparison between 4 mm and 8 mm plates (base bitumen).....	116
Figure 7.10: Repeatability of the 4-mm diameter.....	116
Figure 7.11: Relaxation modulus at 60 seconds and at -10°C showing the effect of CRM content. .....	117
Figure 7.12: Slope coefficient of the relaxation modulus at 60 seconds and at -10°C showing the effect of CRM content.....	118
Figure 7.13: the magnitude (left) and slope coefficient (right) of the relaxation modulus at 60 seconds and at -10°C showing the effect of WMA additives on the base binder. ....	119
Figure 7.14: the magnitude (left) and slope coefficient (right) of the relaxation modulus at 60 seconds and at -10°C showing the effect of WMA additives on the CRMB. ....	119
Figure 8.1: Arrangement of separation tubes in vertical orientation. ....	123
Figure 8.2: The scheme of the polymer modified bitumen high-temperature storage stability evaluation. ....	124
Figure 8.3: The effect of CRM concentration on high-temperature storage stability of CRMB in term of non-recoverable compliance (left) and in term of recovery (right). ....	125
Figure 8.4: The effect of WMA additives on high-temperature storage stability of CRMB in term of non-recoverable compliance (left) and in term of recovery (right). ....	126
Figure 8.5: Storage instability index showing effect of the CRM concentration. ....	127
Figure 8.6: Storage instability index showing effect of the WMA additives. ....	127

## List of tables

Table 2.1: Basic elemental composition of bitumen (Read&Whiteoak 2003). .....	22
Table 2.2: Summary of Performance grading tests (Chin 2018). .....	32
Table 2.3: Summary of the standard PG testing and criteria (ASPHALTINSTITUTE 2005). ....	33
Table 3.1: The chemical components of the base bitumen used in this study. ....	39
Table 3.2: Properties of base bitumen used in this study [NYNAS]. .....	40
Table 3.3: Physical and Chemical Properties of Crumb rubber modifier. ....	41
Table 3.4: Crumb rubber particle gradation. ....	41
Table 3.5: General information of the warm mix additives used in this study (AkzoNobel 2010, Sasolwax 2014) .....	42
Table 3.6: Physical characteristics of wax-based warm-mix additive (Sasolwax 2014). ....	44
Table 3.7: Information of prepared asphalt binders used in this study. ....	46
Table 3.8: MSCR results of the 70/100 samples at different short-term aging simulations. ....	51
Table 4.1: Summary of oscillatory testing parameters (adapted from Laukkanen 2015). ....	57
Table 4.2: Specific functional groups for bituminous binders regarding aging (Lamontagne et al. 2001, Van den Bergh 2011). .....	65
Table 4.3: Comparison between the rheological and chemical aging indices. ....	78
Table 5.1: Summary of MSCR test results of fresh and aged binders. ....	89
Table 5.2: Asphalt Institute Specification for Jnr at different traffic level (Asphalt institute 2010). .....	90
Table 5.3: Rutting properties of the short-term aged binders at 64°C .....	92
Table 6.1: Effect of CRM content on the fatigue law parameters. ....	101
Table 6.2: Effect of the WMA additives on the fatigue law parameters. ....	103
Table 6.3: Effect of aging on the fatigue law parameters. ....	106
Table 6.4: Fatigue properties of the long-term aged binders at 20 °C .....	108
Table 9.1: Summary of the study results. ....	131

# **Chapter1**

## **Introduction**

## 1.1 Introduction and Background

Ideally, pavements must be able to perform satisfactorily throughout their designed service lives. However, in recent decades, dramatic growth in traffic volume, increasing axle loading, and more severe climatic conditions have been causing road maintaining problems. More rapid deterioration and earlier failure of pavements require more frequent road maintenance which results in higher cost of operations and maintenance. The overall performance of pavement is therefore needed to be enhanced in order to minimize rutting (permanent deformation) at high temperatures, fatigue cracking at intermediate temperatures, and thermal cracking at low temperatures. Bitumen modification is one of the effective ways which have been applied to improve road damage resistance over the service-temperature range over years. It is because the service performance of the asphalt mixture highly depends on the character of the bituminous material (Yusoff et al. 2011). The most popular form of asphalt binder modification is polymer modifications which can effectively improve viscoelastic properties of the bitumen (Bahia et al. 2001).

Disposal of End-of-Life Tires (ELT) is one of the most challenging tasks discussed all over the world. ELT is non-biodegradable material which was traditionally managed by illegally dumping or stockpiling. However, none of the mentioned solutions is smart and sustainable because these solutions potentially lead to a threat to human and environment. For instance, tire stockpile supplies a suitable breeding ground for mosquitoes, snakes, and other dangerous animals. Moreover, dumped scrap tires are perfectly combustible material that can pose an accidental fire risk which may release toxic fumes (Siddique 2004). According to the European Tyre and Rubber Manufacturers' Association (ETRMA) report, the number of used tires in Europe was about 3.59 million tons in 2013 (ETRMA 2015).

To tackle the mentioned issues, using a recycled polymer such as crumb rubber is a good alternative and cost-effective compared with using other types of polymer modifiers. It is because scrap tires which were normally considered as unwanted residuals can be transformed into a binder modifier that not only reduces the environmental problems but also enhances the damage resistance of the binder. Farina et al. (2017) carried out the life cycle assessment (LCA) of various road paving technologies namely using crumb rubber in bituminous mixtures and the reclaimed asphalt pavement. The environmental impact investigation results showed that using crumb rubber modified binder in wearing courses can lead to significant benefits in terms of energy-saving, environmental impact, human health, preservation of ecosystems, and minimization of resource depletion. The crumb rubber modified binder technology causes reductions of both gross energy requirement and global warming potential about 36% to 45% compared with standard paving solutions.

The crumb rubber modified binder (CRMB) or rubberized binder is a way of binder modification which was originally developed by Charles McDonald in 1964 so-called "wet method" by utilizing crumb rubber particles to modify asphalt binder properties. In the wet method, up to one-fifth of a total weight of asphalt binder can be substituted by crumb rubber modifier (CRM) (Brown 1993). Many studies have shown that one of the most successful



applications of crumb rubber derived from grinding of recycled scrap tires is to use it as a binder modifier. Addition of CRM into the neat asphalt binder has been proven that it is capable of increasing the resistance to rutting, fatigue cracking, and thermal cracking (Lo Presti 2013, Papagiannakis& Loughheed 1995, Shu& Huang 2014).

The improvement of the asphalt binder service performance is governed by the interaction between crumb rubber particles and bitumen called “swelling process” as shown in Figure1.1 (Abdelrahman& Carpenter 1993, Bahia& Davies 1994). It is reported that bitumen-rubber interaction depends on various factors such as bitumen (e.g., source of bitumen, constitutions of bitumen), rubber (e.g., source, types, particle size, production of CRM, constitutions of CRM), additives (e.g., warm-mix additives, chemical additives, organic additives), and interaction conditions (e.g., mixing time, and temperature) (Abdelrahman& Carpenter 1993). In the process, the rubber particles absorb the aromatic and light fraction components of the bitumen forming a gel-like particle which results in a higher proportion of big molecular component (asphaltenes) in the binder, an increase of rubber particle volume, and a decrease in inter-particle distance of swollen rubber. The viscosity of CRMB is thus significantly increased (Airey et al.2002, Heitzman 1992).

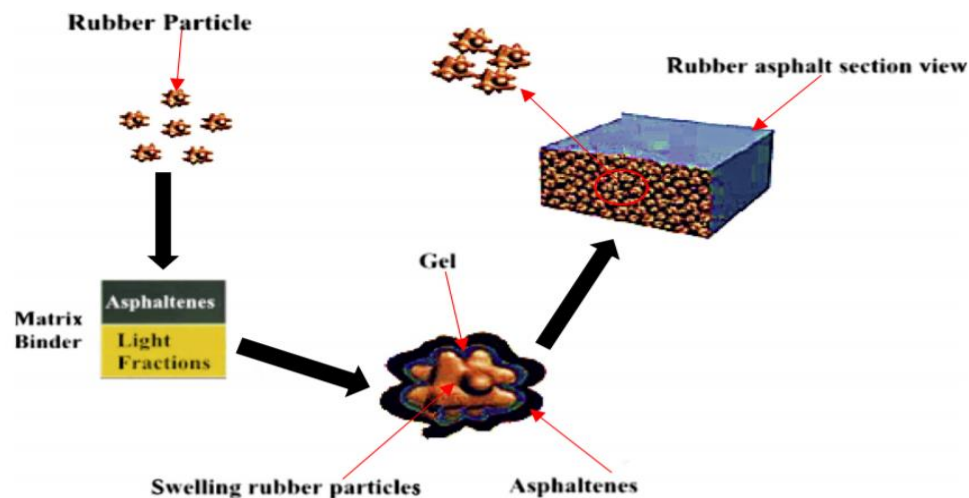


**Figure 1. 1:** Description of swelling of rubber particles and asphalt binder (Heitzman 1992).

However, despite obvious benefits of CRM binder, an infamous drawback of CRMB is the tremendous increase of rubberized asphalt viscosity resulting in lower workability, higher energy consumption (during manufacturing operations), and higher health hazard from asphalt fume exposures (NIOSH 2001). Farina et al. (2017) suggested that the environmental performance of rubberized asphalt (RA) can be further improved by coupling the RA with warm-mix asphalt (WMA) technology. It is because WMA technology requires about 35% less fuel and energy needed during plant mixing (D'Angelo et al. 2008). Furthermore, applying WMA additives in hot mix asphalt (HMA) can lower toxic fumes and greenhouse gas emissions during production and construction which promotes better working conditions. Moreover, the workability and compaction efficiency are enhanced as the WMA additives can remarkably reduce the binder viscosity (Rubio et al. 2012). Therefore, it is believed that the combination of RA and WMA

technologies can contribute more durable and higher environmental performance pavements (Wang et al. 2018).

Although the combination of WMA technologies and the CRMB may sound promising, the effect of the WMA additives on the properties and performance of the CRMB are still questionable. Thus, it is important to investigate the effect of the WMA additive on the properties and performance of the unmodified bitumen and CRMB.

Bitumen has been used as a binding material in asphalt pavements for decades. The viscoelastic properties and behaviors of the flexible pavements are highly dependent on the viscoelastic properties of the asphalt binders (Bahia et al. 2001, Lo Presti 2013). It is because the asphalt binder is the only component in the asphalt mixture that displays temperature- and rate of loading-dependent behavior (Benedetto et al 2011). As a result, asphalt binder surely plays an important role in road service performances over the road service temperatures. Therefore, characterization of the asphalt binder performance definitely provides a better understanding of the overall performance of the pavement.

The response of asphalt binder to traffic loading is a function of three main factors namely age, temperature, and rate of loading. The performance-related asphalt binder specifications were developed to determine whether the binders can provide an acceptable performance against the predominant modes of failure over the whole service temperatures such as rutting (permanent deformation) at high-temperatures, fatigue cracking at intermediate-temperatures, and thermal cracking at low-temperatures. Currently, the Performance Grade (PG) asphalt binder specifications are widely used as the current performance-based specification to characterize mechanical properties of asphalt binders over a range of the pavement service temperature. The Strategic Highway Research Program (SHRP) suggested that dynamic shear modulus ( $G^*$ ) and phase angle ( $\delta$ ) are two main rheological properties (of the virgin and aged binders) used to characterize high and intermediate temperature performances. The value of  $G^*/\sin \delta$  and  $G^*\sin \delta$  measured at a particular temperature and a frequency of 10 rad/sec are the rutting and fatigue cracking resistances of the binder respectively.

The current performance-related specifications were primarily developed and designed for conventional asphalt binders, and these parameters are evaluated and obtained within the linear viscoelastic region (LVE). Research indicated that, in the case of unmodified binders, these parameters did satisfactorily correlate to the service performance over a service temperature range (Bahia et al. 2001). But, in the case of binders containing additives and/or polymer modifiers, the rutting and fatigue cracking parameters did not correlate well with the field mixture performances (D'Angelo 2009, Hintz et al. 2011). Since the response of the polymer modified binder is non-linear, as the polymer chain can be rearranged as the applied stress level goes up (D'Angelo et al. 2007). As a result, many newly developed test methods were proposed for evaluating the binder performance beyond the LVE with respect to rutting and fatigue cracking. This led to the introduction of two new successful test methods which can truly capture the actual performance of both unmodified and polymer-modified binders at high- and intermediate- temperatures respectively namely multiple stress creep and recovery (MSCR) and linear amplitude sweep (LAS)

(Hintz&Bahia 2013, Radhakrishnan et al. 2018, Saboo et al. 2016, Wang et al. 2014). MSCR has been introduced to evaluate the high-temperature rutting resistance of asphalt binders, while LAS was recommended to characterize the intermediate-temperature fatigue cracking resistance of all kind of asphalt binders.

In the case of low service temperature performance evaluation of asphalt binders, the bending beam rheometer test is a typical method determining the low-temperature stiffness( $S[t]$ ) and stress relaxation ability (m-value) of the binders. Recently, Sui et al. (2011) proposed a new low-temperature performance-grading method using 4-mm parallel plates on a dynamic shear rheometer as an alternative method characterizing the low-temperature performance of asphalt binders. This newly developed test can considerably reduce a large amount of bituminous material used in BBR specimen fabrication from approximately 15 g per beam to only 25 mg per binder sample.

In this study, performance characterizations of both unmodified and crumb rubber modified asphalt binders over the whole service temperature range can be carried out by performing the three new generation aforementioned tests (MSCR, LAS, and 4-mm DSR) on only one DSR device. It is believed that the new generation DSR tests will contribute to improving the ability to more accurately characterize the performance of the bituminous materials.

## 1.2 Study goals

The main goal of this study is to get more understanding about the effects of CRM content, and WMA additives on the high-temperature storage stability, and the performance of the asphalt binders over the whole service temperatures by using the storage stability test, and new generation DSR tests respectively. To achieve the study goals, sub-objectives have been defined as follow.

- To experimentally investigate the effect of crumb rubber particle concentration and warm-mix additives on the high-temperature rutting resistance, intermediate-temperature fatigue cracking resistance, and low-temperature thermal cracking resistance of the prepared asphalt binders by using MSCR, LAS, and 4-mm DSR tests respectively.
- To study the effect of crumb rubber particle concentration and warm mix additives on the high-temperature storage stability of prepared CRMBs.
- To validate the new generation DSR tests.

## 1.3 Organization of the thesis

This study consists of 9 chapters which are organized in such a way as presented in Figure 1.2. In an introductory chapter, the background problem, and the goals of the study are defined. In section 2, the literature review presents a basic knowledge about the crumb rubber modified asphalt binder, warm-mix asphalt (WMA) technologies, and performance-based asphalt binder characterization. The physical and chemical properties of materials used in this study and the sample preparation program are described in Chapter 3. In Chapter 4, rheological properties of the study asphalt

binders at different aging conditions were evaluated. The effects of CRM concentration and WMA additive on high-temperature rutting resistance, intermediate-temperature fatigue cracking resistance, low-temperature thermal cracking resistance, and high-temperature storage stability of CRMB are presented in Chapter 5, Chapter 6, Chapter 7, and Chapter 8 respectively. The results and analysis are finally summarized in Chapter 9.

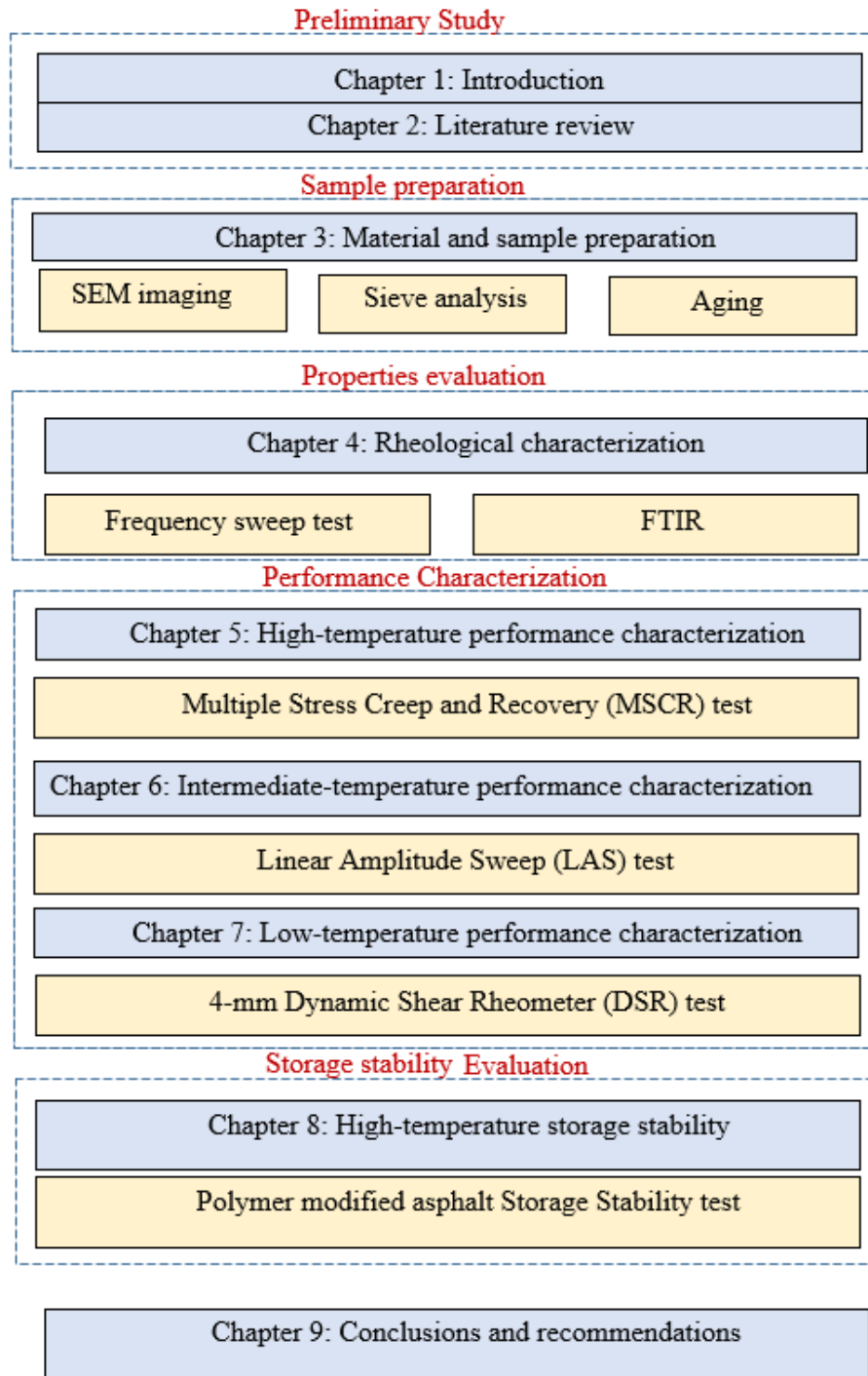


**Figure 1. 2:** Scope and Organization of the study.

# **Chapter 2**

## **Literature review**

## 2.1 Introduction

This literature review covers four different essential topics for this study, namely bitumen, warm-mix asphalt technologies, crumb rubber modified bitumen, and performance evaluations of bituminous asphalt binders. The first section begins with the constitutions of bitumen. It is due to changes in bitumen constitution will result in changes of the final asphalt binder performances. In the second and third parts of the review, the two asphalt technologies, namely the warm-mix asphalt and rubberized asphalt technologies are described. Lastly, the binder performance characterization methods over the whole service temperature in accordance with the current SUPERPAVE specifications are discussed. Thus, to understand changes in the asphalt binder response, it is important to understand how the constitutions of a base bitumen, modified binders, and crumb rubber modified binder influence their final performances over the overall range of road service temperatures.

## 2.2 Bitumen

Generally, bitumen is defined as extremely complex chemical mixtures of molecules which predominantly hydrocarbons derived from petroleum naturally or by distillation. The bitumen that has been currently used in the pavement industries is manufactured from crude oil, and its compositions are highly dependent on the locations of crude oil and the refinery process. As crude oils are produced through various matters accumulated under the earth, therefore it is very difficult to clearly define and determine its composition. However, elementary analysis results of bitumen manufactured from various sources and types of crude oils show that most bitumen commonly contains basic element as described in Table 2.1 (Read&Whiteoak 2003):

**Table 2. 1:** Basic elemental composition of bitumen (Read&Whiteoak 2003).

Element	% by weight
Carbon	82-88
Hydrogen	8-11
Sulfur	0-6
Oxygen	0-1.5
Nitrogen	0-1

As mentioned earlier, the composition and structure of bitumen are complex and varied according to the original of the crude source. Although, the complexity of the bitumen makes it difficult to clearly identify the bitumen composition, its chemical compositions can be categorized into four main groups, namely asphaltenes saturates, aromatics, and resins by means of chromatographic techniques such as SARA (saturates, aromatics, resins, and asphaltenes) analysis as described below.

**Asphaltenes** are insoluble black or brown shapeless solids. They are considered highly polar and complex aromatic materials of high molecular weight, in which their molecular weight ranges from 1,000-100,000 depending on the employed techniques of determining molecular weights. Almost one-fourth of the bitumen is constituted by Asphaltenes. Figure 2.1 shows a typical chemical structure of an asphaltene. Moreover, it was reported that the asphaltenes content has a remarkable effect on the rheological characteristics of a bitumen. It was found that the larger asphaltenes content directly produce harder, more viscous bitumen with a lower penetration, higher softening point and, consequently, higher viscosity. In other words, the stiffness and rigidity of the bitumen increase proportionally to the asphaltenes content (Read&Whiteoak 2003).

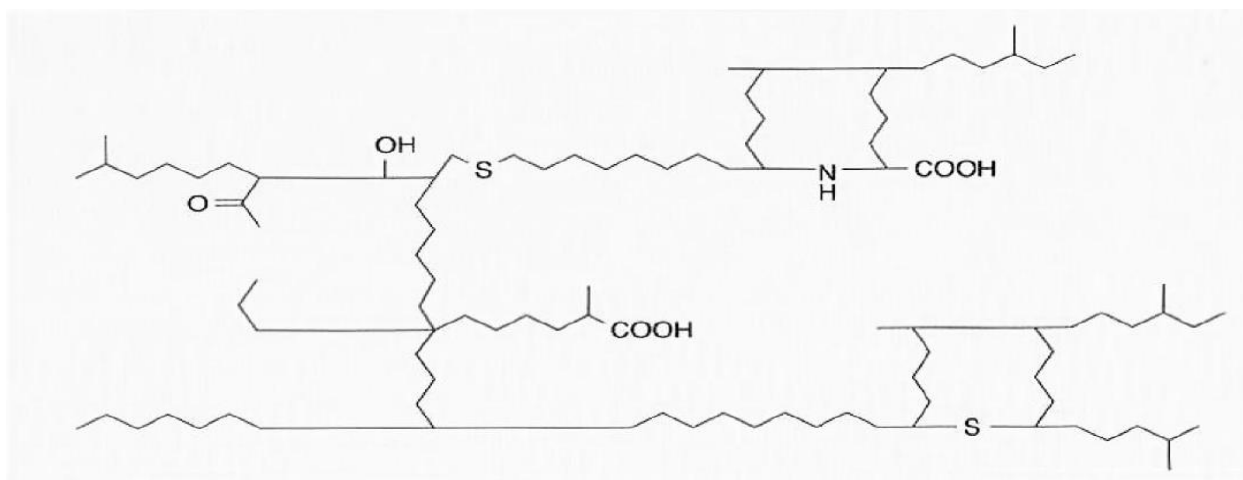


**Figure 2. 1:** Asphaltene chemical structure (Read&Whiteoak 2003).

**Resins** are dark brown solid or semi-solid which are considered as polar molecules. The molecular weight of Resins ranges from 500 to 50,000. In the bitumen, Resins act as dispersing agents or peptisers for the asphaltenes. The proportion of resins to asphaltenes governs characters of the bitumen, namely the solution (SOL) structure, and the gelatinous (GEL) type. The high proportion of Resins results in SOL nature of bitumen, while the GEL nature of bitumen is formed in case of the small proportion of Resins as shown in Figure 2.2 (Read&Whiteoak 2003).

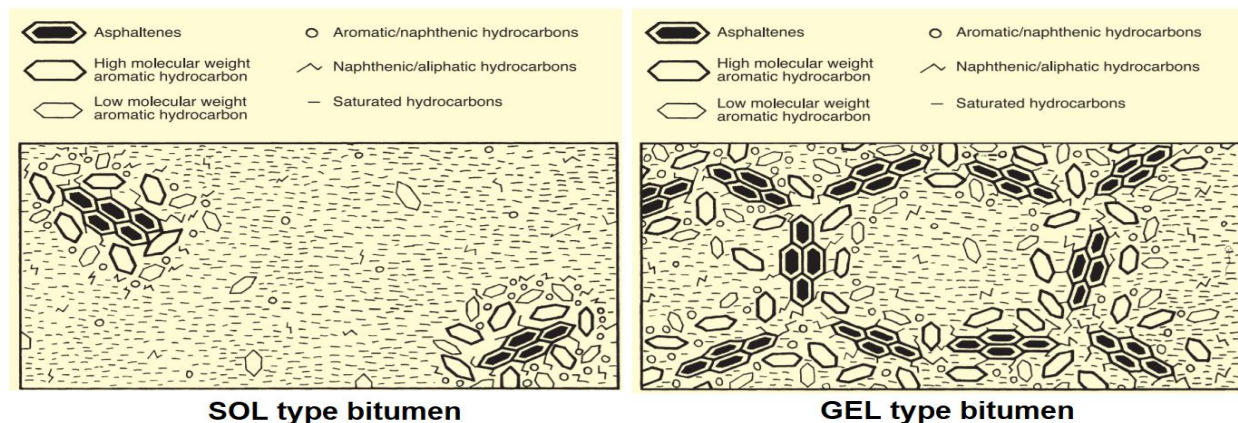


**Figure 2. 2:** Schematic representation of SOL and GEL types of bitumen (Read&Whiteoak 2003).

*Aromatics* are dark brown viscous liquids constituting 40-65% of the total bitumen. The average molecular weight of aromatics varies from only 300-2,000 which is the lowest molecular weight naphthenic aromatic compounds in the bitumen. Their non-polar nature makes them capable of dissolving other higher molecular weight hydrocarbons. The typical structures of aromatics are shown in Figure 2.3 (Read&Whiteoak 2003).

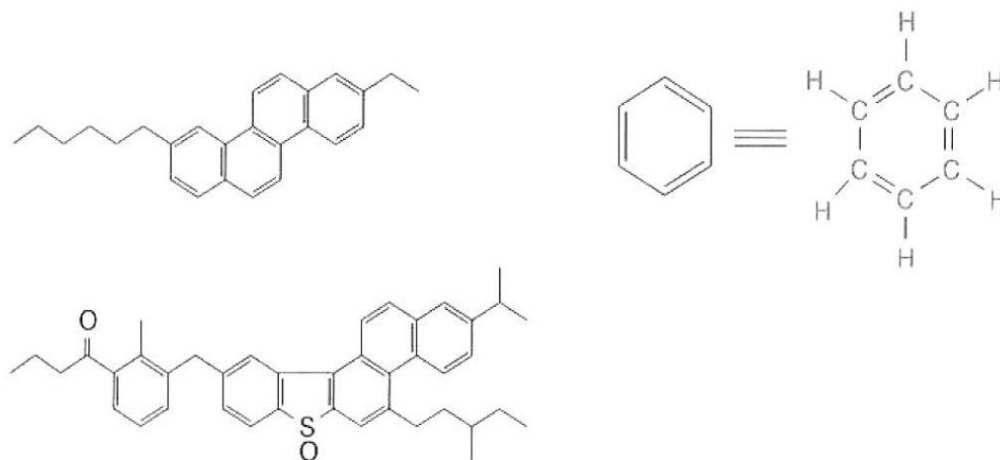


**Figure 2. 3:** Aromatic chemical structures (Read&Whiteoak 2003).

*Saturates* are straw or white viscous oils which are considered as non-polar components in bitumen. The average molecular weight range of saturates is similar to that of aromatics (300-2,000). The components of saturates consist of both waxy and non-waxy saturates, and they constitute 5 to 20% of the total bitumen. Figure 2.4 presents two typical structures of saturate (Read&Whiteoak 2003).

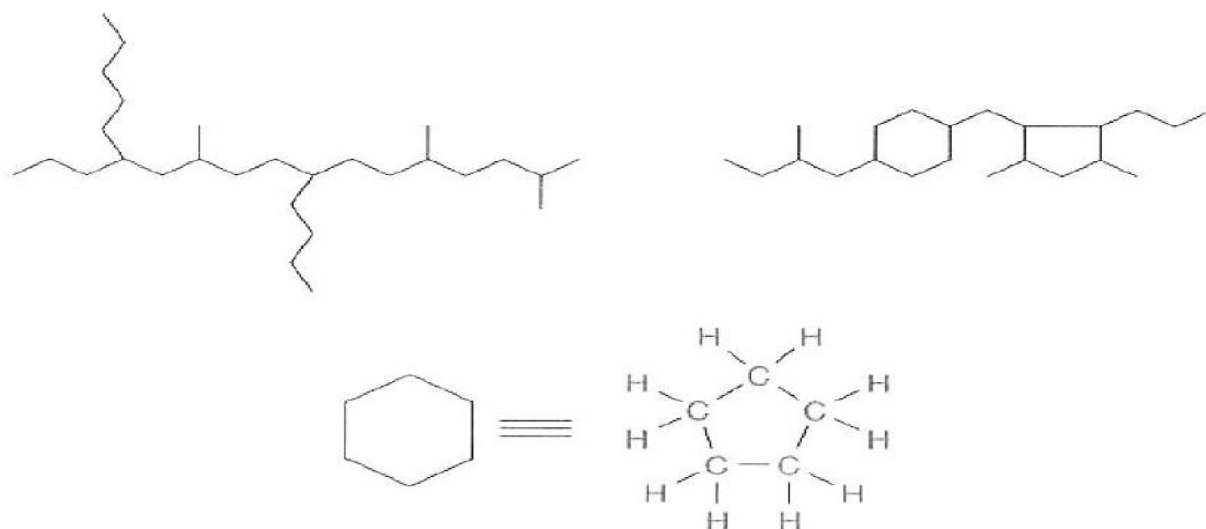


**Figure 2. 4:** Saturates chemical structures (Read&Whiteoak 2003).



## 2.3 Warm mix asphalt (WMA) technologies

Warm mix asphalt (WMA) technologies are relatively new techniques intentionally used to lower the temperature of asphalt mixtures, where the mixture components are manufactured, placed and compacted on the roadways at a temperature 20 - 40°C lower than the conventional HMA (150°C - 190°C) (Rubio et al. 2012). WMA is considered as an environmentally friendly technology as it lowers in fuel consumption results in lower toxic fumes and greenhouse gas emissions during production and construction (Shu et al.2012). This technology requires about 35% less fuel and energy needed during plant mixing which surely can decrease the costs of asphalt production (D'Angelo et al. 2008). Addition of WMA additives also provides paving benefits such as better working condition, higher workability, and compaction efficiency. Moreover, WMA technologies allow asphalt mixtures to be hauled longer distances while still have workability to place and compact, and quicker turnover to traffic due to shorter cooling time. (EAPA 2014, Rubio et al. 2012, Zaumanis 2010)

The key of WMA technologies is to reduce the viscosity binder so that asphalt aggregates can be coated at lower temperatures, or to improve workability. According to the WMA technologies, there are three main techniques to produce asphalt mixture at relatively low mixing temperatures namely foaming processes, addition of organic or wax additives, and addition of chemical additives.

### 2.3.1 Foaming processes

Foaming technologies are intentionally used to expand the contact surface of the binder in the form of foam by adding a small amount of cold water into hot asphalt binder, or in the asphalt mixing chamber. The added water turns to steam when mixing with the hot binder, and the stem is then encapsulated by viscous asphalt binder enabling a temporary increase of binder volume (the formation of voids within the binder). The expansion of the foaming bitumen reduces the viscosity of the mixture, and allows the coating of the aggregates at lower temperatures. There are two commonly used techniques for foaming namely water-containing technologies and water-based technologies (Capitão 2012, EAPA 2014, Rubio et al. 2012).

Water-containing technologies are indirect foaming techniques where a mineral, synthetic zeolite, is used as the source of foaming water. The hydro-thermally crystallized synthetic zeolite contains about 20% of crystalline water, which can be released from the zeolite structure when the temperature is increased above 100°C. The released water causes a controlled foaming effect, which lasts for 6-7 hours, or until the temperature drops below 100°C. It is reported that foaming effect provides better workability of the mixture where mixing temperatures can be reduced around 30°C with the same compaction efficiency as the HMA.

On the other hand, technologies are direct ways of foaming where a specifically controlled amount of water is directly injected into hot bitumen with foaming nozzles. The evaporated water is entrapped in the hot binder, resulting in a temporary increase in the effective volume of the

binder. The large increase in binder volume allows aggregate coating at lower temperatures. This water-based technique promotes a 20-40°C temperature reduction of the asphalt mix.

### **2.3.2 Addition of organic or wax-based additives**

The second method to reduce the viscosity of the asphalt binder is using organic warm mix additives by either mixing an organic wax to bitumen or adding it directly to the mixture. Studies indicated the binder viscosity is decreased as the mixing temperature rises above the melting point of the additives, where the mixing temperature can be effectively reduced around 20–30°C (D'Angelo et al. 2008, Prowell et al. 2011) As the asphalt mixture cools, the added additives crystallize, forming a lattice structure of microscopic particles (Capitão 2012, EAPA 2014). After crystallization, waxes tend to increase the stiffness and plastic deformation (rutting) resistance of the modified asphalt binder due to higher viscosity at intermediate temperatures. However, at low service temperatures where asphalt binder is in the solid phase the low-temperature cracking resistance of the binder is insignificantly affected by the wax-based additives. The melting point of organic additive or wax is one of the critical aspects that must be taken into account. The wax-based additive must have the melting point higher than the expected road service temperatures to prevent permanent deformation (Shang et al. 2011).

It is worth noting that the effect of wax-based additives depends on various factors namely the chemical composition and the rheological characteristics of the asphalt binder, the composition crystallinity of the wax, the application temperature range, and the amount of wax (Edwards&Isacsson 2005).

### **2.3.3 Addition of chemical-based additives**

Chemical based additives are the third method of WMA technologies that are commonly used among the road authorities. It is because the chemical-based technologies require fewer modifications of the asphalt plant and/or mix design process. The aim of these additives is not to directly reduce the binder viscosity but to chemically control the adhesion between aggregates and the binder. At the mixing process, the friction at an interface of the binder and aggregates is chemically reduced in order to enable the asphalt binder coating of aggregate at relatively low temperatures. At the paving field, the additives act as a lubricant promoting better and cooler working conditions. This type of WMA technology is reported that it is capable to decrease about 20 - 40°C of the mix and compaction temperatures (Chowdhury&Button 2009). There are several ways to produce a WMA with this type of chemical-based technology. For example, the chemical additives can be either directly added to the binder or mixed with water and injected into the stream before the mixing chamber (Austroads 2012).

## 2.4 Crumb rubber modified binder (CRMB)

### 2.4.1 History of crumb rubber modified asphalt binder (wet process)

The wet production technique was initially developed by Charles H. McDonald, an engineer working in Phoenix in Arizona (USA), in 1967. The wet process refers to a binder modification process where crumb rubber particles (up to 20% by total binder weight) are incorporated with virgin bitumen by blending them all together for 45-60 minutes at high temperatures (approximately 160°C) to produce a viscous fluid through rubber-bitumen interactions before mixing with the aggregate. In the interaction mechanisms, viscosity and some engineering characteristics of the binder were increased (Abdelrahman&Carpenter 1999, Heitzman 1992). In 1975, the crumb rubber modified binder was primarily used in hot mix asphalt (HMA) in Arizona (Brown 1993).

However, in the early 90s in the States, McDonald wet process was not popularly used due to the various shortcomings of incorporating CRM in the mixtures. It was because the rubberized asphalts were more expensive than the traditional pavements. Furthermore, the rubberized HMA had lower workability than conventional, because of its relatively smaller working-temperature window. Later on, in 1991, Road authorities all around the States were mandated to use the wet process technology by the United States federal law named "Intermodal Surface Transportation Efficiency Act" (recently rescinded). Consequently, the intention to improve the rubberized asphalt-related technologies has been brought back. Since then, the performances of crumb rubber modified binder produced by the wet process have been extensively researched, as the rubberized asphalt mixtures become widely used over the world. (Kuennen 2004, Lo Presti 2013).

### 2.4.2 Crumb rubber modifier production

Crumb rubber modifier (CRM) (also known as ground tire rubber [GTR]) is a product of a grinding process where waste tires are grounded or processed into small pieces. There are two main crumb rubber fracturing methods namely ambient grinding and cryogenic processing (Subhy 2017). Figure 2.5 shows the Scanning Electron Microscope (SEM) images of rubber particles processed by two mentioned methods.

In the ambient grinding process, the fracturing processes are done at or above room temperature where the scrap tires are cut to small pieces then shredded and ground into relatively small-size crumb rubber. This ambient grinding method normally results in irregular-shaped rubber particles with porous and rough surfaces with the size ranging from 0.5 to 5 mm. One of the most popularly used end-of-life-tires processing methods is an ambient grinding method, because of its economic benefits (Lo Presti 2013).

In the cryogenic fracturing, the cut pieces of scrap tires are frozen with liquid nitrogen (typically between -87 to -198 °C). At a temperature below -80 °C, rubber becomes glass-like material where the cooled rubber is very brittle. After that, the frozen rubber is shattered into the

small-size rubber particles by a hammer mill. Cryogenic grinding products usually have an angular shape with a relatively smooth and lower surface area (Memon 2011).

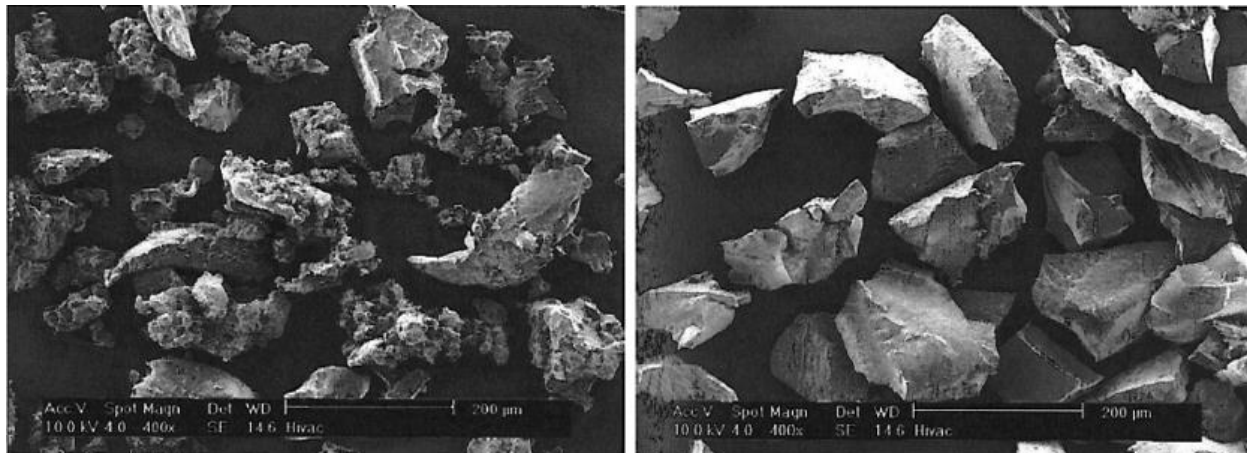


**Figure 2. 5:** Scanning Electron Microscope (SEM) images at 200 microns and 400x magnification of rubber particles processed by ambient grinding (left) and cryogenic fracturing (right) (Memon 2011).

### 2.4.3 Interaction mechanism of crumb rubber particle and bituminous binder

In the wet process, the main purpose of adding crumb rubber modifier in a bituminous binder is to improve the mechanical properties of the conventional binder namely viscosity and elasticity of the unmodified binder. Basically, there are two main simultaneous interaction mechanisms; rubber particle swelling and degradation process of rubber particles (devulcanization /depolymerization) (Abdelrahman&Carpenter 1999, Abdelrahman 2006).

In the particle swelling process, the rubber particles are swollen by absorbing the aromatic oils and light fractions from the binder into the polymer chains of the rubber particles to form a gel-like material ( Figure2.6 b-II) under a high interaction temperature condition (160 °C - 200 °C). This absorption process causes a great increase in the volume of the swollen crumb rubber particles which significantly decreases the inter-particle distances (Figure2.6 c-II). Furthermore, the combination of inter-particle distance reduction and fewer aromatics in the binder results in an enormous increase in viscosity of the binder (Heitzman 1992).

Devulcanization is the process where the sulphur–sulphur (S-S) bonds or carbon–sulphur bonds (S-C) formed by the vulcanization process during tire production are broken. While, depolymerization is the process of decomposing a polymer into monomers. These mentioned reactions can destroy the chemical bonds of the crumb rubber particles and also cause a reduction in the rubber molecular weight. The reduction of stiffness and elasticity of the modified binder is corresponding to the rubber degradation process (devulcanization and/or depolymerization). If the interaction process keeps on continuing after the swelling has reached the maximum swelling equilibrium (Figure 2.6 a-II), the swollen rubber particles will start depolymerizing (Figure 2.6 b-II). After that, under the extremely high mixing temperatures and/or unnecessary long mixing

time, the rubber particles may be fully depolymerized and dispersed into the liquid phase of the binder (Figure 2.6 c-II&III) (Abdelrahman 2006).

The mechanical response and behavior of the CRM binders are directly governed by this interaction. It is reported that the bitumen-rubber interaction is significantly influenced by both material parameters (bitumen, CRM, and additives) and conditions of interaction (mixing conditions). The optimum mixing conditions of particular CRMBs greatly depends on these factors. Therefore, the final performance of any CRMB surely based on the constitutions and mixing conditions (mixing time and mixing temperature).

In this study, all of the materials used are exactly identical to H.Wang's study (2018). According to the H.wang's research, binder samples produced through various mixing times and temperatures were investigated, and the test results indicated that the optimum bitumen-rubber interaction condition was 180°C of mixing temperature for a 30-minute duration. Therefore, in this study, the optimum mixing condition determined in H.wang's research was employed.

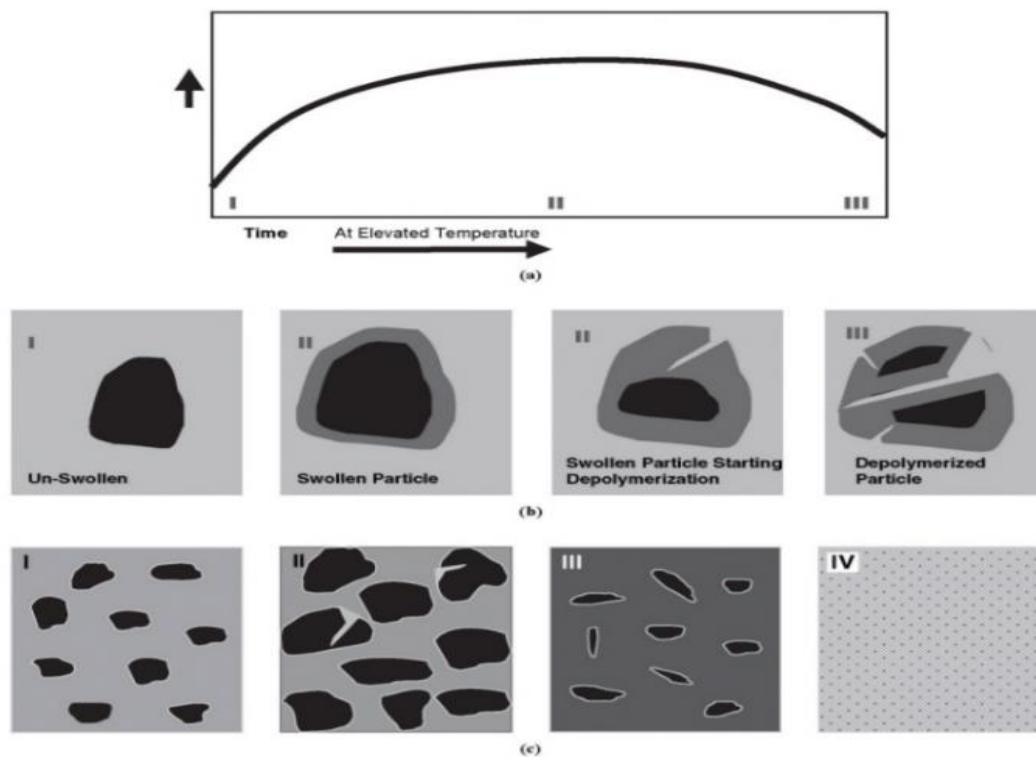


**Figure 2. 6:** Progression of bitumen–rubber interaction at elevated temperature: (a) change in binder viscosity over time, (b) change in particle size over time, and (c) change in binder matrix over time (Abdelrahman 2006).

#### 2.4.4 Storage stability of crumb rubber modified binders

The high-temperature storage stability of the modified bitumen is one of the important criteria of road construction (Navarro et al. 2004). It is because the phase separation normally occurs when the modified bitumen is stored at elevated temperatures. The severity and mechanism of the phase

separation are highly contingent on the type of asphalt binder modifier and the interaction mechanism of the modifiers and bituminous binders (Bahia et al. 1998).

In case of crumb rubber modified binder, its high-temperature storage stability is reported to be one of the main drawbacks because of the incompatibility between swollen CRM particles and the binder (Ghavibazoo et al. 2013, Navarro et al. 2004, Zanzotto et al. 1996). It is because there is a difference in density between CRM particles ( $1.15 \pm 0.05 \text{ g/cm}^3$ ) and the bituminous binder ( $1.02 \text{ g/cm}^3$ ) (Heitzman 1992) which causes the settling down of the CRM particles to the bottom of the hot storage tank due to the gravitational force. As a result of the phase separation, the higher viscosity of the CRMB at the bottom part was reported, conversely, the viscosity of CRMB at the upper part was found reduced (Navarro et al. 2004, Zanzotto et al. 1996) and this affects the mechanical properties of the CRMB. The phase separation significantly causes a variation in mechanical properties of the modified binders between the top and bottom tank due to the non-uniformly distributed of the modifiers which may lead to differences in the mixture performance. In order to prevent variation in mechanical properties between top and bottom of the hot storage tanks, the agitating system is normally installed in the storage tanks to ensure the acceptable level of homogeneity of the modified asphalt binders (Ghavibazoo et al. 2013).

#### **2.4.5 Warm-mix rubberized asphalt binder**

Crumb rubber modified binder or Rubberized binder has been extensively used for decades as it improves the road service performances over the whole range of service temperatures. It is reported that binders modified with crumb rubber exhibit improved resistance to plastic deformation (rutting), fatigue cracking, and low-temperature thermal cracking (Lo Presti 2013, Shen&Amirkhanian 2007). In addition, road safety and comfort are satisfactorily enhanced (Rymer&Donavan 2005). However, the addition of CRM into the base binder causes an enormous increase in viscosity of the crumb rubber modified binders (Abdelrahman 2006). The higher manufacturing and compacting temperatures are thus required in order to provide desirable workability of the mixtures. Consequently, an elevation of mixing and compaction temperatures do not result only in higher fuel consumption but also more difficult and harmful working conditions as the asphalt fumes emission is much higher than the conventional paving technology (Lo Presti 2013).

WMA technologies are widely accepted in the pavement industry as techniques of reducing energy requirements and lowering emissions. WMA can significantly reduce the mixing and compacting temperatures of asphalt mixtures, by either lowering the viscosity of asphalt binders or increasing the workability of the mixtures. Thus, coupling WMA technologies with CRM binder was proposed in order to improve environmental performance, and promote better and safer working conditions. However, the mechanical and engineering properties of CRMB containing WMA additives are still unclear. It is because the addition of WMA additive to CRMB complicates the bitumen-rubber interaction, which may result in a more complex response of CRMBs. The overall performance of the warm CRM binders is thus needed to be characterized.

## 2.5 Performance-based asphalt binder characterization

Bitumen is a viscoelastic material that has been used as an asphalt binder for years. The performance of the asphalt pavements highly depends on the binder properties. It is because an asphalt binder is the only constitute exhibiting both temperature- and time-dependent behaviors. Theoretically, asphalt binder commonly shows Newtonian flow, viscoelastic, and glass-like solid behaviors at high, intermediate, and low service temperatures, respectively (Read&Whiteoak 2003). Under the practical conditions, it is essential to evaluate the binder contribution to the road damage resistance over the whole service temperatures.

Traditionally, empirical binder grading systems (penetration and viscosity based grading system) were used to identify the binder resistant properties. However, due to the empirical nature and various drawbacks of the conventional binder tests, Superior Performing Asphalt Pavements or SUPERPAVE was developed by the Strategic Highway Research Program (SHRP) to overcome the shortcomings of the empirical binder grading systems. According to the SUPERPAVE binder classification system, binders are graded according to their performance in both high and low service temperatures that likely to be experienced by the asphalt binders. The classification system is therefore called the Performance Grade (PG) system.

In the PG system, a set of four physical tests and two age conditioning simulations (refer to Table 2.2 for further detail) is used to measure asphalt binder physical properties at the entire range of pavement service temperatures that can be directly related to the field performance. The two age conditioning methods, the Rolling Thin Film Oven (RTFO) and the Pressure Aging Vessel (PAV), are applied to simulate two critical stages of pavement performance namely after construction stage and long-term service stage of the pavements. Table 2.3 shows the summary of the standard PG testing and criteria which specifically developed to address the binder performance parameters namely rutting ( $G^*/\sin \delta$ ), fatigue cracking ( $G^*\sin \delta$ ), and thermal cracking (creep stiffness and m-value). The binder is graded and reported as PG H-L, where H indicates the average seven-day maximum pavement temperature ( $^{\circ}\text{C}$ ) and -L is the minimum pavement design temperature ( $^{\circ}\text{C}$ ). For example, a PG 64-22 is suitable for the pavement performing from a high pavement temperature of  $64^{\circ}\text{C}$  to a low pavement temperature of  $-22^{\circ}\text{C}$ . For the high temperature performance, the limiting high-temperatures starting from  $46^{\circ}\text{C}$  with  $6^{\circ}\text{C}$  incremental interval up to  $82^{\circ}\text{C}$ . While, the limiting low-temperature is commonly defined from  $-10^{\circ}\text{C}$  down to  $-46^{\circ}\text{C}$  with  $6^{\circ}\text{C}$  step decrements (AASHTO M320).

Rutting, fatigue cracking, and thermal cracking are the predominant modes of failure of the asphalt mixtures at high, intermediate, and low temperatures, respectively. Performance-based asphalt binder characterization are thus needed in order to accurately determine that the asphalt binders can perform at an acceptable level of the road service performance. In the PG system, the binders are classified to meet the criteria corresponding to the expected high and low service temperatures, aging conditions, and traffic loading conditions. Therefore, the PG system uses the set of aforementioned tests (refer to Table 2.2) to characterize physical properties of the binder which can be directly related to field performance of the pavement at its service temperatures.

Table 2. 2: Summary of Performance grading tests (Chin 2018).

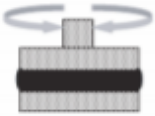
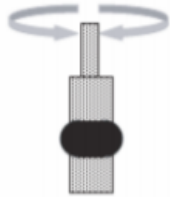


<b>Performance Criteria</b>	Rutting	Fatigue cracking	Low-temperature cracking (Thermal cracking)	
<b>Service Temperature</b>	Average 7-day maximum pavement temperature	Intermediate pavement temperature	Minimum pavement surface temperature	
<b>Critical stage of a binder's life</b>	After construction	Long-term service	Long-term service	
<b>Aging condition</b>	No aging and short-term ageing (RTFO)	Short-term aging (RTFO) plus long-term aging (PAV)		
<b>Test</b>	Dynamic Shear Rheometer (DSR) with 25-mm parallel testing plate 	Dynamic Shear Rheometer (DSR) with 8-mm parallel testing plate 	Bending Beam Rheometer (BBR) 	Direct Tension Test (DTT) 
<b>Point of the test</b>	Measure binder stiffness and viscoelastic properties at high -temperature	Measure binder stiffness and viscoelastic properties at intermediate temperature	Measure low temperature stiffness and stress relaxation ability	Measure binder properties at low service temperatures



Table 2. 3: Summary of the standard PG testing and criteria (ASPHALTINSTITUTE 2005).

Max Design Temp.	PG 46	PG 52						PG 58						PG 64						PG 70						PG 76						PG 82					
Min Design Temp.	-34 -40 -45	-10 -16 -22 -28 -34 -40 -46	-16 -22 -28 -34 -40 -46	-10 -16 -22 -28 -34 -40	-16 -22 -28 -34 -40	-10 -16 -22 -28 -34 -40	-16 -22 -28 -34 -40	-10 -16 -22 -28 -34 -40	-16 -22 -28 -34 -40	-10 -16 -22 -28 -34 -40	-16 -22 -28 -34 -40	-10 -16 -22 -28 -34 -40	-16 -22 -28 -34 -40	-10 -16 -22 -28 -34 -40	-16 -22 -28 -34 -40	-10 -16 -22 -28 -34 -40	-16 -22 -28 -34 -40	-10 -16 -22 -28 -34 -40	-16 -22 -28 -34 -40	-10 -16 -22 -28 -34 -40	-16 -22 -28 -34 -40	-10 -16 -22 -28 -34 -40	-16 -22 -28 -34 -40	-10 -16 -22 -28 -34 -40	-16 -22 -28 -34 -40	-10 -16 -22 -28 -34 -40	-16 -22 -28 -34 -40	-10 -16 -22 -28 -34 -40									
Original																																					
≥ 230°C	Flash point																																				
≤ 3 Pa-s @135°C	Rotational Viscosity																																				
≥ 1.00 kPa	DSR G*/sinδ (Dynamic Shear Rheometer)																																				
	46	52						58						64						70						76						82					
Rolling Thin Flim Oven (RTFO), Mass change ≤ 1.00%																																					
≥ 2.20 kPa	DSR G*/sinδ (Dynamic Shear Rheometer)																																				
	46	52						58						64						70						76						82					
Pressure Aging Vessel (PAV)																																					
20 hours, 2.10 Mpa	90	90						100						100						100 (110)						100 (110)						100 (110)					
≤ 5000 kPa	DSR G*/sinδ (Dynamic Shear Rheometer), Intermediate Temp ( (Max+Min)/2)+4																																				
	10	7	4	25	22	19	16	13	10	7	25	22	19	16	13	31	28	25	22	19	16	34	31	28	25	22	19	37	34	31	28	25	40	37	34	31	28
S<300 MPa m>0.300	Bending Beam Rheometer (BBR), Creep stiffness (S) & m-value																																				
	-24	-30	-36	0	-6	-12	-18	-24	-30	-36	-6	-12	-18	-24	-30	0	-6	-12	-18	-24	-30	0	-6	-12	-18	-24	-30	0	-6	-12	-18	-24	0	-6	-12	-18	-24
If BBR m-value ≥ 0.300 and Creep stiffness is between 300 and 600 Mpa, the Direct Tension failure strain requirement can be used in lieu of the creep stiffness requirement																																					
εt ≥ 1.00 %	Direct Tension Tester (DTT)																																				
	-24	-30	-36	0	-6	-12	-18	-24	-30	-36	-6	-12	-18	-24	-30	0	-6	-12	-18	-24	-30	0	-6	-12	-18	-24	-30	0	-6	-12	-18	-24	0	-6	-12	-18	-24

### 2.5.1 Permanent deformation resistance of asphalt binders

Permanent deformation or rutting is one of the predominant of the pavement distresses typically observed at high service temperatures and/or under heavy traffic loads. In the current performance-based asphalt binder specifications, the SUPERPAVE  $G^*/\sin \delta$  parameter has been widely used to capture the rutting sensitivity of the binder at high temperatures. This binder rutting resistance parameter of unaged and artificial short-term (RTFO) aged binders at the maximum 7-day average pavement design temperature must be at least 1.00 kPa and 2.20 kPa, respectively (ASPHALTINSTITUTE 2005). This  $G^*/\sin \delta$  parameter is based on the dissipated energy concept, where it is assumed that plastic deformation is a resultant of the total energy dissipated per cycle of loading. It is described that at each cycle of traffic loading, the work done in deforming the pavement surface at high temperatures is partially recovered to its original shape by elastic component, and also partially dissipated in the form of permanent deformation by the viscous component. Therefore, in order to minimize the irrecoverable deformation of asphalt, the amount of work dissipated per loading cycle should be minimized, where the work dissipated per loading cycle at a specific stress level can be expressed as the following equation (Stuart et al. 2000).

$$W_c = \pi \sigma_0^2 \left[ \frac{1}{\left( \frac{G^*}{\sin \delta} \right)} \right] \quad (2.1)$$

Where,

- $W_c$  = work dissipated per loading cycle
- $\sigma$  = stress applied during the loading cycle
- $G^*$  = complex shear modulus obtained by DSR test
- $\delta$  = phase angle obtained by DSR test

However, the SUPERPAVE rutting parameter has been criticized for being insufficient in capturing the actual performance of the polymer modified binder. The ineffectiveness of the SUPERPAVE rutting parameter was proven by Accelerated Loading Facility (ALF) testing (Dongre&D'Angelo 2003) and laboratory testing (Bahia et al. 2001). It is because the binder rutting parameter is obtained within the linear viscoelastic (LVE) region, where the binder sample is tested at a low strain level and there is no damage introduced to the binder sample. But, the rutting of asphalt pavements is a non-linear viscoelastic phenomenon, a high-stress concentration induced by complicated traffic loading may cause irreversible damage to pavement structure. On the one hand, in the case of the unmodified binder, it is generally accepted that the SUPERPAVE rutting parameter does actually provide a reasonable correlation between the  $G^*/\sin \delta$  and the field plastic deformation (Bahia et al. 2001, Stuart et al. 2000). On the other hand, in case of the polymer modified binders, it was observed that the  $G^*/\sin \delta$  rutting parameter did not correlate well with the real mixture rutting performance measured in the laboratory (D'Angelo et al 2007). It is because responses of modified asphalt binders are non-linear, and it is unreasonable to evaluate a

non-linear response by the linear testing protocol. It is thus necessary to evaluate the high-temperatures rutting performance of the binder under the non-linear conditions. As a result of Bahia et al. study (2001), many alternative binder rutting parameters have been proposed to replace the current SUPERPAVE rutting parameter. Several comparisons of alternative rutting parameters were made, and it was clearly founded the Multiple Stress Creep and Recovery (MSCR) test did provide more accurate correlations with the rut depth of mixtures as show in Figure 2.7(Radhakrishnan et al. 2018, Saboo&Kumar 2016, Wang&Zhang 2014).

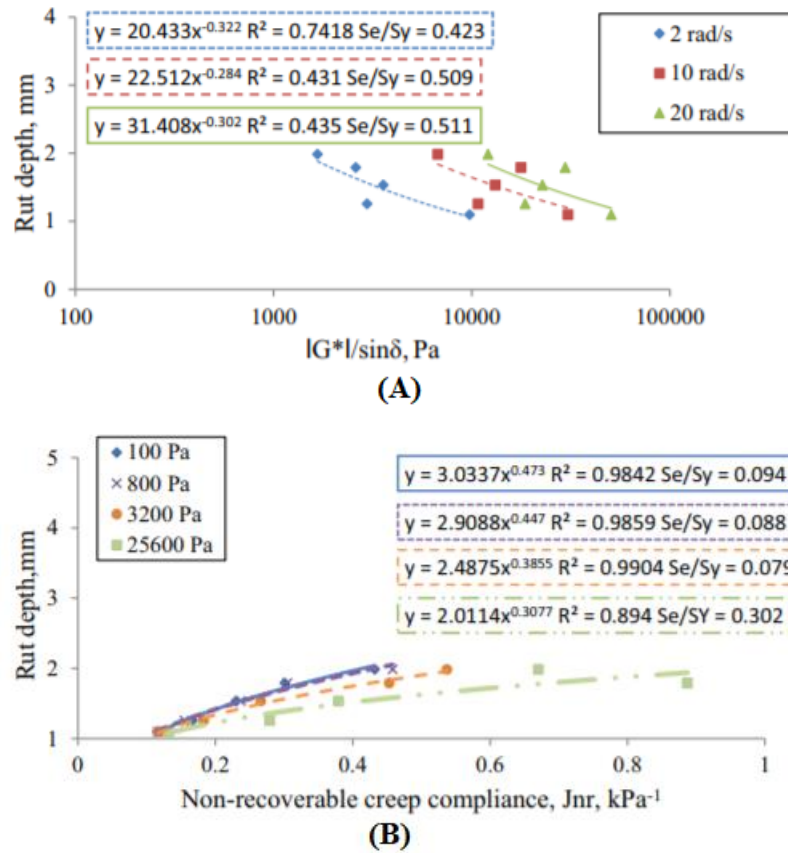


**Figure 2. 7:** Rut depth vs  $G^*/\sin(\delta)$  (A), and rut depth vs  $J_{nr}$  (B) (Radhakrishnan et al. 2018).

### 2.5.2 Fatigue cracking resistance of asphalt binders

At intermediate service temperatures, fatigue cracking is a major concern, especially at the long-term service performance. Cracks normally initiate and propagate within the weakest point of the asphalt mixture such as binder phase or mastic phase. The fatigue resistance of the mixture is therefore directly dependent on the fatigue resistance of the binders. According to the current SUPERPAVE binder specification, the fatigue cracking parameter ( $G^*\sin\delta$ ) is used to assess the fatigue resistance of long-term aged asphalt binders. In the specification, the maximum value of  $G^*\sin\delta$  is specified as 5,000 kPa (ASPHALTINSTITUTE 2005). The concept of energy dissipation is employed to determine binders' ability fatigue to resist fatigue cracking, where the

traffic load is partially dissipated in the form of crack initiation and crack propagation. The work dissipated per loading cycle at a constant strain can be calculated in accordance with equation 2.9 (Anderson&Kennedy 1993). Theoretically, it can be concluded that the smaller amount of energy dissipated the smaller fatigue damage accumulation of the pavement, thus binders with the smallest  $G^* \sin \delta$  value is the most desirable in order to minimize fatigue cracking.

$$W_c = \pi \gamma_0^2 [G^* \sin \delta] \quad (2.9)$$

Where,

$W_c$  = work dissipated per loading cycle

$\gamma_0$  = strain during load cycle

$G^*$  = complex shear modulus obtained by DSR test

$\delta$  = phase angle obtained by DSR test

Many studies indicated that the fatigue performance of asphalt binders, especially modified binders, cannot be sufficiently predicted by the SUPERPAVE fatigue parameter. It is because the parameter  $G^*$  and  $\delta$  are simply measured within the linear viscoelastic regime of asphalt binders, and they do not really represent the real fatigue damage under varied traffic conditions where the pavements experience fluctuating strain levels and wide-ranging traffic loading frequencies. Moreover, in order to accurately evaluate the fatigue resistance of binder, the binder sample should be tested under damaging conditions (Bahia et al. 2002, Johnson&Bahia 2010). Consequently, several approaches for characterizing fatigue resistant properties of both unmodified and modified asphalt binders have been proposed in order to capture the true fatigue performance of binders.

Fatigue cracking is a progressive and permanent structural degradation that occurs in a pavement subjected to repeated traffic loading. Based on this concept, Bahia et al. (2001) proposed the time sweep test method which applies cyclic loading at a constant strain/stress level to quantify the fatigue behavior of asphalt binders by using the 8-mm-diameter parallel plate geometry in the DSR. It is generally acknowledged that the time sweep test performed on the DSR can be reliably used to characterize fatigue properties of the binders (Anderson et al. 2001, Bahia et al. 2002).

### 2.5.3 Thermal cracking resistance of asphalt binders

Low-temperature thermal cracking is predominant distress of asphalt pavements. This failure mode normally manifests when tensile stresses corresponding to shrinkage of the pavement overcomes the fracture strength of the pavement. The stiff asphalt pavements are more susceptible to low-temperature thermal cracking because the ability to dissipate low-temperature stress build up is decreased as temperature falls. The stiffness of the asphalt binder has a predominant effect on the stiffness of the asphalt (Ghavibazoo&Abdelrahman 2014). The low-temperature rheology of asphalt binders plays a dominant role in governing low- temperature performance of asphalt mixture. Thus, understanding, measuring, and controlling the rheological properties of the binders

are the key components of improving the low-temperature performance of pavements (Sui et al. 2010).

The low-temperature thermal cracking resistance of the binders is commonly evaluated by using the bending beam rheometer (BBR) (Bahia et al. 1991). In the BBR test, the deflection under a constant load at temperatures corresponding to the expected lowest pavement service temperature plus 10 degree Celsius ( $T+10^{\circ}\text{C}$ ) of the pre-fabricated binder beam is measured. The sample is normally aged by the rolling thin film oven (RTFO) and then pressure aging vessel (PAV). The built-up tensile stresses in the field are simulated by applying a creep load in the BBR lab test. The creep stiffness ( $S[t]$ ) and the creep relaxation rate (m-value) are two main parameters which are directly calculated from the test results to evaluate the creep resistance of the bitumen and binders' ability to disperse the built-up tensile stresses, respectively. The limiting low temperature of the binders is determined with respect to the maximum temperature at which the creep stiffness at a loading time of 60 seconds ( $S[60]$ ) exceeds 300 MPa, or at which the m-value is less than 0.300. The high value of the creep stiffness indicates that the binders tend to crack, due to the more glass-like the material becomes. Conversely, low-temperature tensile stress can be dissipated more quickly as the creep relaxation rate (m-value) increases (ASPHALT INSTITUTE 1997).

However, in the case of extracted asphalt binders, BBR has limitation due to a limited amount of asphalt binders as the test requires a large amount of asphalt binders in order to pre-mold the sample. This weakness of BBR has encouraged to find a way to link the DSR results to the BBR parameters.

# **Chapter 3**

## **Materials and Sample Preparation**

### 3.1 Introduction

In this chapter, the materials used in this study, namely the base bitumen, crumb rubber modifier, and warm-mix additives are described in detail, including their characteristics and properties. The binder modification methods for base bitumen containing WMA additive, CRMB, and CRMB containing WMA additive are presented. Furthermore, short- and long-term artificial aging simulation procedures employed for conditioning the study asphalt binders are also discussed.

### 3.2 Materials

In this study, both unmodified and modified binders were produced using the following materials:

#### 3.2.1 Base bitumen

70/100 penetration grade bitumen provided by NYNAS (Stockholm, Sweden) was selected as the only base bitumen because this grade of bitumen is commonly used in the Netherlands. Table 3.1 and Table 3.2 show the chemical components and properties of the base bitumen used in this study, respectively. The morphology of base bitumen was captured by using scanning electron microscopy (SEM) as shown in Figure 3.1. According to the SEM picture, it indicated that the 70/100 bitumen contains some impurities, however, the homogeneity of the bitumen is confirmed.

**Table 3. 1:** The chemical components of the base bitumen used in this study.

<b>General</b>	Material	Bitumen
	Source	NYNAS
	Penetration grade	70/100
<b>Chemical compositions</b>	Saturates (%)	7
	Aromatics (%)	51
	Resins (%)	22
	Asphaltenes (%)	20

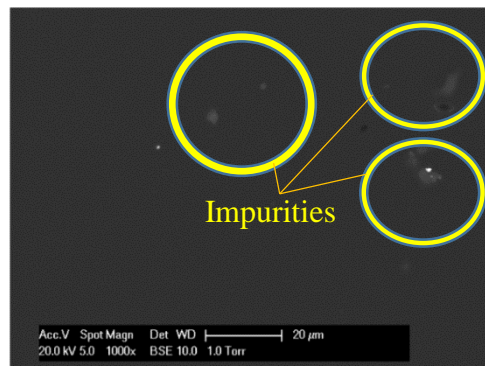


**Figure 3. 1:** Scanning Electron Microscope (SEM) images at 20 microns and 1000x magnification of base bitumen used in this study.

**Table 3. 2:** Properties of base bitumen used in this study [NYNAS].

Properties	Test description	Method	Unit	Min	Max
Consistency at intermediate service temperature	Penetration at 25°C	EN 1426	mm/10	70	100
Consistency at elevated service temperature	Softening Point	EN 1427	°C	43	51
Resistance to hardening at 163°C	Change in mass	EN 12607-1	%	-	0.8
	Retained penetration	EN 1426	%	46	-
	Softening Point after hardening	EN 1427	°C	45	-

### 3.2.2 Crumb rubber modifier (CRM)

Crumb rubber produced from ambient grinding of scrap truck tyre with particle size ranging from 0.0 to 0.5 mm provided by Kargro Recycling was utilized as a bitumen modifier in this thesis as shown in Figure 3.2. The particle shape and texture of the crumb rubber modifier was investigated by using scanning electron microscopy (SEM). Figure 3.3 shows the images of shape and texture at 200 microns and 100 times magnification of the crumb rubber modifier captured by SEM. According to the SEM scanning, the crumb rubber particles were found to have a very porous surface and non-uniformly irregular shapes. Moreover, the physical and chemical properties and the gradation of the crumb rubber particle are presented in Table 3.3-3.4, and Figure 3.4 respectively.

**Figure 3. 2:** Crumb rubber modifier with particle sizes ranging from 0 - 0.5 mm.



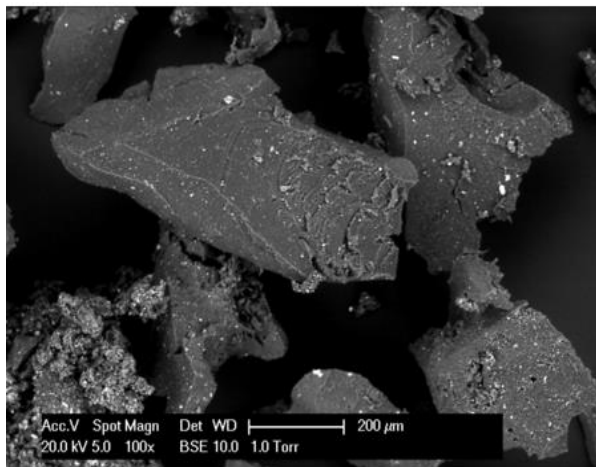


**Figure 3. 3:** Scanning Electron Microscope (SEM) images at 200 microns and 100x magnification of crumb rubber particles used in this study.

**Table 3. 3:** Physical and Chemical Properties of Crumb rubber modifier.

<b>Physical properties</b>	Material	Crumb rubber
	Production method	Ambient grinding
	Source	Scrap truck tyres
	Color	Black
	Morphology	Porous
	Size (mm)	0.00-0.50
	Specific gravity	1.15
	Decomposition temperature (°C)	~200
<b>Chemical properties</b>	Total rubber (natural and synthetic) [%]	55
	Carbon Black (%)	30
	Zinc oxide (%)	1.5
	Sulphur (%)	1
	Benzene extraction (%)	5.5
	Ash content (%)	7

**Table 3. 4:** Crumb rubber particle gradation

Sieve size	% passing
0.710 mm	100
0.500 mm	93
0.355 mm	63
0.180 mm	21
0.125 mm	9
0.063 mm	2

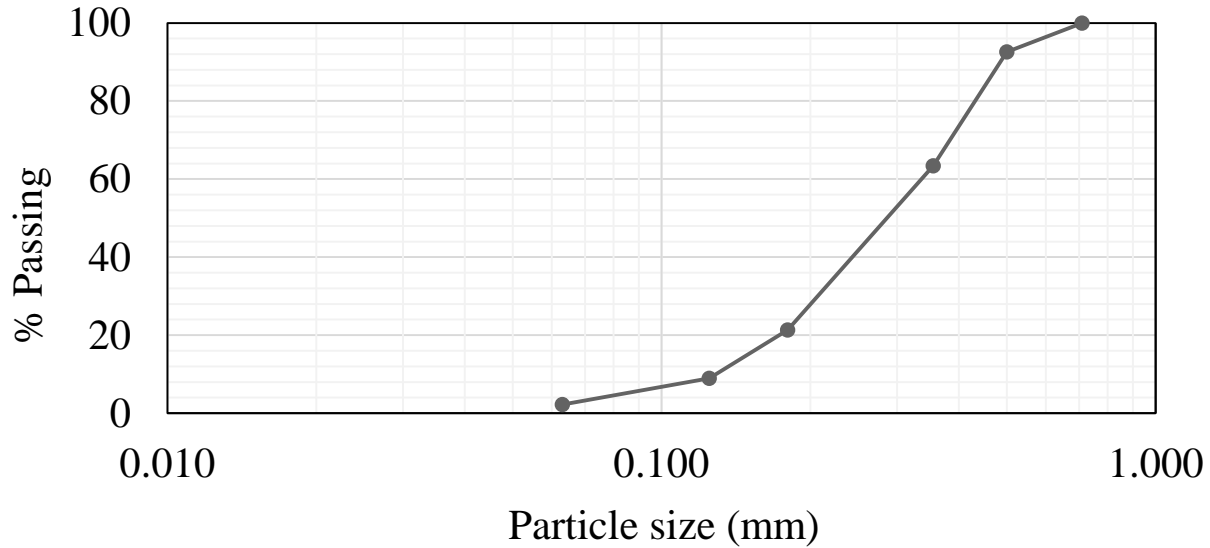


**Figure 3. 4:** Gradation curve of crumb rubber modifier used in this study.

### 3.2.3 Warm-mix additives

In this thesis, two different types of warm mix additive were selected namely: a wax-based warm mix additive and a chemical-based warm mix additive. Table 3.5 shows general information of warm mix additives used in this thesis. The additive products are briefly described and shown in Figure 3.5 and 3.6, respectively.

**Table 3. 5:** General information of the warm mix additives used in this study

Type	Wax-based additive	Chemical-based additive
Appearance	Pastilles	Liquid
Color	Greyish-white	Dark brown
Density (g/cm <sup>3</sup> )	0.590-0.622	0.99
Solubility	Insoluble	Partly soluble
Viscosity (mPa.s at 20 °C)	Not applicable	1.70
Recommend dosage	0.80-4.00% by weight	0.50-3.00% by weight

### 3.2.3.1 Wax-based warm-mix additive

Basically, the wax is a fine crystalline long-chain aliphatic hydrocarbon. It is manufactured from natural gas by using the Fisher-Tropsch process of polymerization. The wax additive is produced in three different solid forms namely: a 5-mm diameter pill, a small 1-mm diameter pill, and a 3-mm chip in flaked form. It is suggested by the manufacturer that the minimum and maximum dosages of the wax additive are 0.8% and 4.0% of the asphalt binder weight, respectively. The wax-based additive is unique from the other types of warm-mix additives as it can be blended with the bitumen or directly added to the asphalt mixture. In this study, the wax in the form of 5-mm diameter pill (Figure 3.5) was chosen to investigate the effect of the wax-based warm mix additive on the performance of the base bitumen and CRMB containing warm-mix additive, and the dosage of the wax was 2.0% by weight of the bitumen. Table 3.6 below shows the physical properties of the wax-based additive.



**Figure 3. 5:** The wax-based warm mix additive used in this study.

**Table 3. 6:** Physical characteristics of wax-based warm-mix additive.

<b>Properties</b>	<b>Description</b>	<b>Unit</b>	<b>Specification</b>	<b>Values and range</b>
<b>Quantitative</b>	Congealing temperature	°C	Min 100	100
	Penetration at 25°C	0.1 mm	Max 1.0	-
	Penetration at 65°C	0.1 mm	Max 13.0	-
	Melting point	°C	Min 75.0	75-115
			Max 115.0	
	Flash point	°C	290	-
	PH		Neutral	-
	Polydispersity index		1.33	-
	Density	kg/m <sup>3</sup>	622 (Pastille)	-
590 (Prill)				
Brookfield Viscosity at 135°C	cP	10-14	12	
<b>Qualitative</b>	Odor			No odor
	Visual color			Greyish-white to yellowish
	Physical state			Pastilles and Prills

### 3.2.3.2 Chemical-based warm-mix additive

The chemical-based additive (Figure 3.6) is a combination of a liquid chemical-based warm mix additive, surfactants, polymers, other additives, anti-stripping agents, etc. It is a multifunctional warm mix additive used to improve the aggregate-surfaces wetting with binder by reducing the surface tension of the asphalt binder, which enables asphalt binder to efficiently coat on surfaces of aggregates. It was claimed that the chemical additive can improve the adhesive strength between asphalt binders and aggregates, and reduce the moisture susceptibility of the asphalt mixture. Furthermore, the chemical additive also contains some additives providing a reduction of the viscosity of the binder and a lubricating effect for easier coating and compaction, thus, resulting in lower manufacturing and compaction temperatures. It can also be used with crumb rubber modified bitumen's. In this study, the chemical-based warm-mix additive was selected to investigate the effect of the warm mix additive on the performance of the base bitumen and CRMB containing warm mix additive, and the dosage of the chemical additive is 0.6% by weight of the bitumen as suggested by the manufacturer.



**Figure 3. 6:** The chemical-based warm mix additive used in this study.

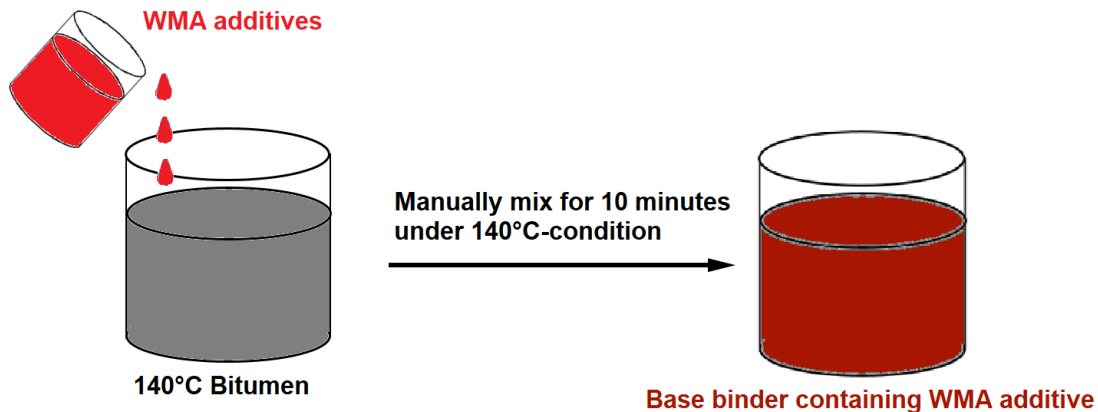
## 3.3 Binder modification method

In order to achieve the study goals, four different types of asphalt binders were prepared namely; unmodified base bitumen, base bitumen containing warm mix additive, crumb rubber modified bitumen, and crumb rubber modified bitumen containing warm mix additive as described in Table 3.7.

**Table 3. 7:** Information of prepared asphalt binders used in this study.

Type of asphalt binders	Code	Base bitumen	CRM dosage (% by weight)	WMA additive
Unmodified base bitumen	70/100	70/100	none	none
Base bitumen containing warm mix additive	70/100-C		none	Chemical-based
	70/100-W		none	Wax-based
Crumb rubber modified bitumen	CRMB-5		5	none
	CRMB-10		10	none
	CRMB-15		15	none
Crumb rubber modified bitumen containing warm mix additive	CRMB-15-C		15	Chemical-based
	CRMB-15-W		15	Wax-based

Base bitumen containing warm mix additive samples were basically prepared by manually blending the hot base bitumen with each warm mix additive at 140°C for 10 minutes as displayed in Figure 3.7. The dosage of both wax-based and chemical-based warm mix additives were 2.0% and 0.6% by unit weight of the asphalt binder as recommended by the producers.

**Figure 3. 7:** Mixing procedures of base bitumen containing warm mix additive.

In case of crumb rubber modified bitumen, three CRM concentrations (5%, 10%, and 15% by total weight of base bitumen) were chosen to experimentally investigate the effect of crumb rubber modifier concentration on asphalt binder performance over the whole service temperatures as mentioned in the sub-objective. The CRMB samples were prepared by using a Silverson high shear mixer (Figure 3.8) at 6000 rpm at 180°C for 30 minutes as suggested by Wang et al. (2018). After that, CRMB containing wax-based warm mix additive and CRMB containing chemical-based warm mix additive were prepared by manually blending each warm mix additive (wax-based and chemical-based additives) with the hot CRMB blend at 160°C immediately after preparing CRMB

as shown in Figure 3.9. Typically, during the interaction between bitumen and CRM, the aromatics are absorbed into the crumb rubber particles. In some cases at asphalt mixing plants, the CRM may excessively absorb the aromatics from the bitumen, causing compatibility problems and reduce the low-temperature flexibility of the CRMB. Thus, in the asphalt production process, various petroleum distillates or extender oil (0-6% of the bitumen weight) are added to improve workability, promote the interaction, and reduce the viscosity of the CRMB (Lo Presti 2013). However, in this study, extender oil was not used to promote the workability of the CRMBs.

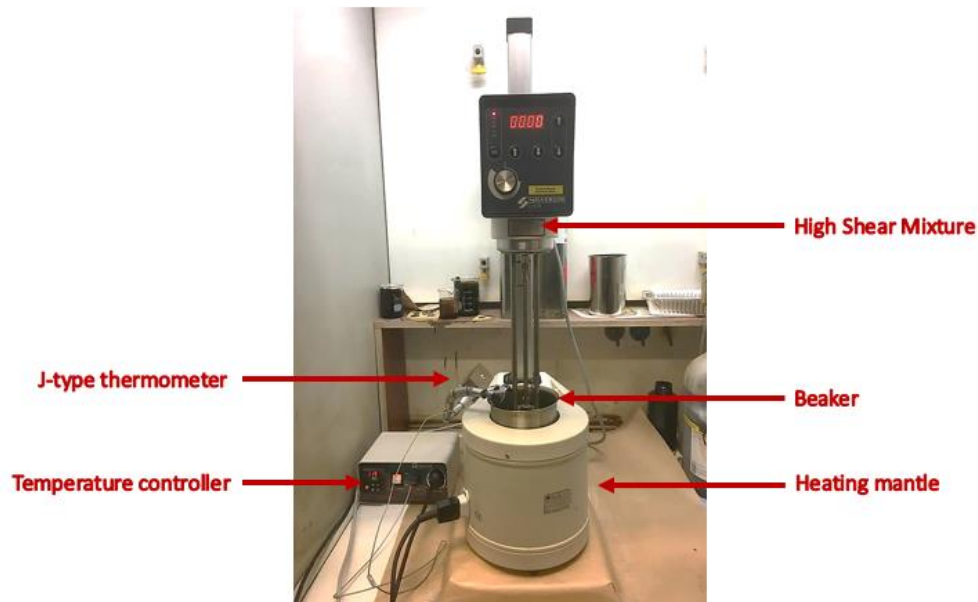


**Figure 3. 8:** Laboratory equipment used to prepare crumb rubber modified bitumen.

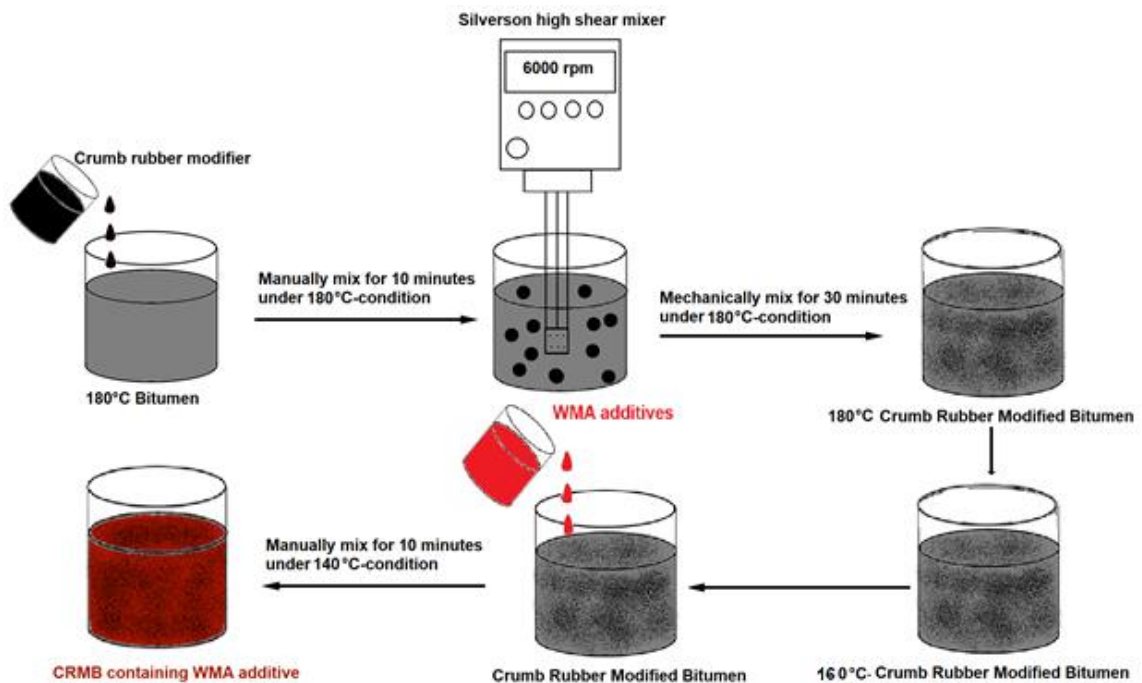


**Figure 3. 9:** Mixing procedures of CRMB and CRMB containing WMA additive.

### 3.4 Laboratory aging methods

Aging of bitumen is one of the major factors which significantly affects physical and rheological properties of asphalt binder. The properties of asphalt binder start changing as the bitumen is exposed to the very first heat in the asphalt mixing process, and this aging process keeps on going as the binder exposed to heat, moisture, oxygen, and ultraviolet radiations during its service life. According to the SUPERPAVE Performance Grading system, the performance and mechanical properties of asphalt binders are normally characterized at three critical aging stages namely: unaged (before mixing with aggregates), short-term aged (after asphalt concrete production and placement), and long-term aged (5 to 10 years after placement) stages. The aging procedures that were employed to condition the binders are described in the following topics.

#### 3.4.1 Short-term aging

The physical hardening process of the asphalt binders after mixing and laying processes is considered as the short-term aging of binders which is normally simulated by the tests such as the thin-film oven test (TFOT) and the rolling thin-film oven test (RTOFT).

The thin film oven test (TFOT) is an aging simulation technique conducted following ASTM Test Method D1754 by conditioning binders in the oven at 163°C for five hours. The 50-ml of asphalt binder is directly poured into a pan (140-mm in diameter) placed on a rotating shelf. After the conditioning, the short-term aged binders might be further tested to evaluate the short-term aging effects. This aging technique simulates conditions that binders are normally experienced during normal hot-mix plant operations.

The rolling thin-film oven test (RTFOT) is considered as an improvement of the TFOT, and being used as the standard short-term aging test. In this test, 35 grams of binder sample is poured into specifically designed glass bottles (Figure 3.10). After that, the bottles are placed horizontally on a cooling rack allows them to cool down for 60-180 minutes before conditioning them in a pre-heated oven where the temperature is maintained at 163 °C for 85 minutes in accordance with AASHTO T240. During the test, the bottles are rotated in a carousel to allow the binders to fully and uniformly coat the bottles (binder film thickness of 1.25 mm) in order to simulate the real asphalt mixing plant conditions. Furthermore, the hot and fresh air is periodically injected into the bottles at a rate of 4000 ml/min to intensify the aging effect. The residue from the RTOFT can be further tested for the effects of short-term aging. The chamber of the RTFOT used in the study is shown in Figure 3.10.



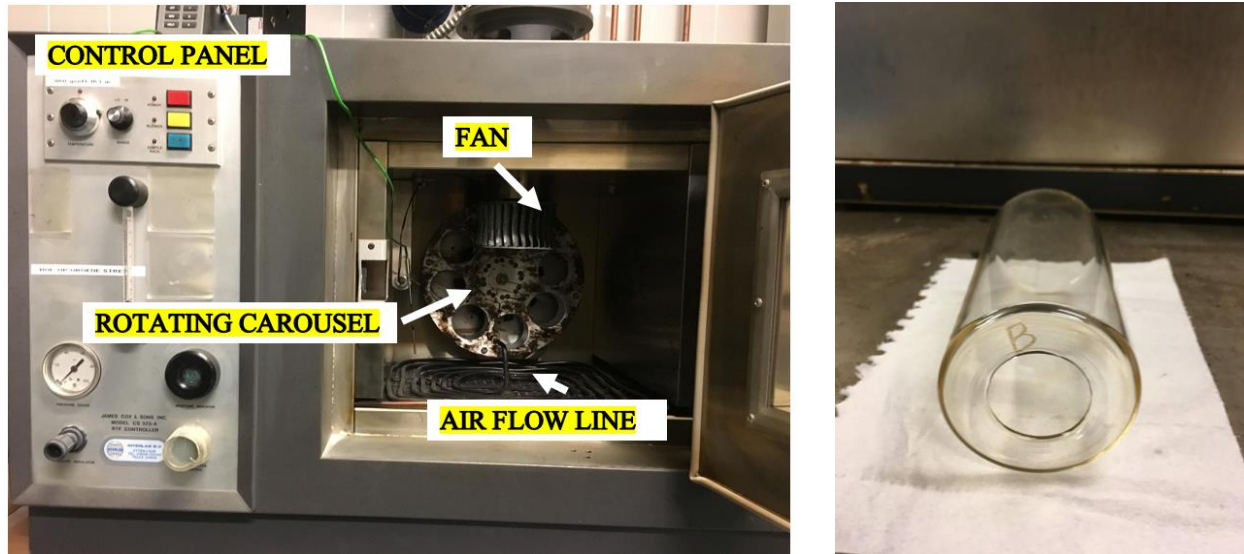


**Figure 3. 10:** Rolling thin film oven test (RTFOT) equipment (left) and the bottles for holding the specimens (right).

However, in this study, the significantly high viscosity of the CRMB may cause problems during the standard short-term aging simulation or the rolling thin-film oven test (RTFOT) as the CRMB may not fully coat the RTFO bottle and/or spill out of the bottle instead of coating it (Bahia et al. 2001, Baumgardner & D'Angelo 2012). According to the original design purpose of the RTFO test, the rolling of the RTFO bottle is to simulate the real asphalt mixing plant conditions where the asphalt binders are continuously stirred by the agitating system in order to avoid skin formation and to ensure uniform aging. Furthermore, it is difficult to obtain sufficient CRMB from the bottles after performing the test due to the very high viscosity of CRMB. It is suggested that other short-term aging simulation such as the thin-film oven (TFO) aging simulation with slight modification could potentially reach the same aging level as the standard RTFOT for the CRMB (Hung et al. 2014). Therefore, in this thesis, the thin-film oven aging simulation was modified to simulate the short-term aging condition of the asphalt binders used in this study, and the detail of the modification is presented below.

The modified static oven aging simulation is ideally based on the thin-film oven test (ASTM D1754) where the hot asphalt binder is placed in 140-mm diameter pans on a shelf in an oven maintained at 163°C for specific duration, but the differences are the static shelf (Figure 3.11) is used instead of rotating shelf and the weight of hot binders is adjusted to be only 20 grams so the thickness of the binder-film is approximately the same as the thickness of the binder in RTFOT (~1.25 mm). Thus, the unknown factor that making the modified static oven aging simulation comparable to the standard RTFO is the test duration.



**Figure 3. 11:** The modified static oven aging simulation

In this experiment, the modified static oven aging simulations were performed at 1h, 2h, 3h and 4h to simulate the short-term aging of the base asphalt binders (70/100 penetration grade) at different testing durations. After that, the modified oven-aged and RTFO-aged samples were tested by performing the frequency sweep test and the MSCR test in order to determine which testing duration can give the comparable short-term aging simulation as the standard RTFOT.

The frequency sweep test and MSCR results show that conditioning asphalt binders in the oven at 163°C for 2 hours can reach approximately the same aging as the RTFO as the results provide about the same rheological properties as shown in Figure 3.12 and Table 3.8, respectively. As a result, from a mechanical point of view, the 2-hour modified static oven aging simulation can be used as an alternative to RTFOT for simulating short-term aging.

Moreover, the FTIR test was also carried out to compare the oxidation products (Check the chapter 4 for further details) between the standard short-term aging simulation (RTFOT) and the oven aging simulations. Figure 3.13 shows the carbonyl and sulfoxide indices of the short-term aging simulations. According to the FTIR results, it is clear that the oven test duration of 2 hours gave the similar oxidation products as the standard RTFOT. Therefore, in this study, 2-hour modified static oven aging is used for conditioning short-term aging of prepared binder samples.

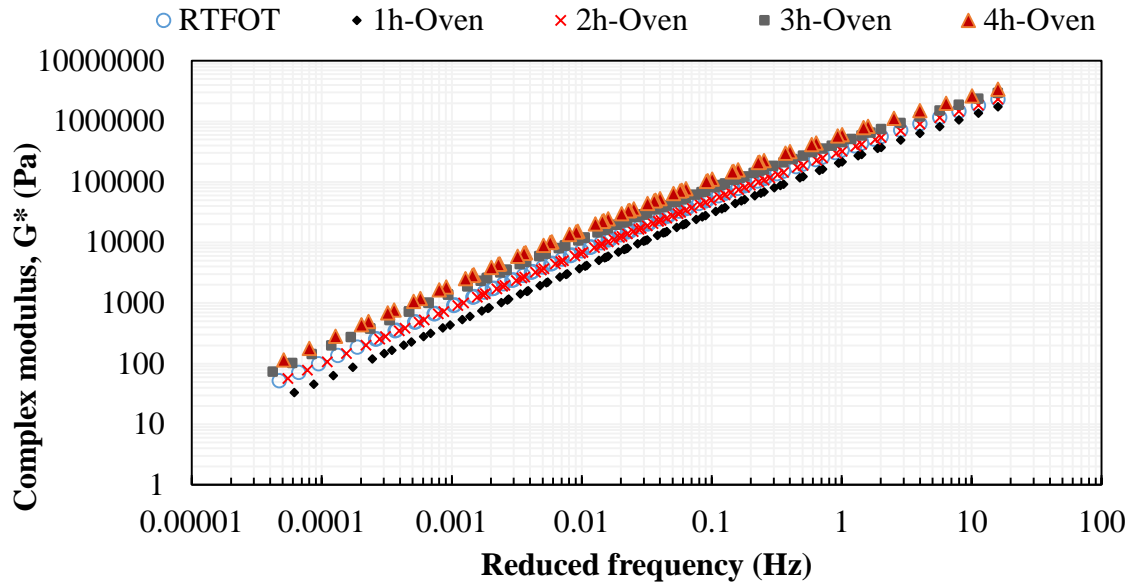


**Figure 3. 12:** Rheological characteristics master curve of 70/100 samples conditioned at different short-term aging simulations (reference temperature = 30°C).

**Table 3. 8:** MSCR results of the 70/100 samples at different short-term aging simulations.

Aging Simulation	Average recovery (%)		Average creep compliance (1/kPa)	
	0.10 kPa	3.20 kPa	0.10 kPa	3.20 kPa
RTFOT	1.40	No recovery	3.90	4.44
1-hour Oven	No recovery	No recovery	5.59	6.22
2-hour Oven	1.55	No recovery	3.49	3.94
3-hour Oven	4.74	No recovery	2.61	3.07
4-hour Oven	6.75	0.29	1.86	2.04

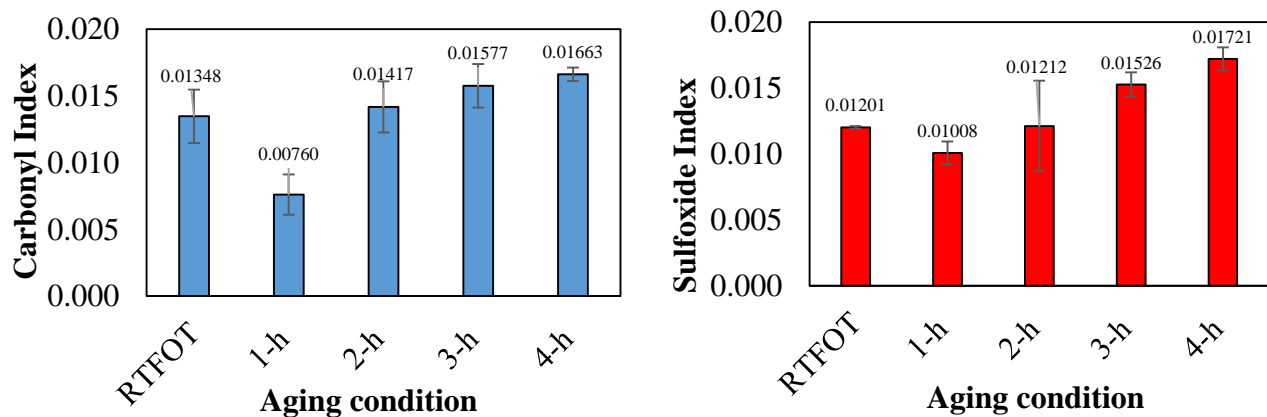


**Figure 3. 13:** Carbonyl index (left) and sulfoxide index (right) of the short-term aging simulations.

### 3.4.2 Long-term aging

The Pressure Aging Vessel (PAV) is used to simulate 5-10 years in-service oxidative aging of asphalt binder. The long-term aged samples were prepared through a Pressure Aging Vessel (PAV) device as shown in Figure 3.14 by exposing the short-term aged (2-hour modified oven-aged) samples to elevated temperatures ( $100^{\circ}\text{C}$ ) in a pressurized environment ( $21 \pm 0.1$  MPa for 20 hours  $\pm 10$  minutes) in accordance with AASHTO R28. In the PAV test, 50-gram of short-term aged residue is poured into in a 140 mm diameter pan (approximately 3.2 mm binder film thickness) and conditioned with the procedures as mentioned.



**Figure 3. 14:** The ATS Pressure Ageing Vessel.

# **Chapter 4**

## **Rheological Characterization**

## 4.1 Introduction

Asphalt binders are generally known as viscoelastic material which properties are dependent on both rates of loading and temperature. Newtonian flow behavior is reported to be the common behavior of asphalt binders at a low rate of loading and/or high service temperatures (above 60 °C). While, at low service temperatures (below -20 °C) and/or high loading frequencies, glass-like solid or elastic behaviors are expected. Moreover, the viscoelastic response is exhibited at the intermediate temperatures (between -20 °C and 60 °C). Therefore, in the typical road service conditions, both viscous and elastic behaviors of asphalt binders are likely to be shown (Bahia et al.2001, Read&Whiteoak 2003).

Rheology is defined as the study of flow and deformation of materials that exhibit time- and temperature-dependent response under applied forces (Bahia et al.2001). The viscoelastic response of asphalt binders is commonly characterized by oscillatory rheological testing with the help of Dynamic Shear Rheometer (DSR). The behavior of viscoelastic materials can be divided into two behavioral domains, namely linear and non-linear viscoelastic. In a linear viscoelastic region, the response of material is independent of the magnitude of the applied stress/strain but affected by the rate of loading (frequency) and temperature. In the non-linear region, the material properties are influenced by all frequency, temperature, and magnitude of applied stress/strain. Thus, it is very difficult to characterize the non-linear response of viscoelastic materials by using the DSR. The main goal of this chapter is to characterize rheological properties of the asphalt binders at different frequencies (time of loading), temperatures, and aging stages within the linear viscoelastic (LVE) region.

## 4.2 Oscillatory rheological testing

### 4.2.1 Background

Oscillatory/dynamic testing is a common method employed to determine rheological characteristics over a range of temperatures and frequencies of viscoelastic materials by using a DSR. In principle, sinusoidal shear stress ( $\tau^*$ ) or shear strain ( $\gamma^*$ ) is induced to a sample in order to measure the amplitude of the applied torque ( $T$ ) and angular displacement ( $\theta$ ) of the sample as shown in Figure 4.1. In the test, the sample is sandwiched between two circular plates where the lower plate is fixed and the oscillating torque is applied through the upper plate. Figure 4.2 presents a stress-strain response of a viscoelastic material in which the lag between the two sinusoidal responses is represented by the phase angle ( $\delta$ ).

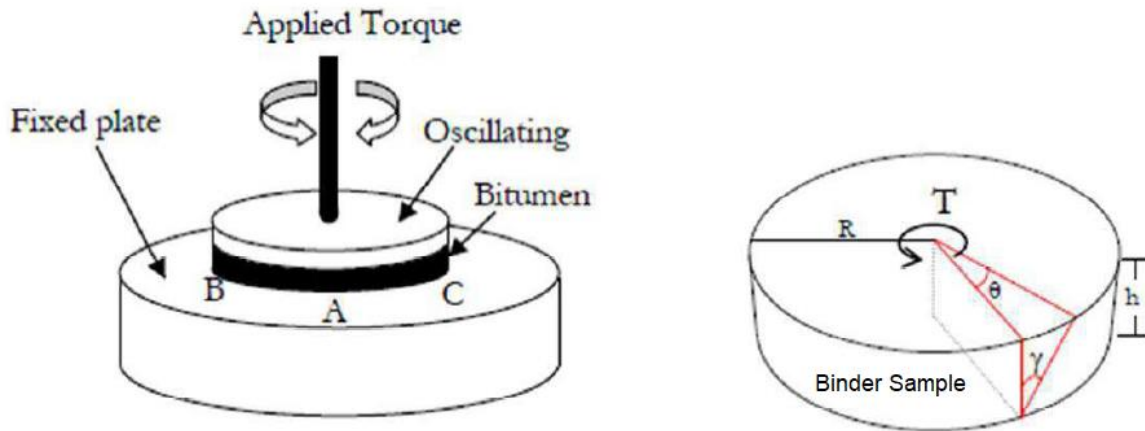


Figure 4. 1: Configuration of DSR parallel plates.

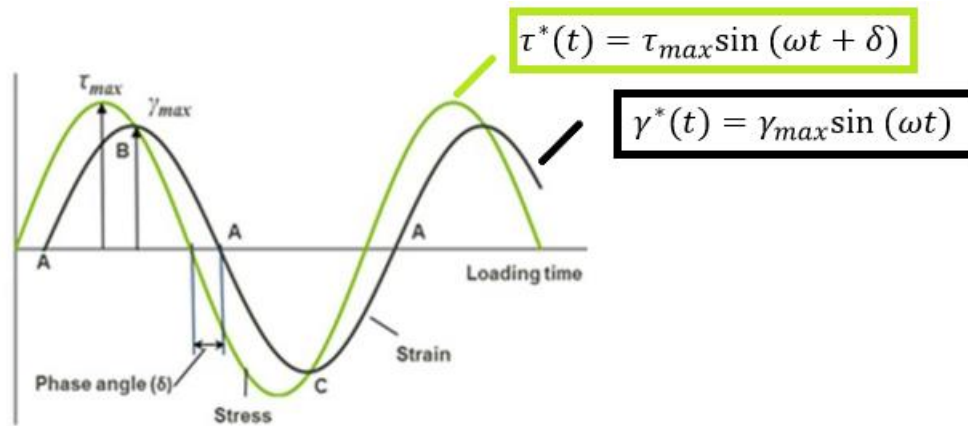


Figure 4. 2: Stress-strain response of a viscoelastic material.

The corresponding strain and stress at any time domain can be calculated based on the measured torque and angular rotation by using the equations 4.1 and 4.2.

$$\gamma^*(t) = \gamma_{max} \sin(\omega t) = \gamma_{max} e^{i\omega t} \quad (4.1)$$

$$\tau^*(t) = \tau_{max} \sin(\omega t + \delta) = \tau_{max} e^{i(\omega t + \delta)} \quad (4.2)$$

Where,

$\tau_{max}$  = maximum shear stress,  $\frac{2T}{\pi R^3}$  (Pa)

$\gamma_{max}$  = maximum shear strain,  $\frac{\theta R}{h}$

$\delta$  = Phase angle or Phase lag between stress and strain responses (radians)

$\omega$  = angular frequency (radian/second)

T = torque (N.m)

R = radius of the parallel plates (mm)

$\theta$  = deflection angle (radians)

h = gap between parallel plates (mm)

Therefore, from the calculation of strain and stress at any time domain, the complex dynamic modulus ( $G^*$ ) at any time domain which represents overall resistance to deformation in term of a ratio of stress and strain can be written as follow:

$$G^* = \frac{\tau^*}{\gamma^*} = \frac{\tau_{max}}{\gamma_{max}} (\cos\delta + i\sin\delta) = \frac{\tau_{max}}{\gamma_{max}} e^{i\delta} \quad (4.3)$$

The above equation (4.3) can be rewritten in the following form, where the complex modulus can be represented by the storage shear modulus ( $G'$ ) and loss shear modulus ( $G''$ ).

$$G^* = G' + iG'' \quad (4.4)$$

Where,

$G'$  = storage shear modulus,  $\frac{\tau_{max}}{\gamma_{max}} (\cos\delta)$  (Pa)

$G''$  = loss shear modulus,  $\frac{\tau_{max}}{\gamma_{max}} (\sin\delta)$  (Pa)

The storage shear modulus ( $G'$ ) is considered as the elastic component of the complex shear modulus which describes a measure of the energy stored and elastically recovered per cycle of sinusoidal deformation. While, the loss modulus ( $G''$ ) is associated with the viscous part of the complex modulus which reflects the dissipation of energy per cycle of sinusoidal deformation. In addition, the loss tangent ( $\tan \delta$ ) or the tangent of phase angle ( $\tan^{-1}\delta$ ) represents the ratio of energy dissipated to energy stored in a cyclic deformation.

The phase lag or difference between the sinusoidal stress and strain is called the phase angle ( $\delta$ ). The amount phase lag parameter indicates the state of viscoelasticity that materials behave. On the one hand, materials with  $0^\circ$  phase angle are considered to be purely elastic where the materials are capable of recovering without accumulating any permanent deformation. On the other hand, purely viscous stage of material is indicated when the phase angle is equal to  $90^\circ$  as shown in Figure 4.3. Table 4.1 shows a summary of parameters and their physical meanings of the oscillatory rheological test.

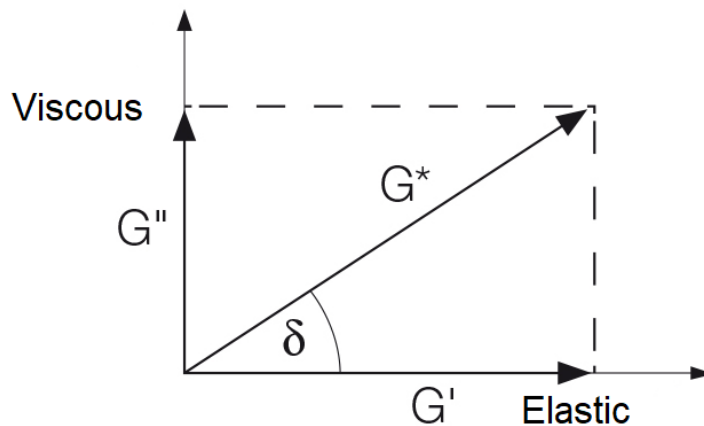


**Figure 4. 3:** Representation of complex shear modulus.



**Table 4. 1:** Summary of oscillatory testing parameters (adapted from Laukkanen 2015)

Parameter	Symbol	Definition	Unit	Physical meaning
Complex modulus	$G^*$	$G' + iG''$	Pa	a measure of the overall resistance of the material to deformation in each oscillation
Storage modulus	$G'$	$\frac{\tau_{max}}{\gamma_{max}} \cos \delta$	Pa	a measure of the energy stored and elastically recovered in each oscillation
Loss modulus	$G''$	$\frac{\tau_{max}}{\gamma_{max}} \sin \delta$	Pa	a measure of the energy dissipated in each oscillation
Loss tangent	$\tan \delta$	$\frac{G''}{G'}$	-	a ratio of energy dissipated to energy stored in each oscillation
Phase angle	$\delta$		rad	phase difference between the stress and strain that reflects the viscoelastic characteristic of the material

## 4.2.2 Rheological data representation

The DSR results are obtained at various temperatures and loading frequencies. The data is thus needed to be represented the viscoelastic behavior of materials in an understandable way in order to enable study on the rheological properties of bituminous binders. There are several useful forms of graphical presentation techniques that could be used to represent the DSR test data as described below.

### 4.2.2.1 Isochronal plots

An isochronal plot is a representation of any viscoelastic parameter (complex shear modulus, phase angle, storage modulus and so on) in the function of temperature at each specific loading frequency. The isochronal plot can show the temperature susceptibility of the materials as the viscoelastic data can be presented over a range of temperatures at a given frequency. Therefore, the comparison of viscoelastic properties at different temperatures can be made. A sample of an isochronal plot can be seen in Figure 4.4.

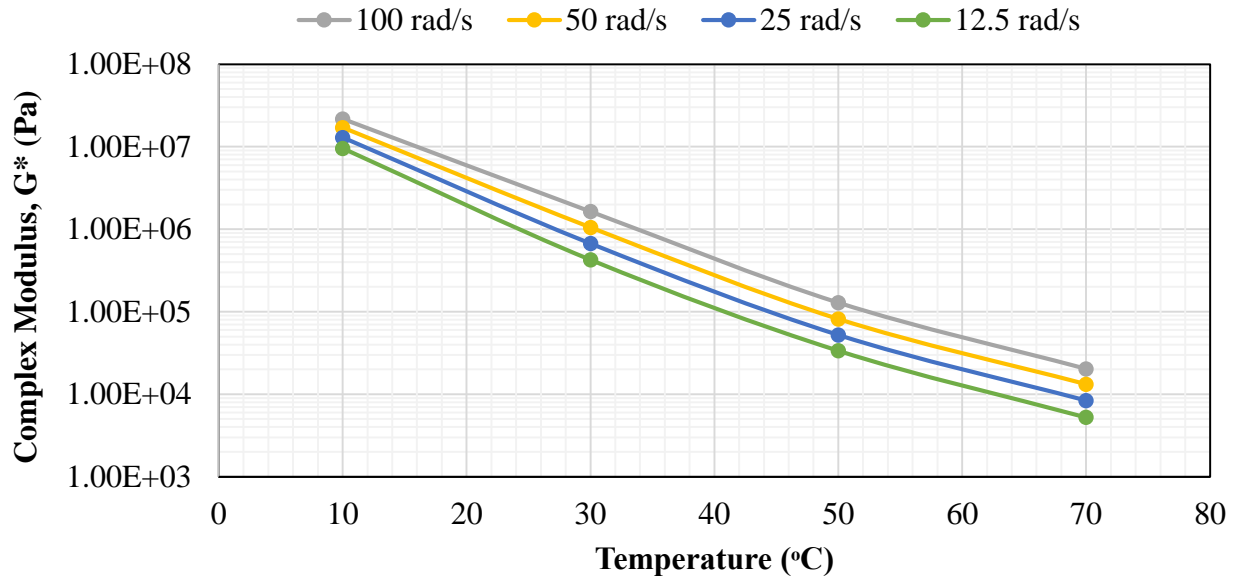


Figure 4. 4: Example of isochronal plot at different frequencies.

#### 4.2.2.2 Isothermal plots

An isothermal plot is a graph representing the viscoelastic parameters in function of loading frequency at any particular temperature. The graph can show a rate of loading dependency of the material at a given temperature as the data is graphically represented over a range of loading frequencies at a constant temperature. Figure 4.5 shows a sample of an isothermal plot.

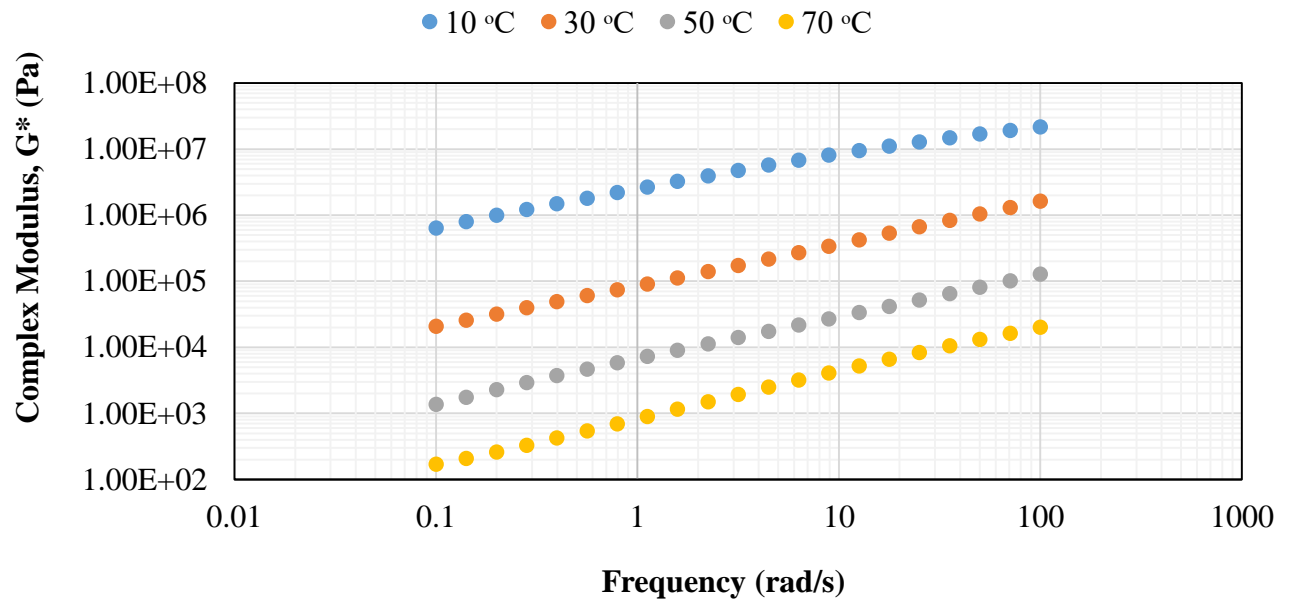
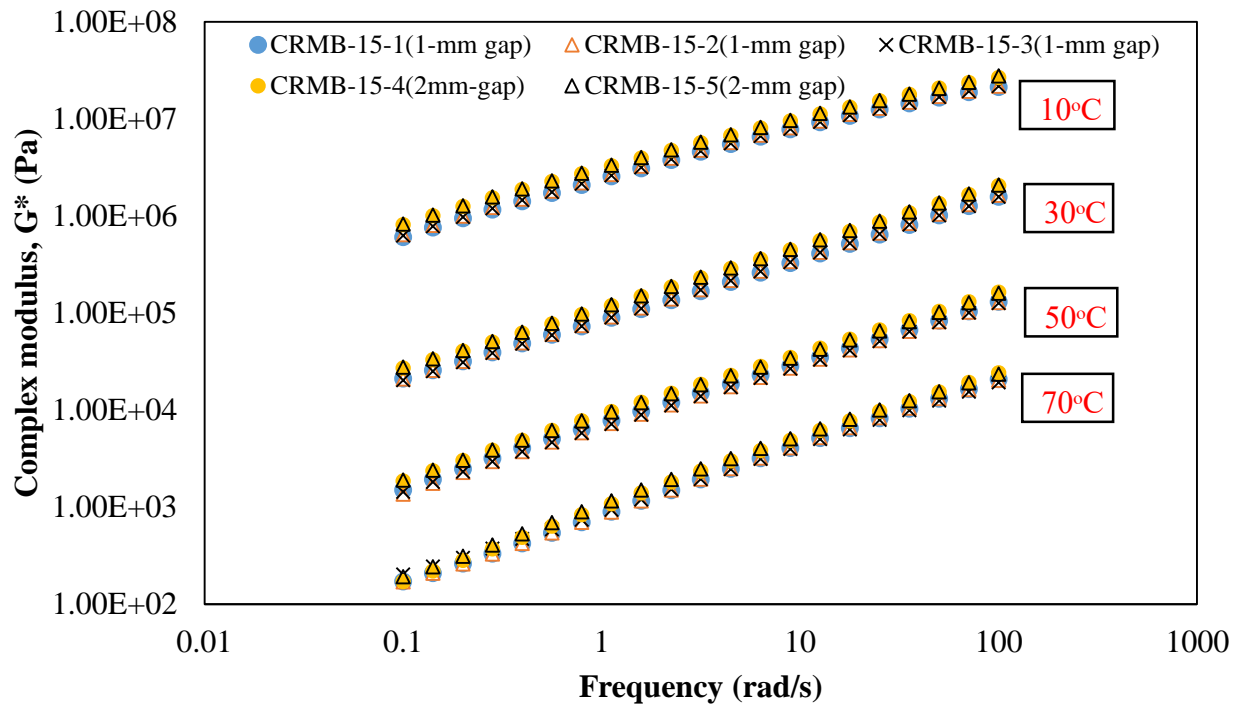


Figure 4. 5: Example of isothermal plot at different temperature.

### 4.2.2.3 Potential issue of the parallel plates' gap-height for modified asphalt binders containing particulate matter.

In the current AASHTO T315, the largest size of the particulate matter within modified asphalt binders should be smaller than one-fourth of the gap-height to ensure accuracy and repeatability of the testing results. The reason is the test results may be dominated or interfered by the characteristics of the particulate matter due to the particle can contact the parallel plates during the test.

In this study, the size of the CRM is ranging from 0 - 0.5 mm which could interfere the DSR measurement with the 1-mm gap test. According to the specification, the height of the gap should be at least 2 mm. In order to verify the validity of the 1-mm gap test results in this study, the results of frequency sweep test using two different gap-heights of the CRMB-15 at the fresh state are presented in Figure 4.6. It can be observed that the frequency sweep test results of 1-mm gap and 2-mm gap (suitable gap-height in accordance with the specification) are similar and stable. Therefore, based on the test results, it can be concluded that the test results are not affected by the CRM particle and representative of the modified binder as a whole.



**Figure 4. 6:** The frequency sweep test results of the CRMB-15.

### 4.2.3 Master curve and time-temperature superposition principle

Master curve is a continuous curve that represent the rheological responses (Phase angle, complex shear modulus, storage modulus, and loss modulus) of viscoelastic materials over an extended range of loading frequency or time scale (several year of loading time) at a specific reference temperature by using the time-temperature superposition principle (TTSP) (Airey 1997. Anderson 1991).

TTSP is a principle that relates the equivalency between time and temperature responses of viscoelastic materials. This principle is considered as an efficient tool that mainly used to represent the viscoelastic behavior of materials over a broad range of time and loading frequency that exceeds the compliance limit of the DSR by shifting measurable rheological data obtained at different temperatures to any chosen reference temperature. The amount of shifting required to shift the curve at each temperature is represented by the shift factor ( $a_T$ ). The shift factor can be calculated using the Williams, Landel, and Ferry equation, or WLF equation (Airey 1997).

$$\log a_T = -\frac{C_1(T-T_0)}{(C_2+T-T_0)} \quad (4.5)$$

Where:

$a_T$  = shift factor at temperature T

T = temperature

$T_0$  = The reference temperature

$C_1, C_2$  = Empirical constants

In this study, master curves at a selected reference temperature were constructed by shifting curves of other test temperatures horizontally to coincide with the reference curve as presented in Figure 4.7. The measured data was fitted into the modified Christensen, Anderson, and Marasteanu model (CAM) to determine the  $C_1$  and  $C_2$  coefficients (Yudoff et al. 2012). Equation 4.6-4.7 describe the mathematical express of the modified CAM model. An example of the master curve constructed by using the modified CAM model is shown in Figure 4.8.

$$G^*(\omega_r) = G_e^* + \frac{G_g^* - G_e^*}{\left[1 + \left(\frac{\omega_r}{\omega_c}\right)^k\right]^{\frac{m}{k}}} \quad (4.6)$$

$$\delta(\omega_r) = \delta_e + \frac{\delta_g - \delta_e}{\left[1 + \left(\frac{\omega_r}{\omega_c}\right)^k\right]^{\frac{m}{k}}} \quad (4.7)$$

Where:

$G^*(\omega_r)$  = The complex shear modulus in a function of the reduced frequency ( $\omega_r$ ), Pa.

$G_e^*$  =  $G^*(\omega \rightarrow 0)$  The complex shear modulus at equilibrium ( $G_e^* = 0$ , for bitumen), Pa.

$G_g^*$  =  $G^*(\omega \rightarrow \infty)$  The glassy complex shear modulus, Pa.

$\omega_c$  = cross over frequency at the defining temperature (frequency at  $G' \approx G''$ ), rad/sec

$\omega_r$  = reduced frequency at the defining temperature, rad/sec

m, k = Shape parameters.

$\delta(\omega_r)$  = The phase angle in a function of the reduced frequency ( $\omega_r$ ), degree.

$\delta_e$  =  $\delta(\omega \rightarrow 0)$ , The phase angle at equilibrium, degree.

$\delta_g$  =  $\delta(\omega \rightarrow \infty)$ , The glassy phase angle, degree.

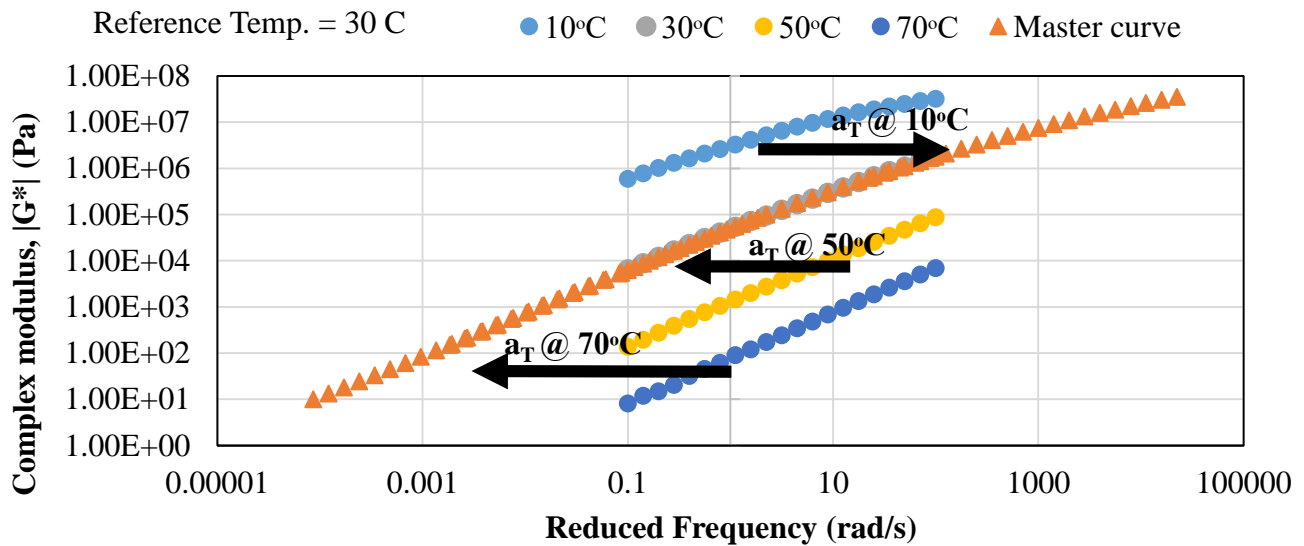


Figure 4. 7: Construction of master curve.

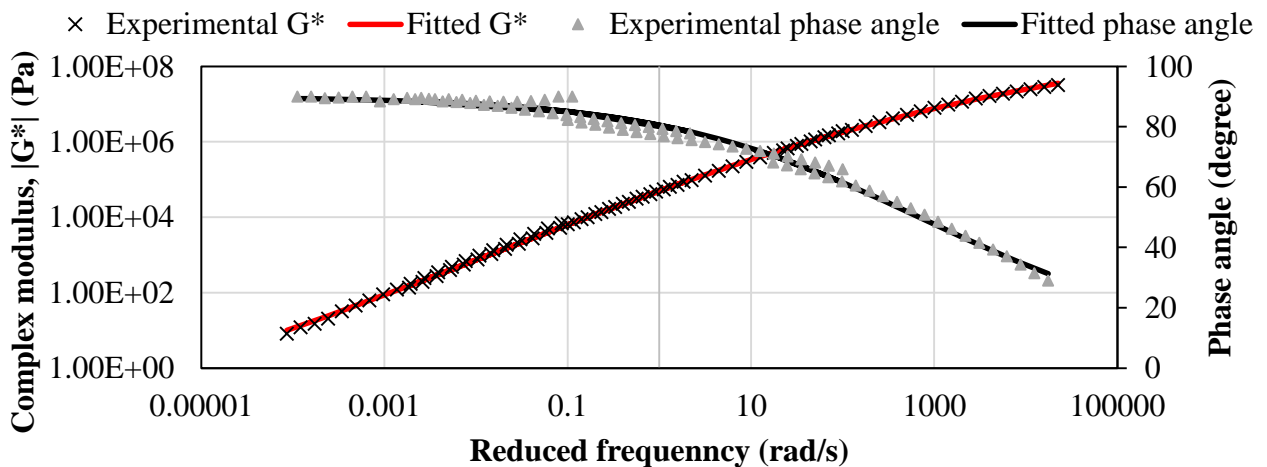


Figure 4. 8: An example of the master curve of the unaged neat bitumen constructed by using the modified CAM model.

#### 4.2.4 Experimental program

The frequency sweep test was conducted at 4 different testing temperatures namely: 10°C, 30°C, 50°C, and 70°C. The test was performed in a strain-controlled mode within the LVE region and the loading frequency varied from 0.1-100 rad/s. The binder samples were conditioned at 3 aging stages (unaged, short-term aged, and long-term aged). The test and sample preparation were carried out in accordance with AASHTO 315-10 specification.

#### 4.3 Fourier transform infrared spectroscopy (FTIR)

Fourier transform infrared (FTIR) spectroscopy is a non-dispersive and non-destructive method of infrared (IR) spectroscopy which is popularly used to analyze chemical functional groups of materials. The FTIR technique was originally developed to overcome the original dispersive infrared spectrometers which measures a spectrum intensity over a narrow range of wavelengths at a time. The working mechanism of the dispersive infrared spectrometer is to separate individual frequencies of energy emitted from the IR source by using a prism or grating. When IR radiation is passed through a sample, some radiation can be transmitted through the sample and some is absorbed by the sample as shown in Figure 4.9. After that, a detector measures the amount of energy at each frequency and the result is presented in a form of spectrum of intensity versus wavelength (or wave number). The original dispersive method may take a considerable amount of time, but FTIR spectroscopy can shorten the testing duration by measuring all infrared frequencies simultaneously. The main advantage of this device is different chemical structures (or molecules) produce different spectral intensities which can be considered as “fingerprints” of the chemical functional groups. Therefore, the chemical structures of individual materials can be characterized according to their chemical fingerprints (Hsu 1997).

An oxidative aging process of asphalt binders is normally caused by two main mechanisms namely photo-oxidation and thermal-oxidation. The oxidation process can alter the chemical compositions of the binder by bonding binder molecular groups with atmospheric oxygen. Sulfoxides (oxidation of sulfide, S=O) and carbonyl compounds (C=O) are commonly formed during chemical transformations caused by oxidation (Lamontagne et al., 2001). The changing of these chemical compositions of the binders can be traced and shown in a form of a spectrum by the FTIT scanning.

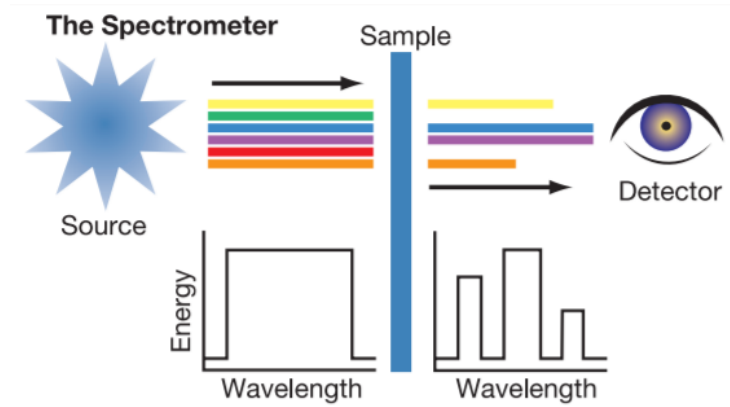


**Figure 4. 9:** FTIR spectrometer working principle  
(Source: <https://tools.thermofisher.com/content>)

Aging of the binder can be investigated by the mean of IR spectrum semi-quantitative analysis such as peak ratio (band height) measurement, or area ratio evaluation. Due to the complex nature of the bitumen chemical composition, Lamontagne et al. (2001) suggested that the areas of peaks measured from valley to valley at specifically selected wavenumbers of the FTIR-obtained spectrum (grey-colored areas) as shown in Figure 4.10 can be used to investigate the changes in the functional groups due to the oxidative ageing. Table 4.2 presents specific functional groups for bituminous binders used for characterizing the aging influence. According to Table 4.2, it was found that there are two functional groups that normally affected by the oxidative aging namely carbonyl and sulfoxide groups. Therefore, in this study, the ageing indices, carbonyl index and sulfoxide index, were calculated by dividing the carbonyl band area ( $A_{1700}$ ) and sulfoxide band area ( $A_{1030}$ ) by the total areas derived from the spectrum quantification (grey-colored areas) as shown in Eq. (4.8-4.10)

$$\text{Carbonyl index} = \frac{A_{1700}}{\sum A} \quad (4.8)$$

$$\text{Sulfoxide index} = \frac{A_{1030}}{\sum A} \quad (4.9)$$

$$\sum A = A_{(2953,2862)} + A_{1700} + A_{1600} + A_{1460} + A_{1376} + A_{1030} + A_{864} + A_{814} + A_{743} + A_{724} \quad (4.10)$$

For the calculation of peak areas within the band limits mentioned in Table 4.2, the peak areas ( $A_3$ ) were defined as an area of the FTIR-obtained spectrum ( $A_1$ ) subtracted by the area under the defined baseline ( $A_2$ ) within the same band limits as illustrated in Figure 4.11.

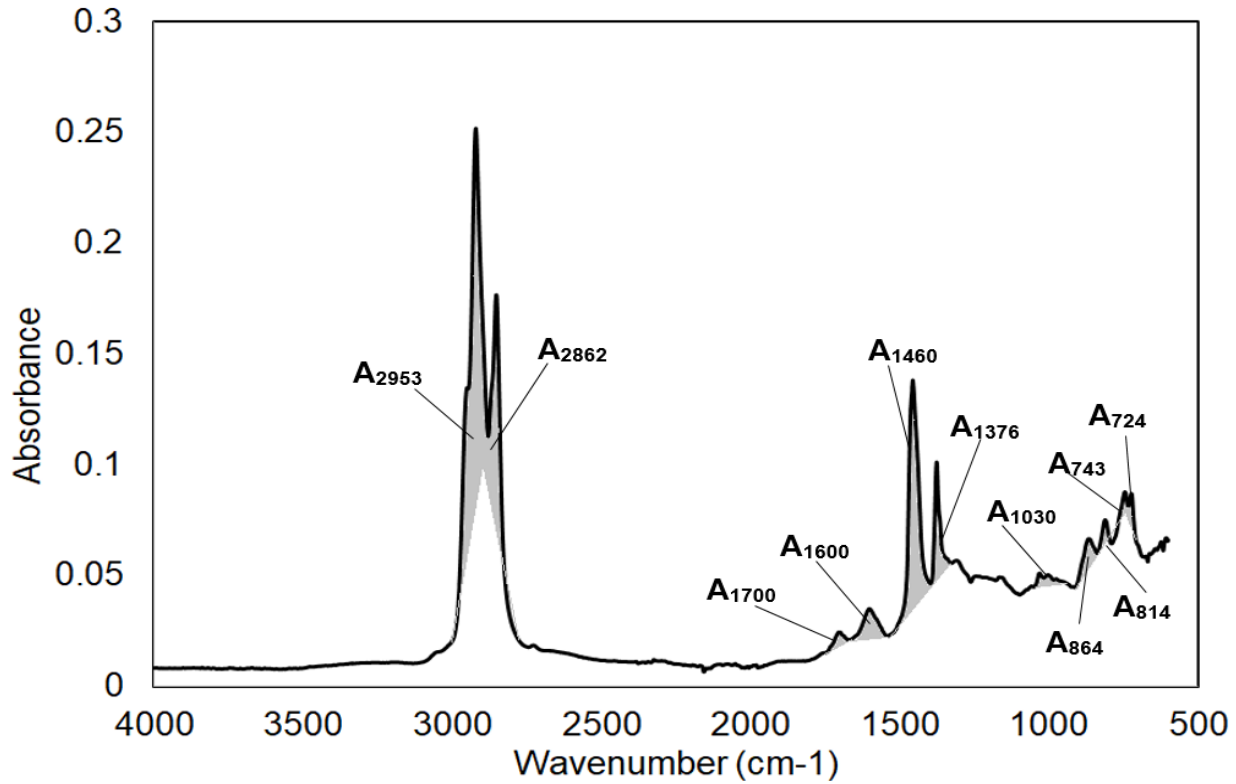


**Figure 4. 10:** Infrared spectrum of an asphalt binder (the colored areas are used for the calculation of specific ageing indices following (Lamontagne et al. 2001).

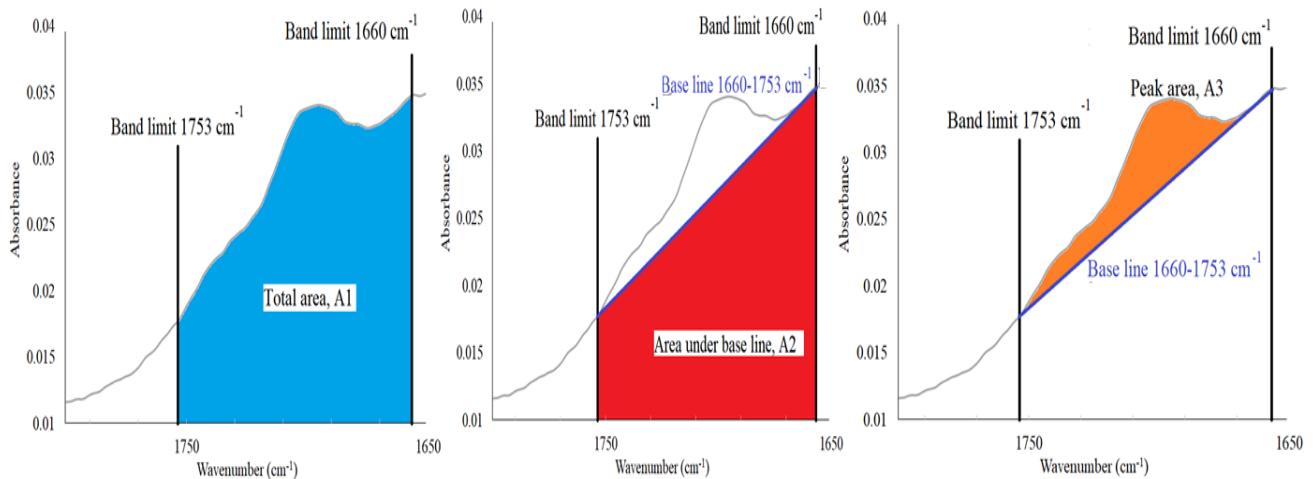


**Figure 4. 11:** Example of a peak area calculation of the band area  $A_{1700}$ .



**Table 4. 2:** Specific functional groups for bituminous binders regarding aging (Lamontagne et al. 2001, Van den Bergh 2011).

Band Area	Band limit (cm <sup>-1</sup> )	Vibration bands	Functional group	Affected by aging
A <sub>724</sub>	710-734	(CH <sub>2</sub> ) <sub>n</sub> Rock (n ≥ 4)	Long chains	No
A <sub>743</sub>	734-783	C-H out of plane bending	Out of plane adjacent	No
A <sub>814</sub>	783-838	C-H out of plane bending	Out of plane adjacent	No
A <sub>864</sub>	838-912	C-H out of plane bending	Out of plane singlet	No
A <sub>1030</sub>	995-1047	S=O stretching	Oxygenated functions - sulfoxide	Yes
A <sub>1376</sub>	1350-1390	C-H bending	Branched aliphatic structures	No
A <sub>1460</sub>	1395-1525	C-H bending	Aliphatic structures	No
A <sub>1600</sub>	1535-1670	C=C stretching	Aromatic structures	No
A <sub>1700</sub>	1660-1753	C=O stretching	Oxygenated functions - carbonyl	Yes
A <sub>2862</sub>	2820-2880	C-H stretching	Stretching symmetric	No
A <sub>2953</sub>	2880-2990	C-H stretching	Stretching aromatic	No

### 4.3.1 FTIR experimental program

The chemical test was carried out by using the Spectrum 100 FTIR spectrometer of Perkin-Elmer as shown in Figure 4.12. The background check and sample were scanned 20 times with the resolution of 4cm<sup>-1</sup>. The test was performed within a wavenumber range of 600 to 4000 cm<sup>-1</sup>. A sample of a normal FTIR-obtained spectrum is presented in Figure 4.13.



**Figure 4. 12:** FTIR spectrometer of Perkin-Elmer.

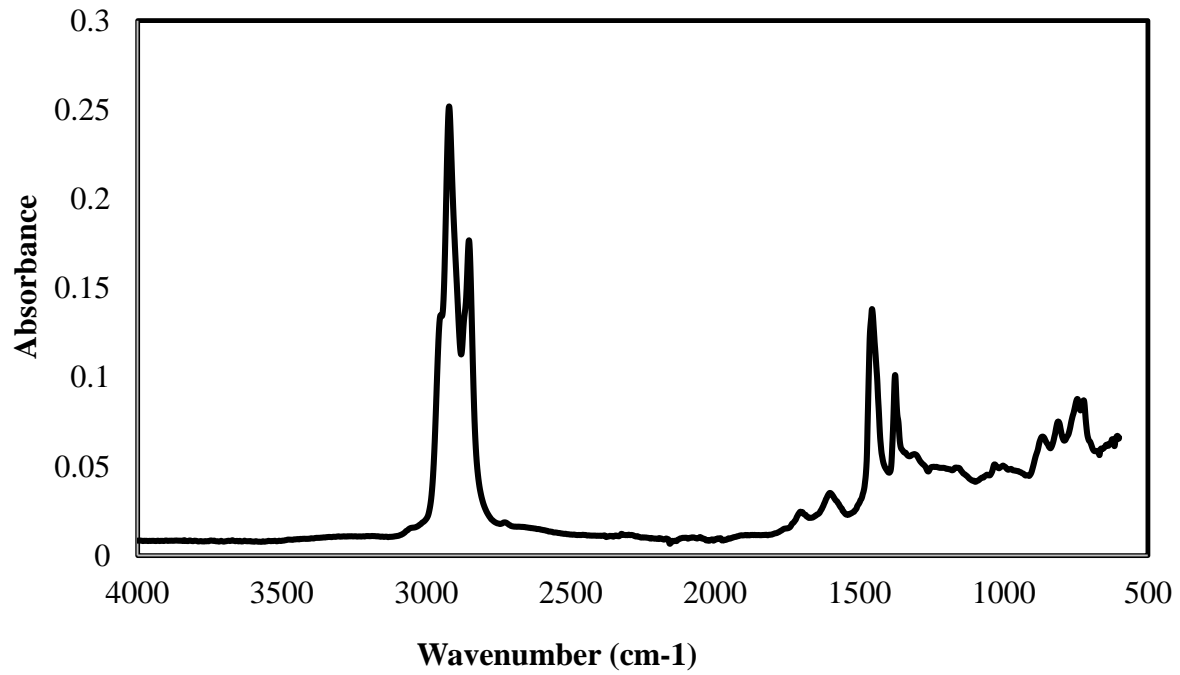


**Figure 4. 13:** Sample of FTIR-obtained spectrum of a bituminous binder.

## 4.4 Results and Analysis

### 4.4.1 Effect of CRM content on the rheological properties

In this part, to only investigate the influence of CRM content on the rheological properties of the binders, the frequency sweep test was carried out on the virgin (unaged) binders (70/100, CRMB-5, CRMB-10, and CRMB-15). Thus, the effect of artificial aging was not considered.

The master curves of the complex shear modulus ( $G^*$ ) and the phase angle ( $\delta$ ) were constructed at a reference temperature of 30°C as shown in Figure 4.14 and 4.15 respectively by using the Time-Temperature Superposition Principle (TTSP) and the equations as mentioned in section 4.2.3 to compare the rheological properties of the binder that interacted with CRM and the base bitumen (70/100).

According to Figure 4.14 and 4.15, it is clear that the binder modification has an obvious effect on the rheological properties of the binders at low loading frequencies (equivalent to high-temperature response). It can be seen that the complex modulus of the binders increased at the higher proportion of CRM. Furthermore, the modification also resulted in an obvious decrease in the phase angle of the CRMBs, especially the CRMB-15. The mentioned results clearly show an increase in stiffness and elastic response of the modified binders, and these effects became stronger at the higher rubber content. The improvement of the elastic response and the modulus can be attributed to the formation of polymer-network within the binder which stiffens the CRMBs. Therefore, the CRM binders can be expected to have a better rutting resistance than the base binder.

However, the effect of CRM concentration seemed to be smaller at high loading frequencies (equivalent to low-temperature). It can be noticed that the curves tend to coincide at high frequencies.

In addition, an isochronal plot of the complex modulus ( $G^*$ ) versus temperature at 10 rad/s for the modified binder is shown in Figure 4.16. Generally, it can be clearly seen that the addition of CRM shows an increase in the value of the complex modulus at high temperatures, but at the low temperature (10°C) where the binder properties are dominated by the characteristics of the base bitumen, both the pure bitumen and CRM binders tend towards the same complex modulus (approximately 10 MPa) regardless of the CRM concentration. As temperature increases, the effect of rubber modification starts to exhibit, and the CRM binders seem to have a better thermal resistance compared to the unmodified as the slopes of complex viscosity versus temperature curves of the modified binders in Figure 4.16 were more gentle than the pure binder.

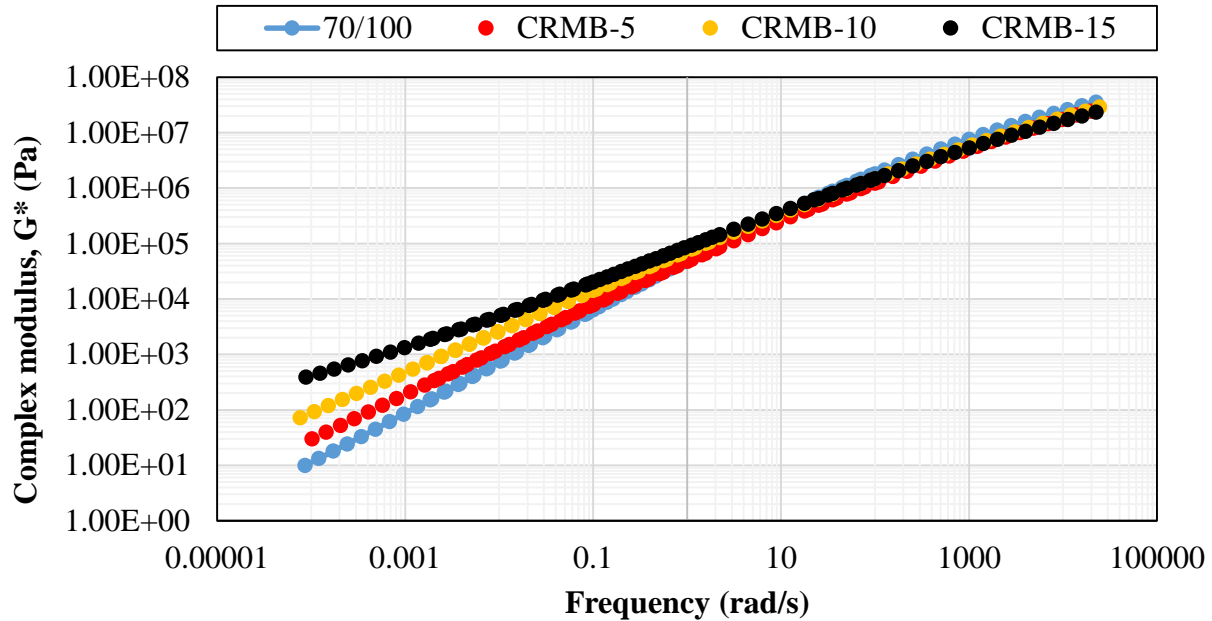


**Figure 4. 14:** Master curves of complex modulus for the unaged binders at a reference temperature of 30°C showing the effect of CRM concentration.

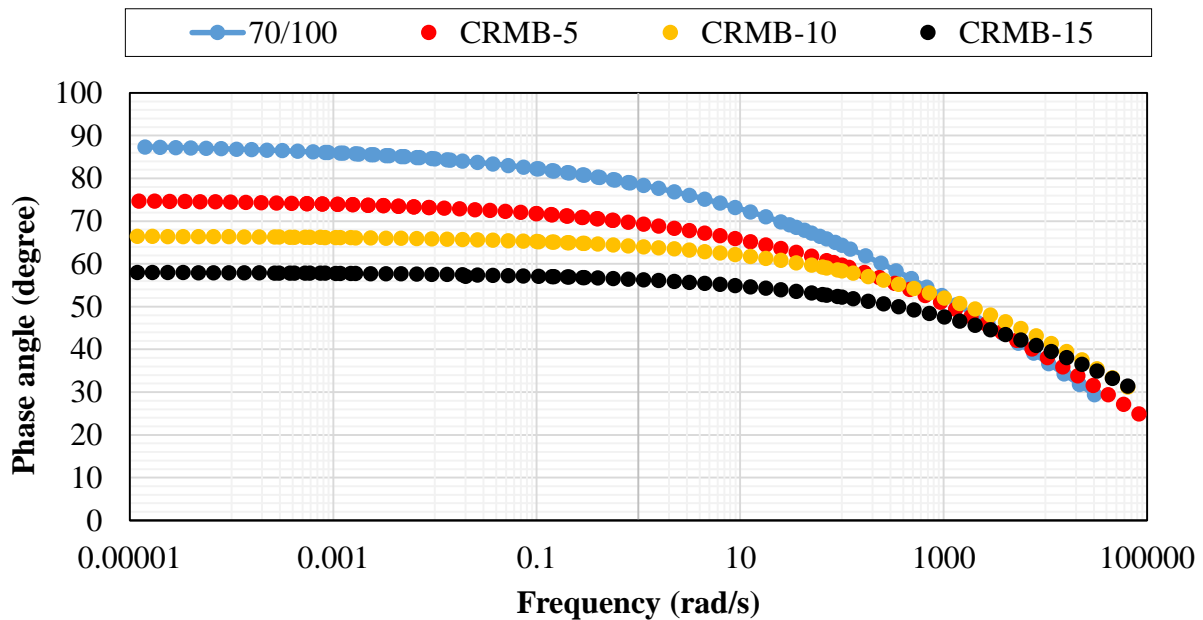


**Figure 4. 15:** Master curves of phase angle for the unaged binders at a reference temperature of 30°C showing the effect of CRM concentration.

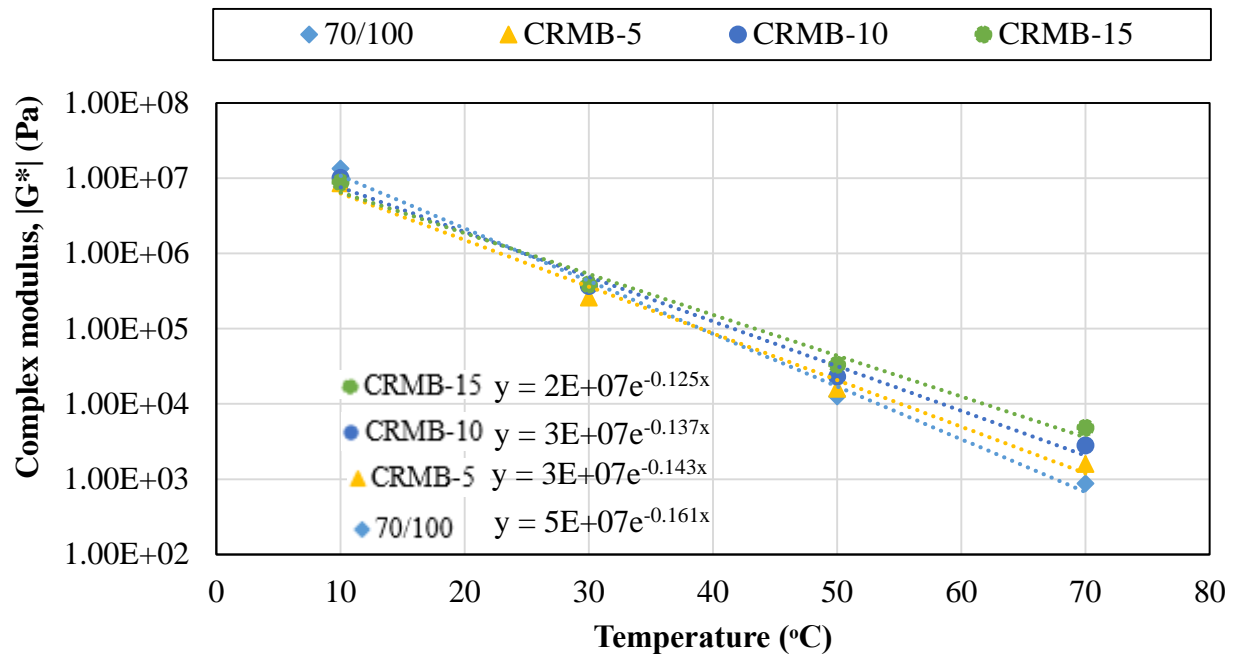
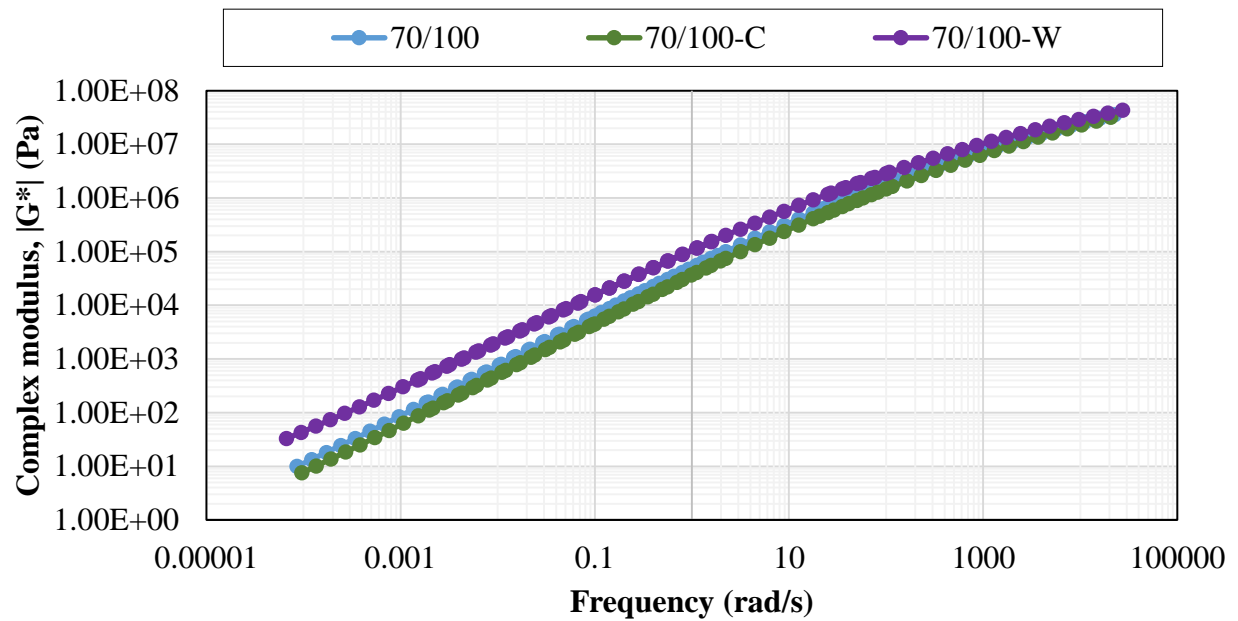


**Figure 4. 16:** Complex modulus versus temperature at 10 rad/s showing the CRM concentration effect.

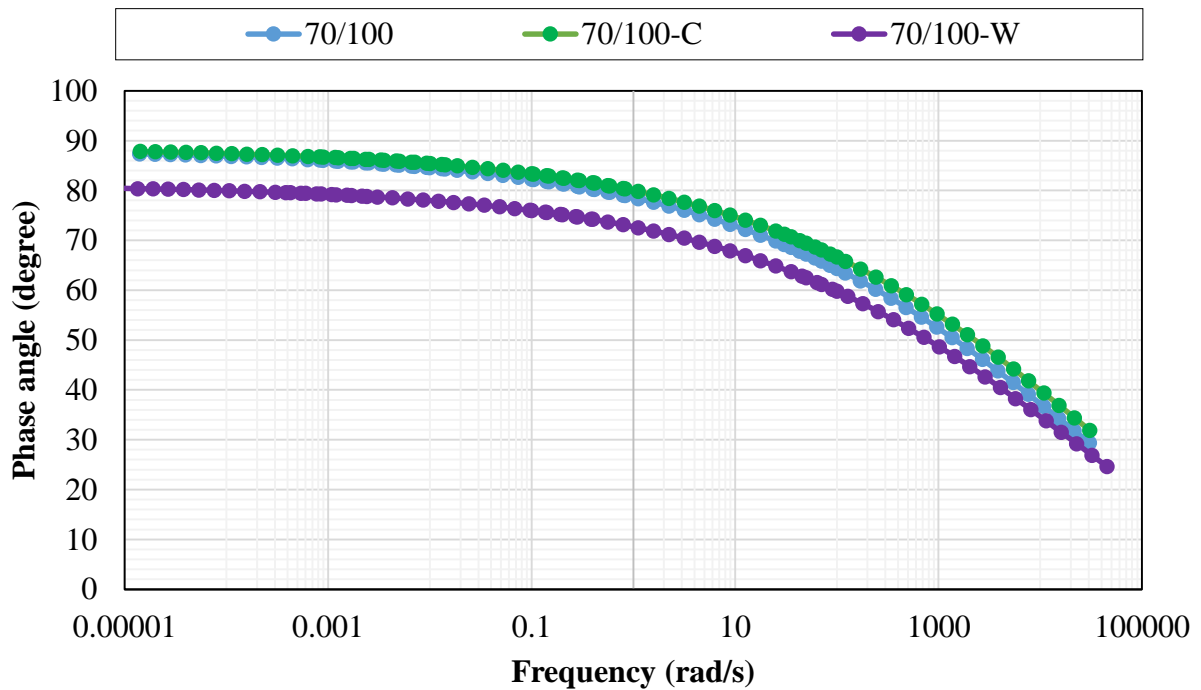
#### 4.4.2 Effect of WMA additives on the rheological properties

Figure 4.17-4.20 show the master curves of the complex modulus and phase angle of the binders containing the WMA additives at the normal road service temperature. In this part, the effect of WMA additives on the rheological properties of both base binder and CRMB is focused on without considering the artificial aging effect.

In the case of the chemical-based warm-mix additive, the curves clearly demonstrate that the additive slightly softened the base binder as evidenced by the reduction of the complex modulus (stiffness) over the whole range of loading frequencies. Moreover, it also lowered the elastic response (increased phase angle) of the base binder. However, the influence of the chemical-base additive on the complex modulus and phase angle of CRMB seems to be less effective as the curves of CRMB-15 and CRMB-15-C are almost identical. On the other hand, the wax-based additive seemed to have an obvious effect on the both unmodified and modified binders at high-temperatures and low frequencies. It is clear that the binders containing the wax additive had a remarkably higher complex modulus than the binders without wax. It is because a crystal lattice structure of wax which was formed at temperatures lower than the wax's melting point (~100°C) stiffens the binders. In addition, an addition of the wax additive can reduce the phase angle of the binders, meaning that the elastic response was improved.



**Figure 4. 17:** Master curves of complex modulus for the unaged binders at a reference temperature of 30°C showing the effect of WMA additives on the base bitumen.



**Figure 4. 18:** Master curves of phase angle for the unaged binders at a reference temperature of 30°C showing the effect of WMA additives on the base bitumen.

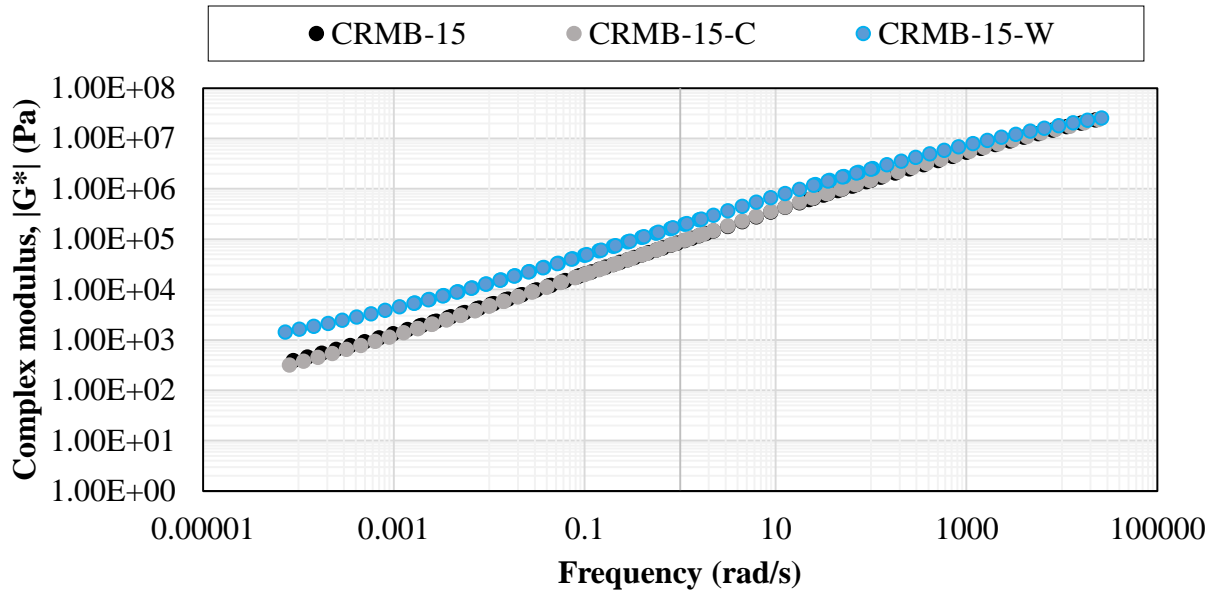


**Figure 4. 19:** Master curves of complex modulus for the unaged binders at a reference temperature of 30°C showing the effect of WMA additives on the CRMB.

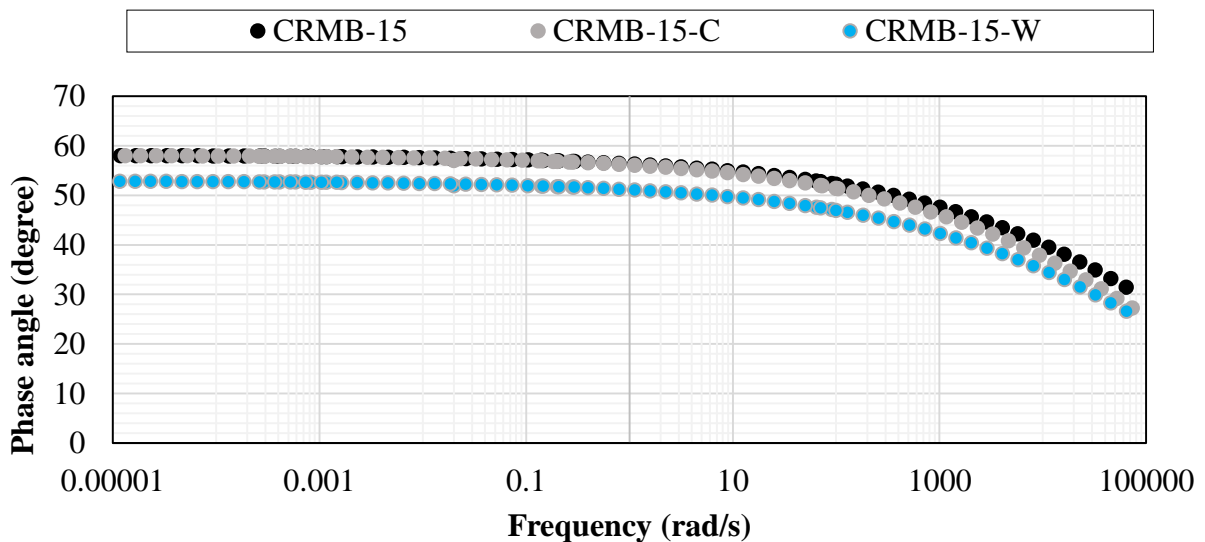


**Figure 4. 20:** Master curves of phase angle for the unaged binders at a reference temperature of 30°C showing the effect of WMA additives on the CRMB.

The effect of the warm-mix additives on the thermal susceptibility of both pure and modified binders are presented in the form of an isochronal plot (Figure 4.21 and 4.22). According to the plots in Figure 4.21 and 4.22, an addition of wax-based additive provided an improvement of thermal susceptibility of both binder types as the slope was smaller than the binders without wax. It was found that the crystallization of wax structure within the binders did not only increased the

stiffness ( $G^*$ ) and decreased phase angle of the binders but also made binders less susceptible to a thermal changing.

Additionally, in the case of the chemical-based additive, its influence on both unmodified and CRM binders seemed to be unnoticeably small because the slopes of the isochronal plots of both binders with and without the chemical additive were almost identical.

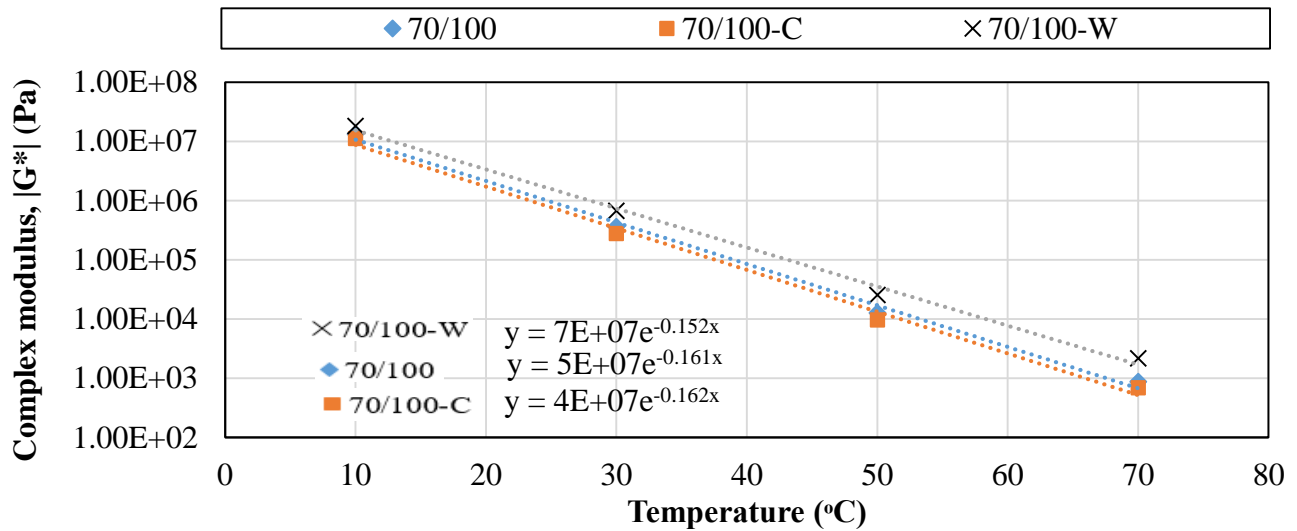


**Figure 4. 21:** Complex modulus versus temperature at 10 rad/s showing the WMA additives effect on the base binder.

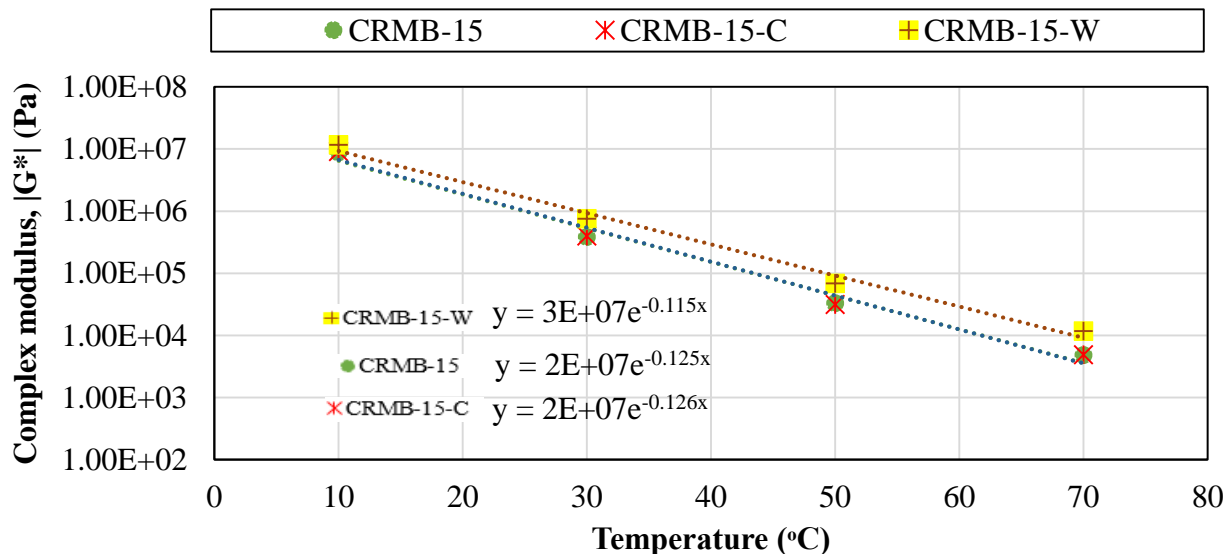


**Figure 4. 22:** Complex modulus versus temperature at 10 rad/s showing the WMA additives effect on the CRM binder.



### 4.4.3 Aging effect on the rheological properties

In this part, the rheological properties of the unaged, short-term aged, and long-term aged binders were compared. Master curves of complex modulus and phase angle for the unaged, short-term aged and long-term aged base bitumen 70/100 at a reference temperature of 30°C are shown in Figures 4.23. Figure 4.24 presents the stiffness index (Equation 4.11) or relative changes of the complex modulus of the study asphalt binders after the short-term and long-term oxidative aging at the frequency of 10 rad/s and at the temperature of 30°C to compare the oxidative aging effect on changes of rheological properties of the binders. Furthermore, the plots of the other binders in this study were also constructed and presented in the Appendix A.

$$\text{Stiffness Index} = \frac{|G_{aged}^*|}{|G_{unaged}^*|} \quad (4.11)$$

According to Figure 4.23, it is clear that the complex modulus (stiffness) of the long-term aged binder was the highest, while the unaged was the lowest. Similarly, the other binders in this study also undergo the same increase of the stiffness after aging (in Appendix A). An increase in stiffness of the binder can be attributed to the formation of Asphaltenes and loss of light molecular weight constituents in bitumen (Lee et al. 2006).

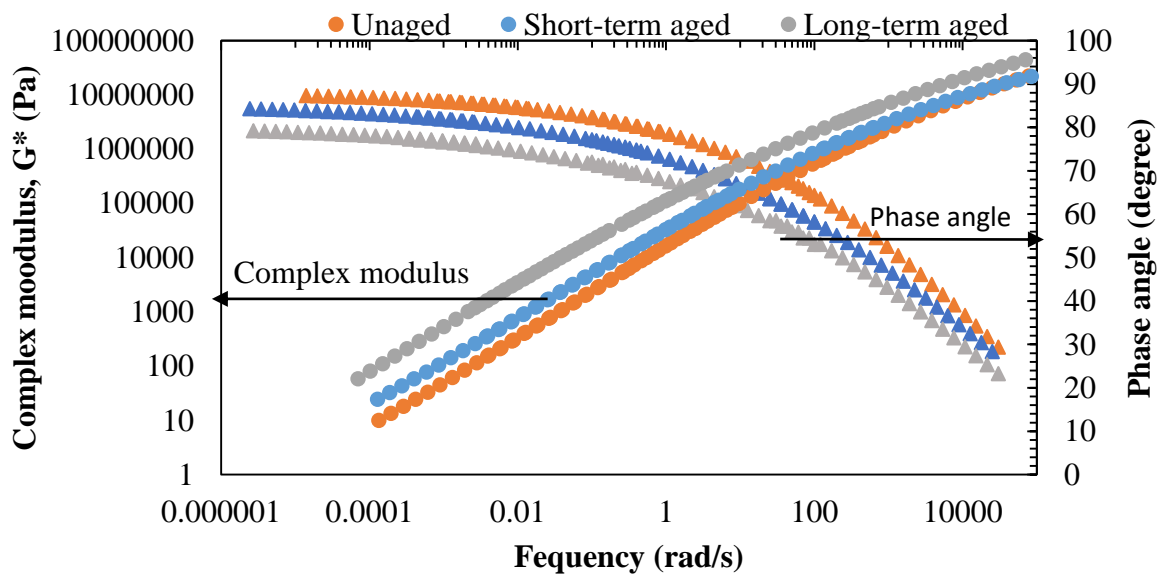


**Figure 4. 23:** Master curves of complex modulus and phase angle for the 70/100 base binder at a reference temperature of 30°C showing the aging effect.

However, it can be observed in Figure 4.24 that the aging effect on the changes of complex modulus (stiffness) of the binders was diverse. The relative changes of modulus reduced as the percentage of CRM increased. The stiffness index in the case of the short-term aging ( $G_{\text{short-term aged}}^*/G_{\text{unaged}}^*$ ) of 70/100 was reduced from 2.03 to 1.98, 1.72, and 1.32 when the %CRM was 5%,

10%, and 15% respectively. The same trend can also be seen in the case of the long-term aging ( $G^*_{\text{long-term aged}}/G^*_{\text{unaged}}$ ) where the stiffness index decreased from 4.31 to 2.08 when 15% of rubber was added.

The chemical-based additive seems to have a negative effect on the aging resistance of the base binder as the stiffness index in both short-term and long-term are higher than the case of the 70/100 binder. However, in the case of the CRM binder, the negative influence of the chemical additive did affect only during the short-term aging period but there was no effect on the long-term aged CRMB sample. This indicated that, based on the complex modulus, an addition of chemical-based WMA additive made both the base and CRM binders more susceptible to the oxidative hardening. In the term of the wax-based warm-mix additive, the relative changes of the base binder stiffness were smaller than the binder without wax, indicating that the wax can improve the aging resistance of the pure bitumen. Additionally, the warm-mix additives effect on the long-term aging resistance of the CRM binder is insignificant as the long-term stiffness index of CRMB-15, CRMB-15-C and CRMB-15-W were about the same.

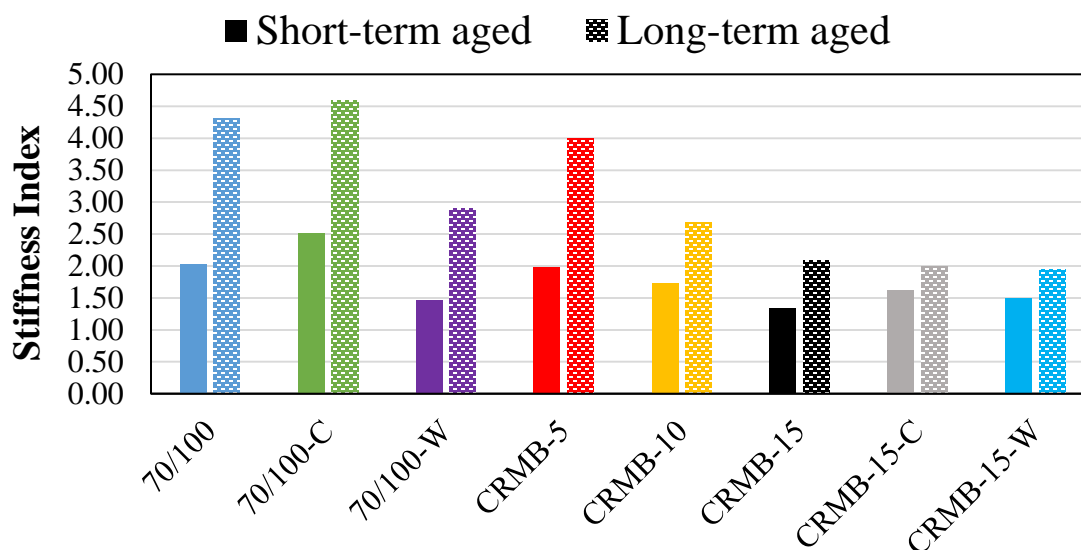


**Figure 4. 24:** Stiffness index of the asphalt binders at 10 rad/s and at temperature of 30°C.

The FTIR spectrometer was employed to scan the bituminous samples at three different aging conditions in order to chemically investigate the effect of CRM content and WMA additives on the aging susceptibility of the study binders. Figure 4.25 show a FITR spectrum of the pure 70/100 bitumen at three aging stages. According to Figure 4.25, it can be observed that there are two functional groups, carbonyl and sulfoxide (in left and right rectangular, respectively), which increased corresponding to the oxidative aging of the asphalt binders. A comparison of carbonyl and sulfoxide indices (calculated in accordance with equation 4.8-4.9) was made to measure the influence of the rubber concentration and the warm-mix additives. Moreover, the carbonyl and sulfoxide indices of the study binders are presented in Figure 4.26-4.28.

However, in order to get the clear picture of the effect of CRM content and the WMA additives on the aging susceptibility of the asphalt binders the oxidation product is defined as a combination of carbonyl and sulfoxide indices at aged-stage divided by the summation of both indices at fresh-stage as shown in an equation 4.12.

$$Oxidation\ product = \frac{(Carbonyl\ index + Sulfoxide\ index)_{aged}}{(Carbonyl\ index + Sulfoxide\ index)_{fresh}} \quad (4.12)$$

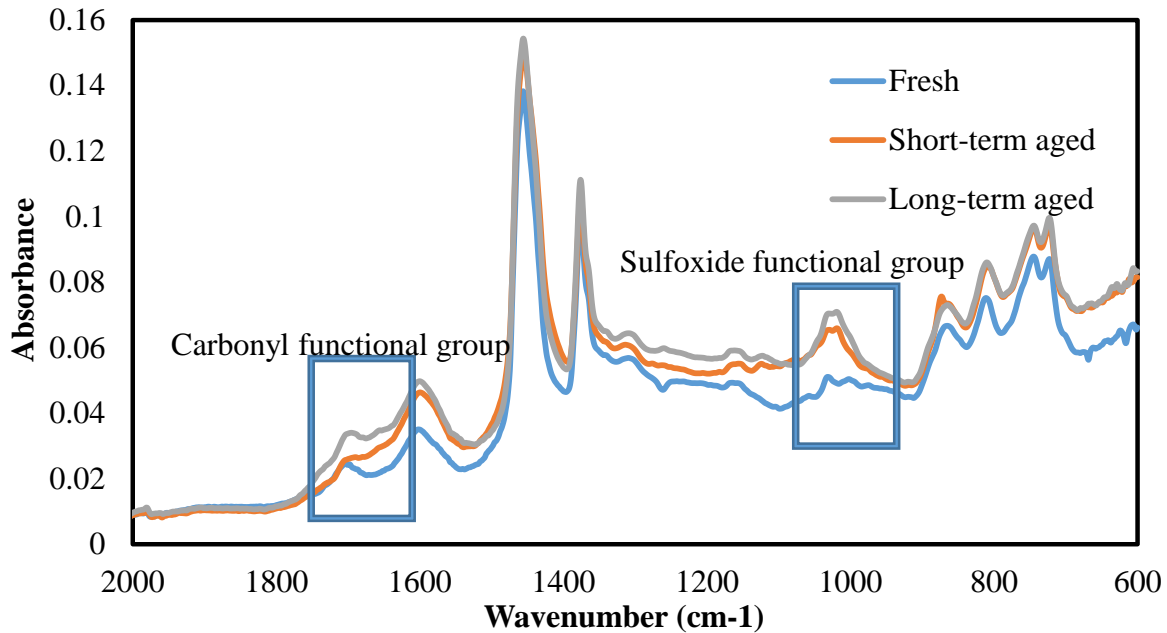


Figure 4. 25: FITR-obtained spectrum of the 70/100 base binder at different aging conditions.

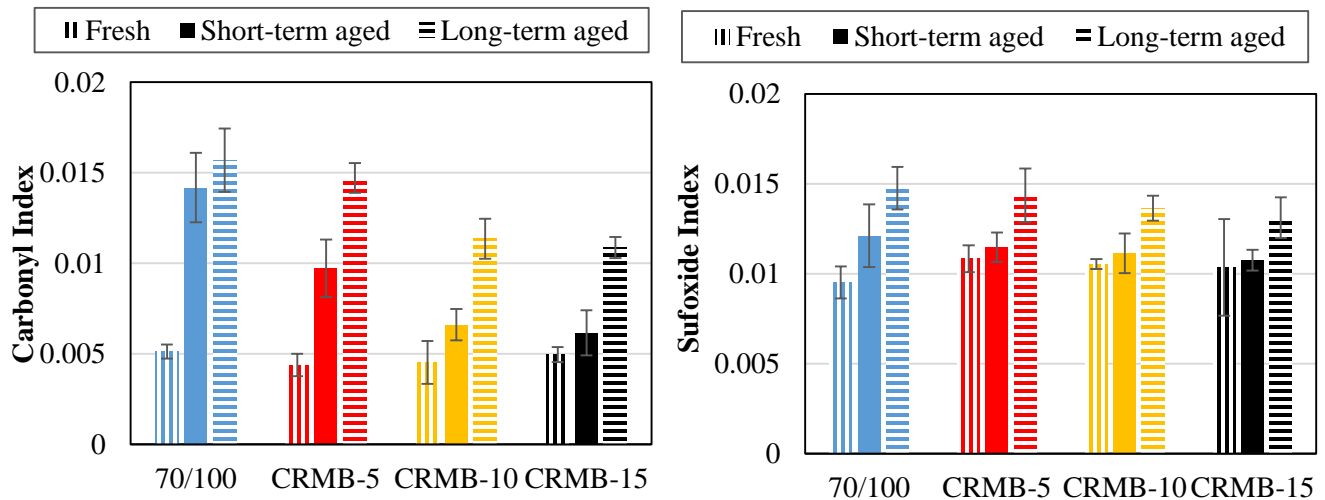


Figure 4. 26: Carbonyl index (left) and sulfoxide index (right) showing the effect of CRM content.

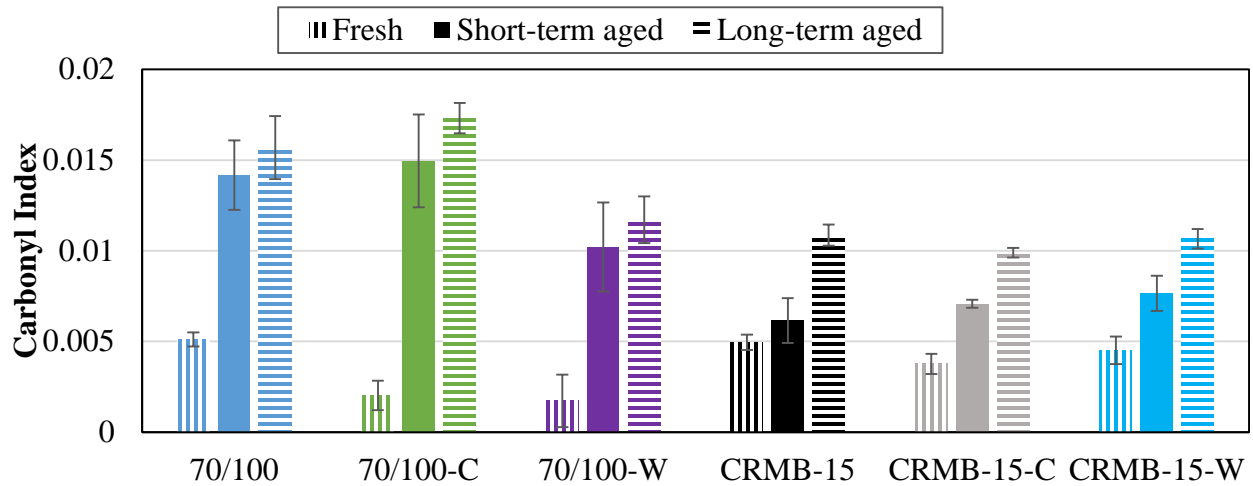


Figure 4. 27: Carbonyl index showing the effect of the WMA additives.

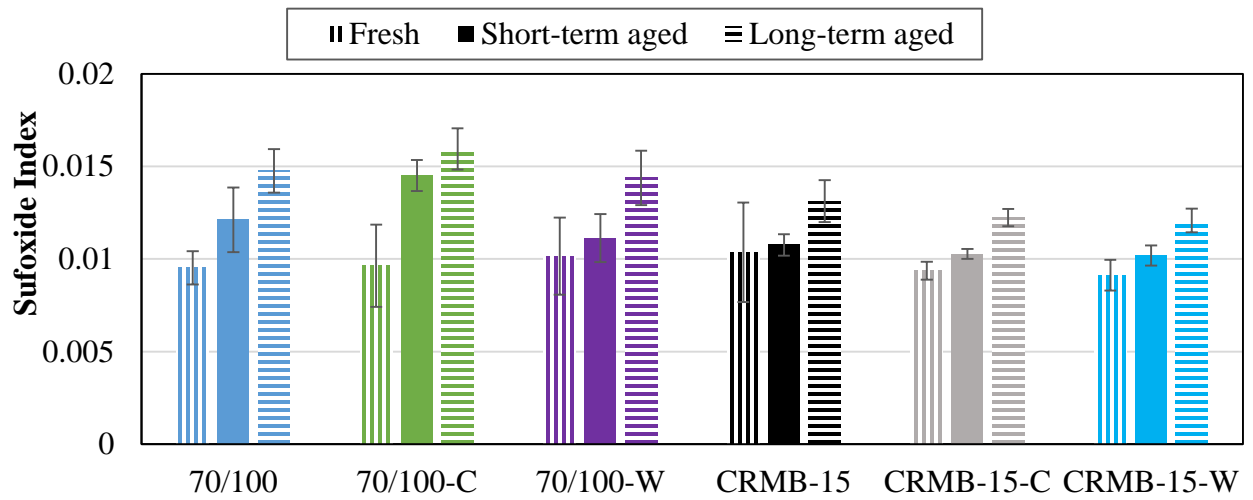


Figure 4. 28: Sulfoxide index showing the effect of the WMA additives.

In general, the value of both indices increased corresponding to the oxidative aging. According to the indices, it is obvious that both indices at both aging stages (short- and long-term aged) were reduced as the CRM concentration increased as evidenced by the smaller values of the indices in Figure 4.26. The rate of oxidation in a function of aging condition of the binders is presented in a form of the oxidation product as shown in Figure 4.29-4.30. According to Figure 4.29, it was found that the rate of formation of the oxidation product was less in the case of the CRMB when compared with the based bitumen, indicating an improved aging susceptibility of the CRM binders which coincides with the mechanical characterization results (stiffness index from frequency sweep test). In other words, the incorporation of rubber and bitumen can lower the aging effect (increase aging resistance) on the performance of the modified binder.

The effect of WMA additives on the aging susceptibility of both unmodified and modified binders are illustrated in Figure 4.27-4.28 and 4.30. It is clear that addition of the chemical-based warm-mix additive negatively affected the base binder as it was found an increase of both carbonyl

and sulfoxide indices of the 70/100-C. The unfavorable effect of the chemical was confirmed by the higher rate of oxidation of both the base and CRM binders. Conversely, the wax seems to improve an aging susceptibility of the base bitumen as the both indices of 70/100-W were reduced. However, the oxidation product indicated that the addition of the wax-based additive did not really improve the aging resistance of the base binder which contradicts the mechanical test result (stiffness index). The stiffening effect of the wax may cause this contradiction between the chemical and mechanical test results (can be seen in Table 4.3). In the case of the CRMB, the wax shows an increase in the carbonyl index at the short-term aged stage. Additionally, based on the oxidation product, the addition of wax also reduced the aging susceptibility of the CRMB as shown in Figure 4.30.

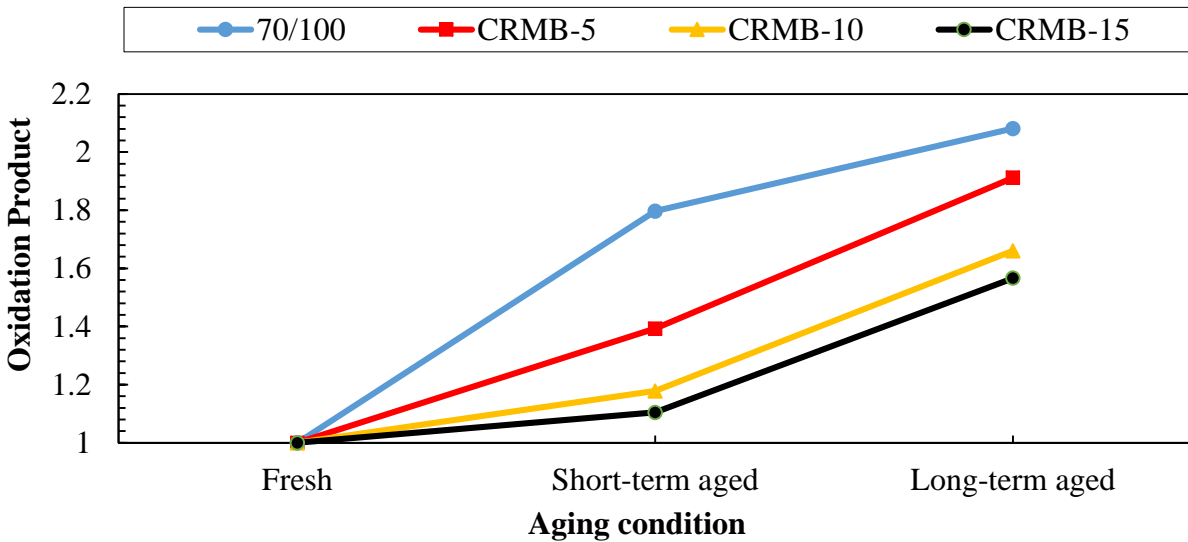


Figure 4. 29: Effect of CRM content on oxidation product.

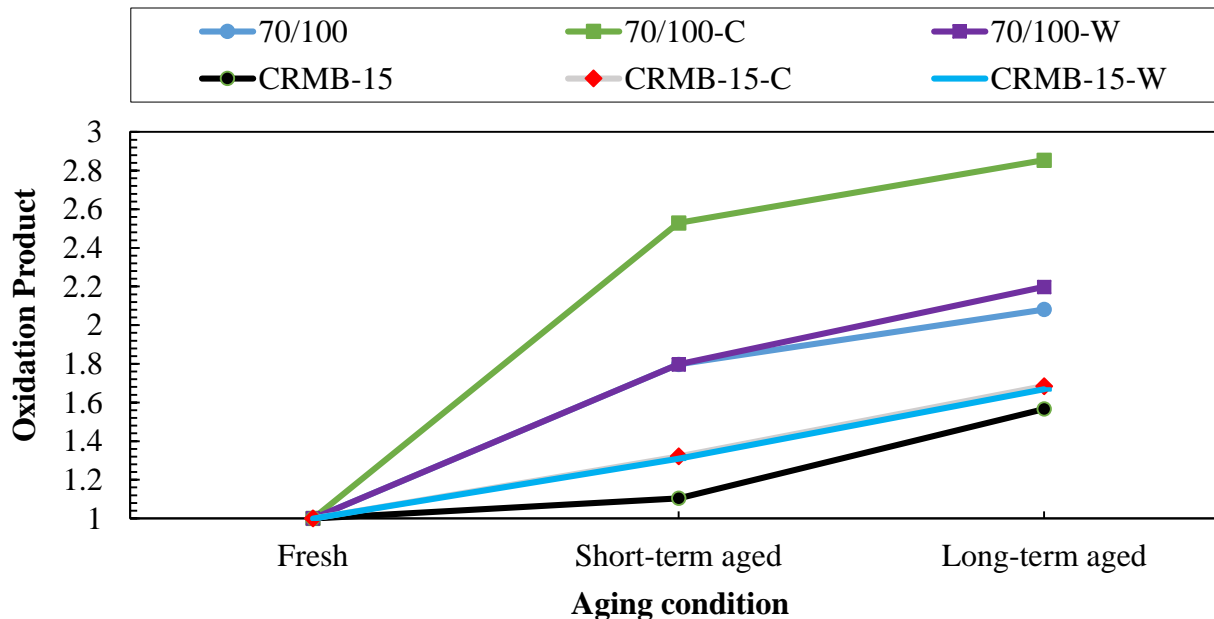


Figure 4. 30: Effect of the WMA additives on oxidation product.

**Table 4. 3:** Comparison between the rheological and chemical aging indices.

Sample code	Short-term aged		Long-term aged	
	Oxidation product (chemical)	Stiffness index (rheological)	Oxidation product (chemical)	Stiffness index (rheological)
70/100	1.80	2.03	2.08	4.31
70/100-C	2.53	2.51	2.85	4.59
70/100-W	1.80	1.46	2.20	2.90
CRMB-5	1.39	1.98	1.91	4.00
CRMB-10	1.18	1.72	1.66	2.68
CRMB-15	1.10	1.34	1.57	2.08
CRMB-15-C	1.32	1.62	1.68	1.98
CRMB-15-W	1.31	1.49	1.67	1.95

## 4.5 Summary

The main purpose of this chapter was to evaluate the effects of CRM concentration, the WMA additives, and the aging effect on the rheological properties of the asphalt binders. All in all, it can be summarized as follow:

- Modification of an asphalt binder with the CRM tends to increase the stiffness (complex modulus) and elastic response of the binder.
- Incorporation with CRM can improve an oxidative aging resistance of the modified binder.
- At 30°C, the wax-based additive can stiffen and improve the elastic behavior of both the unmodified and modified binders. While the chemical-based additive seems to slightly decrease both the complex modulus and phase angles of the binders.
- The binders were hardened by the oxidative aging as evidenced by the increase in complex modulus. Additionally, the phase angles were also reduced when the binders were artificially aged.
- The chemical additive makes the base bitumen more susceptible to the oxidative aging, however, the effect of wax was found to be advantageous to the base binder.
- Based on the stiffness index, both WMA additives insignificantly affected the aging susceptibility of the CRMB, but, according to the FTIR analysis, the addition of the WMA additives decreased aging susceptibility of the modified binder.

# **Chapter 5**

## **High-Temperature Performance Characterization**

## 5.1 Introduction

Rutting or permanent deformation is the major failure mode in flexible pavements at high road service temperatures. Typically, this type of road distress is formed along the pavement's wheel path which can highly affect the safety and driving comfort of road users. Rutting development in the asphalt layer can be generally described as one of these two basic mechanisms namely, consolidation (densification or volume change) of asphalt layer, or shape distortion (plastic flow) which is not associated with volume change.

The type of asphalt binder used in the asphalt mixture is reported to be one of the significant factors affecting the permanent deformation resistance of the mixture. Currently, the SUPERPAVE rutting parameter  $|G^*|/\sin \delta$  is commonly used as an indicator for ranking the binders for their high-temperature performance. However, many studies have recently reported about the inability of the current Performance Grade binder specification (PG) to correctly capture and characterize permanent deformation behavior of asphalt binder, particularly highly modified bitumen such as polymer modified bitumen (Bahia et al. 2001, D'Angelo 2009).

The multiple stress creep and recovery (MSCR) test has been proposed to be a more fundamentally correct test which can be used to measure the accumulated plastic strain in the binder under multiple stress levels of creep stress for a second followed by a recovery period of 9 seconds for 10 cycles at each stress level. The test mechanism makes it possible to capture the rutting susceptibility of the binder by evaluating both recoverable elastic strains, and non-recoverable plastic strains that contribute to permanent deformation of the asphalt mixture under repeated loading situation.

This chapter focusses on quantifying the high-temperature performance of unmodified asphalt binders and CRMB by using the MSCR test. The effect of CRM concentration and the WMA additives on the values of different test parameters has also been evaluated and discussed. This may provide additional benefit in judging the relative performance of CRMB at high service temperature.

## 5.2 Multiple Stress Creep and Recovery Test

### 5.2.1 Background

The idea of characterizing the non-linear response of the binders by using binder creep and recovery testing protocol was originally developed by the National Co-operative Highway Research Program (NCHRP) (Bahia et al. 2001). As a result of the aforementioned idea, the Multiple Stress Creep and Recovery (MSCR) test was proposed to accurately evaluate the rutting susceptibility of both unmodified and polymer modified binders in the non-linear viscoelastic region (D'Angelo et al. 2007, Dongre&D'Angelo 2003). The MSCR test has been validated by various laboratory studies and field investigations (Wang et al. 2014, Radhakrishnan et al. 2018, Saboo et al. 2016).



According to AASHTO T350, in the MSCR test, the DSR device and 25-mm diameter parallel plates are used for conducting the test. The test is usually performed on RTFO-aged samples to simulate the aging after road construction, however, the MSCR can also be conducted on unaged or PAV-aged binder samples. At shear stress level of 100 Pa and 3,200 Pa the binder sample is subjected to 1-second shear loading and then the applied shear stress is removed for 9 seconds allowing the binder to recover as shown in Figure 5.1. At each stress level, the repeated creep and recovery of shear stress is applied for ten cycles. Figure 5.2 illustrates a schematic representation of the MSCR test loading sequence.

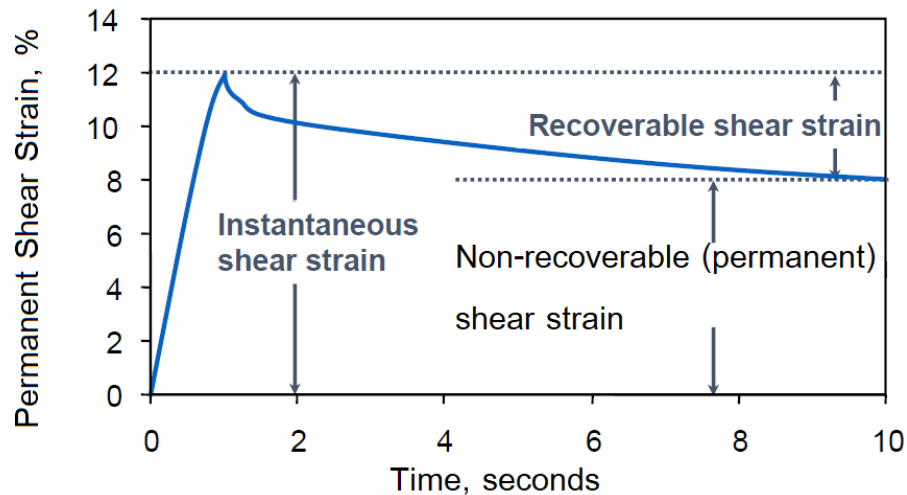


**Figure 5. 1:** A creep and recovery curve for a single cycle (Anderson 2014).

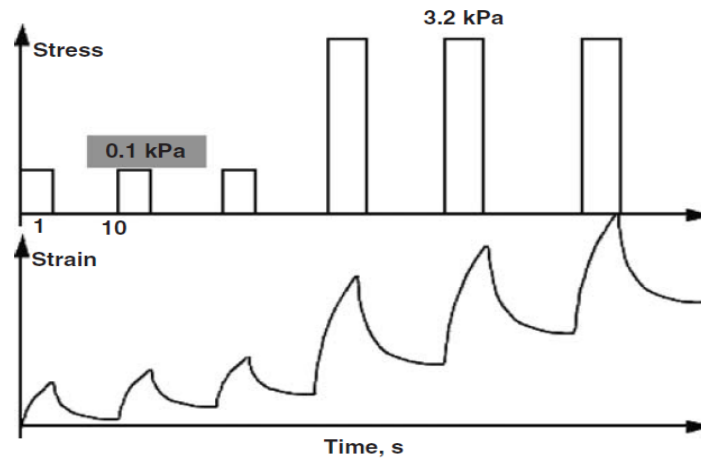


**Figure 5. 2:** schematic representation of the MSCR test loading sequence showing only two stress levels for illustration (D'Angelo 2009).

For each of ten cycles of creep and recovery at each stress levels (0.1kPa and 3.2kPa) the strain values are recorded. These measured values are analyzed to determine the binder's ability to recover under a repeated loading condition and the rutting resistance of the asphalt binders in terms of the average percent recovery (%recovery) and non-recoverable creep compliance ( $J_{nr}$ ),

respectively. The percent recovery of each creep and recovery cycle ( $N=1$  to  $10$ ) at any stress level ( $\sigma$ ) can be calculated by:

$$\%recovery(\sigma, N) = \left( \frac{\varepsilon_1 - \varepsilon_{10}}{\varepsilon_1} \right) \times 100\% \quad (5.1)$$

Where:

$$\varepsilon_1 = \varepsilon_c - \varepsilon_0 \quad (5.2)$$

$$\varepsilon_{10} = \varepsilon_r - \varepsilon_0 \quad (5.3)$$

- $\varepsilon_1$  = the adjusted strain value at the end of creep portion (after 1.0 second) of each cycle  
 $\varepsilon_{10}$  = the adjusted strain value at the end of recovery portion (after 10.0 second) of each cycle  
 $\varepsilon_c$  = the strain value at the end of each creep portion  
 $\varepsilon_0$  = the strain value at the beginning of each creep portion  
 $\varepsilon_r$  = the strain at the end of each recovery cycle

Therefore, the average percentage of recovery at any stress level ( $\sigma$ ) can be obtained from the following formula:

$$\%recovery_{\sigma, average} = \frac{\sum[\varepsilon_r(\sigma, N)]}{10} \text{ for } N = 1 \text{ to } 10 \quad (5.4)$$

Similarly, the average non-recoverable creep compliance at any stress level can be calculated as:

$$J_{nr, \sigma} = \frac{\sum J_{nr}(\sigma, N)]}{10} \text{ for } N = 1 \text{ to } 10 \quad (5.5)$$

Where:

$$J_{nr}(\sigma, N) = \frac{\varepsilon_{10}}{\sigma} \quad (5.6)$$

Moreover, in this test, the stress sensitivity ( $J_{nr, Slope}$ ) of the binders expressed in percentage can also be evaluated by considering difference in the non-recoverable creep compliance between the two different stress levels as follow.

$$J_{nr, Slope} = \frac{J_{nr, 3.2} - J_{nr, 0.1}}{3.2 - 0.1} \times 100\% \quad (5.7)$$

## 5.2.2 Sample preparation and experimental program

In this chapter, Multiple Stress Creep and Recovery (MSCR) test was conducted at  $64^\circ\text{C}$  (the predetermined temperature was stabilized within  $\pm 0.1^\circ\text{C}$  tolerance for 10 minutes) by using Anton Paar Dynamic Shear Rheometer (DSR) with 25-mm diameter parallel plate and a 1-mm gap. The 25-mm diameter samples were pre-molded, and then sandwiched by the 25-mm parallel plates as shown in Figure 5.3. After the required 1-mm binder thickness was achieved, the excess binder was trimmed off by a heated blade. Two stress levels (0.1 and 3.2 kPa) were chosen to characterize the high-temperature rutting properties of the asphalt binder in both linear and in

nonlinear regions in accordance with AASHTO T350. Non-recoverable creep compliance ( $J_{nr}$ ) and percentage recovery (%recovery) of prepared binders (detail given in Table 3.7) were calculated at each stress level and defined temperature to identify the rutting resistant properties, recovery ability, and stress sensitivity of the asphalt binders.

Furthermore, the rutting problem is reported to be critical during the high-temperature conditions of the earlier period of pavement service life, because the asphalt binder is less aged and softer. Thus, in this chapter, the prepared binders at unaged and aged were tested in order to investigate the effect of CRM and WMA additives on the rutting performance before and after the aging of the binders.

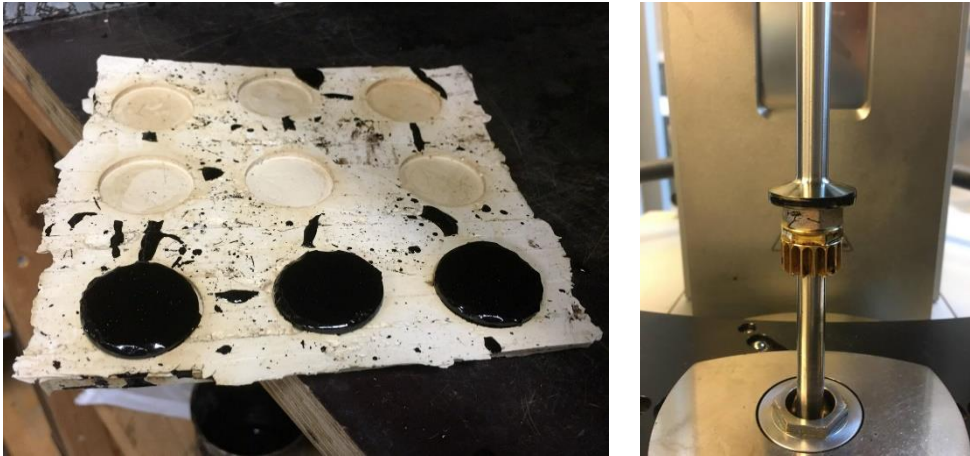


**Figure 5. 3:** Sample preparation and the setup for the MSCR test (25mm plates and 1mm gap).

## 5.3 Results and analysis

### 5.3.1 Effect of CRM content on the high-temperature performance

In this sub-section, the MSCR test was performed on the fresh (unaged) samples, namely 70/100, CRMB-5, CRMB-10, and CRMB-15 in order to solely evaluate the effect of CRM content on the permanent deformation resistance of the binders. The percentage recovery (%recovery), non-recoverable creep compliance ( $J_{nr}$ ) at both stress levels (0.1 and 3.2 kPa), and the stress sensitivity of the binders ( $J_{nr,slope}$ ) are presented in Figure 5.4-5.6, respectively.

According to the MSCR test results shown in Figure 5.4, it is clear that the non-recoverable creep compliance at all stress levels significantly decreased as the rubber content increased, indicating an improved rutting resistance of the crumb rubber modified bitumen. While, a significantly high  $J_{nr}$ -values of the 70/100 indicated a relatively poor resistance to the permanent strain of the base binder. Obviously, it can be seen that crumb rubber modified binders had a considerably higher ability to recover (%recovery) than the unmodified binder at both stress levels. It was found that the CRMB-15 had the largest %recovery-value as compared to the other binders, followed by CRMB-10, CRMB-5, and 70/100 respectively. Moreover, it is worth noting that, at both stress levels, the base bitumen could not recover from the repeated loading situation. It means that the addition of CRM made the asphalt binder capable of resisting higher applied stress levels,

without accumulating unrecoverable deformation. Therefore, it can be summarized that the higher plastic deformation resistance and better recoverability of the modified binders were attributed to the better-interlocked polymer network in the CRMB.

It can be noticed from Figure 5.6 that the CRMB-5 shows the higher stress sensitivity than the neat bitumen, and the  $J_{nr\_slope}$  values were found to be decreased as the rubber content increased. The reason for the increase in the sensitivity value is the polymer chain within the CRMB-5 can be rearranged as the applied stress increased, resulting in more stress sensitive of the CRMB-5. However, in the case of the CRMB-10 and CRMB-15, due to more presence of polymer network formed in the polymer-modified binders so the network becomes more interlocked, therefore, the polymer chain cannot be easily rearranged. An asphalt binder with high value of  $J_{nr\_slope}$  will have a relatively high increasing rate of the permanent deformation at high service temperatures when stress level increases. Thus, a binder with low stress sensitivity is favorable.

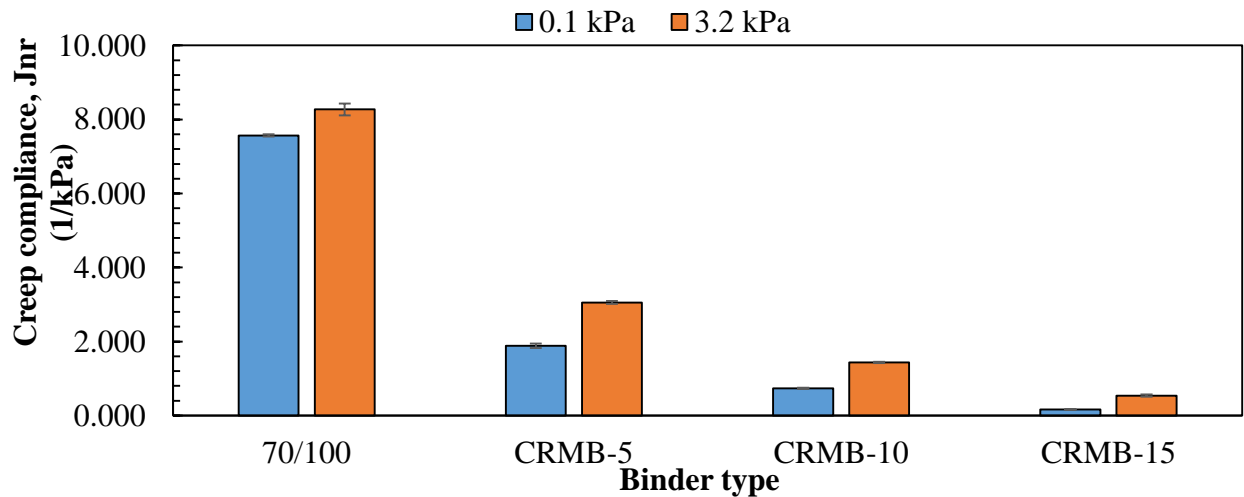


Figure 5. 4: Effect of CRM content on the creep compliance.

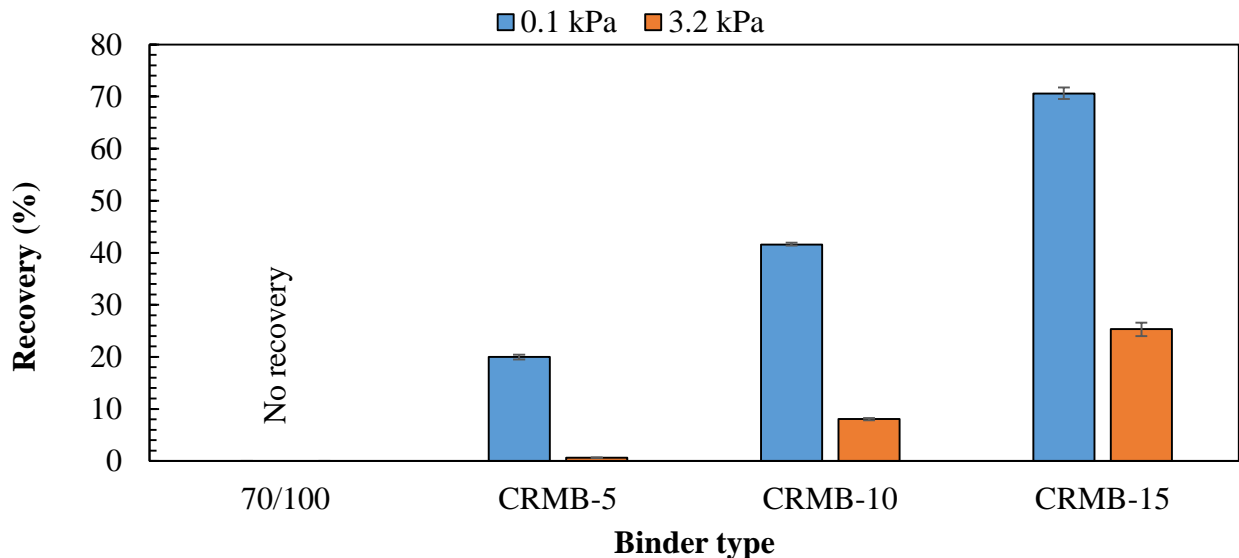
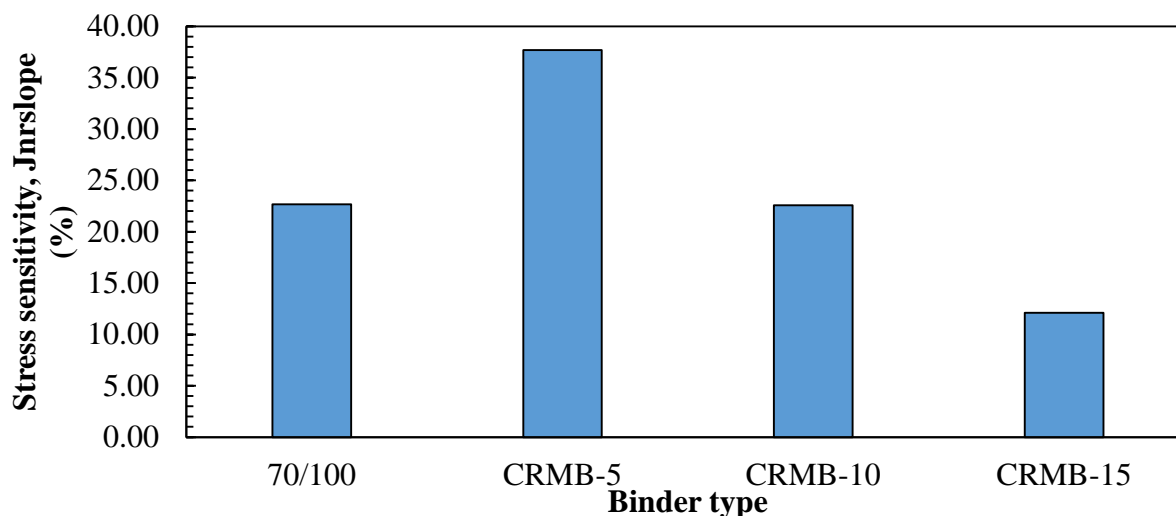


Figure 5. 5: Effect of CRM content on the percent recovery.



**Figure 5. 6:** Effect of CRM content on the stress sensitivity.

### 5.3.2 Effect of WMA additives on the high-temperature performance

In this part, the effects of WMA additives on high-temperature rutting performance of both unmodified binder and CRMB are focused on, thus the test was conducted on the binders without any artificial aging condition. Figure 5.7-5.11 present the effect of WMA additives on the rutting performance of base bitumen and CRMB, respectively.

It can be seen from both Figure 5.7-5.10 that the addition of the wax-based WMA additive positively affected the permanent deformation resistance of both base and CRM binders. In general, the Jnr of the binders was significantly reduced, while the %recovery was notably increased. At low-stress level (0.1 kPa), an addition of wax to 70/100 enormously increased the recoverability from 0% to over 40%. However, it should be noted that, at high-stress level (3.2 kPa Pa), the effect of addition of wax on %recovery of the 70/100-W could not be observed as it was not capable of recovering from the permanent strain under repeated loading condition. In the case of the CRM binder, an addition of wax-based additive also exhibited an improvement of rutting resistance, as the Jnr at 0.1kPa and 3.2 kPa decreased from 0.16 to 0.03 kPa<sup>-1</sup>, and from 0.54 to 0.33 kPa<sup>-1</sup> respectively. Additionally, the elastic response of the CRMB was clearly improved at both stress levels. The improvement of resistance to permanent deformation of 70/100-W and CRMB-15-W was attributed from the crystallization of wax particles which is formed a uniform linked structure when it cools down. This distributed wax-network can highly strengthen the plastic deformation resistance of the binders.

On the one hand, high-temperature permanent deformation resistance of the base bitumen containing chemical-based WMA additive (70/100-C) was improved as evidenced by the reduction of Jnr values around 0.4 kPa<sup>-1</sup> at both stress levels. However, the base bitumen shows no elastic response at both stress levels when mixing with the chemical additive, so, either positive or negative effects of the chemical additive on the ability to recover of base bitumen could not be identified. On the other hand, the addition of the chemical-based WMA additive seemed to have a

negative effect on rutting performance of the CRM binder. It can be noticed that the  $J_{nr}$  values of CRMB-15-C slightly increased from 0.16 to 0.18  $\text{kPa}^{-1}$ , and from 0.54 to 0.59  $\text{kPa}^{-1}$  at 0.1 kPa and 3.2 kPa stress levels respectively. Furthermore, 1-2% of recovery percentage of CRMB was reduced when mixing with the chemical-based additive.

**Figure 5. 7:** Effect of the WMA additives on the creep compliance of the base binder.

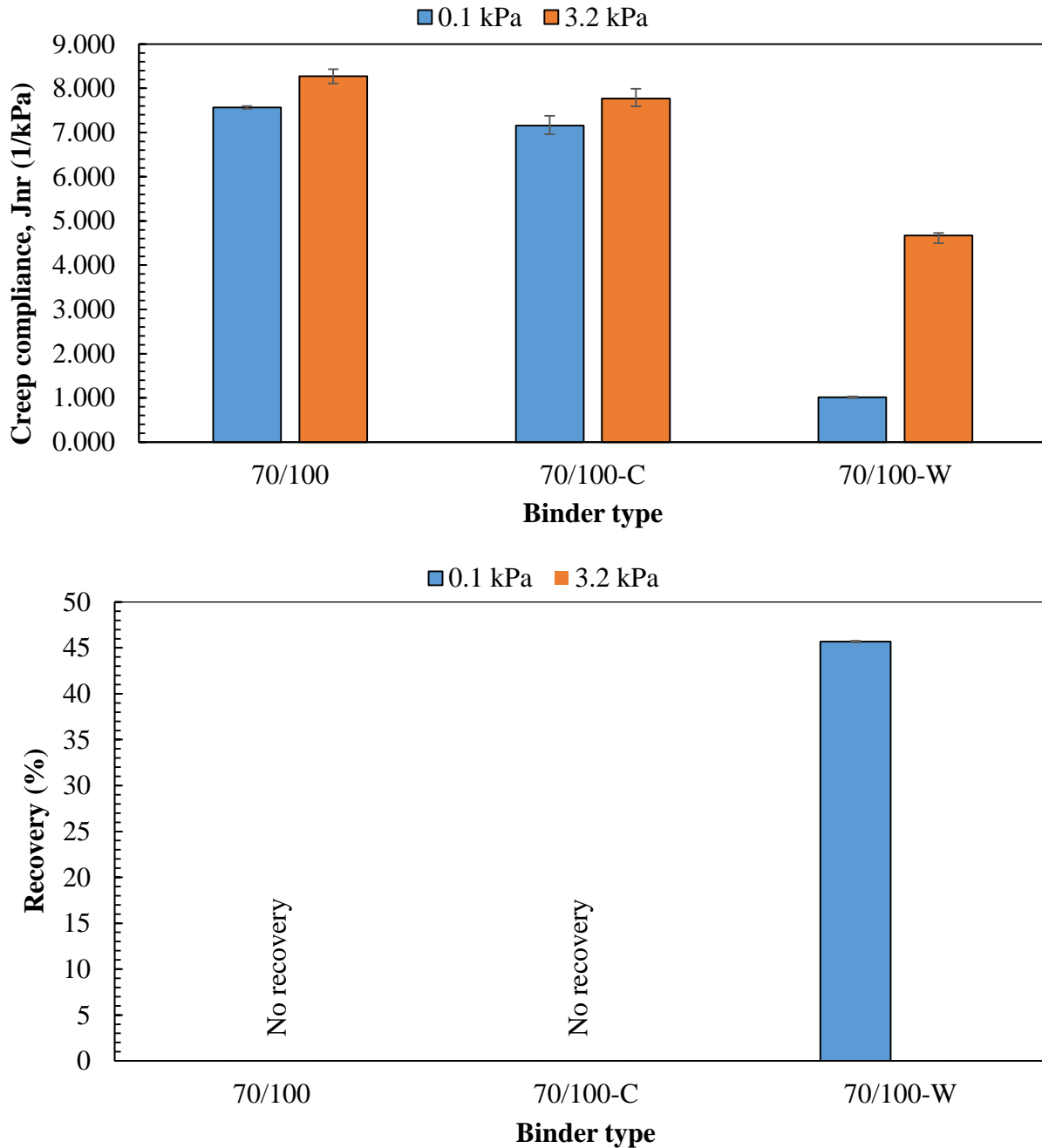


**Figure 5. 8:** Effect of the WMA additives on the percent recovery of the base binder.

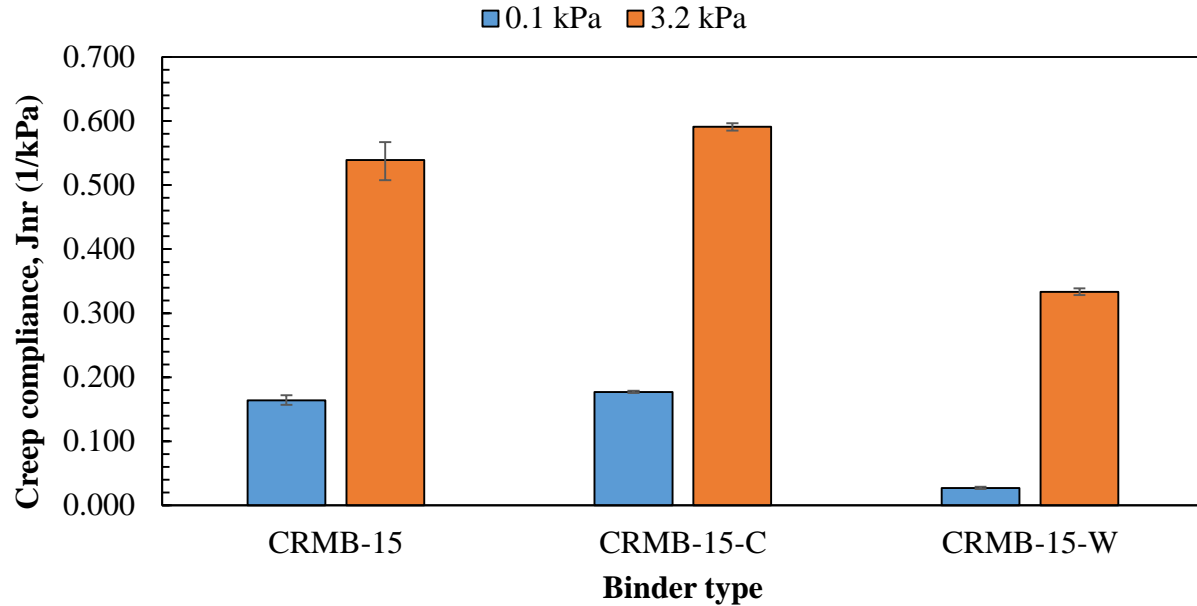


**Figure 5. 9:** Effect of the WMA additives on the creep compliance of the CRMB.

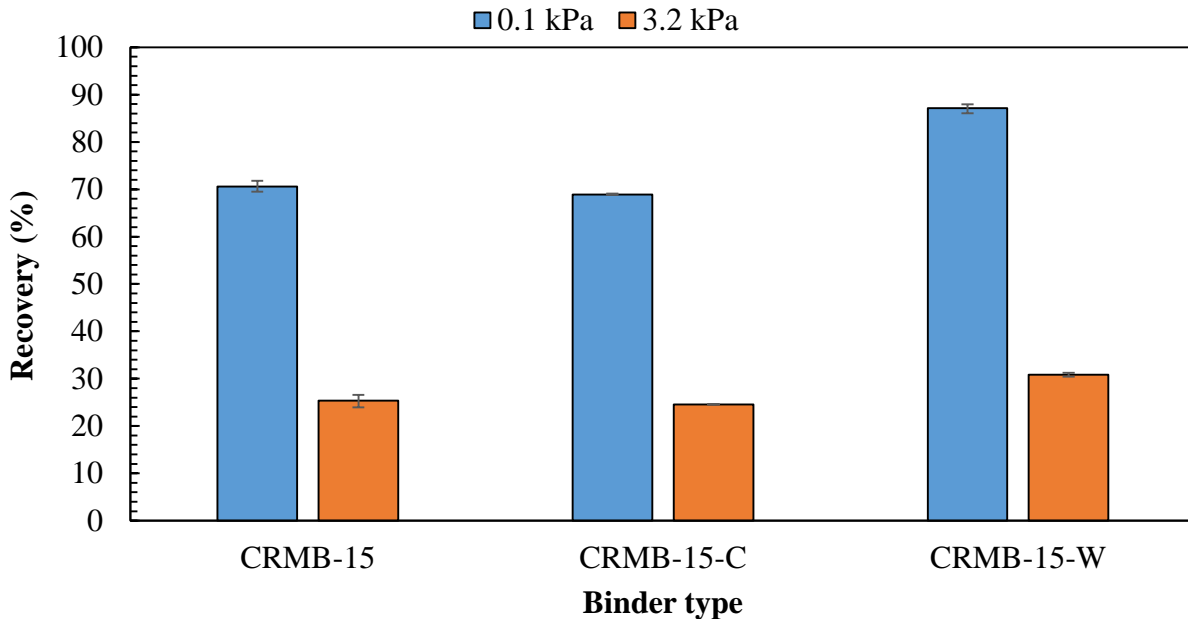


**Figure 5. 10:** Effect of the WMA additives on the percent recovery of the CRMB.

The stress sensitivity of both unmodified and modified binders was also influenced by the WMA additives, especially in the case of the wax-based additive. Apparently, the addition of wax considerably increased the stress sensitivity of the base binder, as the  $J_{nr,slope}$  rose from 22.63% to 118.08%. However, in the case of the CRMB, the wax slightly reduced the stress sensitivity of the modified binder. Although the effect of wax was obvious but the effect of the chemical-based additive on the stress sensitivity of the binders was inconsiderable.

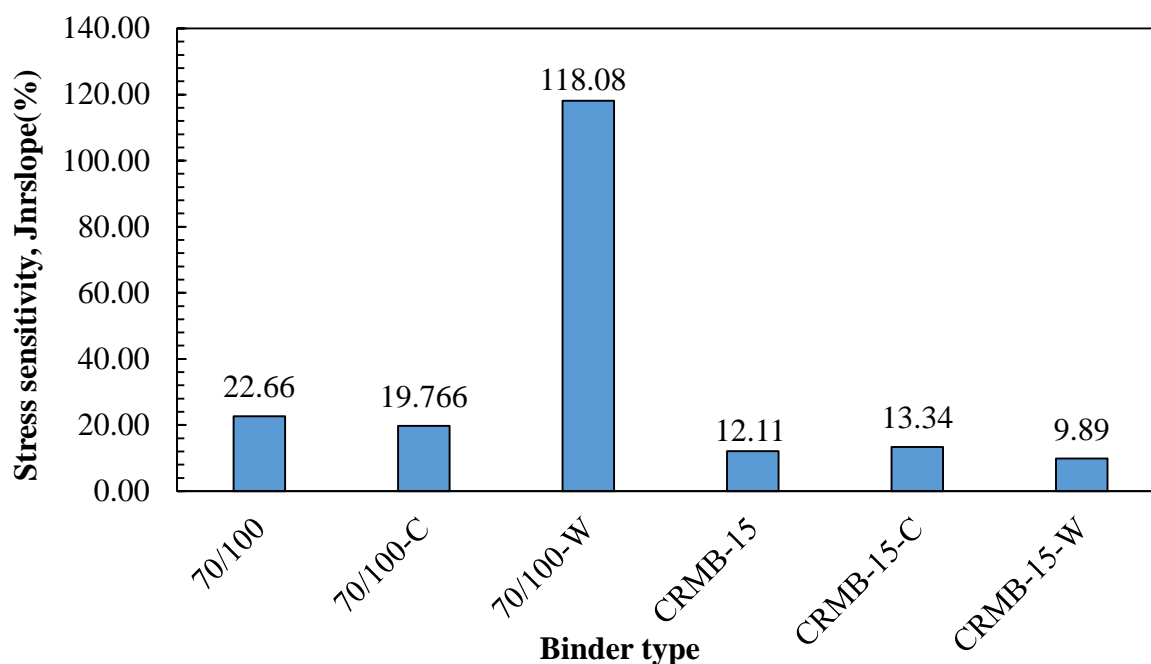


**Figure 5. 11:** Effect of the WMA additives on the stress sensitivity.

### 5.3.3 Effect of aging on the high-temperature performance

As mentioned earlier, the aging of asphalt binders is one of the important factors influencing the final performance of the binders, therefore, in this section, changes of the high-temperature performance of the binders before and after aging simulations were observed. The performance of the aged samples was tested and compared to the unaged binders. Furthermore, the combined effects of CRM percentage and WMA additives were also taken into account. The average values of MSCR test results of both unaged and aged binders are shown in Table 5.1. From the presented data, it can be clearly seen that the binders that were modified with both CRM and/or WMA additives outperformed the unmodified binder. In general, it was observed that the aged binders show the higher rutting resistance than the fresh binders, as evidenced by Table 5.1 showing the smaller value of the average unrecoverable creep compliance ( $J_{nr}$ ), and superior average percent recover (%recovery) at all stress levels.

According to the test results, generally, it can be seen that all binders became less dependent on the stress changes when aged. It is obvious that the 70/100-W was the most sensitive to the applied stress level, as it exhibited the highest stress sensitivity value ( $J_{nr, slope}$ ). While, the CRMB-15-W shows the lowest stress sensitive response, indicating that the microcrystalline structure of wax particles which was formed at a temperature below the melting point of wax ( $\sim 100^{\circ}\text{C}$ ) only influenced the stress dependency of the base bitumen. On the one hand, the stress dependency of the binders increased when incorporated with the CRM as the polymer network within the binder (from the asphalt-rubber interaction) can be rearranged substantially when the applied stress level goes higher as mentioned in topic 5.3.1. On the other hand, the sensitivity of the modified was



reduced when the polymer chain became more interlocked at higher rubber content. Moreover, the chemical-based additive seemed to have no significant effect on the stress sensitivity of the binders.

**Table 5. 1:** Summary of MSCR test results of fresh and aged binders.

Sample code	Stage	Jnr (1/kPa)		Jnr, slope (%)	Percent recovery (%)	
		0.1 kPa	3.2 kPa		0.1 kPa	3.2 kPa
70/100	unaged	7.568	8.271	22.66	0.00	0.00
	short-term aged	3.489	3.938	14.48	1.55	0.00
	long-term aged	0.937	1.093	5.04	10.01	2.80
70/100-C	unaged	7.157	7.770	19.77	0.00	0.00
	short-term aged	3.323	3.778	14.67	1.52	0.00
	long-term aged	1.191	1.390	6.42	7.88	1.53
70/100-W	unaged	1.013	4.674	118.08	45.69	0.00
	short-term aged	0.602	2.478	60.53	45.78	0.18
	long-term aged	0.241	0.692	14.54	45.03	8.37
CRMB-5	unaged	1.884	3.053	37.69	19.99	0.64
	short-term aged	1.336	1.780	14.33	22.35	3.73
	long-term aged	0.403	0.605	6.51	40.21	18.01
CRMB-10	unaged	0.733	1.433	22.58	41.58	8.04
	short-term aged	0.466	0.914	14.45	48.12	15.47
	long-term aged	0.219	0.349	4.19	55.36	33.26
CRMB-15	unaged	0.164	0.539	12.11	70.58	25.35
	short-term aged	0.142	0.413	8.75	76.32	32.45
	long-term aged	0.140	0.327	6.04	76.34	38.79
CRMB-15-C	unaged	0.177	0.591	13.34	68.87	24.58
	short-term aged	0.172	0.462	9.34	73.57	29.89
	long-term aged	0.190	0.318	4.13	61.74	38.11
CRMB-15-W	unaged	0.027	0.333	9.89	87.17	30.82
	short-term aged	0.022	0.192	5.50	91.44	41.66
	long-term aged	0.059	0.143	2.73	72.8	47.36

Based on the specification given by Asphalt Institute (Table 5.2), the base bitumen with and without WMA additives (70/100, 70/100-C, and 70/100-W) after the short-term aging simulation were found to be suitable for standard traffic condition where the minimum value of Jnr is specified as  $2.0 \text{ kPa}^{-1}$ . The appropriate binder for “Heavy” and “Very Heavy” traffic conditions are the CRMB-5 and CRMB-10, respectively. While, the crumb modified bitumen with 15% rubber content with and without WMA additives (CRMB-15, CRMB-15-C, and CRMB-15-W) could be used for locations with “Extremely Heavy” traffic conditions.

**Table 5. 2:** Asphalt Institute Specification for Jnr at different traffic level (Asphalt institute 2010).

Jnr (3.2kPa)	Temperature (°C)	Traffic	ESALs
≤4.0	64	Standard	<10 million and standard traffic loading*
≤2.0		Heavy	10-30 million or slow moving traffic loading**
≤1.0		Very Heavy	>30 million or standing traffic loading***
≤0.5		Extremely Heavy	>30 million and standing traffic loading

Note: \* Standard traffic -- where the average traffic speed is greater than 70km/h

\*\*Slow traffic -- where the average traffic speed ranges from 20km/h to 70km/h

\*\*\*Standing traffic-- where the average traffic speed is less than 20km/h

From the point of high-temperature performance, it is clear that the aging of the asphalt binders positively affected both modified and unmodified binders in this study. However, the aging effect on the binders was also influenced by the CRM and WMA factors. Table 5.2 displays clear decreases in differences of Jnr-value between fresh and aged binders with an increase in CRM percentages. The 15% rubber-concentration binder exhibited the smallest changes of Jnr-value before and after aging. While, in the case of the 70/100 binder, the largest change of Jnr-value was found. However, in the case of the binders containing WMA additives the effect of additives on the aging resistivity was doubtful. In order to get a clear picture of the influences of CRM concentration and WMA additives on the aging effect, therefore, an attempt has been made in this study to evaluate the aging index value at different CRM values and WMA additives based on their creep compliance values at 3.2 kPa stress level. Jnr index of binders was calculated using the following equation (5.8), and plotted as shown in Figure 5.12. A higher value of Jnr index indicates a higher degree of susceptibility towards aging effect and vice versa.

$$\text{Jnr Index} = \frac{J_{nr,3.2kPa-Unaged}}{J_{nr,3.2kPa-Aged}} \quad (5.8)$$

Where:

$J_{nr,3.2kPa-Unaged}$  = Non-recoverable creep compliance value of unaged binders at 3.2 kPa

$J_{nr,3.2kPa-Aged}$  = Non-recoverable creep compliance value of short-term aged binders at 3.2 kPa

According to the plot (Figure 5.12), it is observed that the Jnr index values decrease at a higher proportion of CRM in the binders, meaning that the binders are less susceptible to aging effect as the CRM percentage was more concentrated. The reason is the aging (hardening) of the binder is a process of oxidation and loss of volatile (lightweight) constituents in bitumen. This hardening is attributed to the formation of high molecular weight molecules (asphaltenes), which increases stiffness and viscosity of the asphalt binder (Lee et al. 2006). Theoretically, the interaction of

rubber-bitumen is increased at a higher proportion of CRM in the binder, which results in larger amount of lightweight component absorbed into swollen rubber particles. During the aging process, the low molecular weight constituents that were earlier absorbed by the rubber were ejected into bitumen, resulting in a lower rate of asphaltenes formation (Lee et al. 2011). Therefore, the aging process of the CRMB at higher CRM concentration was reduced.

The influence of the wax additive on the short-term aging resistance of the base binder and CRMB was found to be opposite. According to Figure 5.12, it is clear that the wax slightly improved short- and long-term aging resistances of the 70/100 as evidenced by the lower Jnr index of 70/100-W. Conversely, the aging effect on rutting performance of CRMB containing the wax additive (CRMB-15-W) was relatively higher than the CRMB-15, meaning that the wax increased the aging susceptibility of the CRM binder. In case of chemical additive, an addition of the chemical-based WMA-additive had inconsiderable effect on short-term aging susceptibility of both the base bitumen and CRMB, as the value of the Jnr index of 70/100-C and CRMB-15-C were almost identical to the Jnr index of 70/100 and CRMB, respectively. However, the smaller Jnr index at the long-term aged stage of the 70/100-C compared with the 70/100 shows that the chemical additive positively improved the long-term aging resistance of the base bitumen, but the adverse effect was found in the case of the modified binder (70/100-C).

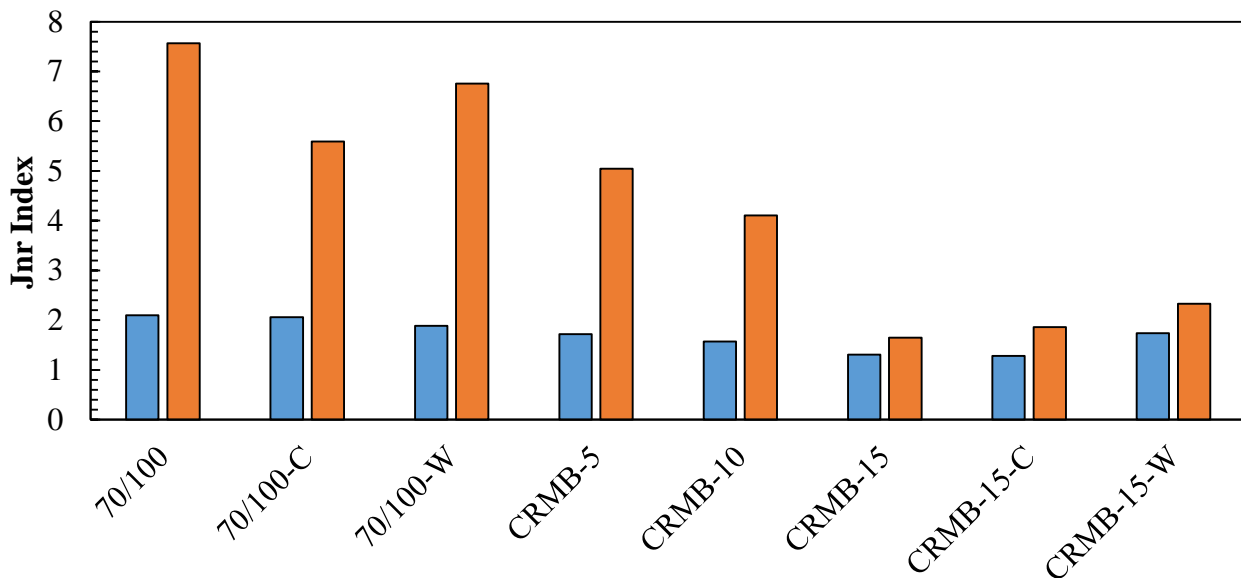


**Figure 5. 12:** Effect of CRM content and the WMA additive on the Jnr index.

### 5.3.4 Comparison of rutting parameters

Table 5.3 presents a comparison between the SUPERPAVE rutting parameter ( $G^*/\sin [\delta]$ ) and the MSCR parameters (Jnr and Recovery). The high-temperature rutting performance of the studied binders were classified based on the SUPERPAVE and MSCR parameters. According the test results, it is clear that the Jnr and Recovery provided the similar ranks of the binder rutting resistance, whereas the  $G^*/\sin (\delta)$  ranked the high-temperature performance differently in some

cases. It is because the MSCR test was intentionally developed to characterize the high-temperature permanent deformation resistance of the binders beyond the LVE, while the  $G^*/\sin(\delta)$  parameter was simply obtained within the LVE. Based on the previous literatures (section 2.5.1), the MSCR results were found to have better correlations to the rut depths of the real mixtures than the  $G^*/\sin(\delta)$ , especially in the case of modified asphalt binders. It is due to the rutting of the pavement is a non-linear failure phenomenon and thus the parameter evaluated within the LVE may not truly relate to the actual rutting performance of the asphalt mixtures. Therefore, the ranking of the non-linear response of the binders is more representative to the real high-temperature performance of the asphalt binder.

**Table 5. 3:** rutting properties of the short-term aged binders at 64°C

Sample code	Rheological properties test	MSCR test		Ranking		
	$G^*/\sin(\delta)$ (kPa)	Jnr, <sub>3.2kPa</sub> (1/kPa)	Recovery, <sub>3.2kPa</sub> (%)	$G^*/\sin(\delta)$	Jnr, <sub>3.2kPa</sub>	Recovery
70/100	2.985	3.938	0.00	7	8	7-8
70/100-C	2.976	3.778	0.00	8	7	
70/100-W	8.937	2.478	0.18	4	6	6
CRMB-5	5.054	1.780	3.73	6	5	5
CRMB-10	8.253	0.914	15.47	5	4	4
CRMB-15	10.776	0.413	32.45	3	2	2
CRMB-15-C	13.518	0.462	29.89	2	3	3
CRMB-15-W	31.384	0.192	41.66	1	1	1

## 5.4 Summary

The main point of this chapter is to experimentally characterize the high-temperature performance of the unmodified and crumb rubber modified binders in order to examine the effect of rubber content and the warm-mix additives on the high-temperature rutting resistance of the binders. The changes of the high service temperature performance of the prepared binders were investigated and compared with corresponding to unaged and aged bitumen. The following summary can be drawn from the results obtained from the MSCR test:

### **5.4.1 Effect of CRM content on high-temperature performance**

- According to the MSCR test results, it can be concluded that the rubber content significantly affects the high-temperature performance of the asphalt binders. It is clear that the non-recoverable deformation resistance, recovery ability, and stress sensitivity of the binders significantly increases at a higher proportion of crumb rubber modifier. Furthermore, the addition of crumb rubber is shown to increase the resistance of the binder aging effects.

### **5.4.2 Effect of the WMA additives on high-temperature performance**

- The wax-based warm-mix additive was proven to be capable of improving high-temperature rutting resistance, and recovery ability of both base and CRM binders. Additionally, the wax additive tremendously increased the stress sensitivity of the base binder.
- While, the chemical-based warm-mix additive did not significantly affect the high-temperature performance and stress sensitivity of base bitumen, but slightly reduced rutting resistance and an ability to recover of the CRMB.
- The addition of the wax and chemical only improved aging resistance of the base binder, but in case of the CRM binder, the aging resistivity potential was found to be reduced.

### **5.4.3 Effect of aging on high-temperature performance**

- Aging seemed to have a positive effect on the high-temperature performance of both unmodified and modified binders as the permanent deformation resistance and recovery percentage were higher at the aged stages. Furthermore, aging also reduced the stress dependency of the binders.

# **Chapter 6**

## **Intermediate-Temperature Performance Characterization**

## 6.1 Introduction

Fatigue cracking is known as a major form of pavement distress at intermediate road service temperatures (15°C~25°C). Once fatigue cracks are initiated, higher rates of pavement deterioration can be found, and life of pavements is drastically shortened as the effects of traffic and environmental damages can be combined with the cracks. It was found that fatigue cracks normally start and propagate at the weakest links in the asphalt mixture, which are the interface between the asphalt binders and the aggregates, and in the binder itself (Hintz et al. 2011, Johnson&Bahia 2010, Kim et al. 2006). Therefore, the characteristics of asphalt binders surely have a significant impact on the fatigue resistance of asphalt mixtures.

Evaluation of fatigue performance and the effect of long-term aging on the material properties of asphalt binders by measuring linear viscoelastic dynamic shear modulus ( $G^*$ ) and phase angle ( $\delta$ ) of the binders has been specified in the current SUPERPAVE specification for binder performance grading for years. The performance grading method has been using the stiffness-based parameter ( $G^*\sin\delta$ ) to characterize the fatigue cracking resistance of the asphalt binders at intermediate road service temperatures. However, this testing method has been reported to be inaccurate as it does not include actual evaluation binder damage resistance. Moreover, the effect of pavement structure and/or traffic loading are not taken into account, as the SUPERPAVE parameter is measured at only one load amplitude (within the LVE range) and fixed frequency (10 rad/sec). In actual traffic conditions where the binders are exposed to complicated strain levels and varied loading frequencies, the more accurate testing method to characterize fatigue behavior of asphalt binders is thus needed in order to identify the contribution of the binders' properties on the fatigue resistance of asphalt mixtures. Therefore, the Linear Amplitude Sweep (LAS) test has been introduced as a newly developed procedure to more accurately quantify the fatigue-related performance of bituminous binders by integrating results from a frequency sweep and a strain sweep into Viscoelastic Continuum Damage (VECD) analysis to calculate the coefficients of a fatigue law in order to estimate the fatigue life of the binders at defined strain levels.

This chapter focuses on characterizing the fatigue performance in term of a number of cycles to failure of both the unmodified asphalt binders and crumb rubber modified bitumen at different CRM dosages including the effects of the warm-mix additives by using LAS test method in accordance with AASHTO TP-101. Additionally, fatigue cracking problem of flexible pavements is more concerned after the long-term service, because hardening (aging) effects of the asphalt binders make it more susceptible to fatigue cracking. Therefore, in this part of the study, the binders at both unaged and long-term aged stages were also investigated in order to evaluate and compare the changes of fatigue performance before and after long-term aging. All binders were aged before testing using the modified static oven aging simulation and Pressure Aging Vessel (PAV).

## 6.2 Linear amplitude sweep test

### 6.2.1 Background

Recently, an accelerated fatigue test named the linear amplitude sweep (LAS) test has been proposed for characterizing fatigue behavior of both unmodified and modified asphalt binders (Hintz et al. 2011, Johnson&Bahia 2010). According to AASHTO TP 101-14 specification, in the LAS test, amplitudes of the applied strain are linearly and systematically increased from 0.1 to 30% at a fixed frequency of 10 Hz in order to accelerate the rate of fatigue damage accumulation. A repeated oscillatory loading test is conducted by using the DSR device with 8-mm parallel plate geometry.

Prior to the Amplitude Sweep test, the frequency sweep test (0.2-30 Hz) is conducted within the LVE region at the strain level of 0.1% to obtain undamaged material properties ( $\alpha$ ). According to the specification, the  $\alpha$ -parameter is defined as a reciprocal of slope coefficient (denoted as 'm' in equation 6.1) of the log-log plot of relation between storage modulus ( $\log G'[\omega]$ ) and angular frequency ( $\log \omega$ ), where the storage modulus can be calculated as  $G^*(\omega) \cos\delta(\omega)$ .

$$\alpha = \frac{1}{m} \quad (6.1)$$

After the frequency sweep test, the LAS is performed on the same binder sample. Amplitude sweep loading begins with 100 cycles of sinusoidal loading at a shear strain of 0.1%. Each successive loading step consists of 100 cycles at a rate of increase of 0.1% applied strain until 30% strain is reached as shown in Figure 6.1.

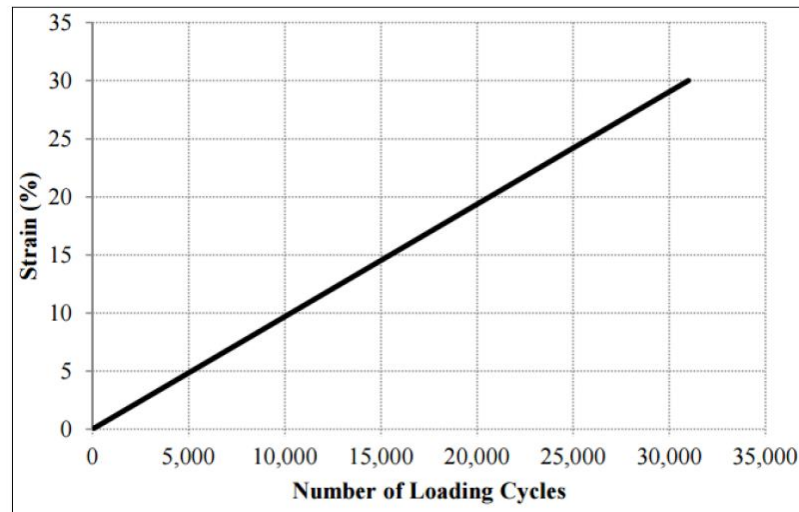


**Figure 6. 1:** Loading Scheme for Amplitude Sweep Test.

The LAS test results can be analyzed by using viscoelastic continuum damage (VECD) analysis. The basis of VECD principle is based on the idea of Schaperly's theory of work potential to model damage growth (Kim et al. 2006). This theory is inspired by the thermodynamics of



irreversible processes and Paris' Law of crack growth. Thus, the Schapery's work potential theory defines an equation for the damage rate ( $\frac{dD}{dt}$ ) for viscoelastic material as the change in the material's energy potential ( $W$ ) with respect to the change in the amount of damage ( $D$ ) in the material in the relation based on Paris' Law of crack growth:

$$\frac{dD}{dt} = \left( -\frac{\partial W}{\partial D} \right)^\alpha \quad (6.2)$$

Under cyclic loading, Kim et al. (Kim et al. 2006) suggested that changes in the dissipated energy are an indication of the fatigue damage accumulation of viscoelastic materials. Therefore, incorporating the application of the Schapery's theory of work potential (equation 6.2) and the dissipated energy (equation 2.9) allows for the estimation of fatigue life at any strain amplitude. The fatigue damage accumulation in the specimen at any testing time ( $D[t]$ ) can be determined as the following equation.

$$D(t) \cong \sum_{i=1}^N [\pi \gamma_0^2 (C_{i-1} - C_i)]^{\frac{\alpha}{1+\alpha}} (t_i - t_{i-1})^{\frac{\alpha}{1+\alpha}} \quad (6.3)$$

Where:

$C(t) = \frac{|G^*(t)|}{|G^*_{initial}|}$ , a ratio of the complex shear modulus at time ( $t$ ) and the initial undamaged

complex shear modulus, or the material integrity, (MPa).

$\gamma_0$  = Applied strain for a given data point (%)

$t$  = Testing time, (second).

$i$  = Loading time step.

Then, the simple power law (Kim et al. 2006) is used to create and fit the plot of relationship between the material integrity ( $C [t]$ ) and damage intensity ( $D [t]$ ) in order compare the material integrity at varying level of fatigue damage.

$$C_{(t)} = C_0 - C_1 (D_{(t)})^{C_2} \quad (6.4)$$

Where:

$C_0$  = 1, the initial value of  $C$

$C_1 C_2$  = curve-fit coefficients derived through linearization of the Power law.

The fatigue life of the binders in a number of cycles to failure ( $N_f$ ) can be determined using equation 6.5. In addition, the value of binder fatigue performance parameter ( $N_f$ ) is in a function of the maximum expected binder strain value ( $\gamma_{max}$ ) which depends on a structure of the considered pavement.

$$N_f = A (\gamma_{max})^{-B} \quad (6.5)$$

Where:

$$A = \frac{f(D_f)^k}{k(\pi C_1 C_2)^\alpha}$$

$f$  = loading frequency (10Hz)

$K$  =  $1 + (1 - C_2) \alpha$

$D_f$  =  $\left( \frac{C_0 - C_{at\ Peak\ Stress}}{C_1} \right)^{\frac{1}{C_2}}$ , The damage value at failure

$B$  =  $2\alpha$

### 6.2.2 Sample preparation and experimental program

Linear Amplitude Sweep (LAS) test was conducted at 20°C (where the  $G^*$ -value of the 70/100 binder > 10 MPa) using Anton Paar Dynamic Shear Rheometer (DSR) where the test temperature was maintained within +/- 0.1 °C tolerance for 10 minutes. The 8-mm diameter parallel plate and a 2-mm gap were employed to determine the fatigue law parameter  $A$  and  $B$  (as shown in the equation 6.5), in order to estimate the fatigue life ( $N_f$ ) of the prepared binders (detail given in Table 3.7) at any particular strain levels ( $\gamma_{max}$ ). The parameter  $A$  and  $B$  are VECD model coefficients that depend on the material characteristics. The “A” parameter represents the integrity of binder sample against accumulated damage whereas “B” parameter is related to the sensitivity of binder sample against any changes in loading amplitude (strain) (Kim et al. 2006). The LAS test was carried out in accordance with the AASHTO TP101 as described in section 6.2.1.

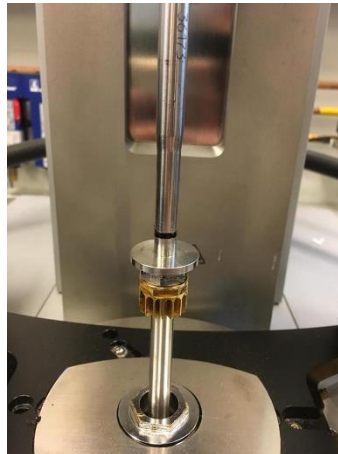


**Figure 6. 2:** The LAS test setup (8mm plate with 2mm gap)

### 6.3 Results and analysis

Figure 6.3-6.5 present the plots of the apparent stress-strain (stress/strain values were calculated based on an assumption of a constant sample geometry) diagram obtained from the amplitude sweep test results, showing material behavior when the binders were subjected to the load. It can be observed that, for the initial part of the curves, the slope of the curve increases linearly as the shear stress is directly proportional to the applied strain level. After reaching a particular strain level, it can be seen that all binder displayed a considerable reduction in the shear stress indicating initiation of fatigue failure in the binder samples. The effects of CRM content, WMA additives, and aging on the fatigue life of the binders are presented in detail in the sub-sections 6.3.1-6.3.3 below. It should be noted that the term

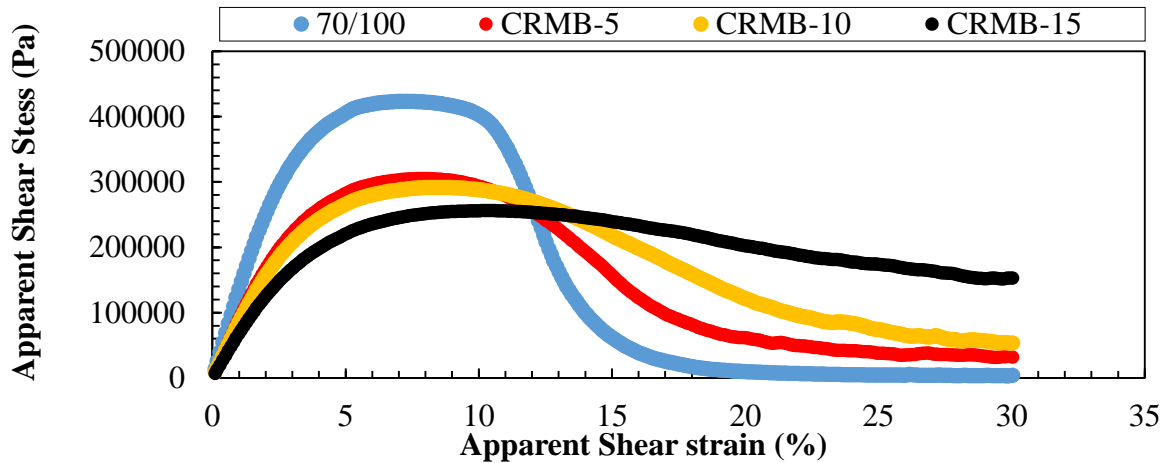


**Figure 6. 3:** Shear stress and strain diagram from amplitude sweep test showing the effect of CRM content.

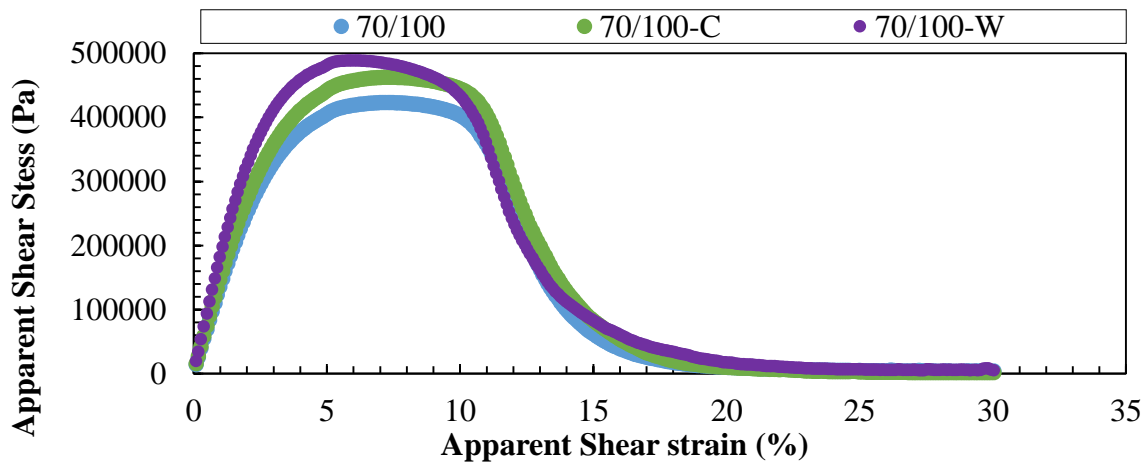


**Figure 6. 4:** Shear stress and strain diagram from amplitude sweep test showing the effect of the WMA additives on the base bitumen.

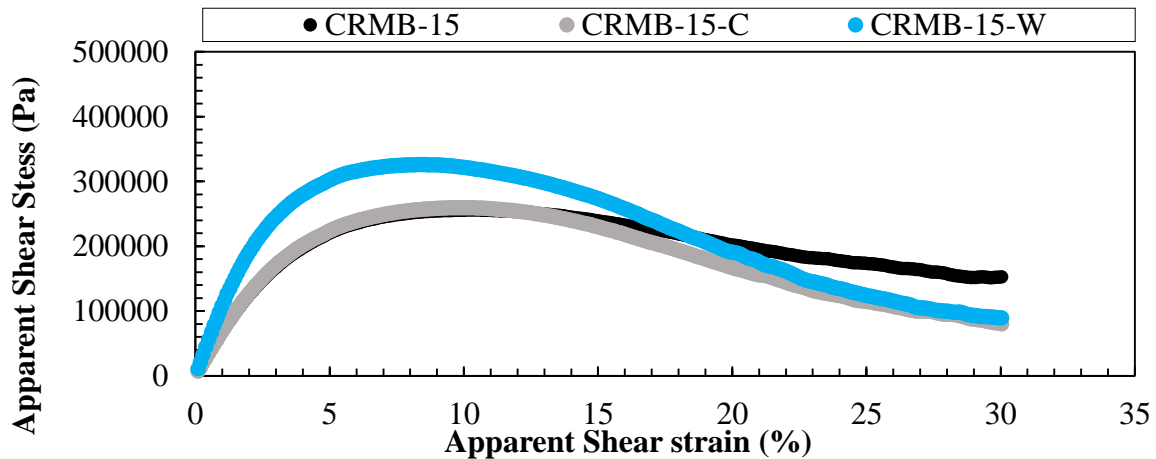
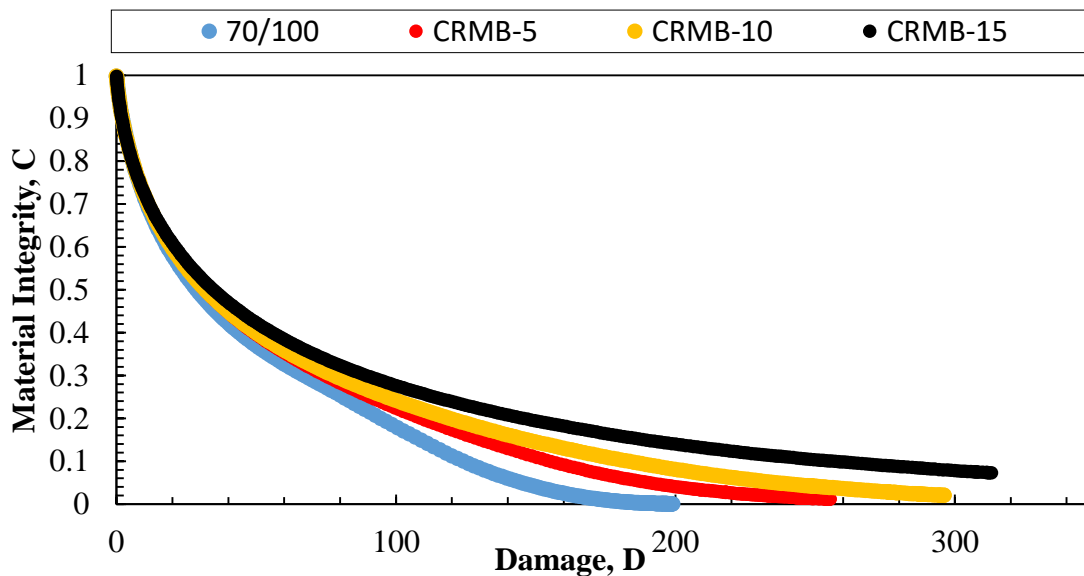


**Figure 6. 5:** Shear stress and strain diagram from amplitude sweep test showing the effect of the WMA additives on the CRMB.

### 6.3.1 Effect of CRM content on the intermediate-temperature performance

According to the diagram 6.3, it is clear that the shear stress of the neat 70/100 penetration grade binder reached a peak value of 0.42 MPa at the strain level of 7.30% at a relatively higher hardening rate of shear stress compared to the CRM modified binders. Generally, the CRMBs had a slower rate of stress increasing, and the peak shear stress values of CRMB-5, CRMB-10, and CRMB-15 were recorded at 0.30MPa, 0.29MPa, and 0.26MPa respectively. Furthermore, the CRMB-15 was found to have the fatigue failure initiation at the largest strain level (10.30%) followed by CRMB-10 (8.46%), CRMB-5 (7.78%), and 70/100 (7.30%) respectively, meaning that, based on Figure 6.3, the highest damage tolerance can be expected from the CRMB-15.

Figure 6.6 shows a plot of damage characteristic (material integrity [C] versus damage [D]) showing the effect of CRM concentration on the damage resistance of the binders. The graph presents the behavior of materials regarding damage development within the binders. In general, it can be seen that the integrity of materials decreases as the damage increases. The material integrity presented here represents the value of normalized dynamic shear modulus  $\left(\frac{|G^*|}{|G^*_{initial}|}\right)$  of asphalt binders, where the 1.0-value of integrity indicates the undamaged stage of binders. According to Figure 6.6, the base binder has a relatively rapid decrease in its material integrity, and the integrity reached the zero at the damage intensity of approximately 200. While, in the case of the rubber modified binders, their material integrity values do not seem to reach zero integrity at the end of the test (strain amplitude of 30%). As expected, the CRMB-15 shows the slowest rate of integrity reduction followed by CRMB-10 and CRMB-5, respectively.



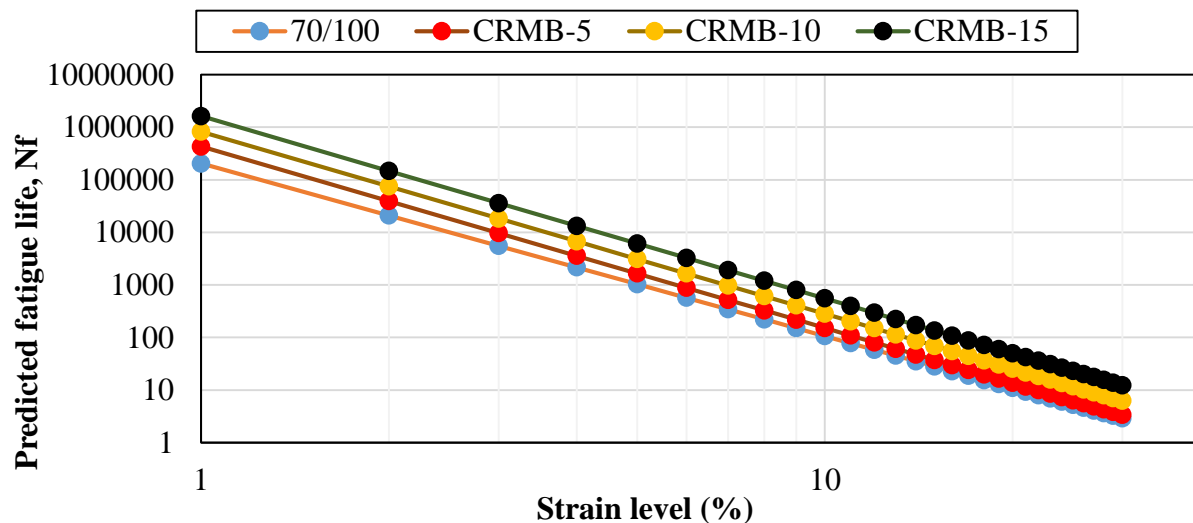
**Figure 6. 6:** Damage characteristic curve showing effect of CRM content.

Figure 6.7 presents predicted fatigue lives of the binders in term of a number of cycles to failure at various strain levels. The predictions were carried out in accordance with the fatigue law equation (Eq. 6.5), and the parameters used for analysis were presented in Table 6.1. From the

plot, it is obvious that the unmodified binder had the lowest fatigue life, and the number of cycles to failure obviously increased corresponding to the percentage of added rubber content, especially at low strain amplitudes. In addition, it can be noticed that the parameter “B” which represents applied load sensitivity of the binder decreased at the higher CRM proportion indicating more load susceptibility of the CRM modified binders. In other words, increasing the CRM content was not only capable of improving intermediate-temperature damage tolerance, but also affected strain sensitivity of binders.

**Table 6. 1:** Effect of CRM content on the fatigue law parameters.

Sample code	A	B
70/100	204317.4	-3.28378
CRMB-5	429274.7	-3.45342
CRMB-10	825583.9	-3.46614
CRMB-15	1626826	-3.46838



**Figure 6. 7:** Fatigue life prediction in function of strain level showing effect of CRM content.

### 6.3.2 Effect of WMA additives on the intermediate-temperature performance

According to the stress-strain diagrams showing effects of WMA additives (Figure 6.4-6.5), the effects of the WMA additives on stress-strain response of base bitumen and CRMB-15 were observed. In case of the wax-based additive, the uniformly distributed wax-network after its crystallization seemed to stiffen both base bitumen and CRMB binders at the intermediate service temperature as evidenced by the obviously higher peak of the curves. However, the damage tolerance of the materials was founded to be reduced due to the addition of the wax additive. It is because the strain levels where the failure initiated in binders (at the peak of stress) in the case of 70/100-W and CRMB-15-W were found to be lower than the base and CRM binders without the

wax additive. The strains at the peak of the stress of 70/100 and CRMB-15 were 7.30% and 10.30%, while, the peaks of 70/100-W and CRMB-15-W were observed at 5.94% and 8.27% strain amplitudes respectively. In case of the effect of chemical-based additive, the addition of the chemical additive slightly reduced the damage tolerance of the CRM binder, but improve stiffness and the resistant ability of the base binder. The 70/100-C binder had a peak value of the shear stress of 0.46 MPa at 7.39% strain, and the CRMB-15-R had the peak of 0.26 MPa 9.92% strain.

Based on the damage characteristic curves shown in Figure 6.8 and 6.9, it is clear that the wax-based additive negatively affected the damage resistance of both base and CRM binders, as evidenced by noticeably faster decreases of material integrity values of 70/100-W and CRMB-15-W. At the end of LAS test, 70/100-W had a zero integrity at approximately 180 damage intensity, while CRMB-15-W could not reach zero integrity. Moreover, in the case of the chemical additive, its influence was very small, the difference of the 70/100 and 70/100-C curves was hardly seen. It should be noted that the unfavorable effect of the chemical on the CRM binder became noticeable when the integrity below 0.3.

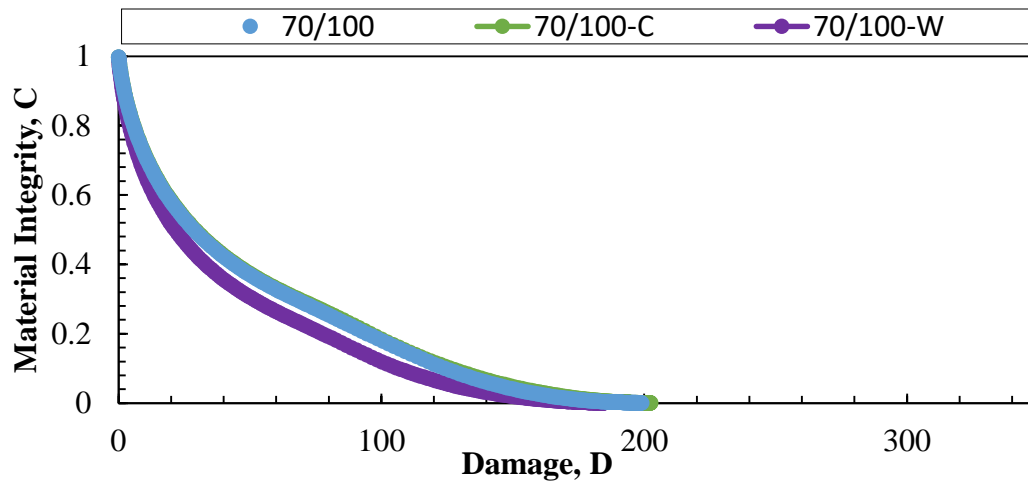


**Figure 6. 8:** Damage characteristic curve showing effect of WMA additives on the base binder.

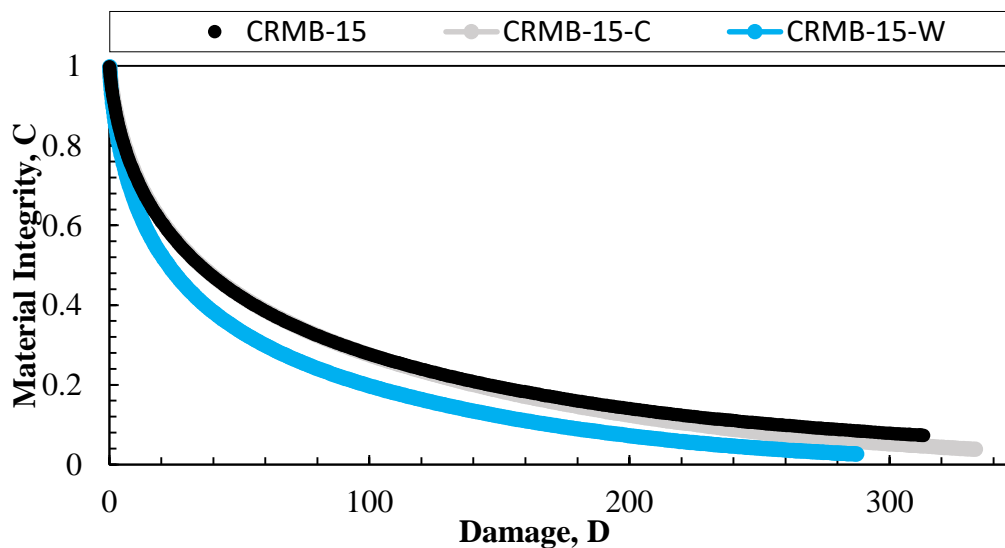


**Figure 6. 9:** Damage characteristic curve showing effect of WMA additives on the CRMB.

The effect of the WMA additives on the fatigue parameters are given in detail in Table 6.2. Fatigue lives of the binders containing WMA additives were predicted based on the Fatigue's law, and presented in Figure 6.10 and 6.11. It can be clearly seen from both figures that the fatigue resistance of both modified and neat binders which contain the wax-based additive were dramatically lower than the binders without the wax additive. Moreover, based on the parameter "B", the addition of wax also made both the modified and unmodified binders more susceptible to the changes in loading.

**Table 6. 2:** Effect of the WMA additives on the fatigue law parameters.

Sample code	A	B
70/100	204317.4	-3.28378
70/100-C	200510.7	-3.24005
70/100-W	146372.7	-3.55501
CRMB-15	1626826.0	-3.46838
CRMB-15-C	1140317.4	-3.40770
CRMB-15-W	1204180.5	-3.69775

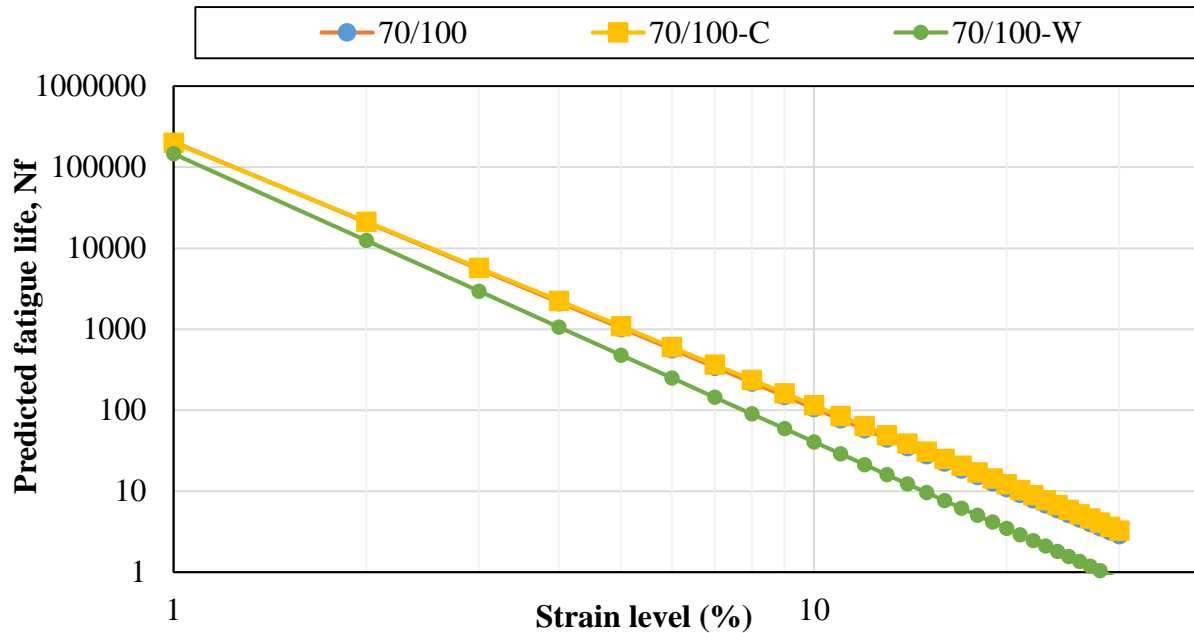


**Figure 6. 10:** Fatigue life prediction in function of strain level showing effect of WMA additives on the base binder.

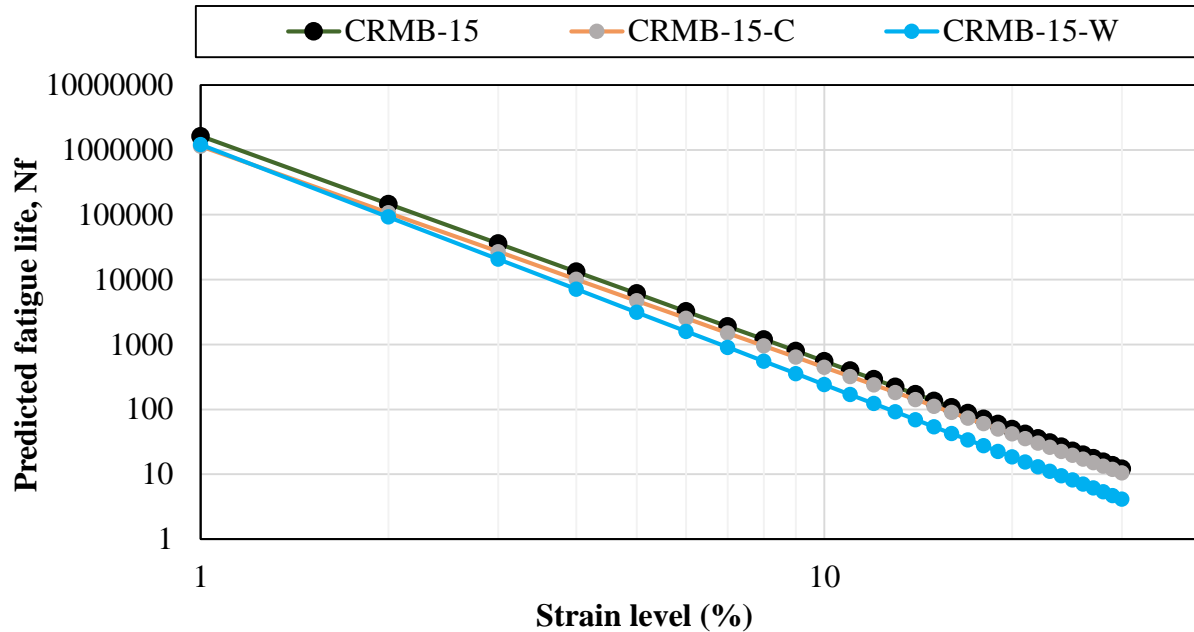


**Figure 6. 11:** Fatigue life prediction in function of strain level showing effect of WMA additives on the CRMB.

Although the wax's effect was very obvious, the effect of the chemical-based additive was difficult to distinguish, especially in the case of the base bitumen. The strain in the asphalt binder is normally assumed to be about 50 times of the strain occurred in the asphalt mixture (Masad et al. 2001). Thus, in order to clearly define the effect of the chemical additive, the predicted fatigue lives of the binders containing WMA additives at 2.5% strain corresponding to 500 micro strain (in the binder) were selected for comparison. The predicted fatigue life chart (Figure 6.12) of 70/100-C shows that the chemical effect was unnoticeably small, meaning that the fatigue resistance of 70/100-C was neither better nor worse than the neat bitumen at an intermediate road service temperature. However, the chemical effect on the CRMB was found to be negative as the chemical-based additive lower the fatigue life of CRMB-15-C. It should be noted that the negative effect of the chemical-based additive on the predicted fatigue life of the CRM binder seemed to be smaller than the wax-based additive. Furthermore, the addition of the chemical additive improved the stress sensitivity of both neat bitumen and CRMB at the intermediate temperature. Additionally, based on the predicted fatigue lives at 2.5% strain, even the addition of the WMA additives lowered the fatigue resistance of the CRMB but the fatigue performance of the CRMB containing WMA additives were still better than the base bitumen with or without additives.



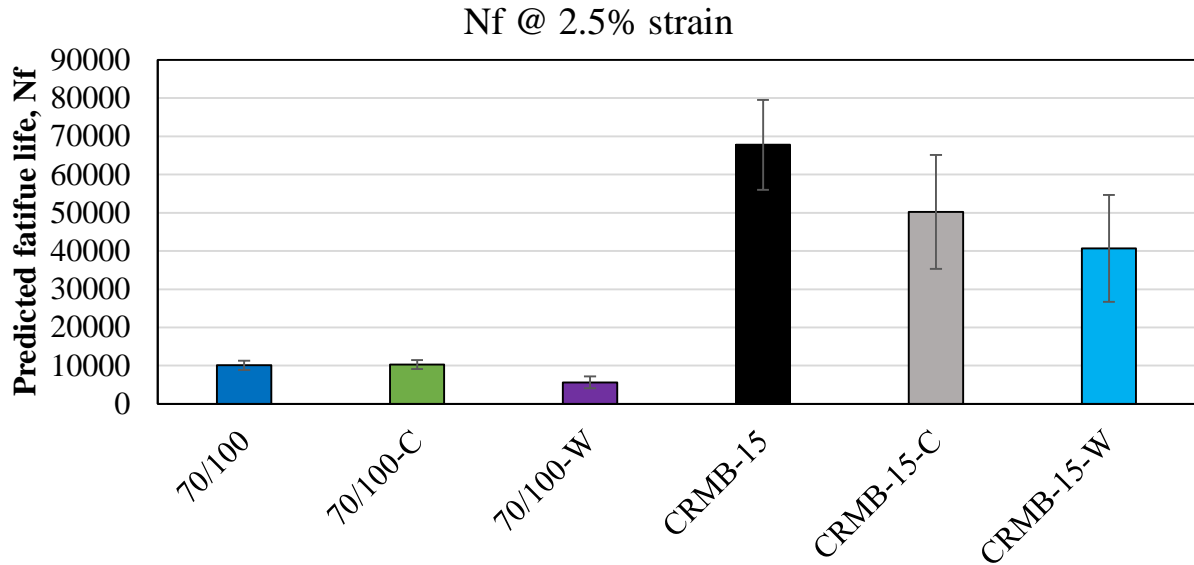


**Figure 6. 12:** Predicted fatigue lives at 2.5% strain showing effect of the WMA additives.

### 6.3.3 Effect of aging on the intermediate-temperature performance

Aging is one of the significant factors that influence the cracking progression of pavements by embrittling asphalt binders. In this section, the effects of artificial long-term aging (denoted as -PAV) on the fatigue parameters of the study binders were shown in Table 6.3. Moreover, an example of the aging effect on the fatigue tolerance of binders is presented in the forms of damage characteristic curves and predicted fatigue lives of the neat bitumen in Figure 6.13 and 6.14, respectively. The other binders in this study also experienced the same changes after aging as the base binder, and their characteristic curves and the predicted fatigue lives can be found in Appendix B.

According to Table 6.3, parameter “A” generally increased with age, but, conversely, aging decreased the value of parameter “B”. It can be observed that the changes of the fatigue parameters due to aging effect are diverse. It is clear that the aging influence decreased as the rubber content increased. The addition of the wax additive lowered parameter “A” for both base and CRM binder, while the chemical decreased “A” only in the case of the neat bitumen. The addition of the WMA additives affected the base and CRM binder differently as it decreased the changes of “B” in the case of base bitumen, but increased the changes of “B” for the CRMB.

In general, based on the damage characteristic curves, it can be seen that the long-term aged sample had lower damage tolerance than the fresh binder as evidenced by the higher deteriorating rates as shown in Figure 6.13. It is because the hardening phenomenon of the binder after the continuous oxidative aging process has changed the behavior of the material into more brittle and rigid which made them more susceptible to fatigue damage. The higher rate of material degradation of the PAV-aged samples indicates that the fatigue resistant behavior of the asphalt binder was negatively affected by the oxidative aging process.

However, it also can be observed from Figure 6.14 that at the low strain levels the PAV-aged sample have longer predicted fatigue lives, but when the strain increases to a certain level the predicted number of cycle to a failure of the long-term aged binder became lower than the unaged binder. It is because after the artificial aging simulation the binders became stiffer, but, simultaneously, their ductility was reduced due to a formation of Asphaltenes and loss of low-molecular-weight components. The results indicate that at the lower strain level the hardening of asphalt binders positively influenced the fatigue damage resistance, but after reaching a certain strain level a loss of ductility of the aged binder shows a relative higher decreasing rate of fatigue lives compared to the unaged. The reason of an improvement of the predicted fatigue lives at low strain levels can be attributed to an increase in the fatigue parameter “A”, and the steeper slope of the predicted fatigue curve was due to a decrease in the parameter “B”.

**Table 6. 3:** Effect of aging on the fatigue law parameters.

Sample code	Aging condition	A	B	$A_{aged}/A_{fresh}$	$B_{aged}/B_{fresh}$
70/100	Fresh	36990.6	-2.32242	5.52	1.41
	Long-term aged	204317.4	-3.28378		
70/100-C	Fresh	44156.8	-2.40306	4.54	1.35
	Long-term aged	200510.7	-3.24005		
70/100-W	Fresh	61051.3	-2.6008	2.40	1.37
	Long-term aged	146372.7	-3.55501		
CRMB-5	Fresh	79529.6	-2.51712	5.40	1.37
	Long-term aged	429274.7	-3.45342		
CRMB-10	Fresh	246325.1	-2.81891	3.35	1.23
	Long-term aged	825583.9	-3.46614		
CRMB-15	Fresh	885777.9	-3.08982	1.84	1.12
	Long-term aged	1626826.0	-3.46838		
CRMB-15-C	Fresh	613362.1	-2.99329	1.86	1.14
	Long-term aged	1140317.4	-3.4077		
CRMB-15-W	Fresh	765955.4	-3.23827	1.57	1.14
	Long-term aged	1204180.5	-3.69775		

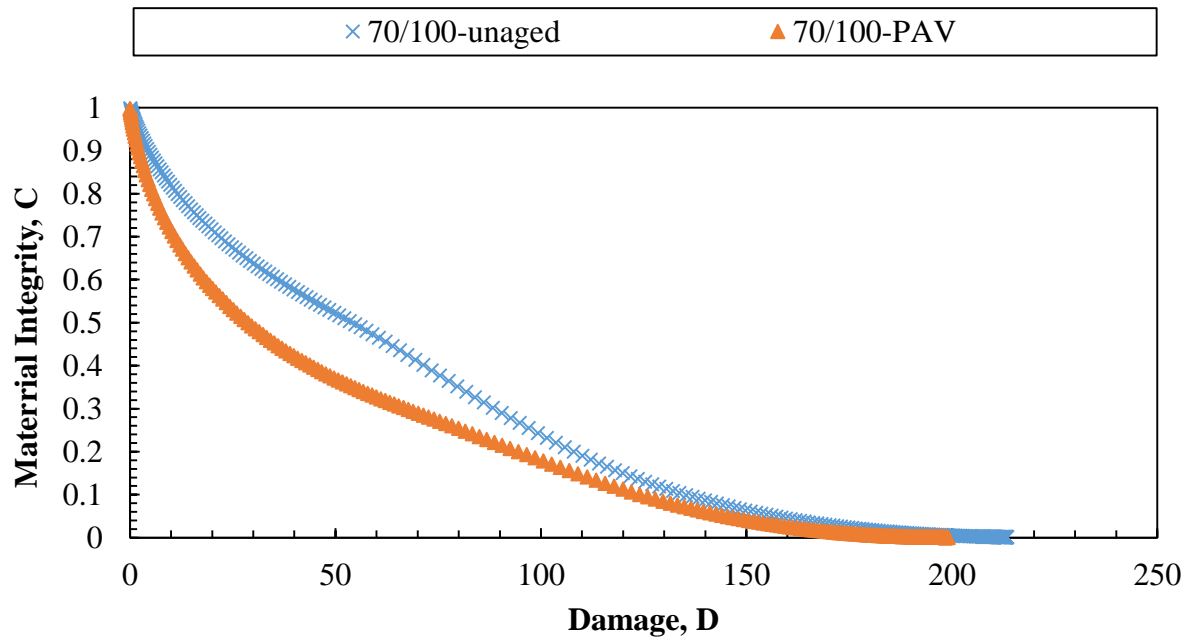


**Figure 6. 13:** Damage characteristic curves showing effect of artificial long-term ageing on the base binder.

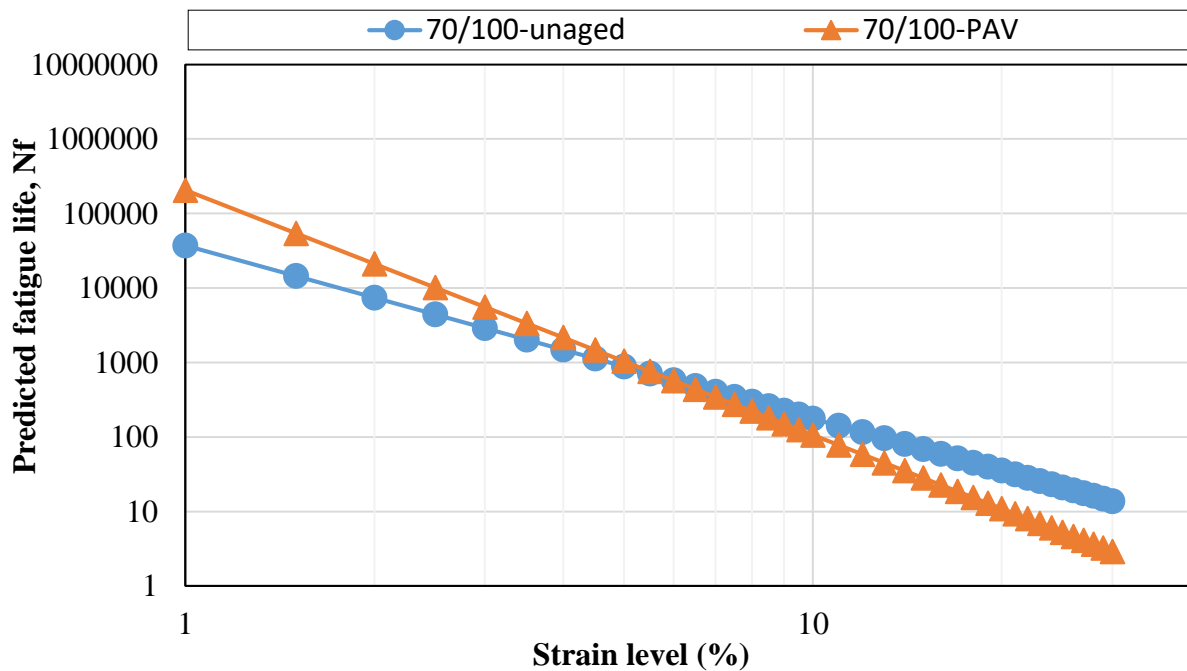


**Figure 6. 14:** Fatigue life predictions in function of strain level showing effect of artificial long-term ageing on the base binder.

### 6.3.4 Comparison of asphalt binder fatigue parameters

In this sub-section, the predicted fatigue life obtained by the LAS test are compared with the time sweep-measured fatigue life and the SUPERPAVE fatigue parameter as shown in Table 6.4. It can be noticed that the LAS predicted fatigue lives at 2.5% strain are different from the real fatigue test at the same strain level. Generally, it is clear that all the studied binders had longer fatigue lives than the prediction. Apparently, the difference in fatigue lives of two methods was due to the different loading rate which affected the fatigue damage accumulation of the binders. The LAS applies loading strain at an increasing rate, whereas the applied strain in the case of the time sweep test is constant. However, the rank of fatigue performance provided by the LAS and time sweep tests indicate that the LAS has an ability to capture the fatigue properties of the binders, and can be used as a surrogate to the conventional fatigue test to characterize the binder fatigue performance at intermediate-temperatures.

Currently, the SUPERPAVE fatigue parameter ( $G^*\sin[\delta]$ ) is used to evaluate the effect of the long-term aging on the material properties as described in section 2.5.2. However, the SUPERPAVE has been questioned about its validity due to the fatigue properties of asphalt binders are measured at only one loading amplitude which does not account for the effect of pavement structure and traffic loading. According to Table 6.4, it can be observed that the SUPERPAVE parameter differently ranks the intermediate-temperature performance of the binders. Therefore, based on the laboratory testing results, the SUPERPAVE fatigue parameter lacks ability to accurately characterize the actual fatigue damage resistance of the asphalt binders, especially when incorporated with CRM and WMA additives.

**Table 6. 4:** Fatigue properties of the long-term aged binders at 20 °C

Sample	LAS test		Time sweep test		Rheological properties test	
	Predicted fatigue life at 2.5% strain (N)	Rank	Fatigue life at 2.5% strain (N)	Rank	$G^*\sin(\delta)$ (MPa)	Rank
70/100	10082	6-7	29700	6-7	4.33	7
70/100-C	10299		29800		3.08	3
70/100-W	5633	8	23600	8	6.52	8
CRMB-5	18133	2	54400	2	3.67	5
CRMB-10	31452	4	94500	4	3.23	4
CRMB-15	67785	1	335200	1-3	2.49	1
CRMB-15-C	50230	2	335900		2.62	2
CRMB-15-W	40664	3	336300		3.68	6

## 6.4 Conclusions

The main point of this chapter was to characterize the fatigue resistance of the asphalt binders at the intermediate-temperature, where the LAS test was employed to measure the effect of rubber content and the warm-mix additives on the fatigue damage tolerance of the binders in an accelerated manner. Based on the LAS testing results, the major findings are as follows:

### 6.4.1 Effect of CRM content on intermediate-temperature performance

- The CRM content plays an important role in the fatigue damage tolerance of the asphalt binders as the CRM binders showed a better fatigue performance than the unmodified binder at the intermediate-temperature.

### 6.4.2 Effect of WMA additives on intermediate-temperature performance

- The wax-based additive clearly reduced the fatigue performance of both the base and CRM binders.
- The chemical-base additive slightly improved the fatigue resistance of the base asphalt binder, but lowered the fatigue life of the CRM binder.

### 6.4.3 Effect of aging on intermediate-temperature performance

- Oxidative aging increased the rate of material degradation as it changed the behavior of the material in a brittle way. However, it positively impacted the fatigue life of the binders at low loading strain levels.

# **Chapter 7**

## **Low-Temperature Performance Characterization**

## 7.1 Introduction

Thermal cracking is one of the important modes of failure of asphalt pavements, especially in cold-climate regions. It is because when the temperature drops, the thermal tensile stress corresponding to shrinkage of the pavement will be developed to the point that the built-up tensile stress overcomes the tensile strength of the asphalt, so, the cracks is initiated. The thermal cracking commonly occurs in the form of transverse cracks. This type of distress is usually initiated when the asphalt mixture cannot sufficiently dissipate the built-up tensile stress. It was found that the rheological properties of the asphalt binders significantly affect the low-temperature thermal cracking performance of the pavements (Ghavibazoo&Abdelrahman 2014, Sui et al. 2011). Therefore, the better stress-relaxation ability of the binders is desirable for improving the thermal cracking resistance.

Currently, the bending beam rheometer (BBR) is employed to characterize the stress relaxation ability, and an ability to resist low-temperature cracking of bituminous materials at low-temperatures. However, it is difficult to perform the test when a binder extraction from pavement cores is required for the field monitoring because the BBR test requires large amounts of binder to pre-mold a beam sample.

Recently, a newly developed technique using 4-mm dynamic shear rheometer (DSR) was proposed as an alternative to characterize low-temperature performance of the asphalt binders. In the new test, the rheological properties of the binders at low-temperatures can be measured by using 4-mm parallel plate geometry in a dynamic shear rheometer (DSR). The use of 4-mm plates reduces a needed amount of binders to only a few grams which is advantageous when characterizing the asphalt binders recovered from a pavement core.

The main objective of this chapter is to experimentally characterize the low-temperature performance of the study binders to examine the effects of CRM content, and the WMA additives on the low-temperature performance of the binders by using the new 4-mm DSR test.

## 7.2 Dynamic shear rheometer test with application of 4-mm plates

### 7.2.1 Background

In 2011, Sui et al. (2011) proposed a newly developed technique to characterize the low-temperature performance of asphalt binders by using 4-mm parallel plates on a dynamic shear rheometer. The 4-mm DSR test was performed on eleven different unmodified asphalt binders, and it was observed that the 4-mm DSR results can correlate to the BBR test results. Based on Sui et al. study , they found the high linear correlation between the BBR creep stiffness at the low performance grade temperature plus 10 degree Celsius and at loading time of 60 seconds ( $S[60\text{ s, low PG temp} +10^{\circ}\text{C}]$ ) and the 4-mm DSR shear stress relaxation modulus ( $G[t]$ ) at 2 hours and at the true low performance grade temperature collected from stress relaxation master curves ( $G[7200\text{s, low PG temp}]$ ) as shown in Figure 7.1. It was also observed a strong relation between the BBR stress relaxation rate at the low performance grade temperature plus 10 degree Celsius

and at loading time of 60 seconds ( $m_c$  [60, low PG temp +10°C], and shear stress relaxation rate at 2 hours and at the true low performance grade temperature collected from stress relaxation master curves ( $m_r$  [7200s, low PG temp]) as shown in Figure 7.2. Thus, it was concluded that 4-mm DSR could be used as an alternative low-temperature performance grading method.

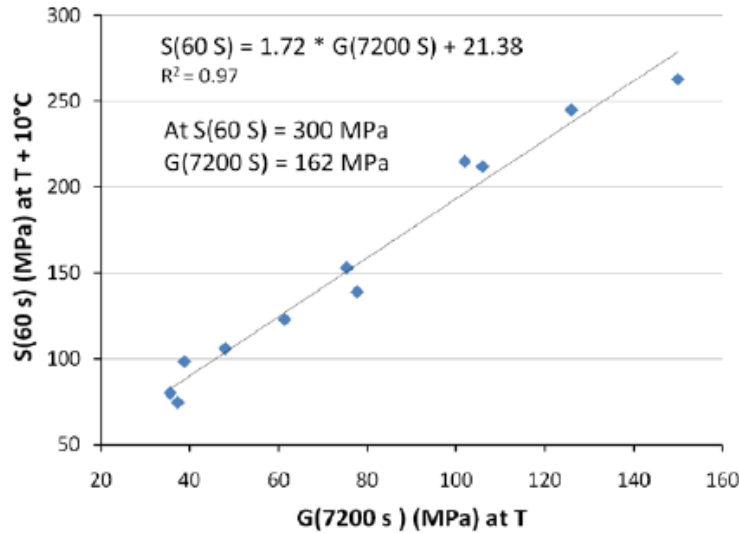


**Figure 7. 1:** Correlation between BBR  $S(60s)$  and 4-mm DSR  $G(7200 s)$  (Sui. et al 2011).

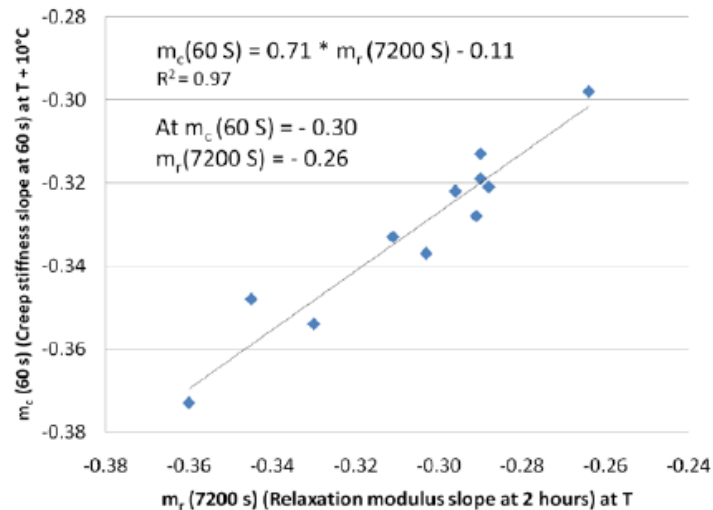


**Figure 7. 2:** Correlation between BBR  $m_c(60s)$  and 4-mm DSR  $m_r(7200 s)$  (Sui. et al 2011).

Recently, Farrer et al (2015) from the Western Research Institute (WRI) modified the 4-mm DSR method characterizing low-temperature performance which was originally proposed by Sui et al. (2011). Farrer et al. (2015) suggested that the results of the 4-mm DSR can be linked to the BBR parameters at the same loading time and temperature. The WRI proposed a method to correlate between the shear relaxation modulus and its slope coefficient at 60 seconds from the 4-mm DSR test and the low-temperature rheological properties of the asphalt binders, namely the BBR creep stiffness  $S(t)$  and  $m$ -value through the following procedures:



- (1) Construct a master curve of the storage shear modulus in the function of the angular frequency  $G'(\omega)$  at a pre-determined reference temperature as shown in Figure 7.3.

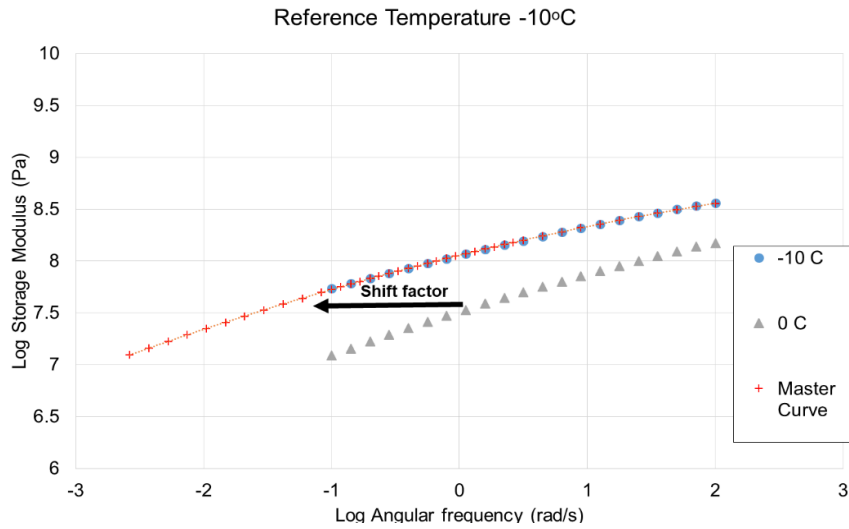


**Figure 7. 3:** Storage modulus master curve at a reference temperature.

- (2) Converse the storage modulus in function of angular frequency  $G'(\omega)$  into the relaxation modulus in a function of time  $G(t)$  through the approximate expression (eq. 7.1) developed by Christensen (1982). The master curve of relaxation modulus can be obtained through the interconversion as shown in Figure 7.4.

$$G(t) \approx G'(\omega) \Big|_{\omega = \frac{2}{\pi t}} \tag{7.1}$$

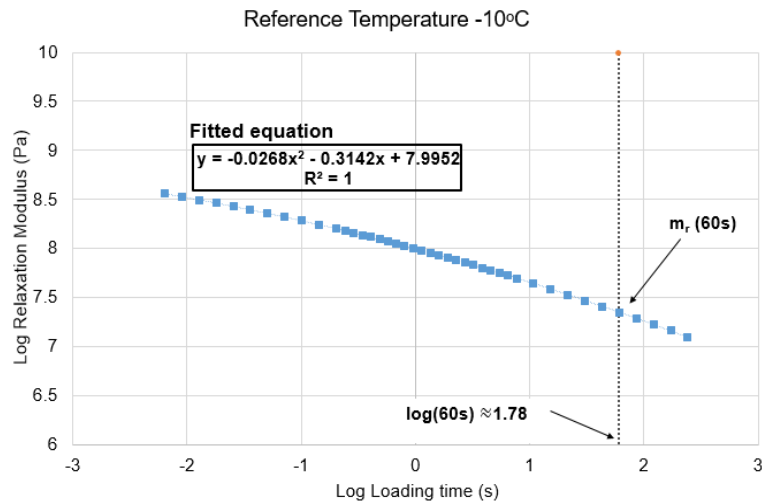


**Figure 7. 4:** Relaxation modulus master curve at a reference temperature.

- (3) Fit the relaxation modulus master curve with a second-order polynomial as shown in Figure 7.4. Then, determine the value of relaxation modulus at 60 seconds  $G(60s)$  through the fitted equation. The slope coefficient of the relaxation modulus  $m_r(60s)$  can be calculated by taking the first derivative of the second-order polynomial fitted equation.

According to the WRI's study, it was found that the magnitude of the 4-mm-DSR-obtained relaxation modulus and its slope coefficient at 60 seconds and at 10 °C higher than the PG temperature ( $G[60\text{ s, low PG temp} + 10\text{ °C}]$ ) provided the strong linear correlation to the BBR low temperature stiffness and m-value at 60 seconds and at 10 °C higher than the PG temperature ( $S[60\text{ s, low PG temp} + 10\text{ °C}]$ ) as shown in Figure 7.5-7.6. Based on the linear correlation of Farrer et al (2015), the limiting shear relaxation modulus and relaxation rate at PG + 10°C are  $G(60s) < 143\text{ MPa}$  and  $m_r(60s) > 0.28$  which correspond to the limiting value of BBR parameters. The fitted equation of the correlation are as follow:

$$S(60s) = 2.01G(60s) + 12.72 \quad (7.2)$$

$$m_c(60s) = 0.72m_r(60s) - 0.10 \quad (7.3)$$

Where:

$S(60s)$  = BBR-obtained creep stiffness at 60-second loading time (at PG +10°C)

$G(60s)$  = DSR-obtained relaxation modulus at 60-second loading time(at PG +10°C)

$m_c(60s)$  = BBR-obtained relaxation rate at 60-second loading time (at PG +10°C)

$m_r(60s)$  = DSR-obtained relaxation rate at 60-second loading time (at PG +10°C)

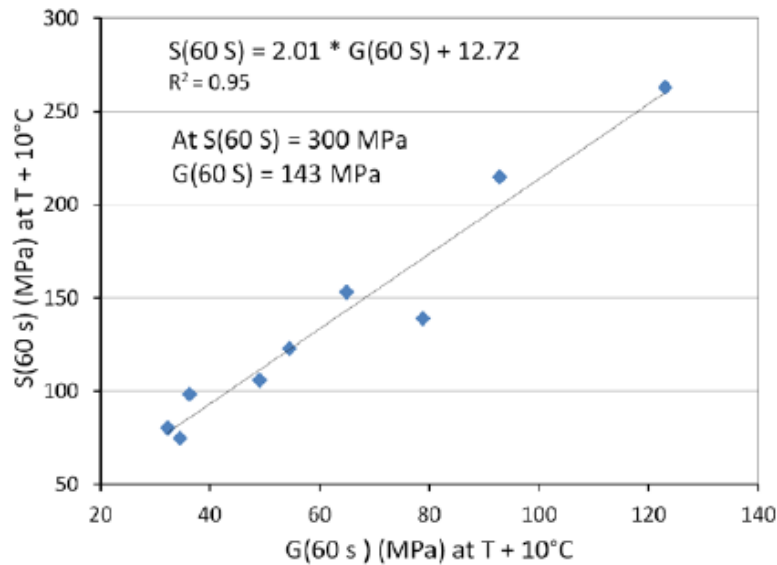


**Figure 7. 5:** Correlation between BBR  $S(60s)$  and 4-mm DSR  $G(60\text{ s})$  Farrar et al. (2015).

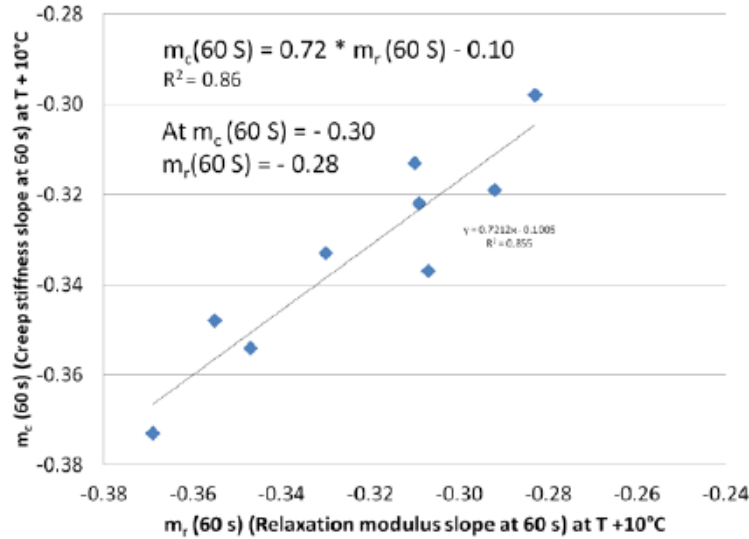


**Figure 7. 6:** Correlation between BBR  $m_c(60s)$  and 4-mm DSR  $m_r(60\text{ s})$  Farrar et al. (2015).

### 7.2.2 Experimental program

The specimens were carefully prepared in accordance with a draft AASHTO standard method for 4-mm DSR test (detail given in Farrar et al. [2015]). The excessive sample after sandwiched in 4-mm plates was removed by a heat Anton Paar spatula as shown in Figure 7.7.



**Figure 7. 7:** Anton Paar spatula for sample trimming.

The low-temperature linear viscoelastic properties of the asphalt binders in this study were determined by performing frequency sweep tests with 4-mm parallel plate geometry with a 1.75-mm gap (Figure 7.8) from 0.1-100 rad/s at two different temperature ( $-10^\circ\text{C}$ , and  $0^\circ\text{C}$ ) on the Anton Paar DSR device. The linear viscoelastic regions of the binders were defined as Wang et al. (2018). Thus, the tests were performed at a strain level of 0.1% under strain-controlled mode. The radial instrument compliance corrections were automatically carried out by a real-time online instrument compliance correction of the Anton Paar software. The comparison between the complex modulus obtained by the 4-mm and 8-mm plates is shown in Figure 7.9. According to the comparison, the results from 8-mm and 4-mm tests were found to be similar, indicating no compliance effects of the parallel plate geometries. In addition, the repeatability of the 4-mm parallel plate is shown in Figure 7.10.

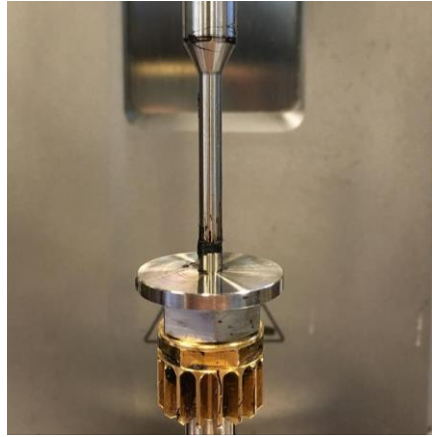


Figure 7. 8: Setup for the 4-mm DSR test (4-mm plates and 1.75-mm gap).

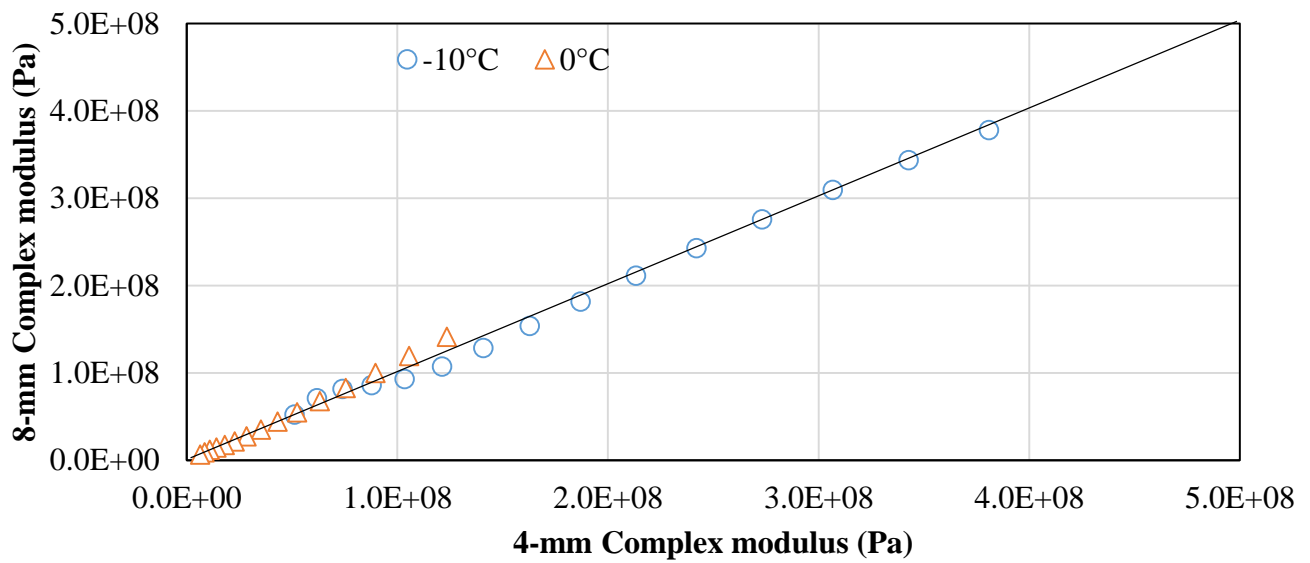


Figure 7. 9: Comparison between 4 mm and 8 mm plates (base bitumen).

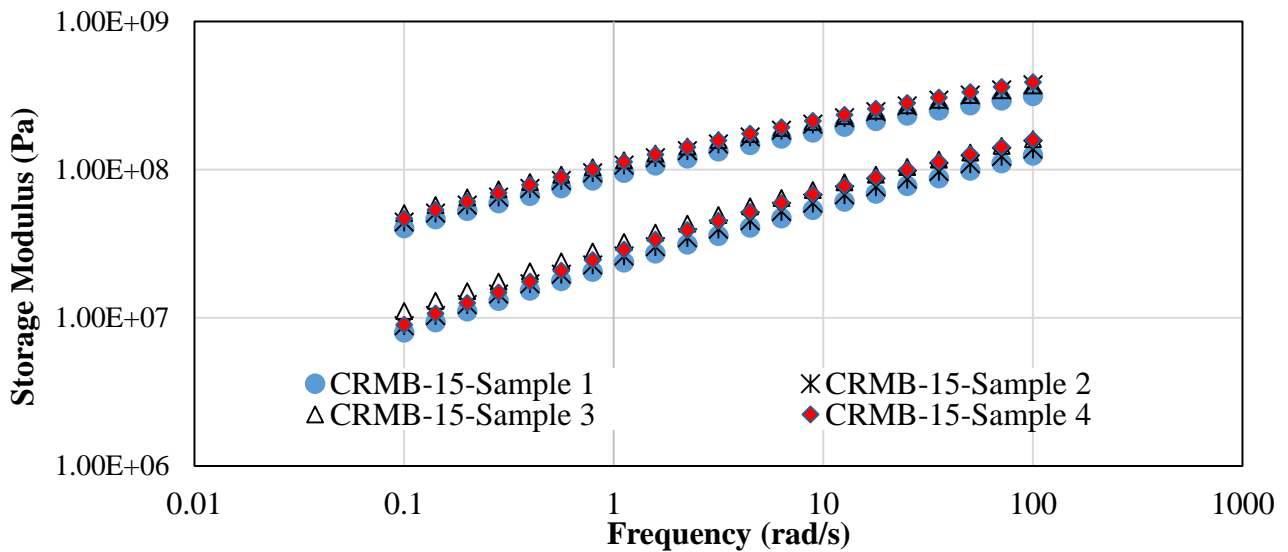
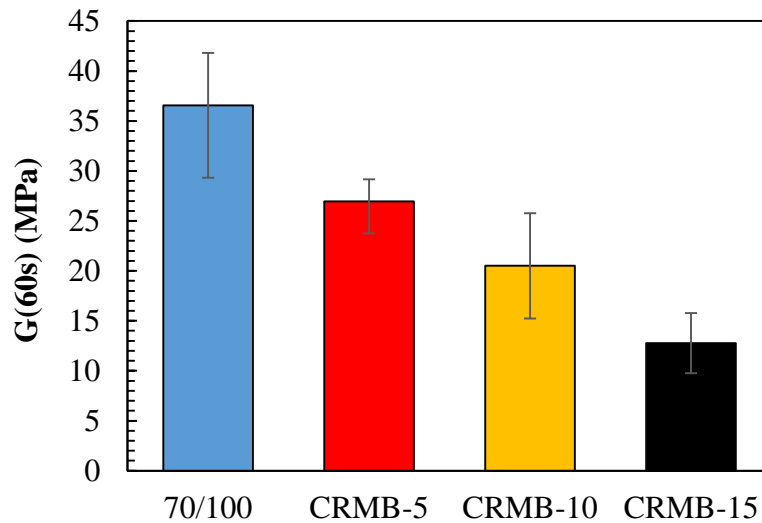


Figure 7. 10: Repeatability of the 4-mm diameter

## 7.3 Results and analysis

### 7.3.1 Effect of CRM content on the low-temperature performance

The effect of CRM content on the low-temperature thermal cracking resistance of the binders were examined at the long-term aged stage. Generally, asphalt binders with lower stiffness and higher relaxation rate are preferred as they have better resistance to low-temperature cracking. The relaxation modulus and the relaxation rate of the study binders are presented in Figure 7.11 and 7.12, respectively. According to Figure 7.11, it is clear that the addition of CRM can lower the relaxation modulus (stiffness) of the binders as the modified binders show superior low-temperature performance. In general, the modified binder containing the highest percentage of CRM (15%) showed the lowest stiffness and highest relaxation ability. The value of the relaxation modulus and its slope at 60 seconds of the base binder were decreased from nearly 37 MPa to be lower than 14 MPa, and increased from 0.43 to almost 0.47 at 15% CRM concentration, respectively. Furthermore, it can be seen that the CRM binders containing the higher rubber content exhibited the better the relaxation rates of the binders compared to the base binder. The improvement of low-temperature performance of the CRM binders can be attributed to the presence of the CRM particles within the binder mastic which enhanced the elastic response of the binders at the low-temperature. Thus, the higher proportion of rubber in the asphalt binder mastic resulted in the more elastic particles which lower the low-temperature stiffness and improve the stress-relaxation ability of the binders.



**Figure 7. 11:** Relaxation modulus at 60 seconds and at  $-10^{\circ}\text{C}$  showing the effect of CRM content.

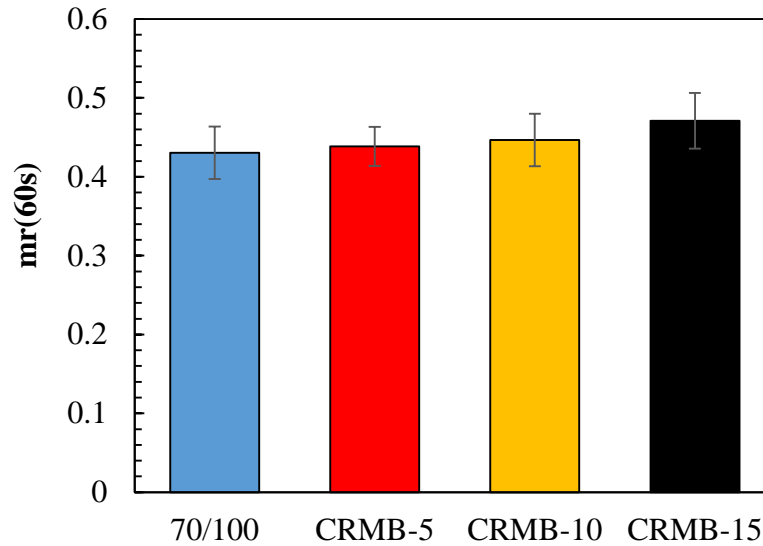


**Figure 7. 12:** Slope coefficient of the relaxation modulus at 60 seconds and at  $-10^{\circ}\text{C}$  showing the effect of CRM content.

### 7.3.2 Effect of WMA additives on the low-temperature performance

The effect of the WMA additives on low-temperature performance of the base bitumen and the CRM binders are presented in Figure 7.13-7.14. According to the diagrams, it can be clearly observed that an addition of the wax-based WMA additive negatively impacted both base and CRM binders. Generally, both unmodified and modified binders with the wax-based additive showed a significantly higher low-temperature stiffness compared to the binders without the wax additive. In the case of the base binder, the stiffness increased from below 30 MPa to almost 40 MPa when the wax was added into the base binder. The addition of wax also doubled the stiffness of the CRM binders which made it more susceptible to the low-temperature thermal cracking. Moreover, the relaxation rate of both base and CRM binders were decreased due to the stiffening effect of the wax-based additive. The increase in stiffness and the decrease in relaxation ability of the binders were due to the formation of the crystalline structure of wax in the binder matrix at the temperature below its melting point ( $\sim 100^{\circ}\text{C}$ ).

On the one hand, the effect of the chemical-based additive on the low-temperature cracking resistance of the base binder was found to be desirable. The chart 7.13 demonstrates a relatively low stiffness of the base binder with the chemical compared to the base binder without the chemical-based additive. An obvious improvement of 70/100-C's relaxation rate was also recognized in Figure 7.13. On the other hand, the effect of the chemical additive on the CRM binder (Figure 7.14) was found to be opposed to the case of the base binder. The chemical additive seemed to lower an elastic response of the CRM binder at low temperature as the chemical slightly increased the stiffness and lowered the relaxation rate of the CRMB.

Even though the addition of both wax-based and chemical-based additives decreased the low-temperature thermal cracking resistance of the modified binder, their low-temperature stiffness values were still relatively low compared to the base bitumen with and without the WMA additive. This result indicated that the binder modification with the CRM can truly improve the low-temperature road damage resistance.

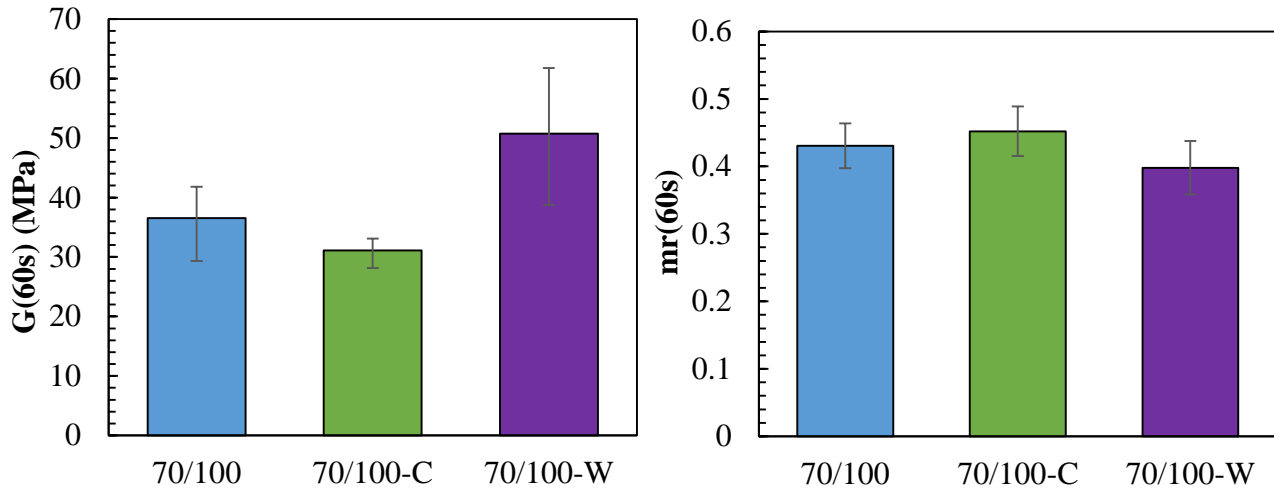


**Figure 7. 13:** the magnitude (left) and slope coefficient (right) of the relaxation modulus at 60 seconds and at  $-10^{\circ}\text{C}$  showing the effect of WMA additives on the base binder.

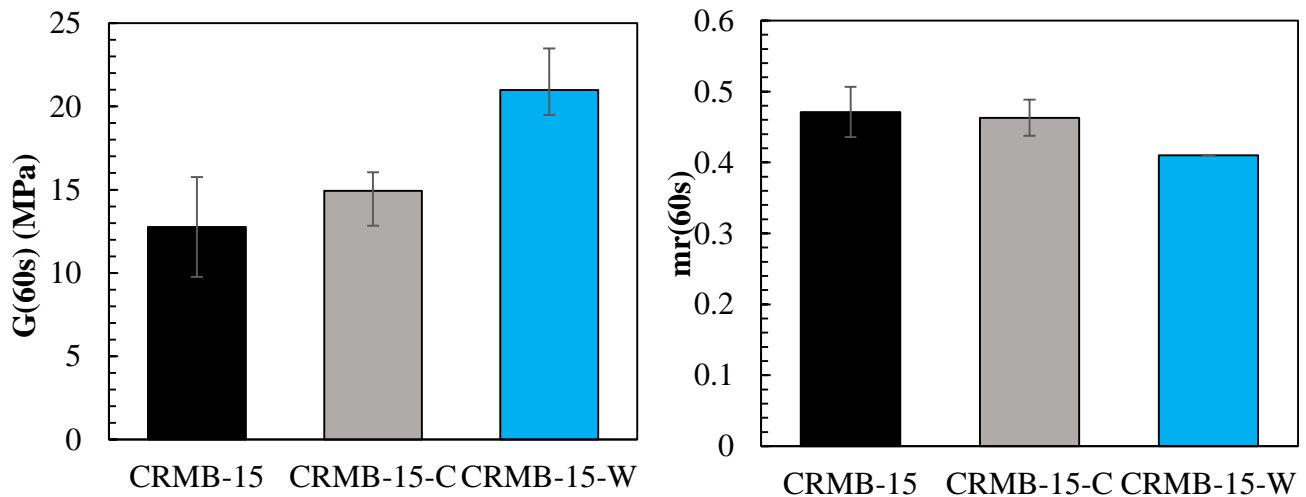


**Figure 7. 14:** the magnitude (left) and slope coefficient (right) of the relaxation modulus at 60 seconds and at  $-10^{\circ}\text{C}$  showing the effect of WMA additives on the CRMB.

## 7.4 Summary

This chapter focused on characterizing low-temperature rheological properties of the binders to investigate the effect of CRM content and WMA additives on the low-temperature damage resistance of the binders. Although, the BBR test was not conducted to verify the correlation of the findings in this chapter due to the unavailability of the BBR device, and there is an uncertainty

about the difference of cooling media between the BBR and the DSR which may affect the performance of the binders (Marasteanu & Cannone Falchetto, 2018). However, the idea of characterization and the results in this chapter can be used for ranking the low-temperature performance of the binder.

#### **7.4.1 Effect of CRM content on low-temperature performance of the binders**

- According to the 4-mm DSR test results, it can be concluded that the CRM content significantly affects the low-temperature stiffness and stress relaxation rate of the asphalt binders. It is clear that the low-temperature performance of the binders was improved when incorporated with the crumb rubber.

#### **7.4.2 Effect of WMA additives on low-temperature performance of the binders**

- In the case of low-temperature performance, the addition of the wax-based warm-mix additive was proven to be disadvantageous for both unmodified and modified binders as it made the binders become more susceptible to the low-temperature thermal cracking by increasing the binders' stiffness. While, the chemical-based warm-mix additive differently affected the base and the modified binders. The chemical slightly improved the low-temperature damage resistance of the base binder, but lowered the low-temperature performance of the CRMB.



# **Chapter 8**

## **High-Temperature Storage Stability**

## 8.1 Introduction

Crumb rubber modifier (CRM) recycled from scrap tyres has been used as a bitumen modifier in pavement industry for decades, but the use of this type of asphalt binder modifier is not popular like other polymers. It is because of its lower storage stability at elevated temperatures. Storage stability of the CRMB at high temperature is one of the critical issues of the CRMB as it has a very high tendency of CRM to separate from the CRMB. Higher density of the CRM particles causes them to settle down to the bottom of hot storage tanks due to the gravitational force, and therefore cause variation between CRMB's physical properties of the top part and bottom part of the hot-storage tanks. The mechanism of separation significantly depends on the type and dosage of bitumen modifier and its interaction with asphalt binder (Bahia et al. 1998, Ghavibazoo et al. 2013). Therefore, variation in CRM dosage and warm mix additives will surely result in different interaction, and consequently different high-temperature storage stability of CRMB.

Even hot storage tanks with agitation system are typically applied when highly modified or polymer-modified asphalt binder is used in road constructions to ensure uniform temperature and homogeneity of the modified binder, especially CRMB. However, a phase separation of the constituents still occurs resulting in an increase in road construction cost. Thus, getting more insight about the storage stability of the CRMB will contribute to an improvement of storage stability of CRMB, and ultimately results in cost reduction.

The main objective of this Chapter is to experimentally investigate the effects of CRM concentration and warm mix additive on the tendency of CRM particles to separate from CRMB under static high-temperature storage. In this chapter, the storage stability of five different crumb rubber modified binders (as shown in detail in Table 8.1) was carried out in accordance with ASTM D7173 and AASHTO-350 (MSCR) respectively, in order to observe and mechanically evaluate the effects of CRM and the WMA additives on the storage stability of the CRMB.

**Table 8. 1:** Modified binders used for storage stability test.

Type of asphalt binders	Code	Base bitumen	CRM content (%)	WMA additive
Crumb rubber modified bitumen	CRMB-5	70/100	5	none
	CRMB-10		10	none
	CRMB-15		15	none
Crumb rubber modified bitumen containing warm mix additive	CRMB-15-W		15	Wax-based
	CRMB-15-C		15	Chemical-based

## 8.2 Experimental program

According to the Standard Practice for Determining the Separation Tendency of Polymer from Polymer Modified Asphalt (ASTM D7173),  $50 \pm 0.5$  g of each hot CRMB blend (as mentioned in table 8.1) was poured into standard aluminum tubes- 25-mm diameter by 125-mm to 140-mm length. After that, filled tubes were oriented in the vertical direction as shown in Figure 8.1 and kept in the oven at  $163^\circ\text{C} \pm 5^\circ\text{C}$  for  $48 \pm 1$  h. Then, the tubes were cooled to  $-10^\circ\text{C} \pm 10^\circ\text{C}$  in order to solidify the binders. After cooling, the frozen tubes were cut into three equal parts (40-mm each), and the samples from the top, middle, and bottom parts of the tube were stored for further testing as shown in Figure 8.2.

Typically, the storage stability of the prepared samples is evaluated by means of softening point and/or penetration technique. The difference between top-part and bottom-part properties is normally used as an indicator of the storage stability of the asphalt binder, but the empirical nature of these tests was reported to be insufficient in evaluating the presence of modifier particles.

In this study, the MSCR test was carried out at  $64^\circ\text{C}$  to mechanically evaluate the presence of the elastic response of each part of the prepared samples in term of percent recovery (%rec) and an ability to resist a permanent deformation under repeated loading in term of non-recoverable compliance (Jnr) of the asphalt binders. Furthermore, the differences in the mechanical properties of the prepared specimens were analyzed to get a proper understanding of the phase separation of CRMB during hot storage.



**Figure 8. 1:** Arrangement of separation tubes in vertical orientation.

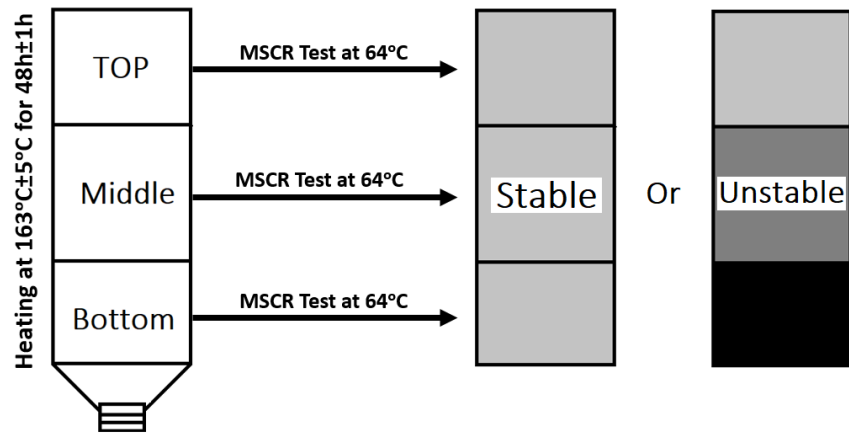


**Figure 8. 2:** The scheme of the polymer modified bitumen high-temperature storage stability evaluation.

### 8.3 Results and analysis

As mentioned earlier, the MSCR test was conducted to quantify the amount of separation or non-uniformity of the modified material after heated storage. The results from the entire MSCR test are shown in Table 8.2.

**Table 8. 2:** MSCR test results of different sections of the aluminum tubes.

Sample Code	Creep Compliance, Jnr (1/kPa)					
	Load level 0.1kPa			Load level 3.2kPa		
	Top	Middle	Bottom	Top	Middle	Bottom
CRMB-5	5.902	5.639	0.576	6.777	6.465	2.735
CRMB-10	1.517	0.317	0.229	1.994	1.277	1.115
CRMB-15	0.228	0.121	0.062	0.800	0.796	0.632
CRMB-15-C	0.612	0.123	0.010	0.918	0.531	0.453
CRMB-15-W	0.085	0.017	0.010	0.411	0.332	0.183

Sample Code	Recovery, rec (%)					
	Load level 0.1kPa			Load level 3.2kPa		
	Top	Middle	Bottom	Top	Middle	Bottom
CRMB-5	0.000	0.000	69.317	0.000	0.000	7.580
CRMB-10	22.740	79.770	79.277	5.540	20.670	23.470
CRMB-15	74.177	85.995	91.895	26.690	29.145	35.375
CRMB-15-C	40.575	82.730	91.705	35.210	41.611	53.020
CRMB-15-W	91.410	94.665	96.040	38.765	40.410	46.065

Based on the results at 3.2kPa load level, the values of non-recoverable creep compliance ( $J_{nr, 3.2kPa}$ ) and recovery of three different sections were plotted in Figure 8.3 and 8.4. According to Figure 8.3, it can be clearly seen that at the higher CRM concentration, the differences between the values of creep compliance and recovery were significantly decreased. The binder that possessed the highest difference for the creep compliance and recovery values was determined to be the crumb rubber modified bitumen with 5% rubber content (CRMB-5). It was found that presence of elastic response (%recovery) at top and middle sections of CRMB-5 are 0%, while the bottom part was found to be around 8%. This result suggested that the CRM particles are mostly in the bottom section of the conditioned CRMB-5 tube, meaning that the storage stability of CRMB-5 was relatively low. Conversely, the binder with the lowest difference for  $J_{nr}$  and %rec values from the MSCR test was found to be the binder with 15% CRM concentration (CRMB-15). CRMB-15 shows significantly more uniform value of creep compliance and %recovery.

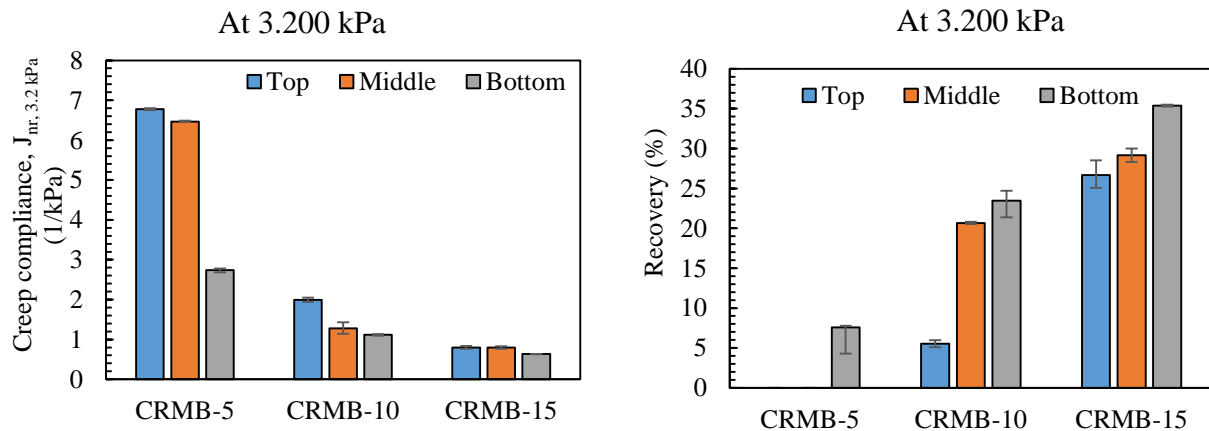


**Figure 8. 3:** The effect of CRM concentration on high-temperature storage stability of CRMB in term of non-recoverable compliance (left) and in term of recovery (right).

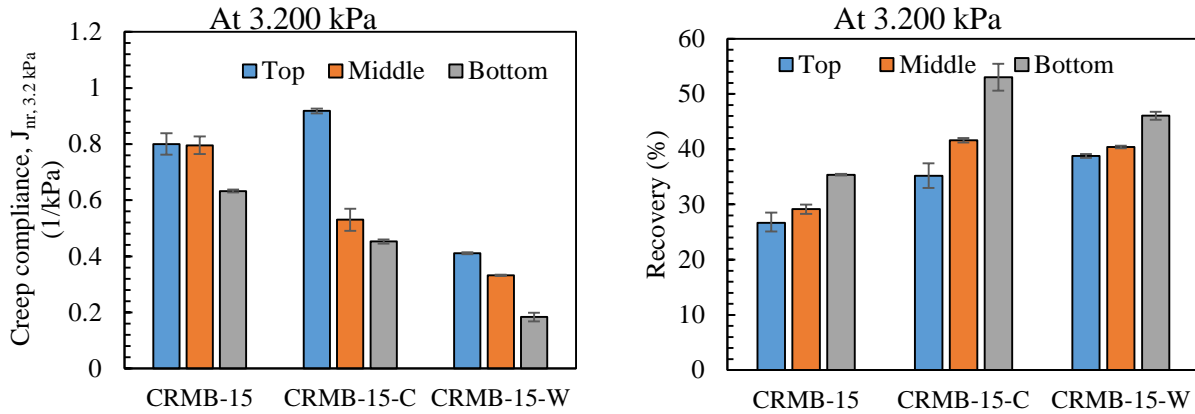


**Figure 8. 4:** The effect of WMA additives on high-temperature storage stability of CRMB in term of non-recoverable compliance (left) and in term of recovery (right).

In case of CRMB with the additives, the chart showing values of  $J_{nr}$  and %recovery at 3.2kPa load level were drawn as shown in Figure 8.4 in order to compare the amount of separation or non-uniformity of the modified material after conditioning. Based on Figure 8.4, the effect of warm-mix additives on the storage stability of the conditioned materials can hardly indicated because of the effect of the warm-mix additives on the rutting susceptibility of the binder.

In order to identify the effects of the warm-mix additives on the high-temperature storage stability of the CRM binders, the storage instability index based on the non-recoverable creep compliance at 3.2kPa ( $J_{nr,3.2kPa}$ ) of the conditioned samples was therefore employed as an indicator to capture the actual effect of the CRM content and WMA additives on the storage stability of the CRMB at elevated temperatures. The  $J_{nr}$  value at 3.2kPa load level was selected as an indicator because at very high stress level the presence of elastic particles can be clearly distinguished. The storage instability index was calculated as followed:

$$\text{Storage Instability Index} = \frac{J_{nr,3.2kPa-Top} - J_{nr,3.2kPa-Bottom}}{J_{nr,3.2kPa-Average}} \quad (8.1)$$

Where:

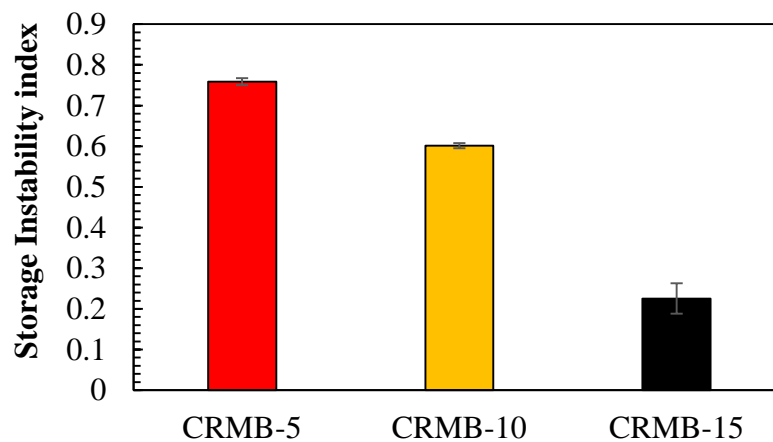
$J_{nr,3.2kPa-Top}$  = the non-recoverable creep compliance at 3.2 kPa of the top part of the tube.

$J_{nr,3.2kPa-Bottom}$  = the non-recoverable creep compliance at 3.2 kPa of the bottom part of the tube.

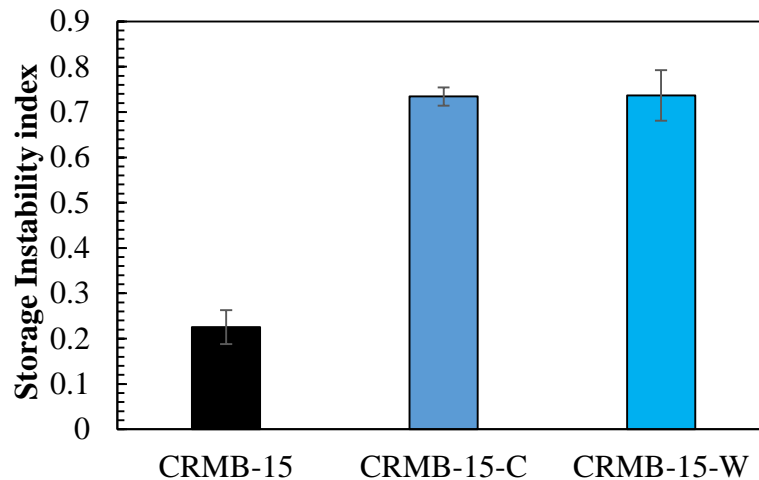
$J_{nr,3.2kPa-Average}$  = the average value of the non-recoverable creep compliance at 3.2 kPa of the whole tube.

Figure 8.5 and 8.6 present the storage instability index showing the effect of CRM concentration and the WMA additives, respectively. According to the storage instability index chart (Figure 8.5), it is clear that the addition of CRM can significantly improve the storage stability of the CRM binders. The CRMB-5 shows the largest value of the instability index, indicating the worst high-temperature storage stability. While, the CRMB-15 possessed the smallest index of storage instability which shows the best performance. The reason is due to at the higher CRM concentration results in the more interaction between rubber particles and bitumen

which reduces rubber inter-particle distance, and increases the viscosity of the CRMB. The higher value of viscosity and smaller inter-particle distance have improved the resistance of the settling down of the CRM particles because the movement of the CRM particles was reduced. Moreover, it can be observed that the storage instability index of the CRMB with the warm-mix additives (both wax-based and chemical-based) in Figure 8.6 were larger than the index of CRMB without a warm-mix additive. It was because the warm-mix additives were intentionally designed to reduce the viscosity of asphalt binders at the mixing and placing temperatures (above 160°C). The lower viscosity of the CRMB with the warm-mix additives allowed the CRM particles to settle down more easily as evidenced by the bigger difference in the rutting properties of the top and bottom sections.



**Figure 8. 5:** Storage instability index showing effect of the CRM concentration.



**Figure 8. 6:** Storage instability index showing effect of the WMA additives.

## 8.4 Summary

### 8.4.1 Effect of CRM content on storage stability of CRMB

- According to MSCR test results, the CRMB with the lowest CRM concentration (5%-CRM) was found to be the most unstable material as its degree of separation was the highest among the samples. CRMB blends produced with the CRM at 15% concentration were found to be relatively stable compared to the others. From the observation, it is obvious that the viscosity of the CRMB significantly increased as the CRM concentration became higher. The increase of CRMB viscosity could reduce the settle down of swollen CRM particles to the bottom section of the tube, which resulted in more stable asphalt binding material. Furthermore, the increased amount of CRM surely shorten the inter-particle distance of swollen CRM and improve interconnection between swollen rubber particles, which results in prevention of rubber particles movement during the hot-storage period. Therefore, CRM content plays an important role in storage stability, and the results indicated that the increase of CRM concentration leads to improvement of storage stability.

### 8.4.2 Effect of WMA additives on storage stability of CRMB

- The comparison results of the CRMB with and without warm-mix additive illustrated that the warm-mix additives had a measurable effect on storage stability of the CRMB. Based on the storage instability index, both wax-based and chemical-based warm-mix additives increased a separation tendency of CRMB, especially the wax-based additive.



# **Chapter 9**

## **Conclusions and Recommendations**

## 9.1 Conclusions

The primary aim of this study was to characterize the rheological and performance-related properties of the binders by means of traditional (Frequency sweep test) and newly developed (MSCR, LAS, and 4-mm DSR) testing methods in order to investigate the effect of crumb rubber content and the warm-mix additives on the binder properties. Based upon the results of the study presented in the previous chapters the following conclusions and key findings can be drawn (more detail of the summary of the study results can be found in Table 9.1):

1. The addition of CRM can enhance rheological and performance-related properties of the binders over the whole road service temperatures. It was found that the incorporation of CRM into the base bitumen can improve the stiffness, elastic response, and aging resistance of the binder at the normal road service temperature.
2. The CRMBs show an improved road damage resistance and recoverability over the whole road service temperatures. A dosage of the CRM plays an important role in the improvement of the overall performance, and the high-temperature storage stability of the CRMB.
3. The wax-based WMA additives similarly affected the performance of the base bitumen and CRMB. The addition of the wax additive can only enhance the high-temperature performance of the binders, but the effect of wax on the performance of the bituminous binder at intermediate and low road service temperatures were found to be adverse as it lowered the fatigue and thermal cracking resistances of both base and CRM binders.
4. The influences of the chemical-based WMA additive on the performance of the base bitumen and CRMB were different. The addition of the chemical additive was observed to be disadvantageous for the CRMB as it reduced the overall damage resistance of the CRMB. However, the negative effects of the chemical additive on the CRMB's performances at intermediate- and low-temperatures were less severe than the negative effect of the wax-based additive. In the case of the base binder, the addition of the chemical can slightly increase the overall road damage resistance of the base binder.
5. The addition of the WMA additives obviously reduced the high-temperature storage stability of the CRMB.

Table 9.1: Summary of the study results.

Property	Parameters	% CRM	Effect of the chemical-based warm-mix additive on		Effect of the wax-based warm-mix additive on	
			Base bitumen	CRMB	Base bitumen	CRMB
Rheological properties	Complex modulus (G*) at 30°C	√	•	•	√	√
	Phase angle at 30°C	√	•	•	√	√
	Thermal susceptibility	√	•	•	√	√
High-temperature performance	Rutting resistance (Jnr) at 64°C	√	√	x	√	√
	Recoverability (%recovery) at 64°C	√	•	x	√	√
	Stress sensitivity (Jnr, slope) at 64°C	√	•	•	√	•
Intermediate-temperature performance	Fatigue damage resistance at 20°C	√	•	x	x	x
Low-temperature performance	Low-temperature stiffness (G[60s]) at -10°C	√	√	x	x	x
	Stress relaxation rate (mr[60s]) at -10°C	√	√	x	x	x
High-temperature storage stability	based on Storage instability index	√	-	√	-	√
Short-term aging resistance	based on Stiffness Index	√	x	x	√	x
	based on Oxidation product	√	x	x	•	x
	based on Jnr Index	√	•	•	√	x
Long-term aging resistance	based on Stiffness Index	√	x	•	√	•
	based on Oxidation product	√	x	x	x	x
	based on Jnr Index	√	√	x	√	x

\*Note: √ = increase, x = decrease, • = inconsiderable, and - = not applicable.

## 9.2 Recommendations

In this thesis, the properties and performance of the warm-mix CRMB were only characterized in a bitumen-level, and the materials used in this study were very limited in extent. Therefore, in this section, a list of recommendations for future research are presented.

1. In order to get more comprehensive results, the base bitumen and CRM with varying origins and compositions should be included to validate the effects of the CRM and the WMA additives used in this study.
2. In this study, only two common commercial available products of WMA additives were investigated. However, there are many other WMA additive types on the market that their effects on the CRMB properties need to be investigated.
3. Due to the unavailability of the BBR, the correlation of the 4-mm DSR results and the BBR parameters in the case of the CRMB was not verified. Thus, BBR test should be conducted to confirm the validity of the 4-mm DSR test.
4. The predicted fatigue lives of the long-term aged binders in this study were found to be longer than the fresh binders which were unexpected. The reason is that the LAS test does not take the healing ability of the binder into account. Thus, in order to get more realistic fatigue resistance of the asphalt binders, the healing capacity of the binders at different aging conditions should be considered.
5. Performance characterizations should be extended in the higher levels such as mastic (binder+filler), mixture, and road scale to clearly verify the effect of CRM and WMA additives.
6. Although it may be time-consuming, more verification need to be done to establish a unified DSR test methodology for binder performance testing.

---

## References

AASHTO M 320-10: *Standard Specification for Performance Graded Asphalt Binder*. American Association of State Highway and Transportation Officials. 2010.

Abdelrahman, M. *Controlling performance of crumb rubber-modified binders through addition of polymer modifiers*. Transportation Research Record: Journal of the Transportation Research Board (1962), 2006, pp.64-70.

Abdelrahman, M.A. and Carpenter, S.H. *Mechanism of interaction of asphalt cement with crumb rubber modifier*. Transportation Research Record: Journal of the Transportation Research, Vol. 1661, 1999, pp. 106–113. <http://dx.doi.org/10.3141/1661-15>

Airey, G.D. *Rheological Characteristics of Polymer Modified and Aged Bitumens*, PhD Thesis, The University of Nottingham, 1997.

Airey, G.D., Singleton, T.M. and Collop, A.C. *Properties of polymer modified bitumen after rubber-bitumen interaction*. ASCE Journal of Civil Engineering Materials, 14 (4), 2002, pp. 344-354.

Anderson, D. A., and Kennedy, T. W. *Development of SHRP Binder Specification*, Journal of the Association of Asphalt Paving Technologists, Vol .62, 1993, pp. 481–507.

Anderson, D. A., Le Hir, Y.M., Marasteanu, M.O., Planche, J -, Martin, D., Gauthier, G. *Evaluation of fatigue criteria for asphalt binders*, Transportation Research Record: Journal of the Transportation Research Board, Vol. 1766(1), 2001, pp. 48-56. <https://doi.org/10.3141/1766-07>

Anderson, D.A., Christenson, D.W and Bahia, H.U. *Physical Properties of Asphalt Cement and the Development of Performance-Related Specifications*, Journal of the Association of Asphalt Paving Technologists, vol.60, 1991, pp. 437-475.

Asphalt Institute Technical Advisory Committee, *Guidance on the Use of the MSCR Test With the AASHTO M320 Specification*, Asphalt Institute, Lexington, KY, 2010.

ASPHALT INSTITUTE. *Summary of the standard PG testing and criteria*, The specifications for performance Graded (PG) asphalt binders are given by AASHTO M 320 or ASTM D6373, 2005. <http://www.asphaltinstitute.org/engineering/specification-databases/us-state-binder-specifications/>

ASPHALT INSTITUTE. *Superpave performance graded asphalt binder specification and testing*, Superpave series no.1, ASPHALT INSTITUTE, Kentucky, 1997, pp. 15–19.

Austroroads. *Review of Overseas Trials of Warm Mix Asphalt Pavements and Current Usage by Austroroads Members*; AUSTROROADS TECHNICAL REPORT; AP-T215-12; November 2012; ISBN 978-1-921991-57-8; Australia.

BAHIA H. U., ANDERSON, D. A., CHRISTENSEN D.W. *The bending beam rheometer: a simple device for measuring low-temperature rheology of asphalt binders*. Journal of the association of asphalt paving technologists, Association of Asphalt Paving Technologists, Seattle, 1991, pp. 117–135.

Bahia, H. U., Zhai, H., Rangel, A. *Evaluation of Stability, Nature of Modifier, and Short-Term Aging of Modified Binders Using New Tests: LAST, PAT, and Modified RTFO*. In Transportation Research Record 1638, TRB, National Research Council, Washington, D.C., 1998, pp. 64–71.

Bahia, H.U. and Davies, R. *Effect of crumb rubber modifiers (CRM) on performance-related properties of asphalt binders*. Journal of the Association of Asphalt Paving Technologists, Vol. 63, 1994, pp. 414–438.

Bahia, H.U., Hanson, D.I., Zeng, M., Zhai, H., Khatri, M.A., Anderson, R.M. *Characterization of modified asphalt binders in superpave mix design*. Report No. 459, National Cooperative Highway Research Program, National Academy Press, Washington, D.C., 2001.

Bahia, H.U., Zhai, H. *A new method for the storage stability test of modified asphalt*. Prep Am Chem Soc, Div Fuel Chem 4, 1998, 1041–1045.

Bahia, H.U., Zhai, H., Zeng, M., Hu, Y., Turner, P. *Development of binder specification parameters based on characterization of damage behavior*. Journal of the Association of Asphalt Paving Technologists, Vol.70, 2002, pp. 442-470.

Baumgardner, G. and D'Angelo, J.A. *Evaluation of New DSR Testing Geometry for Performance Testing of Crumb Rubber Modified (CRM) Binder*. Transportation Research Record: Journal of the Transportation Research Board, No.2293, 2012, pp. 73-79.

Brown, R. *Historical Development: History of Use of Crumb Rubber in Asphalt Paving Materials*, Auburn, AL: National Center for Asphalt Technology, 1993.

Capitão, S.D., Picado-Santos, L.G., Martinho F. *Pavement engineering materials: Review on the use of warm-mix asphalt*. Construction and Building Materials, Vol.36, 2012, pp. 1016-1024.

Chin, C. *PERFORMANCE GRADED BITUMEN SPECIFICATIONS*, 2018.

Chowdhury, A., Button, J. W. *A Review of Warm Mix Asphalt*. Springfield, Virginia: National Technical Information Service, 2008.

D'Angelo, John A., Kluttz, R., Dongre, R.N., Stephens, K., Zanzotto, L., *Revision of the superpave high temperature binder specification: the multiple stress creep recovery test (With Discussion)*. Journal of the Association of Asphalt Paving Technologists: From the Proceedings of the Technical Sessions Paving Technology, Vol. 76, 2007.

D'Angelo, J. A., Harm, E. E., Bartoszek, J. C., Baumgardner, Gaylon L., Corrigan, Matthew R., Cowsert, Jack E., Harman, Thomas P., et al. *Warm mix Asphalt: European Practice. No. FHWA-pl-08-007*. USA. 2008.

D'Angelo, John A. *The Relationship of the MSCR Test to Rutting*. Road Materials and Pavement Design, 10:sup1, 2009, pp. 61-80. <https://doi.org/10.1080/14680629.2009.9690236>

Di Benedetto, H., Sauzeat, C., Bilodeau, K., Buannic, M., Mangiafico, S., Nguyen, QT., Pouget, S., Tapsoba, N. & Van Rompu, J. *General Overview of the time-temperature superposition principle validity for materials containing bituminous binder*. International Journal of Roads and Airports, Vol. 1, 2011, pp.35–52. <https://doi.org/10.5568/ijra.2011-01-03.3552>

Dongre R., D'Angelo J. *Evaluation of Different Parameters for Superpave High Temperature Binder Specification Based on Rutting Performance in the Accelerated Loading Facility at FHWA*, Transportation Research Record, TRB, 2003, Transportation Research Board, National Research Council, Washington D.C., 2003.

Edwards Y, Isacson U. *Wax in bitumen-State of the art: Part2- Characterization and effects*. Road Mater Pavement Des 2005;6(4):1–30.

ETRMA. *End-of-life Tyre Report 2015*. European Tyre & Rubber manufacturers' association. 2015. <http://www.etrma.org/uploads/Modules/Documentsmanager/elt-report-v9a---final.pdf>

Farina, A., Zanetti, M.C., Santagata, E., Blengini, G.A. *Life cycle assessment applied to bituminous mixtures containing recycled materials: Crumb rubber and reclaimed asphalt pavement*. Resources, Conservation and Recycling, Vol. 117, 2017, pp. 204–212. <https://doi.org/10.1016/j.resconrec.2016.10.015>

Ghavibazoo, A., Abdelrahman, M. *Effect of Crumb Rubber Dissolution on Low-Temperature Performance and Aging of Asphalt–Rubber Binder*. Transportation Research Record: Journal of the Transportation Research Board, No. 2445, Transportation Research Board of the National Academies, Washington, D.C., 2014, pp. 47–55. DOI: 10.3141/2445-06

- Ghavibazoo, A., Abdelrahman, M., Ragab, M., 2013. *Effect of crumb rubber modifier dissolution on storage stability of crumb rubber-modified asphalt*. Transportation Research Record: Journal of the Transportation Research Board, No. 2370, Transportation Research Board of the National Academies, Washington, D.C., 2013, pp. 109–115. DOI: 10.3141/2370-14
- Heitzman, State of the practice: *Design and construction of asphalt paving materials with crumb-rubber modifier*. Final report, Asphalt Rubber 47 (2), 1992, pp. 171–174.
- Hintz, C., & Bahia, H. *Simplification of Linear Amplitude Sweep Test and Specification Parameters*. Transportation Research Record: Journal of Transportation Research Board, Vol.2370, 2013, pp.10-16.
- Hintz, C., and Bahia, H., *Understanding Mechanisms Leading to Asphalt Binder Fatigue in Dynamic Shear Rheometer*. Road Materials and Pavement Design, 14(2), 2013.
- Hintz, C., Velasquez, R., Johnson, C., and Bahia, H. *Modification and Validation of Linear Amplitude Sweep Test for Binder Fatigue Specification*. Transportation Research Record: Journal of the Transportation Research Board, 2207, 2011, pp.99–106.
- Hsu, C.-P.S. *Infrared Spectroscopy*. Handbook of Instrumental Techniques for Analytical Chemistry. F.A. Settle, ed. Prentice Hall PTR, Upper Saddle River, NJ. 1997, pp. 247-283
- Hung, S.S Farshidi, F. Jones, D. Alavi, M.Z. Harvey J.T. and Sadraie H.. *Investigation of Wet-Process Asphalt Rubber Binder Testing with Modified Dynamic Shear Rheometer: Interim Report on Screening Tests*. Technical Memorandum: UCPRC-TM-2014-02. California Department of Transportation. August 2014.
- Johnson, C., Bahia, H. U. *Evaluation of an accelerated procedure for fatigue characterization of asphalt binders*, submitted for publication in Road Materials and Pavement Design. 2010.
- Kim, Y., H. J. Lee, D. N. Little, and Y. R. Kim. *A simple testing method to evaluate fatigue fracture and damage performance of asphalt mixtures*. Journal of Association of Asphalt Paving Technologists, Vol. 75, 2006, pp. 755–788
- Lamontagne, J., et al., *Comparison by Fourier transform infrared (FTIR) spectroscopy of different ageing techniques: application to road bitumens*. Fuel 80(4), 2001. p. 483-488.
- Lee, S.-J. Hu, J. Kim, H. Amirkhanian, S. N. and Jeong, K.-D. *Aging analysis of rubberized asphalt binders and mixes using gel permeation chromatography*, Construction and Building Materials, vol.25, no.3, 2011, pp.1485–1490.



Lee, S-J., Amirkhanian, S., Shatanawi, K. *Effects of crumb rubber on aging of asphalt binders*, asphalt rubber 2006, vol. 3. California: Palm Springs; 2006. pp. 779–95.

Lo Presti, D. *Recycled Tyre rubber modified bitumens for road asphalt mixtures: a literature review*, Construction and Building Materials 49, 2013, pp. 863–881. <http://dx.doi.org/10.1016/j.conbuildmat.2013.09.007>

Masad, E., Somadevan, N., Bahia, H. U., & Kose, S. *Modeling and Experimental Measurements of Strain Distribution in Asphalt Mixes*. Journal of Transportation Engineering, 127(6), 2001, pp. 477–485.

Memon N. *Characterization of conventional and chemically dispersed crumb rubber modified bitumen and mixtures*. PhD thesis, University of Nottingham. 2011.

Mike Anderson. *Introduction to the Multiple-Stress Creep-Recovery (MSCR) Test and its Use in the PG Binder Specification*, 54th Annual Idaho Asphalt Conference Moscow, Idaho .23 October 2014

Navarro, F.J., Partal, P., Martinez-Boza, F, Gallegos, C. *Thermo-rheological behaviour and storage stability of ground tyre rubber-modified bitumens*. Fuel Volume83, Issue 14–15, October 2004, pp. 2041-2049. <https://doi.org/10.1016/j.fuel.2004.04.003>

NIOSH. *Crumb-rubber Modified Asphalt Paving Occupational Exposures and Acute Health Effects*. National Institute for Occupational Safety and Health, Cincinnati, Ohio, USA. 2001. <https://www.cdc.gov/niosh/hhe/reports/pdfs/2001-0536-2864.pdf>

Olli-Ville . *Low-temperature rheology of bitumen and its relationship with chemical and thermal properties*, 2015.

Papagiannakis, A. T. Loughheed, TJ. *A Review of Crumb-Rubber Modified Asphalt Concrete Technology*. Final research report, 1995.

Prowell B, Hurley G, Frank B. *Warm-mix asphalt: best practices*. Lanham (MD): NAPA – National Asphalt Pavement Association; 2011.

Radhakrishnan, V., Ramya Sri, M., Sudhakar Reddy, K. *Evaluation of asphalt binder rutting parameters*. Construction and Building Materials, Vol.173, 2018, pp. 298–307. <https://doi.org/10.1016/j.conbuildmat.2018.04.058>

- Rafat Siddique, T. R. *Properties of Concrete Containing Scrap Tire Rubber-An Overview*. Waste Management, 2004.
- Read, J., and D., Whiteoak, *the Shell Bitumen Handbook, 5th Edition*, London: Thomas Telford Publishing, 2003
- Rubio, C.M., Martínez, G., Baena, L., Moreno, F. *Warm mix asphalt: an overview*. Journal of Cleaner Production, Vol. 24, 2012, pp. 76-84. <https://doi.org/10.1016/j.jclepro.2011.11.053>
- Rubio, M.C., Martínez, G., Baena, L., Moreno, F. *Warm mix asphalt: an overview*. Journal of Cleaner Production, Vol.24, 2012, pp. 76-84. <https://doi.org/10.1016/j.jclepro.2011.11.053>
- Rymer, B., Donavan, P. *Tire-pavement noise Intensity testing in Europe: the NITE study and its relationship to ongoing caltrans quiet pavement activities*. Journal of the Association of Asphalt Paving Technologists, Vol. 74, 2005, pp. 1107-1160.
- Saboo, N., Kumar, P. *Analysis of Different Test Methods for Quantifying Rutting Susceptibility of Asphalt Binders*. Journal of Materials in Civil Engineering, Vol .28, 2016. 10.1061/(ASCE)MT.1943-5533.0001553.
- Shang, L., Wang, S., Zhang, Y., Zhang, Y. *Pyrolyzed wax from recycled crosslinked polyethylene as warm mix asphalt (WMA) additive for SBS modified asphalt*. Construction and Building Materials 25 (2), 2011, pp.886-891.
- Shen, J., Amirkhanian, S. *The influence of crumb rubber modifier (CRM) microstructures on the high temperature properties of CRM binders*. International Journal of Pavement Engineers. 6 (4), 2007, pp. 265-271.
- Shu, X., and B. S. Huang. *Recycling of waste tire rubber in asphalt and Portland cement concrete: An overview*. Construction and Building Materials, Vol. 67, 2014, pp. 217-224. <https://doi.org/10.1016/j.conbuildmat.2013.11.027>
- Shu, X., Huang, B., Shrum, E.D., Jia, X. *Laboratory evaluation of moisture susceptibility of foamed warm mix asphalt containing high percentages of RAP*. Construction and Building Materials, Vol.35, 2012, pp. 125-130.
- Stuart, K.D., Mogawer, W. S., Romer, P. *Validation of Asphalt Binder and Mixture Tests That Measure Rutting Susceptibility*, Report No. FHWA-RD-99-204, 2000.

Subhy, A.T. *Characterisation and development of rubberised bitumen and asphalt mixture based on performance-related requirements*. PhD thesis, University of Nottingham. 2017.

Sui, C., Farrar, M. J., Harnsberger, P. M., Tuminello, W.H., Turner, T. F. *New Low-Temperature Performance-Grading Method Using 4-mm Parallel Plates on a Dynamic Shear Rheometer*, Transportation Research Record: Journal of the Transportation Research Board, No. 2207, Transportation Research Board of the National Academies, Washington, D.C., 2011, pp. 43–48. <https://doi.org/10.3141/2207-06>

Sui, C., Farrar, M.J., Tuminello, W.H., Thomas, F. Turner. *New Technique for Measuring Low-Temperature Properties of Asphalt Binders with Small Amounts of Material*. Transportation Research Record: Journal of the Transportation Research Board, No. 2179, Transportation Research Board of the National Academies, Washington, D.C., 2010, pp. 23–28.DOI: 10.3141/2179-03

The binder *Nynas 70/100 product data sheet*,

[https://nyport.nynas.com/Apps/1112.nsf/wpds/EE\\_EN\\_Nynas\\_70\\_100/\\$File/Nynas\\_70\\_100\\_EE\\_EN\\_PDS.pdf](https://nyport.nynas.com/Apps/1112.nsf/wpds/EE_EN_Nynas_70_100/$File/Nynas_70_100_EE_EN_PDS.pdf)

The use of Warm Mix Asphalt, European Asphalt Pavement Association – Position Paper, 2014. <http://www.eapa.org/userfiles/2/Publications/EAPA%20paper%20-%20Warm%20Mix%20Asphalt%20-%20version%202014.pdf>

Use of the Multiple Stress Creep Recovery (MSCR) Test Method to Characterize Polymer-Modified Asphalt Binders. Available from:

[https://www.researchgate.net/publication/282522397\\_Use\\_of\\_the\\_Multiple\\_Stress\\_Creep\\_Recovery\\_MSCR\\_Test\\_Method\\_to\\_Characterize\\_Polymer-Modified\\_Aspphalt\\_Binders](https://www.researchgate.net/publication/282522397_Use_of_the_Multiple_Stress_Creep_Recovery_MSCR_Test_Method_to_Characterize_Polymer-Modified_Aspphalt_Binders) [accessed Mar 02 2019].

Van den Bergh, W., *The effect of ageing on the fatigue and healing properties of bituminous mortars* (doctoral thesis). Delft University of Technology. 2011.

Wang, C., Zhang, J. *Evaluation of Rutting Parameters of Asphalt Binder Based on Rheological Test*. International Journal of Engineering and Technology, Vol. 6, 2014, pp. 30-33.

Wang, H., Liu, X., Apostolidis, P., Scarpas T. *Review of warm mix rubberized asphalt concrete: Towards a sustainable paving technology*, Journal of Cleaner Production. Vol .177, 2018, pp. 302-314. <https://doi.org/10.1016/j.jclepro.2017.12.245>

Wang, H., Liu, X., Zhang, H., Apostolidis, P., Scarpas T., Erkens, S. *Asphalt-rubber interaction and performance evaluation of rubberised asphalt binders containing non-foaming warm-mix additives*, Road Materials and Pavement Design, 2018.

WMA Technology Production, Testing and Compaction Details, AkzoNobel. 2010. <https://www.dot.ny.gov/divisions/engineering/technical-services/technical-services-repository/details/rediset.pdf>

Yusoff, Md. N.I., Hainin, M.R., Airey, G. *What You Need to Know About Bitumen Rheology*, 2011.

Yusoff N.I.Md.. *Modelling the Linear Viscoelastic Rheological Properties of Bituminous Binders*. PhD thesis, University of Nottingham, 2012.

Zanzotto, L., Kennepohl, GJ. *Development of rubber and asphalt binders by depolymerization and devulcanization of scrap tires in asphalt*. Transportation Research Record:Transportation Research Board, No. 1530, 1996, pp. 51–58.

Zaumanis M. *Warm mix asphalt investigation*. Master of Science thesis. Kgs.Lyngby: Technical University of Denmark in cooperation with the Danish Road Institute, Department of Civil Engineering, 2010. [http://www.warmmixasphalt.org/submissions/117\\_20100630\\_M.Zaumanis\\_WMA\\_Master\\_thesis.pdf](http://www.warmmixasphalt.org/submissions/117_20100630_M.Zaumanis_WMA_Master_thesis.pdf)

# **Appendix A**

## **Effect of aging on rheological properties**

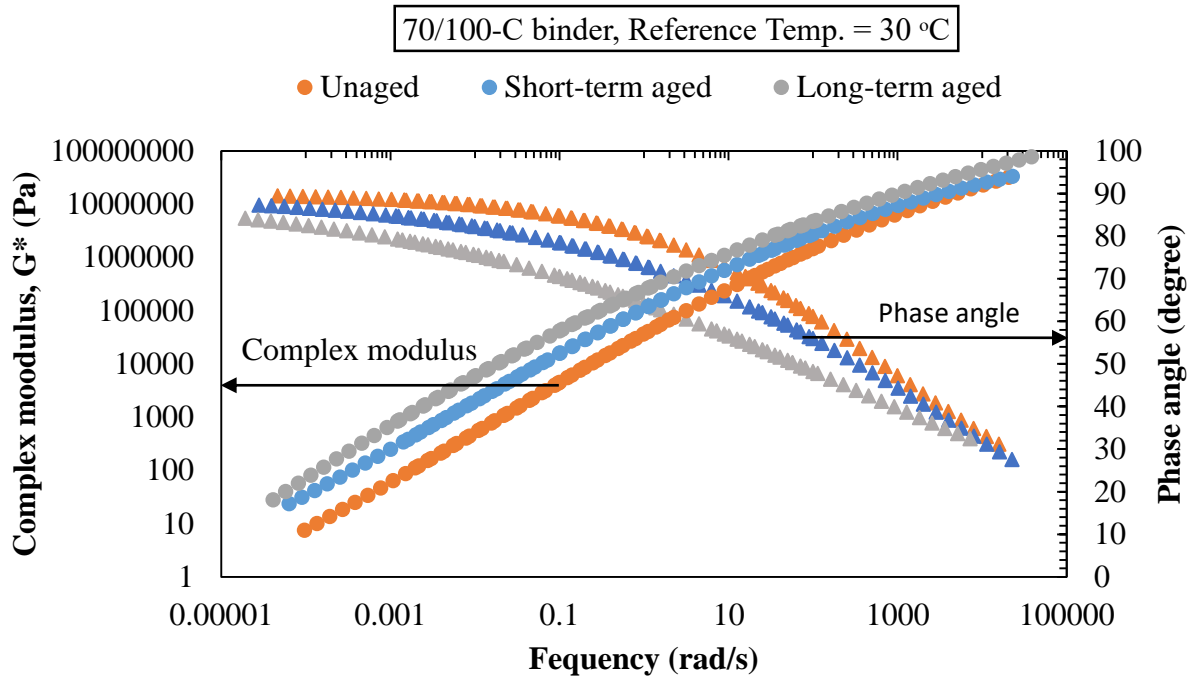


**Figure A.1:** Master curves of complex modulus and phase angle for the 70/100-C binder at a reference temperature of 30°C showing the aging effect.

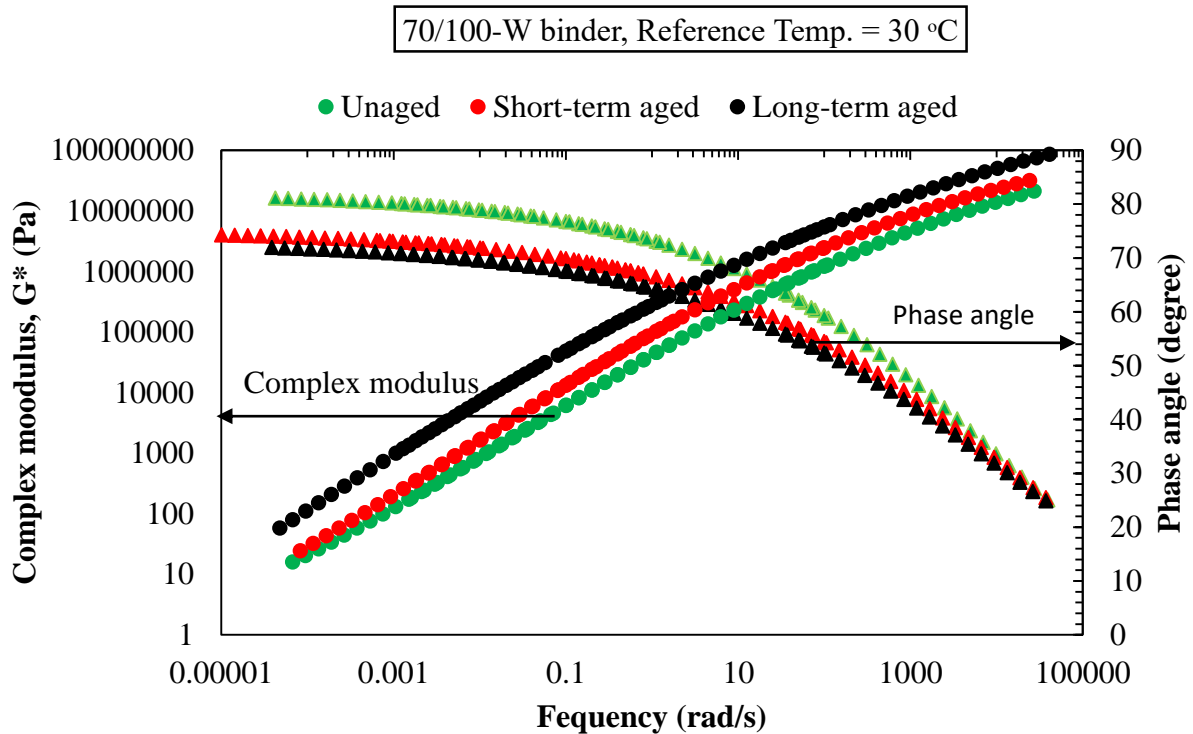


**Figure A.2:** Master curves of complex modulus and phase angle for the 70/100-W binder at a reference temperature of 30°C showing the aging effect.

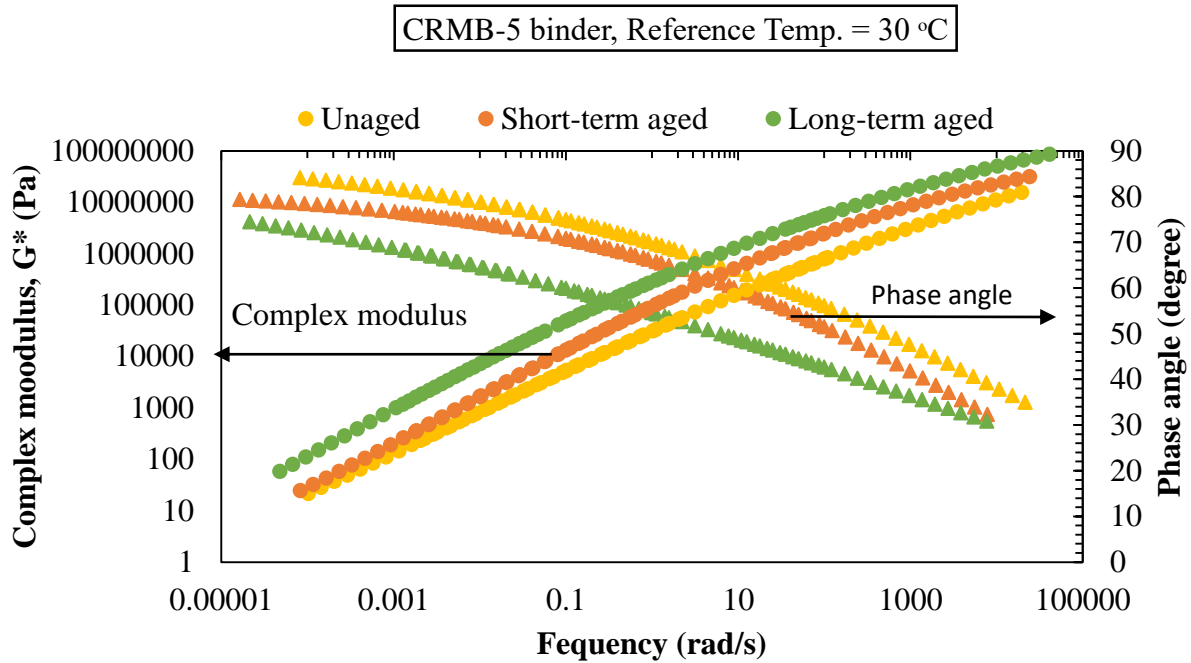


**Figure A.3:** Master curves of complex modulus and phase angle for the CRMB-5 binder at a reference temperature of 30°C showing the aging effect.

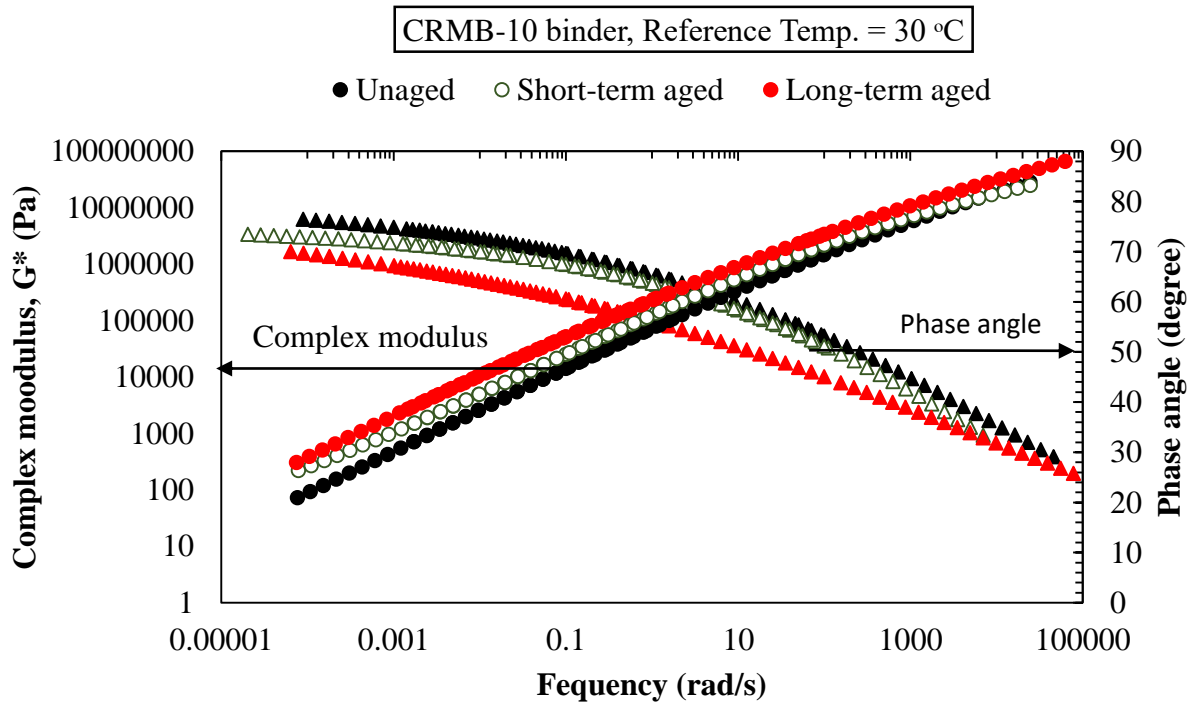


**Figure A.4:** Master curves of complex modulus and phase angle for the CRMB-5 binder at a reference temperature of 30°C showing the aging effect.

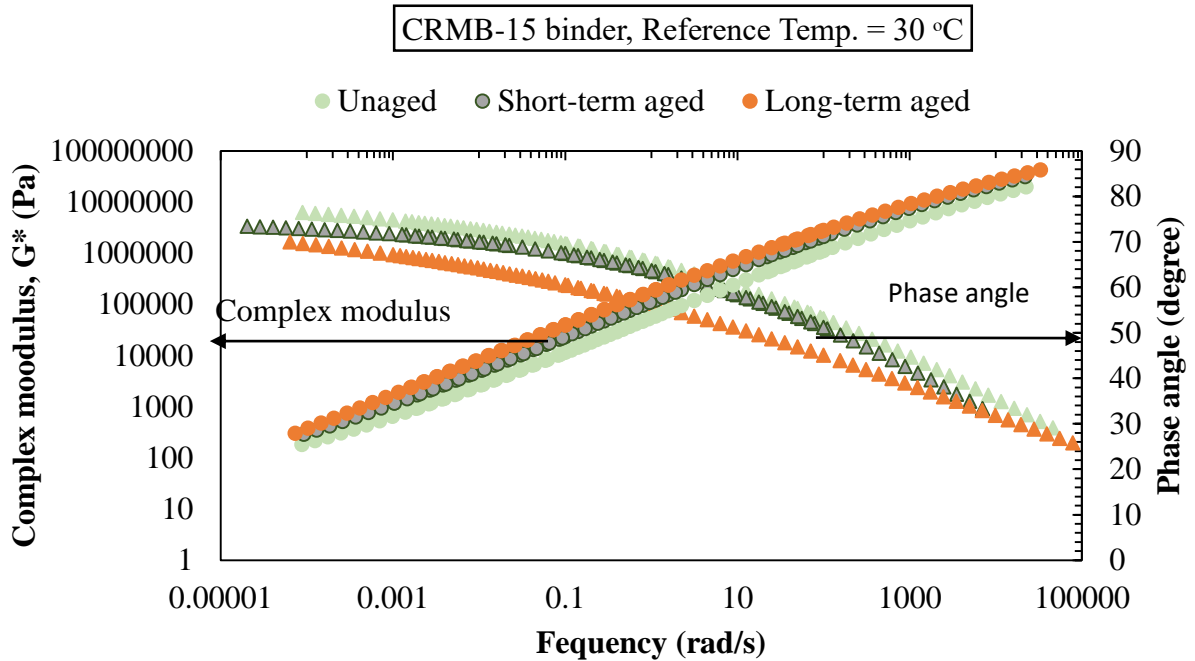


**Figure A.5:** Master curves of complex modulus and phase angle for the CRMB-15 binder at a reference temperature of 30°C showing the aging effect.

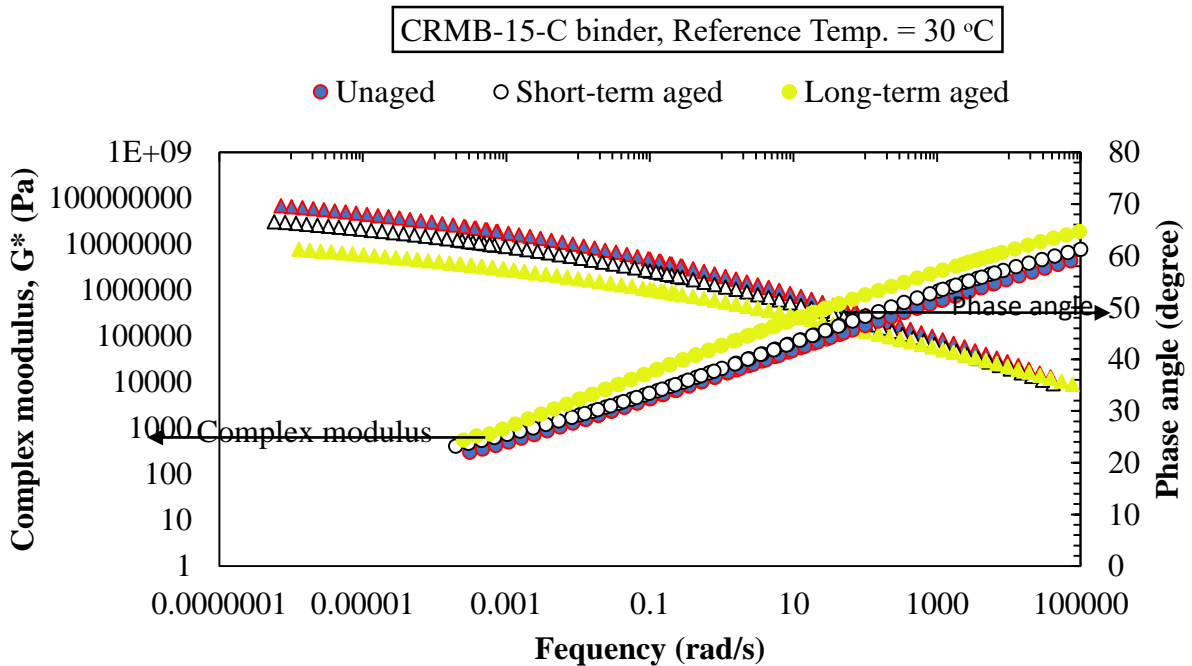


**Figure A.6:** Master curves of complex modulus and phase angle for the CRMB-15-C binder at a reference temperature of 30°C showing the aging effect



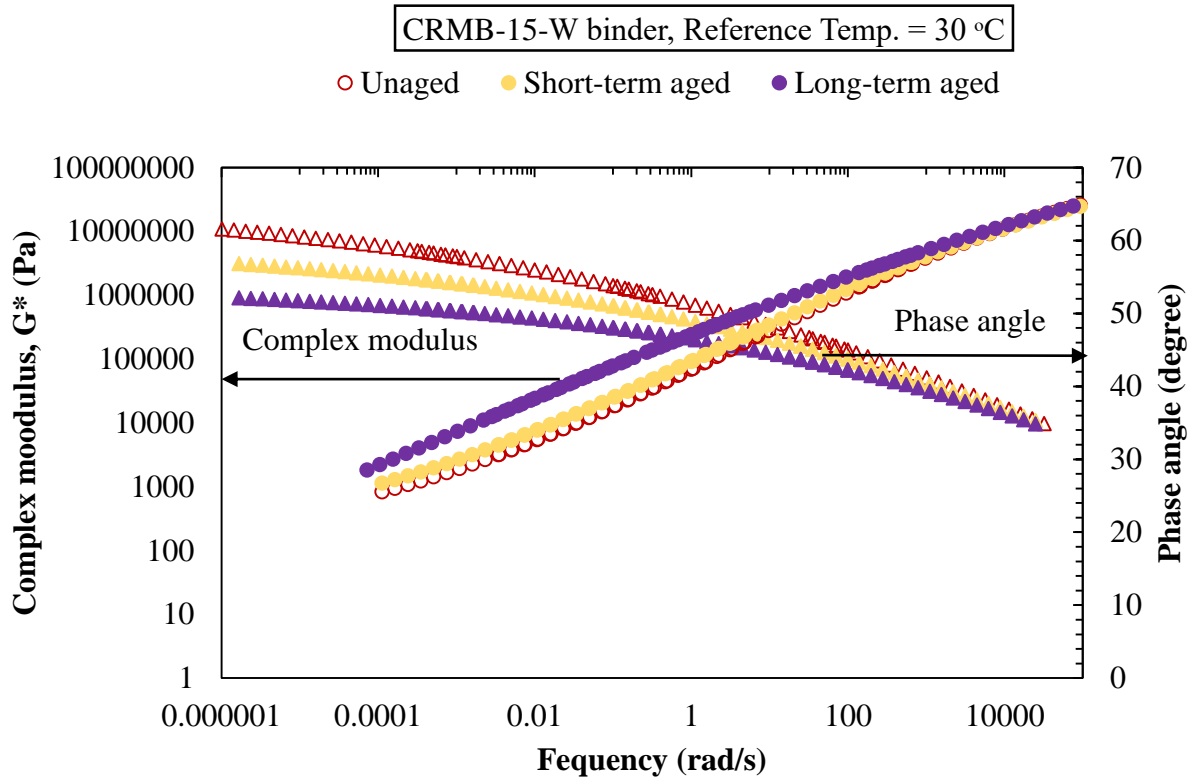


**Figure A.7:** Master curves of complex modulus and phase angle for the CRMB-15-W binder at a reference temperature of 30°C showing the aging effect.

**Appendix B**  
**Effect of aging on fatigue**  
**damage resistance of the binder at**  
**the intermediate-temperature**

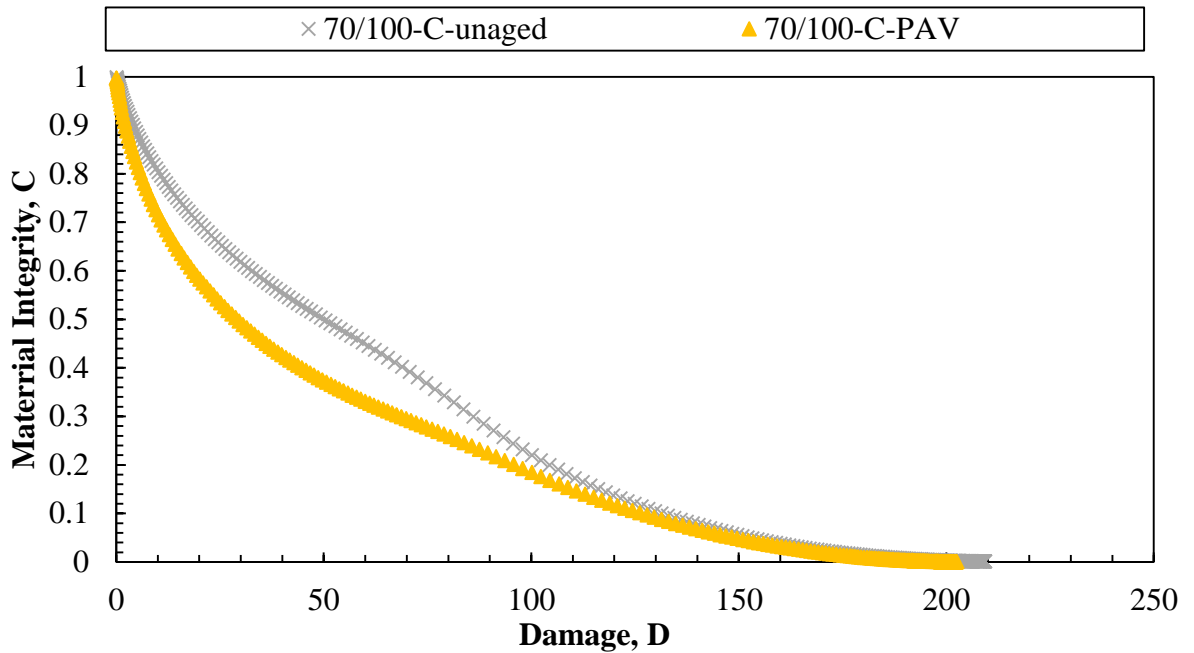


**Figure B.1:** Damage characteristic curves showing effect of artificial long-term ageing on the 70/100-C.

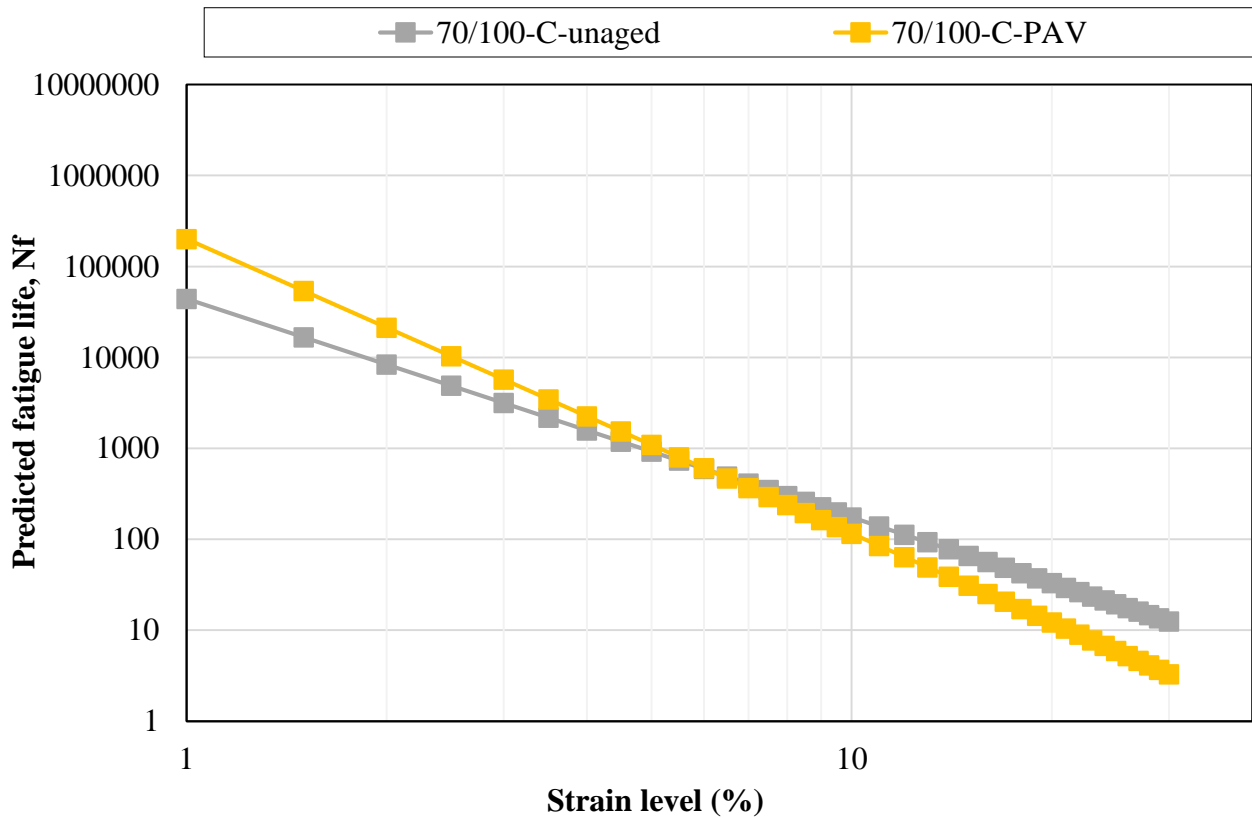


**Figure B.2:** Fatigue life predictions in function of strain level showing effect of artificial long-term ageing on the base 70/100-C.

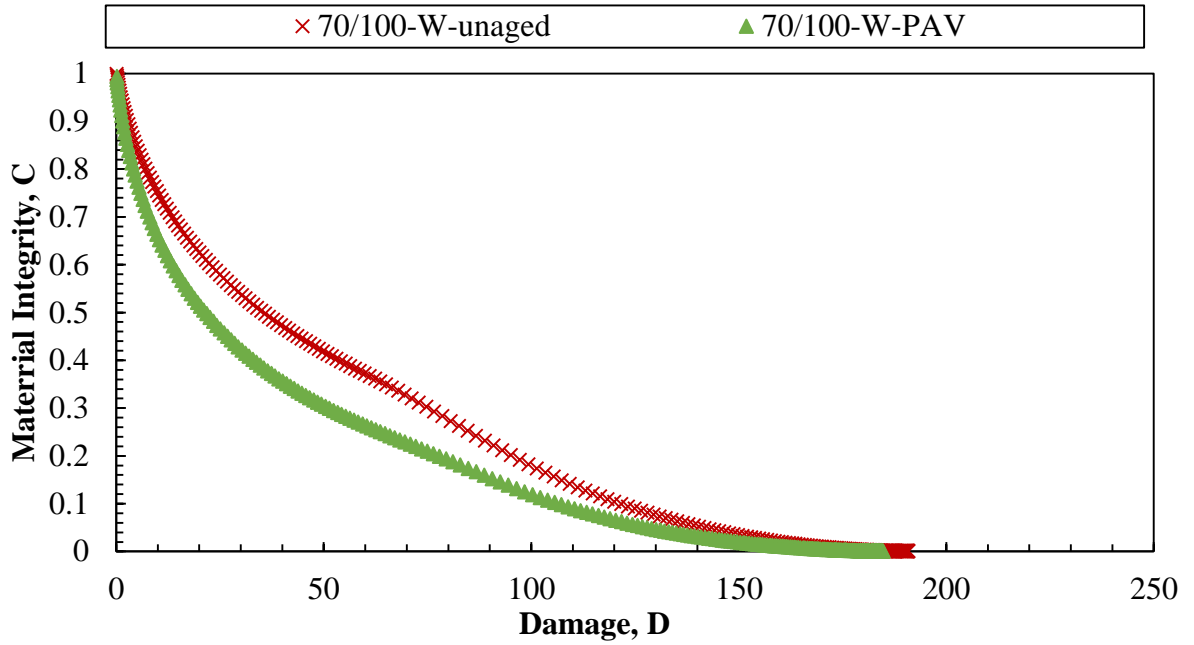


**Figure B.3:** Damage characteristic curves showing effect of artificial long-term ageing on the 70/100-W.

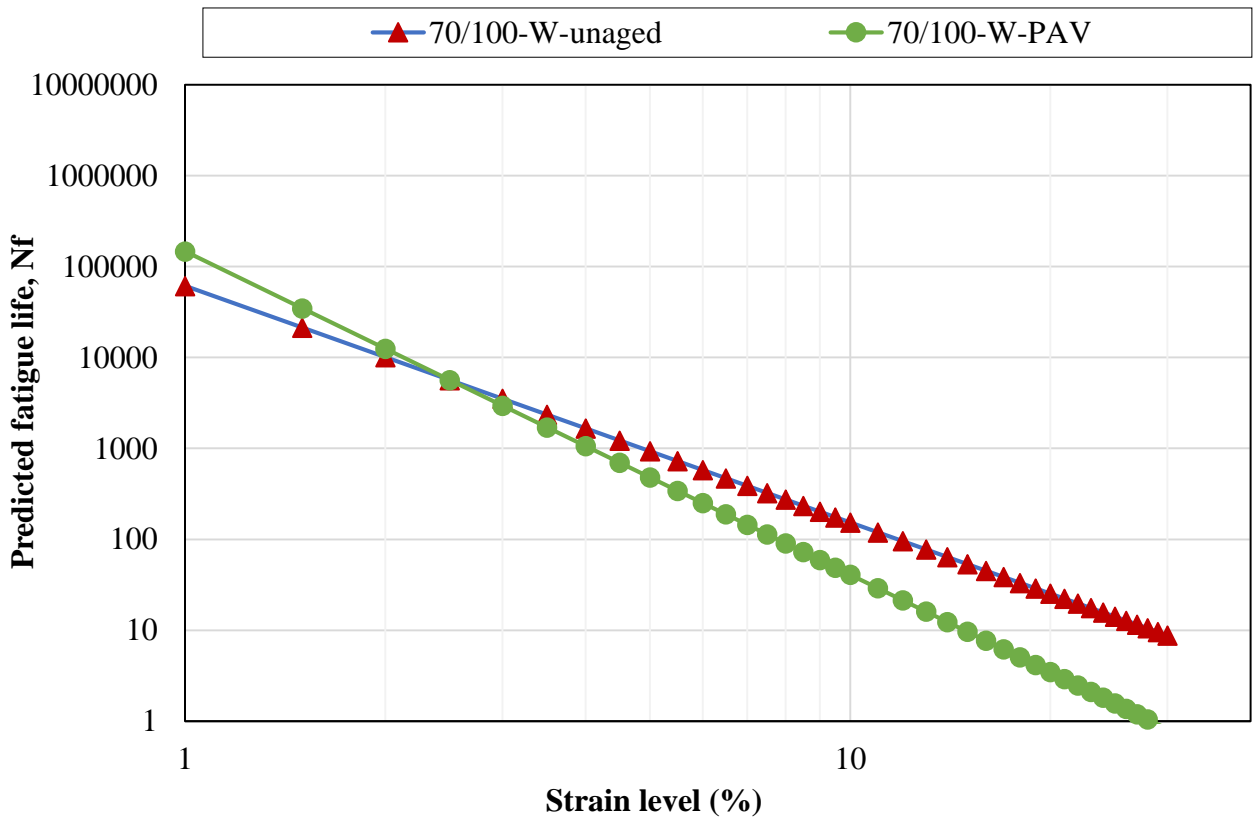


**Figure B.4:** Fatigue life predictions in function of strain level showing effect of artificial long-term ageing on the base 70/100-W.

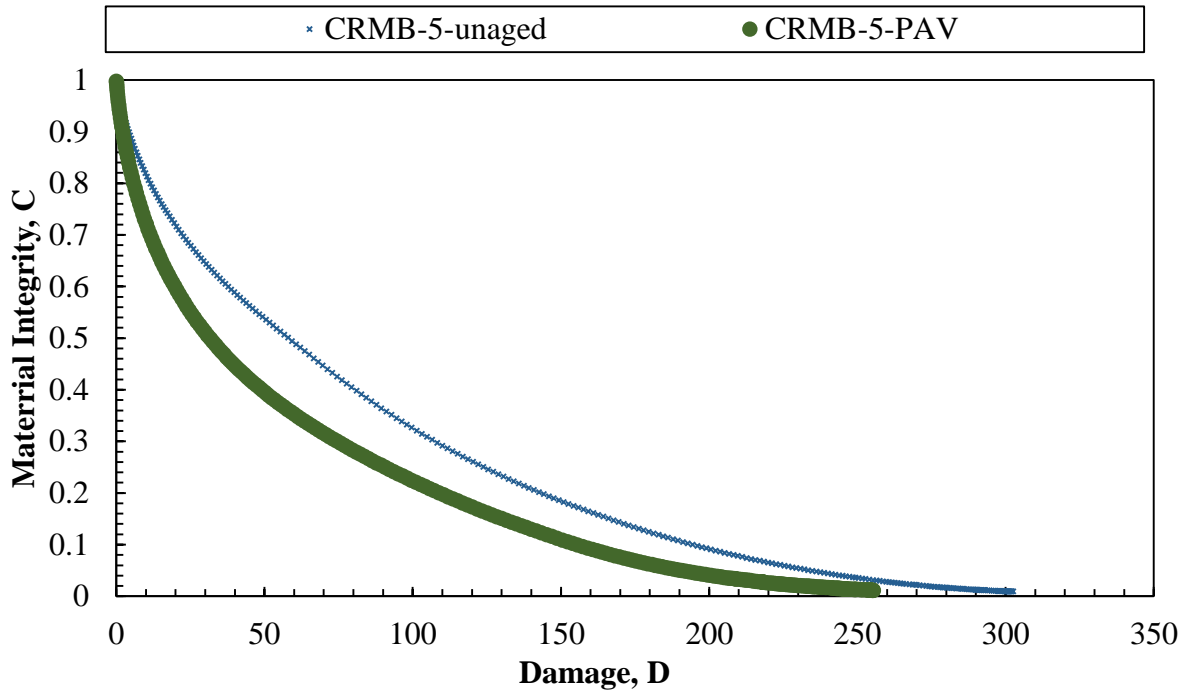


**Figure B.5:** Damage characteristic curves showing effect of artificial long-term ageing on the CRMB-5.

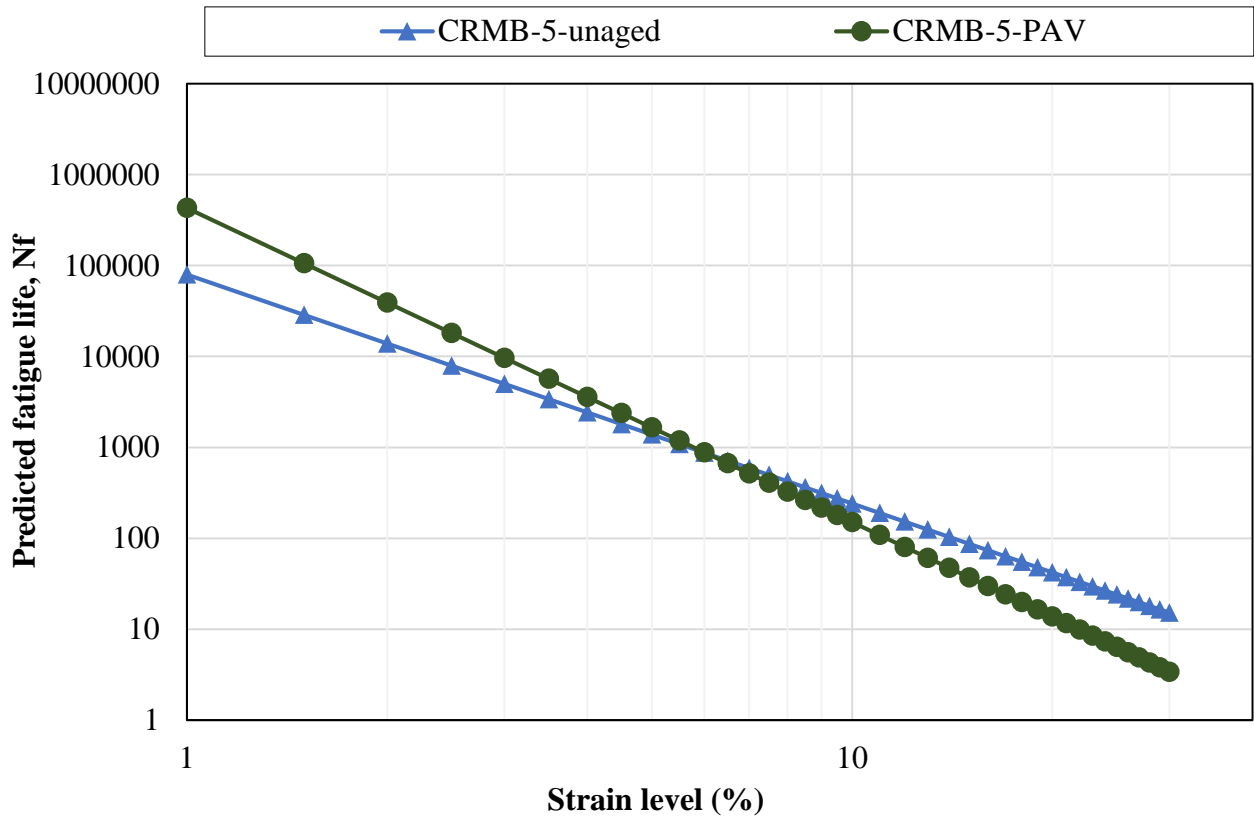


**Figure B.6:** Fatigue life predictions in function of strain level showing effect of artificial long-term ageing on the base CRMB-5.

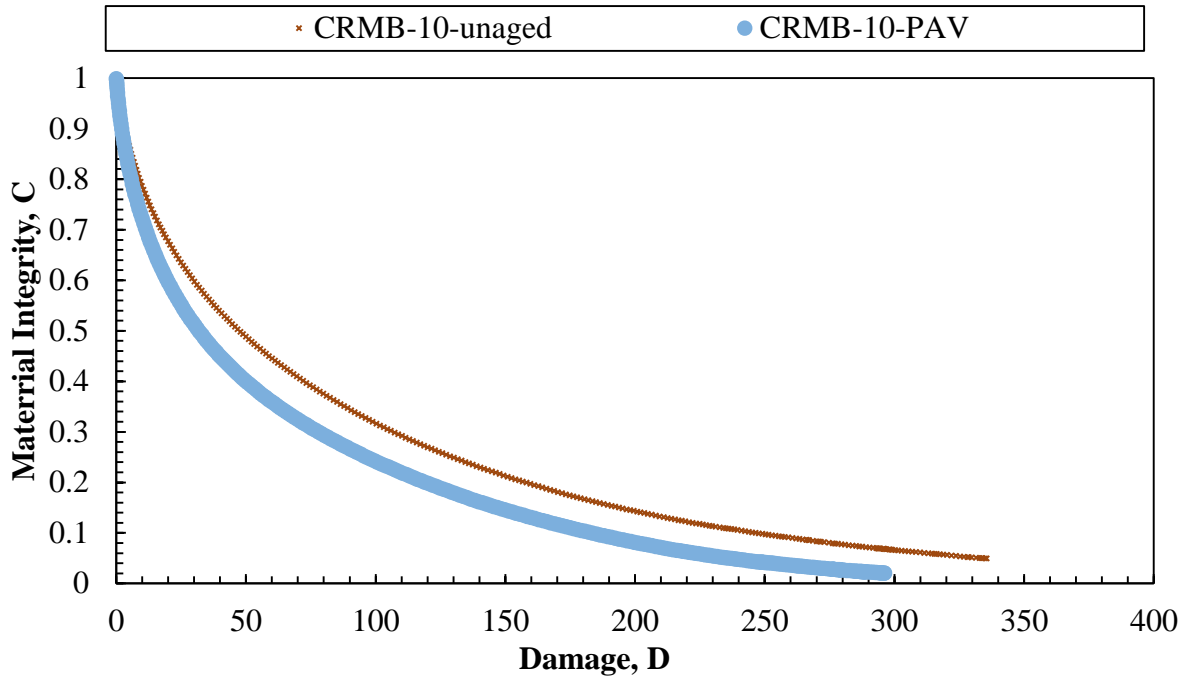


**Figure B.7:** Damage characteristic curves showing effect of artificial long-term ageing on the CRMB-10.

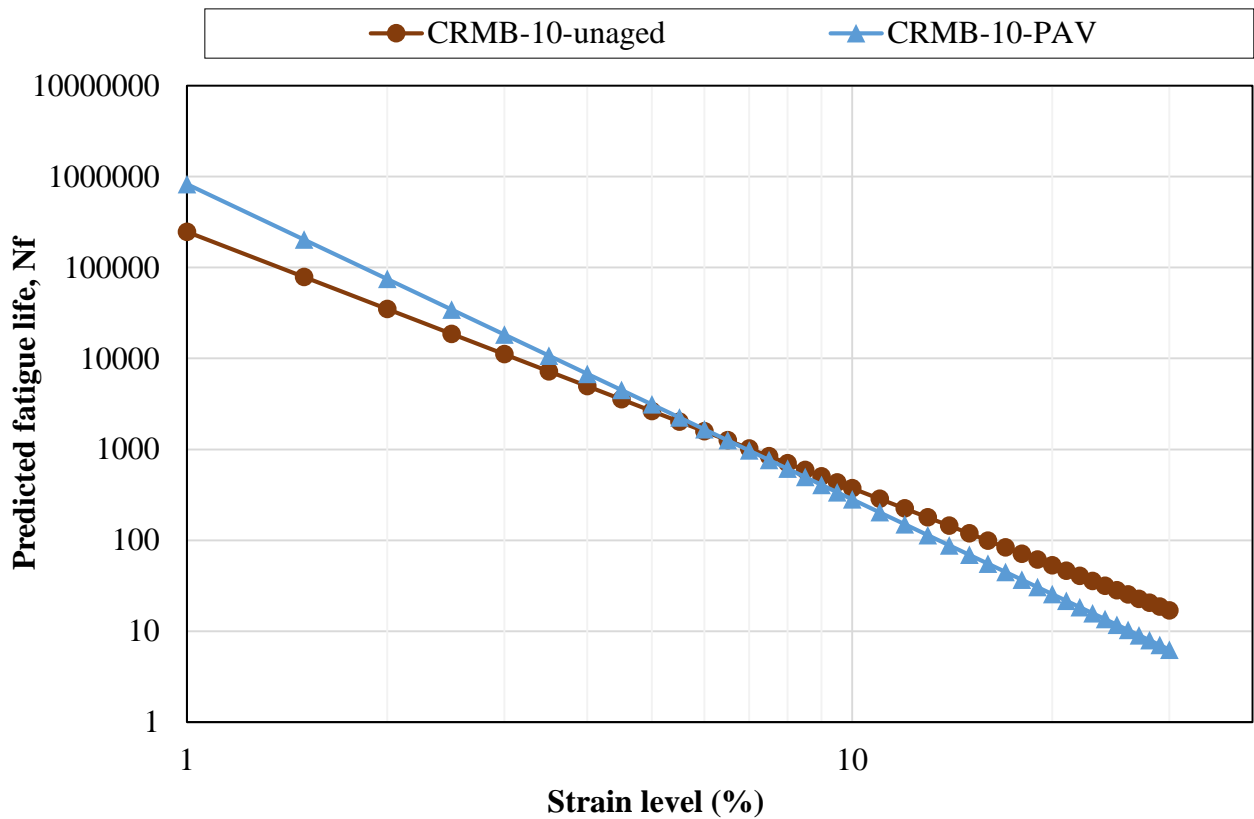


**Figure B.8:** Fatigue life predictions in function of strain level showing effect of artificial long-term ageing on the base CRMB-10.

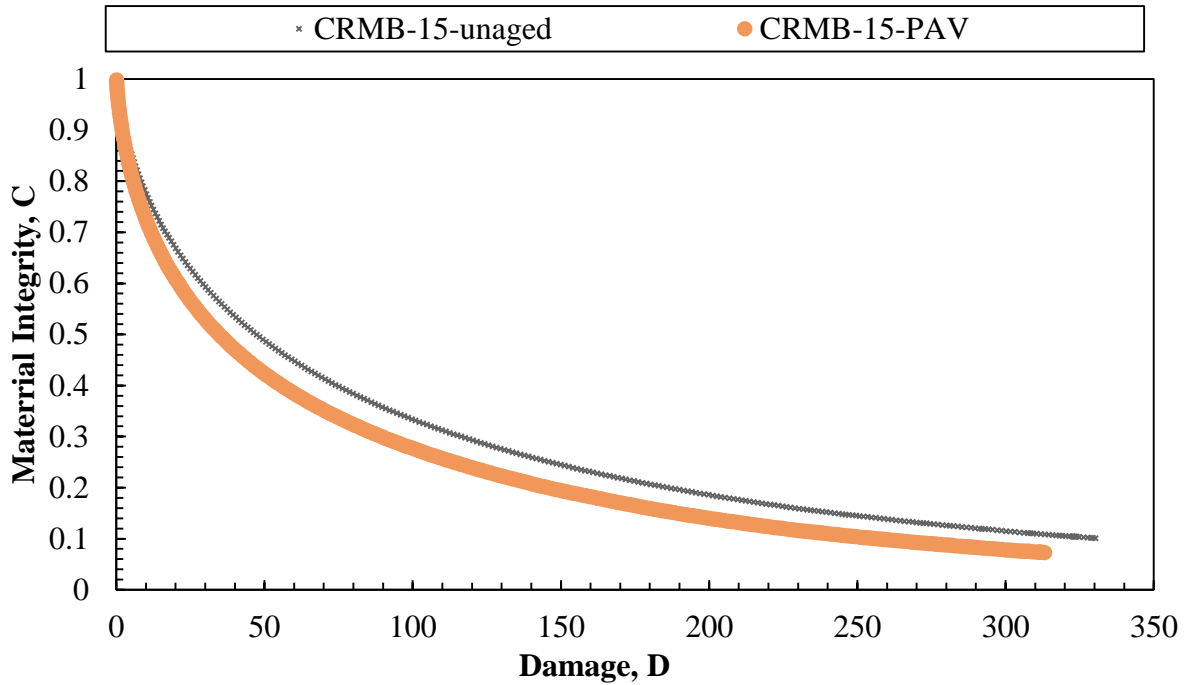


**Figure B.9:** Damage characteristic curves showing effect of artificial long-term ageing on the CRMB-15.

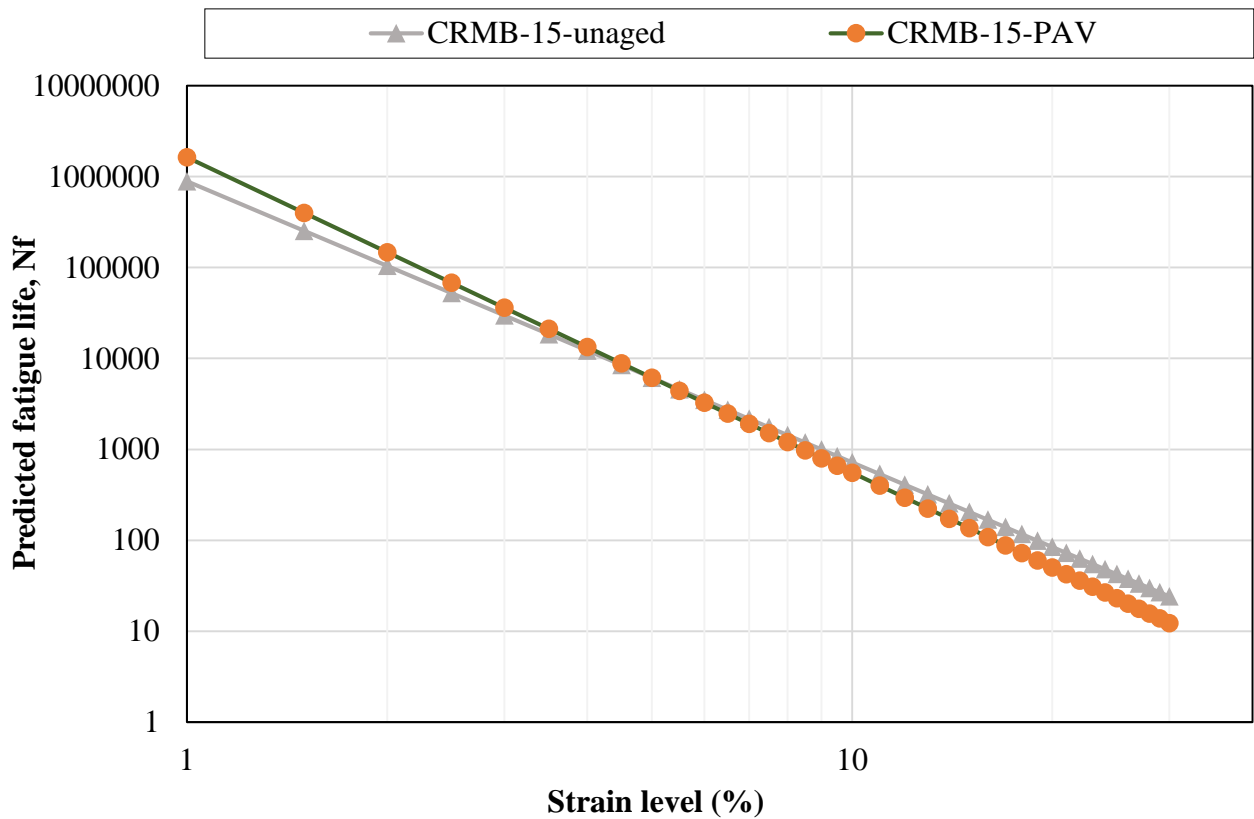


**Figure B.10:** Fatigue life predictions in function of strain level showing effect of artificial long-term ageing on the base CRMB-15.

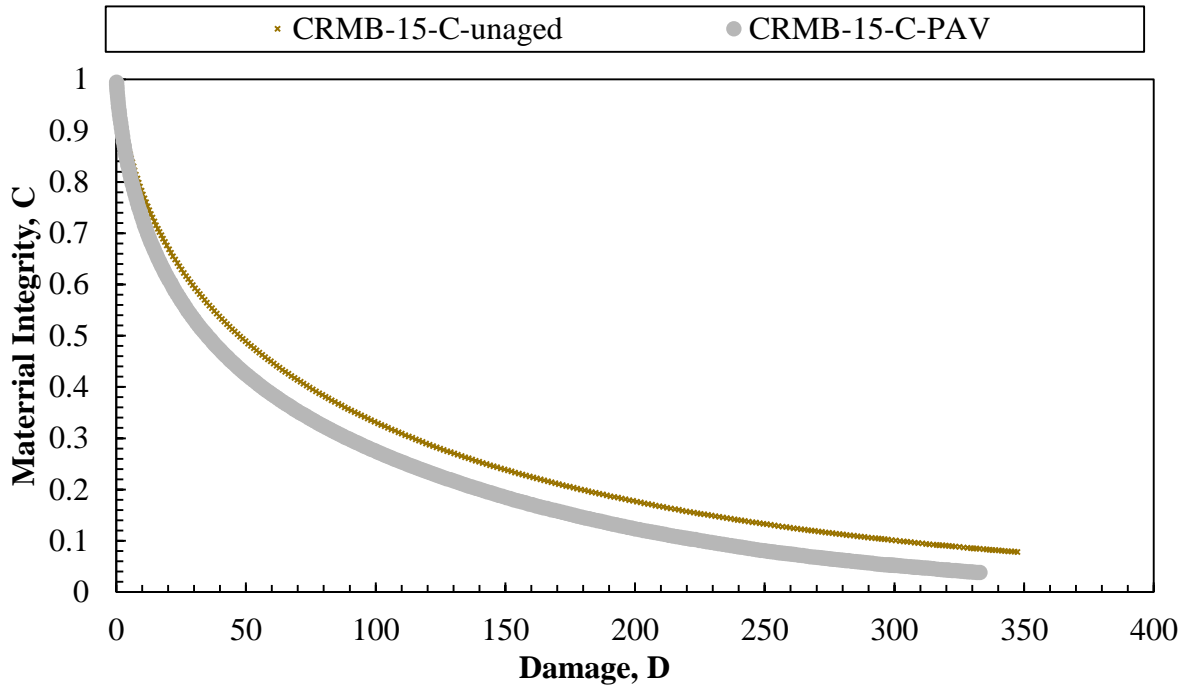


**Figure B.11:** Damage characteristic curves showing effect of artificial long-term ageing on the CRMB-15-C.

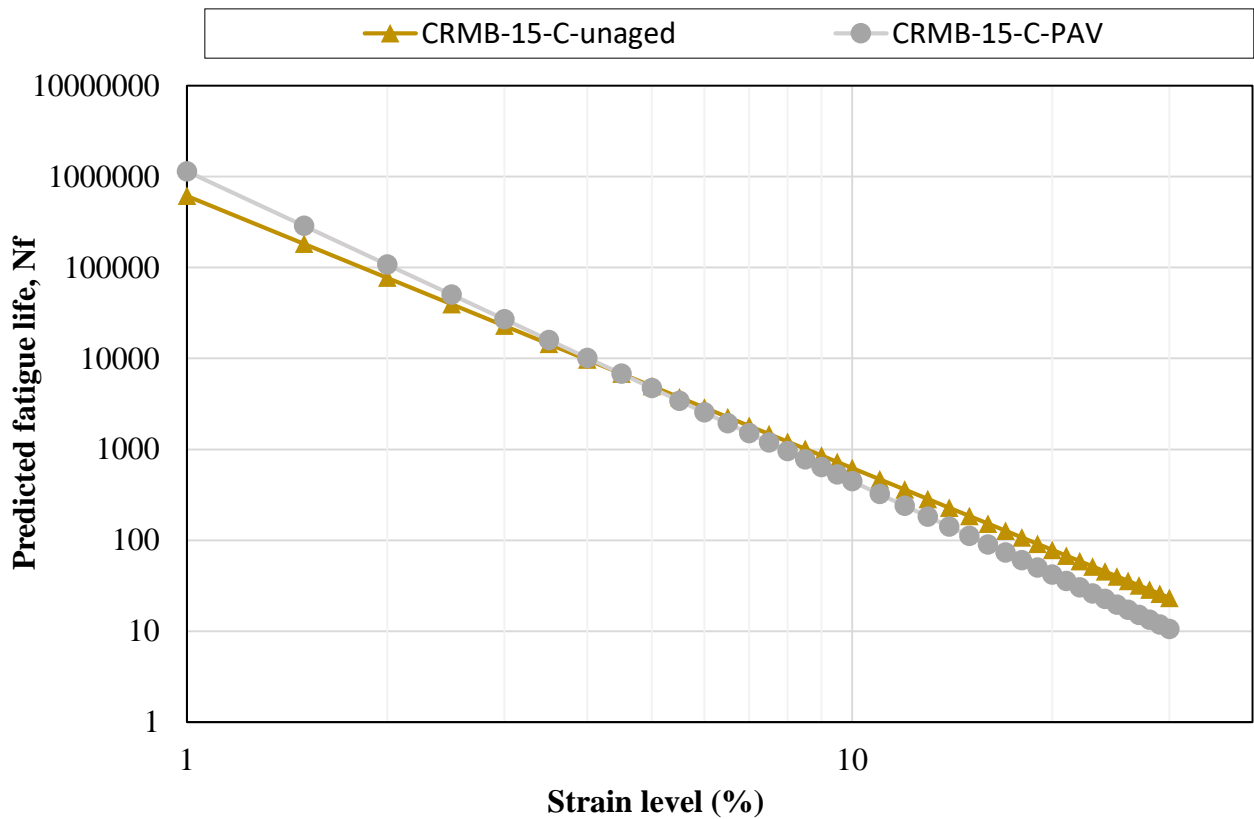


**Figure B.12:** Fatigue life predictions in function of strain level showing effect of artificial long-term ageing on the base CRMB-15-C.



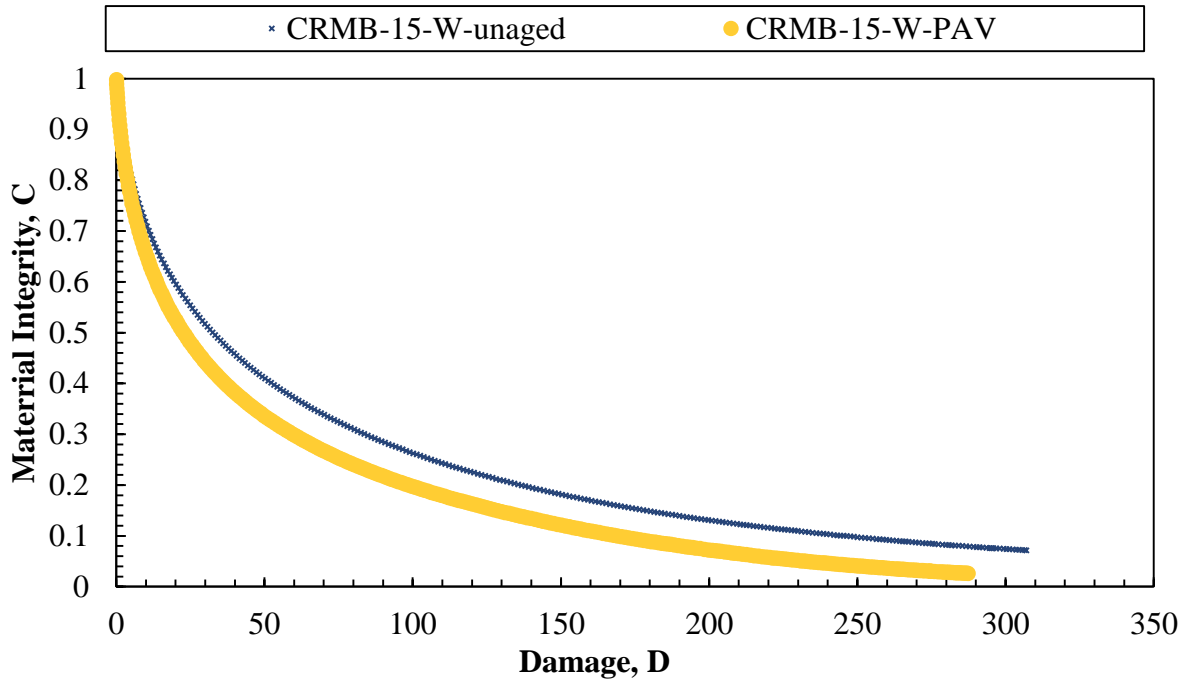


**Figure B.13:** Damage characteristic curves showing effect of artificial long-term ageing on the CRMB-15-W.

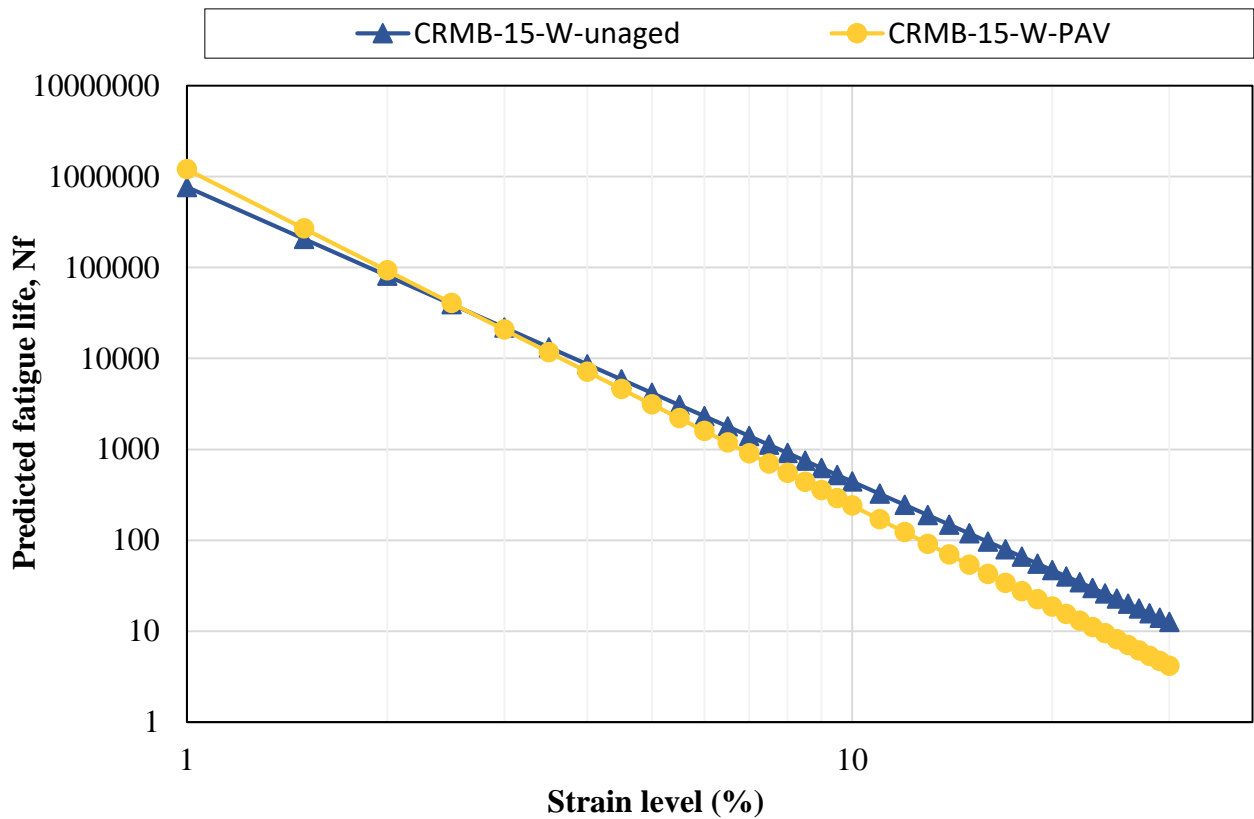


**Figure B.14:** Fatigue life predictions in function of strain level showing effect of artificial long-term ageing on the base CRMB-15-W.